

THE CATHOLIC UNIVERSITY OF AMERICA

Influence of Lubricant on Horizontal Convective Boiling in a Micro-fin Tube

A DISSERTATION

Submitted to the Faculty of the
Department of Mechanical Engineering
School of Engineering
Of The Catholic University of America
In Partial Fulfillment of the Requirements
For the Degree
Doctor of Philosophy

By

Nitin N. Sawant

Washington, D.C.

2012

Influence of Lubricant on Horizontal Convective Boiling in a Micro-fin Tube

Nitin N. Sawant, Ph.D.

Director: J. Steven Brown, Ph.D., P.E.

The goal of this dissertation is to measure local convective boiling heat transfer coefficients in a micro-fin tube operating with pure R-410A and with R-410A/lubricant mixture and to develop a “user-friendly” correlation from these data so that it can be easily applied by designers, practitioners, and researchers in the heating, ventilating and air-conditioning industry. The motivation for this study is the fact that there is little documentation in the literature of the effect of lubricant on the flow boiling heat transfer of R-410A. This dissertation represents the first, and only, study of the effects of lubricant on the heat transfer rate of R-410A during flow boiling using a fluid heating technique. (Note: all of the other studies apply the electrical resistance heating technique, which has been shown by Kedzierski (1995) to strongly influence the measurement.)

One of the objectives of this study, therefore, is to provide a source of data for the boiling of R-410A in a micro-fin tube with and without the addition of a Polyol ester (POE) lubricant. The evaporative heat transfer characteristics of R-410A and R-410A/POE were measured in a fluid-heated, 9.52 mm OD micro-fin tube. Data were measured for temperatures ranging from 7.2 °C to 10 °C. Baseline performance was established by measuring the convective boiling heat transfer of pure R-410A. In addition,

measurements of an R-410A/POE (99.6/0.4 by mass) mixture were taken and then compared to the pure R-410A baseline. The mean degradation in the heat transfer performance with the addition of lubricant was approximately 6.7 %.

A second objective of this study is to compare the experimental data to the existing NIST database of alternative refrigerants to determine the effect of the axial bulk lubricant concentration gradient on evaporative heat transfer. The experimental data were also compared with relevant correlations of R-410A and R-410A/lubricant mixtures.

A heat transfer correlation was developed from the measured data and then compared to them. The correlation predicted 70 % of the experimental data within a deviation of ± 30 %. The average and absolute average deviations of the model correlation are -3 % and 25.4 %, respectively.

This dissertation by Nitin N. Sawant fulfills the dissertation requirement for the doctoral degree in Mechanical Engineering approved by J. Steven Brown, Ph.D., P.E., as Director, Mark A. Kedzierski, Ph.D., as co-Director, and by Sen Nieh, Ph.D., and Rene Gabbai, Ph.D. as Readers.

J. Steven Brown, Ph.D., P.E., Director

Mark A. Kedzierski, Ph.D., Co-Director

Sen Nieh, Ph.D., Reader

Rene Gabbai, Ph.D., Reader

Dedication

This dissertation is dedicated to my parents Mr. Narayan D. Sawant and Mrs. Nalini N. Sawant for instilling the importance of higher education. There is no doubt in my mind that without their sacrifices, continued support, encouragement and counsel I could not have completed this journey.

Table of Contents

Title Page		
Abstract		
Signature Page		ii
Dedication		iii
Table of Contents		iv
List of Illustrations		x
List of Tables		xiii
List of Abbreviations		xv
Acknowledgements		xxi
Chapter 1	BACKGROUND AND SCOPE	1
1.1	The Montreal Protocol (1987)	2
1.2	The Kyoto Protocol (1997)	2
1.3	Alternative Refrigerants to CFCs and HCFCs	3
1.4	Refrigerant R-410A	5
1.4.1	Thermodynamic and Transport Properties	6
1.4.2	Safety Considerations	8
1.4.3	Materials Compatibility	10
1.4.4	Components for R-410A Systems	11
1.4.5	Applications of R-410A	12
1.4.6	Disadvantages of R-410A	12

Table of Contents

1.5	Difference between Mixtures and Pure Fluids	13
1.6	General Description of Boiling	15
1.7	Heat Transfer Augmentation	16
1.7.1	Micro-fin Tube	18
1.8	Lubrication Effects	18
1.9	Text Organization	20
Chapter 2	LITERATURE REVIEW	22
2.1	Test Rigs for Boiling Heat Transfer	23
2.2	Summary of Visual Evidence	25
2.3	Classification of Literature Review – Experimental Evidence	27
2.3.1	Enhancement	27
2.3.2	Comparison with Correlations/Models	31
2.3.3	Geometric Effects	36
2.3.4	Lubricant Effects	38
Chapter 3	EXPERIMENTAL SETUP AND MEASUREMENTS	50
3.1	Apparatus	50
3.2	Test Section	52
3.3	Micro-fin Tube Details	55
3.4	Charging the Refrigerant	57

Table of Contents

3.5	Measurements	57
3.5.1	Measurements for Temperature	58
3.5.2	Measurements for Pressure	58
3.5.3	Measurements for Mass Flow Rate	59
3.5.4	Single Phase Heating Tests for Energy Balance	59
3.5.5	Testing Protocol	60
3.5.6	Data Acquisition System	62
3.5.7	Problems	63
3.5.8	Summary of Experimental Data	64
3.6	Uncertainty in Measurements	64
3.7	Equilibrium Refrigerant Temperature	66
3.8	Fluid Heating and Electrical Resistance Heating	71
Chapter 4	HEAT TRANSFER: RESULTS AND DISCUSSION	74
4.1	Background	74
4.2	Thermodynamic Approach by Thome (1995)	75
4.3	Experimental Methodology and Data Reduction	76
4.4	Results and Discussion	79
Chapter 5	COMPARISON WITH CORRELATIONS	88
5.1	Principal Dimensionless Numbers	88
5.2	Correlation by Kim et al. (2002)	91

Table of Contents

5.3	Correlation by Ding et al. (2008)	95
5.4	Correlation by Hamilton et al. (2005)	100
Chapter 6	MODEL DEVELOPMENT	105
6.1	Introduction	105
6.2	Thome's Model (1995)	106
6.3	Semi-theoretical Model by Kedzierski (2003)	109
6.3.1	Basis of the Model by Kedzierski (2003)	112
6.3.2	Excess Surface Density	114
6.3.3	Derivation of the Model by Kedzierski (2003)	114
6.4	Basis of Proposed Model	120
6.5	Model Development	121
6.6	Discussion	124
Chapter 7	CONCLUSIONS AND RECOMMENDATIONS FOR FURTHER RESEARCH	128
7.1	Concluding Remarks	128
7.1.1	Originality and Contribution	130
7.2	Future Work	131
7.2.1	Two-phase Flow Patterns	131
7.2.2	Fluorescence Technique	132
7.2.3	Effect of Lubricant Concentration	132

Table of Contents

7.2.4	Model using Refrigerant-lubricant Mixture Properties	133
7.2.5	Apparatus Modifications	133
Appendix A	GENERAL DESCRIPTION OF BOILING	135
A1	Regimes of Boiling	136
A2	Horizontal Convective Boiling Heat Transfer	138
Appendix B	CORRELATIONS	141
B1	Superposition Model	141
B2	Asymptotic Model	146
B3	Enhancement Model	147
Appendix C	EXPERIMENTAL DATA	151
C1	Pure R-410A Data	151
C2	R-410A/Lubricant Data	156
Appendix D	COMPUTER PROGRAM	159
Appendix E	TEST RIG OPERATION	201
E1	LabView Program on Computer	201
E2	Test Rig Startup	201
E3	Recording Data	201
E4	At the End of the Day	202

Table of Contents

Appendix F	CALCULATION OF RCL AND ATEL FOR R-410A	203
F1	Acute-Toxicity Exposure Limit (ATEL)	203
F2	Example: ATEL Calculation for R-410A	205
F3	Refrigerant Concentration Limit for R-410A	206
Appendix G	REFRIGERANT HISTORY AND REFRIGERANTS	207
G1	Refrigeration History	207
G2	Refrigerants	210
	BIBLIOGRAPHY	212

List of Illustrations

Figure No.	Title	Page
1-1	Refrigerant Safety Group Classification	9
1-2	T-x Diagram for Vaporization of Near-azeotropic Binary Mixture	14
2-1	Typical Test Rig in Literature	24
3-1	Schematic of Test Rig	51
3-2	Test Section Detail	53
3-3	Cross Sectional View of Test Section and Micro-fin Tube Details	56
3-4	Single-phase Energy Balance with R-134a	60
3-5	Vapor-Liquid Equilibrium Measurements of R-410A	67
3-6	Comparison of Measurements with REFPROP 7.1 (2006)	68
3-7	Difference between R-410A and R-410A/POE at Saturated Liquid Equilibrium Conditions	70
4-1	Refrigerant and Water-side Temperature Profiles	78
4-2	Heat Flux Distribution for R-410A and R-410A/POE	80
4-3	Heat Flux Distribution for Tests with R-410A and R-410A/POE	81
4-4	Effect of Saturation Temperature on Heat Flux	83
4-5	Detail Cross Section of Micro-fin Tube	84
4-6	Comparison of Two-phase Heat Transfer Coefficient for R-410A and R-410A/POE	85

List of Illustrations

Figure No.	Title	Page
4-7	Effect of Lubricant on Two-phase Heat Transfer Coefficient of R-410A	87
5-1	Comparison of Experimental Data with Correlation of Kim et al. (2002)	94
5-2	Comparison of Experimental Data with Correlation of Ding et al. (2008)	99
5-3	Comparison of Experimental Data with Correlation of Hamilton et al. (2005)	102
5-4	Apparent Heat Transfer Degradation due to Lubricant with Correlation of Hamilton et al. (2005)	103
6-1	Bubble on a Heated Wall	113
6-2	Schematic of the Average Departure Bubble for Three R-123/lubricant Mixtures with Corresponding Excess Layers	115
6-3	Comparison of Experimental Data with the New Correlation for R-410A/POE	125
6-4	Measured and Predicted Heat Transfer Coefficients of R-410A/POE	126

List of Illustrations

Figure No.	Title	Page
6-5	Average Deviation versus Quality for the New Correlation of R-410A/POE	127
A-1	Regimes of Flow Boiling	148
A-2	Two-phase Flow Patterns in a Horizontal Tube	149

List of Tables

Table No.	Title	Page
1-1	ODP and GWP of R-22 and Alternative Refrigerants	4
1-2	Comparison of R-410A with R-22 and its Replacements using Refprop	7
1-3	Safety Data for R-22 and Alternative Refrigerants	10
2-1	Comparison of Heat Transfer Enhancement Factors (EF) for R-134a and R-12	29
2-2	Comparison of Pressure Drop Penalty Factors (PF) for R-134a and R-12	30
2-3	Flow Conditions for Pure Refrigerants Flowing Inside Micro-fin Tubes	34
2-4	Tube Geometries for Pure Refrigerants Flowing Inside Micro-fin Tubes	35
3-1	Geometric Parameters of Turbo-AII™ Micro-fin Tube	55
3-2	Tested Range of Measurements	61
3-3	Instrument Range and Uncertainty	65
3-4	Median Estimated 95 % Relative Expanded Uncertainties and Range for Measurements	65

List of Tables

Table No.	Title	Page
5-1	Coefficients of Correlation by Kim et al. (2002)	92
6-1	Values of Empirical Constants	108

List of Abbreviations

Variable	Description
A	Heat transfer area, m^2
$A1$	Safety group
A_c	Cross sectional flow area, m^2
A_i	Internal Surface Area, m^2
A_0, A_1, A_2, A_3	Constants
AL	Atmospheric lifetime, years
AREP	Alternative Refrigerants Evaluation Program
ARI	Air-conditioning and Refrigeration Institute
ASCII	American Standard Code for Information Interchange
ASHRAE	American Society of Heating Ventilation and Air-conditioning Engineers
ATEL	Acute-toxicity exposure limit, ppm
a_0 through a_4	Constants
a_n	Mortality indicator, ppm
Bo	Boiling number
b_0 through b_4	Constants
b_n	Cardiac sensitization indicator, ppm
C	Constant
C_1 through C_9	Constants
Co	Convection number
CFC	Chlorofluorocarbon
CH_4	Methane
COP	Coefficient of performance
CO_2	Carbon dioxide
CST	Critical solution temperature, $^{\circ}C$
c_n	Anesthetic effect indicator, ppm
c_p	Specific heat, J/kg-K
c_{pf}	Water specific heat, J/kg-K
$(c_p)_L$	Specific heat of liquid refrigerant-lubricant mixture, J/kg-K
$(c_p)_V$	Specific heat of pure refrigerant vapor, J/kg-K
D	Diameter, mm
D_r	Diameter of micro-fin tube at the fin root, mm
D_e	Equivalent diameter of micro-fin tube, mm
D_h	Hydraulic diameter, mm
d	Diameter, m
d_f	Diameter at the bottom of fin, mm
dP_f/dz	Water pressure gradient
dT_f/dz	Local axial water temperature gradient

List of Abbreviations

Variable	Description
E	Two-phase Convection Multiplier
E_{RB}	Ribbed tube enhancement factor
EF or E_f	Enhancement factor
e or e_f	Fin height, mm
Fr	Froude number
f	Fin height, mm
G	Mass flux, $\text{kg}/\text{m}^2\text{s}$
g	Gravitational acceleration, m/s^2
GWP	Global warming potential
h	Heat transfer coefficient, $\text{W}/\text{m}^2\text{K}$
$h_{2\Phi}$	Two-phase heat transfer coefficient, $\text{W}/\text{m}^2\text{K}$
h_{fg} or h_{LV}	Latent heat of vaporization, kJ/kg
HC	Hydrocarbon
HCFC	Hydrochlorofluorocarbon
HFC	Hydrofluorocarbon
HP	Hewlett Packard
HVAC&R	Heating Ventilation Air-conditioning and Refrigeration
HOC	Heat of Combustion
ISO	International Standards Organization
ID	Inside diameter, m
ISO	International Standards Organization
k	Thermal conductivity, W/mK
L	Length, m
l_a	Van der Waal's excess layer, m
l_e	Thickness of excess layer, m
l_f	Axial pitch from fin to fin, m
LCCP	Life Cycle Climate Performance
LFL	Lower Flammability Limit
$LMTD$	Logarithmic Mean Temperature Difference, K
LOEL	Lowest observed effect level
M_L	Mass of lubricant, kg
M_w	Molecular weight, kg/kmol
M_r	Molar mass of refrigerant, kg/kmol
M_{rv}	Mass of refrigerant vapor, kg
m	Mass flow rate, kg/s
m_f	Measured water mass flow rate, kg/s
mf_n	Mole fraction for component n
N_2O	Nitrous oxide

List of Abbreviations

Variable	Description
NBP	Normal boiling point, °C
N_f	Total number of fins
NIST	National Institute of Standards and Technology
Nu	Nusselt number
NOEL	No-observed-effect-level
Nu_m	Measured Nusselt number of refrigerant/lubricant mixture
Nu_p	Nusselt Number obtained from correlation
n	Number of fins
OD	Outside diameter, m
ODL	Oxygen deprivation limit, ppm
OEL	Occupational exposure limit, ppm
ODP	Ozone Depletion Potential
ODS	Ozone Depleting Substances
P	Pressure, MPa
PEL	Permissible exposure level, ppm
PF	Penalty factor
PFC	Perfluorocarbon
POE	Polyol Ester Oil
Pr	Prandtl number
P_r	Refrigerant pressure, MPa
P_{re}	Reduced pressure, MPa
P_s	Saturation pressure, MPa
p	Wetted perimeter of the inside of micro-fin tube, m
Q	Heat transfer rate or heat duty, Watts
q or q''	Heat flux, W/m^2
R	Universal gas constant, J/K.mol
RCL	Refrigerant concentration limit, ppm
Re	Reynolds number
r_b	Bubble departure radius, m
S	Boiling suppression factor
SA	Simple Asphyxiate
SES	Service engineer's section
SF ₆	Sulfur hexafluoride
S_p	Perimeter of a fin and channel taken perpendicular to the axis of fin, m
SS	Stainless steel
SUS	Saybolt Universal Seconds
s	Spacing between fins, mm
T	Temperature, °C

List of Abbreviations

Variable	Description
T_b	Bubble point temperature of mixture, °C
T_{bub}	Local bubble point temperature of bulk liquid mixture
T_c	Refrigerant-lubricant critical solution temperature (lower limit), °C
TCF	Toxic concentration factor
T_d	Dew point temperature of mixture, °C
T_e	Temperature at excess layer/bulk fluid interface, °C
T_i	Temperature of interface, °C
TLV	Threshold Limit Value, ppm
T_r	Average refrigeration saturation temperature, °C
T_s	Saturation temperature, °C
T_w	Wall temperature, °C
t_b	Thickness of the fin at its base, mm
t_w	tube wall thickness at root of fin
U	Overall heat transfer coefficient, W/m ² K
U_m	Expanded measurement uncertainty
u_i	Standard uncertainty
v_f	Specific volume of water, m ³ /kg
w_b	All-liquid lubricant mass fraction
w_l or w_{local}	Local lubricant mass fraction
w_{oil}	Oil concentration
X_{tt}	Lockhart-Martinelli parameter
x	Quality
x_b	Lubricant mass fraction
x_l	Mass fraction of vapor
x_q	Thermodynamic mass quality
x_v	Mass fraction of liquid
z	Axial position

Subscripts

a	Micro-fin tube
a'	Micro-fin tube with oil
b	Bulk
c	Critical condition
DB	Dittus-Boelter
diff	Difference
e	Fin height, mm

List of Abbreviations

Variable	Description
f	Fin
g	Gas or vapor
h	Heating or hydraulic
i	Inner
in	Inlet
L or l	Liquid
LV	Least Volatile Component
MV	More Volatile Component
nb	Nucleate boiling
o	Outer
out	Outlet
r	Refrigerant
rv	Refrigerant vapor
s	Smooth tube
sat	Saturation
s'	Smooth tube with oil
ss	Stainless steel
t	Minimum wall thickness, mm
tp	Two-phase
V	Vapor
w	Wall

Greek symbols

α	Heat transfer coefficient, W/m ² -K
β	Helix angle, degrees
β_f	Helix angle of micro-fin, degrees
δ	Liquid film thickness, mm
ϵ	Void fraction
ζ	Fraction of excess layer removed per bubble
Θ	Dimensionless thermal boundary layer temperature profile
λ	Thermal boundary constant
$\lambda_{r,o,L}$	Heat conductivity or liquid refrigerant-lubricant mixture, W/m-K
μ	Viscosity, kg/m-s
ρ	Mass density, kg/m ³
Γ	Excess surface density, kg/m ²

List of Abbreviations

Variable	Description
γ	Helix angle, degrees
Δ	Difference
ΔT_s	Wall superheat, K
ΔT_{le}	Temperature drop across excess layer, K
σ	Surface tension (N/m)
ν	Viscosity, m ² /s

Acknowledgements

The pages of this dissertation reflect the relationships with many generous and inspiring people I have met since beginning my Ph.D. I would like to acknowledge and extend my heartfelt gratitude towards many people for their support and encouragement that helped me tremendously to pursue this dream of a doctoral degree.

First and foremost, I would like to express my deepest gratitude towards my advisor, Dr. J. Steven Brown for his kind support and guidance in completing this dissertation. As Chairman of the Catholic University's Mechanical Engineering Department, he was instrumental in admitting me to the doctoral program. His constant source of encouragement and motivation helped me scale and surpass several levels of difficulties. Without his understanding and help, caring and patience, this doctoral program would have been impossible. I will always treasure all the advice I have received from Dr. Brown over the course of the past ten plus years that I have known him.

Dr. Mark Kedzierski of the National Institute of Standards and Technology (NIST) has served as co-advisor for this research. He gave me the great opportunity to undertake an R-410A project and unhesitatingly put all of his facilities at my disposal. I am greatly indebted to Mark for his enormous co-operation and for never stopping to act as a great mentor to me and for providing me with unending motivation to finish the dissertation.

The other members of my dissertation committee, Dr. Sen Nieh and Dr. Rene Gabbai, have generously given their time and expertise to better my work. I thank them for their time and attention during busy semesters, contribution and good-natured support.

My thanks and appreciation goes out to Dr. Sen Nieh for all his valuable support and his time while guiding his own doctoral and masters degree students. His inspiration could not have come at any more perfect timing in order for me to finish my dissertation. He also made financial assistance available to me during the period when things were starting to look difficult. I have come to appreciate him as a personable man.

It is an honor for me to have come across a warm and kind-hearted person like Dr. Piotr A. Domanski, who gave me the first ever opportunity to be a part of a brilliant HVAC&R Equipment and Performance Group at NIST and also graciously extended the hospitality of the NIST organization. My personal and heart-felt thanks go out to Dr. William Vance Payne II for being a mentor to me during my stay at NIST and also for reviewing this dissertation. I would also like to show my gratitude towards Dr. Sukumar Devotta, who introduced me to the research opportunities in the field of refrigeration and air-conditioning.

Thanks also go to Wolverine Tube, Inc. for supplying the Turbo-AIITM micro-fin tube for the test section. The RL68H (POE) lubricant that was donated by Dr. S. Randles of ICI is much appreciated. The naphthenic mineral oil was donated by Mr. K. Starner and Dr. M. Naduvath of York International and is much appreciated.

I am grateful to Ms. Ruth Hicks, the Mechanical Engineering Department's assistant to the Chair, for assisting me with the administrative tasks necessary for completing my doctoral program. She is one of the nicest lady I have ever met and an equally great credit to the university. I would also like to thank Ms. Peggy Bruce and Ms.

Mary Kate Zabroske of the Office of the Dean of Engineering for their help in monitoring my graduate course and maintaining my immigrant status clean.

I also appreciate the help and encouragement of technician, Mr. John Wamsley, of the Two-Phase Heat Transfer Laboratory at NIST. John was always been there for me when it came to modifying a part of test rig or adding an accessory to equipment.

I am deeply indebted to my family for their encouragement to keep me going in order to complete this dissertation. I want to extend gratefulness toward my parents for their undying support and love and for always understanding the person that I am during the long years of my education. My brothers, Bipin and Sachin and their respective families have provided me with timely doses of motivation, support, laughter and affection.

Last but not the least; I want to express my utmost appreciation and gratitude towards my dearest friend and wife, Jyoti, the most right person to have understood me best and who has never faltered to be the backbone of my quest to achieve my dreams. She has encouraged me non-stop during this monumental journey and I can't thank her enough from the bottom of my heart for all the sacrifices she has made, for all the challenges she has withstood during the time of completion of my dissertation. I want to thank her to have consistently helped me keep perspective on what is important in life and shown me how to deal with reality. I am truly blessed to have got such a fantastic life-companion.

I offer my regards to all of those who supported me in any respect during the completion of my dissertation.

Chapter 1

BACKGROUND AND SCOPE

Industrial refrigeration has evolved since early 19th century up until now. During this period, the type of refrigerant (working fluid) has changed from being familiar solvents and other volatile fluids (ethers, carbon dioxide, ammonia, sulphur dioxide, hydrocarbons, water, carbon tetrachloride, etc.) from 1830s to 1930s - to chlorofluorocarbons (CFCs), hydrochlorofluorocarbons (HCFCs), ammonia, water, etc. from 1931 to 1990s (Calm, 2007).

Growing environmental concerns and increasing governmental regulations over the last several decades has generated an increasing need for “environmentally friendly” refrigerant alternatives since many of the most commonly used refrigerants have been found to have negative environmental impacts. In particular, two recent global agreements have compelled the Heating, Ventilating, Air Conditioning, and Refrigeration (HVAC&R) industry to search for alternative refrigerants: (1) the Montreal Protocol on Substances that Deplete the Ozone Layer (1987) and (2) the Kyoto Protocol to the United Nations Framework Convention on Climate Change (1997).

As a result, chemical and equipment manufacturers have been searching to identify potential alternative refrigerants and refrigerant blends. This activity is also forcing the industry to develop safety and application data for these substitutes, to redesign products and service practices, to qualify new lubricants and other fabrication materials, and to test and rate new equipment (Calm, 2003).

1.1 The Montreal Protocol (1987)

The Montreal Protocol was adopted in September 1987 for the protection of stratospheric ozone. This agreement specified control measures for the reduction and phaseout of Ozone Depleting Substances (ODSs), namely, CFCs, (HCFCs), halons, carbon tetrachloride (CCl₄), 1,1,1-trichloroethane, and methylbromide (CH₃Br). Of these, CFCs and HCFCs were (and are) used extensively as refrigerants for a wide range of applications. This agreement aimed to eliminate these refrigerants and to replace them with environmentally safe substitutes. Perhaps the clearest example of this was the elimination of R-12, which was widely used in applications such as automotive air-conditioning and household refrigerators and R-22, which was widely used in applications such as heat pumps and chillers. R-134a was agreed upon as the most widely accepted replacement to R-12 since it has zero Ozone Depletion Potential (ODP) and thermodynamic properties similar to those of R-12. The Montreal Protocol does not address non-ozone depleting chemicals.

1.2 The Kyoto Protocol (1997)

The Montreal Protocol had an additional benefit in that as a class CFC refrigerants also have large global warming potentials (GWP). Therefore, the Montreal Protocol not only addressed the ozone crisis but also inadvertently helped to address the global warming problem. However, soon after the Montreal Protocol, people began to understand that many of the HFC refrigerants being used to replace CFC and HCFC refrigerants also have

relatively large GWPs. Thus the world community came together and adopted the Kyoto Protocol (1997).

The Kyoto Protocol has Articles on policies and measures, on the considerations of reductions together with sources (sinks), on emissions trading, on a certain non-compliance regime, and on a financial mechanism for developing countries (the so-called "Clean Development Mechanism"). While the emphasis of the Montreal Protocol was on the use of chemicals, the Kyoto Protocol addresses emissions of greenhouse gases. HFC refrigerants are one of the six regulated families of gases, the others being carbon dioxide (CO₂), nitrous oxide (N₂O), methane (CH₄), perfluorocarbons (PFCs), and sulfur hexafluoride (SF₆).

1.3 Alternative Refrigerants for CFCs and HCFCs

The refrigeration history and refrigerant progression is discussed in Appendix G. Calm and Domanski (2004) discussed the status of replacing R-22 with promising alternative refrigerants. The authors cited leading replacements for different refrigeration applications. The authors point out that the comparative efficiencies of alternative refrigerants to CFCs and HCFCs depend primarily on five factors: thermodynamic properties; transport properties; application; safety considerations; and materials compatibility. They emphasized the fact that R-22 phaseout will be manageable and at the same time spur significant technological advances.

Table 1-1 shows examples of some commonly used refrigerants and their relative ODP and GWP (Note: R-11 is defined to have an ODP of 1.0). Both, the ODP and GWP

are calculated from the atmospheric lifetime, measured chemical properties, and other atmospheric data (Calm and Domanski, 2004). ODP and GWP, in addition to criteria such as performance, safety, chemical and thermal stability must be accounted for when selecting a refrigerant. The data shown in Table 1-1 are the modeled values adopted by international scientific assessments. The ODP shown for blends are mass weighted averages.

Table 1-1: ODP and GWP of R-22 and Alternative Refrigerants
(Calm and Domanski, 2004)

Refrigerant	AL* (yr)	ODP	GWP (100 yr)	Refrigerant	AL* (yr)	ODP	GWP (100 yr)
R-22	12.0	0.034	1780	R-32	4.9	~0.0	543
R-123	1.3	0.012	76	R-32/R-600a (95/5)	a	~0.0	520
R-134a	14.0	~0.0	1320	R-32/R-600a (90/10)	a	~0.0	490
R-407C	a	~0.0	1700	R-290	b	0.0	~ 20
R-407E	a	~0.0	1400	R-717	b	0.0	< 1
R410A	a	~0.0	2000	R-744	> 50	0.0	= 1

* AL = Atmospheric Lifetime

a Atmospheric lifetimes are not given for blends since the components separate in the atmosphere

b Unknown

As per the guidelines of the Montreal Protocol and the Kyoto Protocol, the HVAC&R industry is earnestly seeking alternative refrigerants to halocarbons. In an attempt to screen alternative refrigerants, the Alternative Refrigerants Evaluation Program (AREP) was established (ARI, 1997). The program sought refrigerants that were nonflammable, nontoxic, stable inside the system, and unstable in the atmosphere with harmless decomposition products and had good thermodynamic properties. Practical

considerations called for low cost and full compatibility with system materials including lubricants and machining fluids. The environmental criteria included the impact of the refrigerant on stratospheric ozone layer and climate change.

After assessing several refrigerants, 14 candidates were selected as potential replacements for R-22. They were R-134a; R-32/R-125 (60/40); R-32/R-134a (20/280), (25/75), (30/70), and (40/60); R-32/R-227ea (35/65); R-125/R-143a (45/55); R-32/R-125/R-134a (10/70/20), (24/16/60), and (30/10/60); and R-32/R-125/HC-290/R-134a (20/55/5/20); HC-290; and R-717 (Ammonia). (Note: the numbers in parentheses represent the mass percentages of the refrigerants contained in the blends.) Based on the findings, most small compressor and unitary equipment manufacturers converged on R-32/R-125 blends, later reformulated to R-32/R-125 (50/50), also known as R-410A, to maximize performance, while avoiding flammability.

Because this dissertation studies the evaporative characteristics of R-410A and R-410A/lubricant mixture in a micro-fin tube, the following sections in this chapter focuses on: (a) discussing the criterion for choosing R-410A for this study; (b) giving background of boiling in general and flow boiling in particular; (c) discussing the significance of micro-fin tubes; and (d) giving a preview of how lubricant can affect the heat transfer coefficient of R-410A.

1.4 Refrigerant R-410A

R-410A is a non-flammable and non-toxic binary blend of hydrofluorocarbon compounds, comprising by mass 50 % of R-32 and 50 % of R-125. Of the two

components, R-32 offers better thermodynamic performance than R-125 for the conditions of interest, while R-125 offsets R-32's limited flammability. R-410A does not contain any chlorine. It has zero ODP and a GWP of 1890. The molecular mass of R-410A is 72.6 kg/kmol and its normal boiling point temperature is -48.5°C . This near-azeotropic mixture has 50-60 % higher operating pressures than R-22, which provides for energy efficient systems with greater refrigerant mass flow rates, leading to reductions in equipment size and improved system capacity. While R-410A has a temperature glide of only approximately 0.1 K, transfers should always be made from the liquid phase.

1.4.1 Thermodynamic and Transport Properties

Table 1-2 summarizes some of the thermodynamic properties of R-410A and other common refrigerants at an evaporation temperature of -15°C , which is representative of the operating temperature for common evaporators for typical applications.

Although operating pressures of R-410A are significantly higher than those of R-22, R-410A has the advantage of a lower drop of saturation temperature for an equal pressure drop in the heat exchangers (Domanski, 1999). Also, compressors with R-410A have a higher efficiency due to lower pressure ratio compared with R-22. The balance of property impacts provides the opportunity to produce R-410A air-to-air systems equivalent in COP to systems operating with R-22 (Hughes, 1997). At a given temperature, the molar vapor heat capacity of R-410A is higher than that of R-22. This is advantageous for R-410A because the refrigeration cycle avoids wet compression and may also provide a better COP than R-22 (Domanski, 1999).

Table 1-2: Comparison of R-410A with R-22 and its Replacements using Refprop (Lemmon et al., 2010)

Properties/ Refrigerant	R-22	R-134a	R-290	R-744	R-717	R-410A
Molecular weight	86.468	102.03	44.096	44.01	17.03	72.585
Saturated pressure, kPa	296.2	163.94	291.6	2290.8	236.17	481.65
Liquid specific heat, kJ/kg-K	1.1328	1.304	2.391	2.2283	4.5385	1.4552
Vapor specific heat, kJ/kg-K	0.6816	0.8345	1.6165	1.3877	2.4807	1.0173
Vapor ratio of specific heats	1.26	1.16	1.19	1.76	1.36	1.3134
Liquid density, kg/m ³	1330.8	1342.8	548.19	1008	658.65	1227.1
Vapor density, kg/m ³	12.901	8.287	6.5012	60.728	1.9659	18.446
Heat of vaporization, kJ/kg	216.47	209.49	394.65	270.93	1313.2	230
Liquid thermal conductivity, W/m-K	0.101	0.0987	0.1138	0.1285	0.6059	0.1118
Vapor thermal conductivity, W/m-K	0.0084	0.0102	0.0141	0.0159	0.0221	0.0108
Liquid viscosity, μ Pa-s	254.89	324.56	146.76	128.29	201.73	194.24
Vapor viscosity, μ Pa-s	10.741	10.181	7.022	13.474	8.599	11.549

* Properties are calculated at saturation temperature of -15°C

In addition, R-410A exhibits excellent heat transfer performance because of its lower viscosity and higher thermal conductivity. R-410A has a higher volumetric cooling capacity compared to R-22 and has better heat transfer properties, which results in overall performance gains in terms of system efficiency.

As seen in Table 1-2, the transport properties of R-410A are favorable compared to R-22, which results in lower pressure drop (reduced viscous losses) in the system and within the compressor itself, and also yields improved heat transfer characteristics in the

evaporator and condenser. This leads to improved energy efficiency for R-410A systems over R-22 systems for typical conditions for air conditioning. The greater density of the vapor in R-410A permits higher system velocities, reduces pressure drop losses and allows smaller diameter tubing to be used. In other words, a smaller unit can be developed using a smaller displacement compressor, less coil volume and less refrigerant while maintaining system efficiencies comparable to state-of-the-art R-22 equipment. All the above listed attributes have important impacts on cycle performance and system design.

1.4.2 Safety Considerations

Refrigerant safety classification is based on toxicity and flammability. R-410A is given a safety classification A1 by ASHRAE Standard 34 (ASHRAE, 2010), which means it is nonflammable at atmospheric pressure and is non toxic. The toxicity and flammability classifications for refrigerants are described in Fig. 1-1. The blends, such as R-410A and R-407C are assigned classification based on the worst case of fractionation. The classification consists of two alphanumeric characters (e.g., A1 or B2), where the capital letter indicates the toxicity and the arabic numeral denotes the flammability.

The toxicity is based on two classes – A or B – based on either permissible exposure level (PEL) or occupational exposure limit (OEL). Refrigerants are assigned to one of the three classes of flammability (1, 2 or 3) and one optional subclass (2L) based on lower flammability limit testing, heat of combustion, and the optional burning velocity measurement. A refrigerant with classification A1 is low in toxicity and flammability, whereas, any refrigerant with classification B3 is highly toxic and highly flammable.

		SAFETY GROUP		
F L A M M A B I L I T Y	↑	Higher Flammability	A3	B3
		Lower Flammability	A2 A2L*	B2 B2L*
		No Flame Propagation	A1	B1
			Lower Toxicity	Higher Toxicity
				→ INCREASING TOXICITY

* A2L and B2L are lower flammability refrigerants with a maximum burning velocity of ≤ 10 cm/s (3.9 in./s).

Figure 1-1: Refrigerant Safety Group Classification (ASHRAE, 2010)

As per ASHRAE Standard 34 (ASHRAE, 2010), the safety data for R-22 and selected alternative refrigerants, including OEL, refrigerant concentration limit (RCL) and the safety group classification are presented in Table 1-3. The calculation of RCL for R-410A is shown in Appendix F. (Note: OEL is the time-weighted average concentration for a normal eight-hour workday and a 40-hour workweek to which nearly all workers can be repeatedly exposed without adverse effect; and RCL is the refrigerant concentration limit, in air, determined in accordance with this standard and intended to reduce the risks of acute toxicity, asphyxiation, and flammability hazards in normally occupied, enclosed spaces.)

Table 1-3: Safety Data for R-22 and Alternative Refrigerants
(ASHRAE Standard 34, 2010)

Refrigerant	Chemical Formula ^a	OEL ^g , (ppm v/v)	Safety Group	RCL ^{a, c}		
				(ppm v/v)	(g/m ³)	(lb/Mcf)
R-22	CHClF ₂	1000	A1	59,000	210	13
R-134a	CH ₂ FCF ₃	1000	A1	50,000	210	13
R-290	CH ₃ CH ₂ CH ₃	1000	A3	5300	9.5	0.56
R-407C ^h	-	1000	A1	76,000	270	17
R-410A ^j	-	1000	A1	130,000	390	25
R-717	NH ₃	25	B2	320	0.22	0.014
R-744	CO ₂	5000	A1	40,000	72	4.5

^a Data taken from Calm (2001); Calm (1996); Wilson and Richard (2002); Coombs (2004); Coombs (2005); and other toxicity studies

^c The exact composition of this azeotrope is in question, and additional experimental studies are needed.

^g *Highly toxic, toxic, or neither*, where *highly toxic* and *toxic* are as defined in the *International Fire Code, Uniform Fire Code*, and OSHA regulations, and *neither* identifies those refrigerants having lesser toxicity than either of those groups.

^h At locations with altitudes higher than 1500 m, the ODL and RCL shall be 69, 100 ppm.

^j At locations with altitudes higher than 1000 m but below or equal to 1500 m, the ODL and RCL shall be 112,000 ppm, and at altitudes higher than 1500 m, the ODL and RCL shall be 69,100 ppm.

Although flammability is a major concern for hydrocarbons (Safety Group A3), some national safety codes permit the use of flammable refrigerants. The minimization of risks associated with the use of flammable refrigerants can be accomplished either by means of adding safety features to the system or by mixing the flammable refrigerant with other non-flammable refrigerants to obtain a non-flammable mixture (Treadwell, 1994).

1.4.3 Materials Compatibility

R-410A is highly stable in the presence of metals. Laboratory tests have shown that it is compatible with steel, copper, aluminum and brass (SES Technical Bulletin, 2004). Another significant issue is an appropriate choice of lubricant.

1.4.4 Components for R-410A systems

Compressor: Characteristics of R-410A permit using a smaller displacement compressor than ones used in R-22 systems. Additionally, compressors used in R-410A air conditioners use thicker metals to withstand the higher operating pressures. Therefore, only a compressor designed for R-410A should be used with R-410A.

Lubricants for compressor: Good solubility of a lubricant in the refrigerant is desirable. R-410A uses Polyol Ester oils (POE), which are hygroscopic in nature, can be irritating to the skin and can improve heat transfer in the compressor. R-410A and POE when used in an air-conditioning unit mix and circulate more efficiently to keep the moving parts in the compressor lubricated, reducing wear and extending their life.

Heat Exchangers: Heat exchanger coils (evaporator or condenser) designed for R-410A will, due to the properties of R-410A, utilize smaller diameter tubing than ones for equivalent R-22 systems. In practice it is possible to reduce the number of circuits in a heat exchanger for a given load when using R-410A. This may yield an additional benefit of lower air side pressure drop; however, the heat transfer properties and pressure drop characteristics of R-410A in heat exchangers needs more investigation. The efficiencies and weights of heat exchangers for R-410A systems can be designed to be comparable to those used with conventional refrigerants. New microchannel heat exchangers show favorable energetic performance and also have the advantage of lower weight and size. There is a need to address dryout problems during boiling heat transfer processes in the evaporator.

Filter/Drier: The proper selection of a filter/drier is important to the overall reliability of the systems and must be appropriately rated for the higher working pressures.

1.4.5 Applications of R-410A

R-410A is the leading HFC refrigerant for replacing R-22 in positive displacement residential air conditioning and heat pump systems. R-410A is widely used in residential and light commercial unitary air conditioning systems. Most manufacturers are now producing, or soon will be, air conditioning units using R-410A. R-410A also is the leading replacement for redesigned window air conditioners, packaged terminal air conditioners, ground- and water-source heat pumps, and small chillers (Calm and Domanski, 2004). Presently, there are several applications for R-410A, with more expected in the near future, R-410A solutions should be superior to present solutions, with respect to environment impact and also with respect to energy efficiency.

1.4.6 Disadvantages of R-410A

A significant, or even complete, redesign of an R-22 system is required if R-410A is used. The high operating pressures can also restrict the use of R-410A to smaller systems, especially for water cooled systems.

The critical pressure for R-410A is 4.902 MPa and the critical temperature is 71.35°C (160.43°F). R-410A has a lower critical temperature than R-22. As a result, the throttling irreversibilities are greater for R-410A than for R-22, which causes a reduction in the refrigeration effect (Calm and Domanski, 2004). R-410A compressors have a rapid

decrease in performance as the condenser temperature approaches 65.5°C (150°F) and above (Payne and Domanski, 2002). The critical temperature of R-410A is also lower than other R-22 alternatives such as R-407C, which has a critical temperature of 86.1°C (187°F).

1.5 Difference between Mixtures and Pure Fluids

In this section a review is presented of the additional characteristics which must be considered when a fluid is a near-azeotropic mixture, like R-410A. The review is not intended to be comprehensive, but stresses the most important features of near-azeotropic mixtures as applied to flow boiling. Figure 1-2 displays a temperature-composition phase diagram for a near-azeotropic binary mixture in general showing equilibrium conditions at start of vaporization and after 25 % buildup. Examination of the figure reveals immediately the two most important mixture features:

- The evaporation process is non-isothermal.
- As the fluid begins to evaporate, vapor is formed preferentially of one component (the more volatile or “light” component).

The non-isothermal nature of the mixture is advantageous in terms of use in a counter-flow heat exchanger (a higher effectiveness is possible since a constant temperature difference can be maintained throughout the exchanger). On the other hand, the non-isothermal nature also causes a portion of heat input to a flowing mixture to be used for vapor generation; the remainder is required to heat sensibly the liquid and vapor streams.

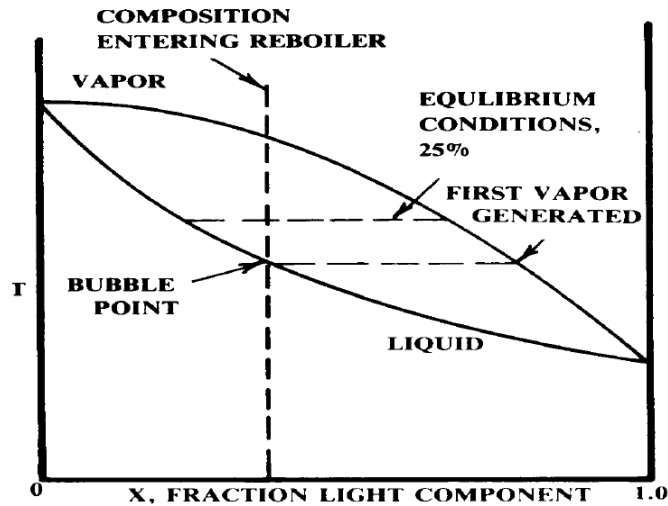


Figure 1-2: T-x Diagram for Vaporization of Near-azeotropic Binary Mixture
(taken from Wolverine Tube Inc., 2004)

For a flowing evaporating liquid, for vapor generation to occur, the vapor already formed must be further heated, and the liquid heated as well to remain in near-equilibrium at their interface (where the evaporation is taking place). In the case of mixtures, the sensible heating may represent more than 20 % of the overall heating required (Ross, 1986).

The composition difference between vapor and liquid reveals that physical properties, both thermodynamic and transport, vary substantially throughout the evaporation process even in the absence of pressure drop. For example, with pure fluids, one tends to think of liquid density as constant under conditions when the fluid begins to evaporate. With mixtures however, with one component stripped preferentially away from the liquid layer during evaporation, the liquid density may vary by 50 % or more, even without pressure drop from inlet to outlet of an evaporator tube (Ross, 1986). Other

thermodynamic properties such as latent heat of vaporization also possess this complicating feature. Thus thermodynamic properties must be reevaluated continuously during the evaporation process.

A great difficulty appears with mixtures in that the addition of a second component into a pure fluid may have spectacular effects on surface tension or viscosity. Surface tension directly affects the nature of nucleate boiling, yet may be impossible to even estimate since general mixing rules are unavailable.

In addition to the property complications, the vapor-liquid composition difference introduces mass transfer resistance. The interfacial composition is different from the bulk liquid and vapor streams. The addition of mass transfer resistance suggests that mass diffusivities should be known; yet these are rarely known for refrigerants. In turbulent flow one needs to estimate the eddy (mass) diffusivity, a process which itself is uncertain, and made even more complicated in the presence of nucleate boiling.

1.6 General Description of Boiling

When evaporation occurs at a solid-liquid interface, it is termed as boiling (Incropera and DeWitt, 1996). The process occurs when the difference, between the temperature of the surface and the saturation temperature corresponding to the liquid pressure, is positive. Appendix A describes the fundamental aspects of the process of boiling describes the various types of boiling: pool boiling, nucleate boiling, convective boiling and film boiling. It also illustrates the different regimes of boiling. These regimes help in understanding the type of boiling occurring at various locations in a heat

exchanger. Also described is the horizontal convective boiling heat transfer to illustrate the various flow patterns at different thermodynamic qualities along the length of a tube in which boiling is occurring. The phenomenon of suppression of nucleate boiling is explained in Appendix A as well.

1.7 Heat Transfer Augmentation

The objective of a heat exchanger is to transfer thermal energy from one fluid to another, with a major design criterion being to maximize the heat transfer rate. In many heat exchanger designs, the main resistance to heat transfer is the low convective heat transfer coefficient of the fluid, often resulting from limiting the maximum fluid velocity over the surface. One way to address this shortcoming is to increase the surface area available for heat transfer, which, among other ways, can be achieved by providing projections (fins) on the parent surfaces. The thermal conductivity of the fin material is an important parameter in determining the degree to which heat transfer is enhanced (Incropera and DeWitt, 1996). Ideally, the fin material should have a large thermal conductivity to minimize temperature variations from its base to its tip. Enhancement techniques can also reduce the size of the heat exchanger and reduce the approach temperature difference. With increasing emphasis on energy conservation and the high costs of heat exchanger materials, enhancement techniques have become increasingly more important in recent years.

As applied to refrigeration and air-conditioning systems, several different techniques to augment two-phase heat transfer have been reported in order to reduce the

size and cost of heat exchangers, and to improve their effectiveness. One of the most promising and widely used techniques for evaporators and condensers is to use internally finned tubes. The surfaces are available in a variety of materials and the surfaces are joined by soldering, brazing or welding, and most often formed by extrusion. The selection of a specific fin configuration is usually a compromise between increasing the heat transfer, which is desirable, and increasing the pressure drop (pumping power). There are slight variations in size, thickness or configuration of these surfaces among all manufacturers such that exact duplication is unusual, and, hence, rating or specifying such surfaces is most often done on an individual basis by manufacturers.

There are various types of internally finned tubes and other enhanced surfaces that are used in the HVAC&R industry. Some of the most popular ones are “spiral grooved,” “inner-grooved,” “ripped-fin,” “multi-groove,” “helical-fin,” “micro-fin”, and “twisted-tape inserts”. The common feature among them are their excellent thermal-hydraulic performances; however, the micro-fin tube geometry is superior to the others because the fins are smaller (typical heights of less than 0.18 mm) and more numerous (typically greater than 60 fins).

Since annular flow occurs over a significant portion of the tube length in evaporators and condensers used in the HVAC&R industry, the liquid annular film attached to the tube wall becomes the major thermal resistance affecting heat transfer (Rohsenow et al., 1985). Therefore, heat transfer in micro-fin tubes is increased not only because of large surface area but also because the liquid film is disturbed.

1.7.1 Micro-fin Tube

For approximately the first 50 years, heat exchangers used in automotive and residential air conditioners were constructed using smooth tubes. Then by the beginning of the 21st century, due in part to government efficiency requirements and in part to competition, approximately 50 % of new evaporators and condensers in the residential air conditioning industry employed enhanced micro-fin tubes rather than smooth tubes. The micro-fin tube dominates unitary equipment design because it provides high heat transfer rate enhancements while maintaining modest pressure drop penalties among all commercially available internal enhancements (Webb, 1994).

Within a thermally effective annular flow regime, the entire internal micro-fin tube wall perimeter is wetted and active rather than only the lower wetted fraction in plain tubes. This represents the principal reason for their very large augmentation ratios at low mass velocities. Higher heat transfer coefficients in micro-fin tube are partly due to (a) the mere increase in the effective exchange area; (b) the turbulence induced in the liquid film by the micro-fins; (c) the surface tension effect on the liquid drainage and wall wetting and (d) the favorable nucleation sites formed between the fins (Cavallini et al., 1999).

1.8 Lubricant Effects

Nearly all vapor-compression refrigeration systems require a lubricant to be charged into the system along with the refrigerant. Although the lubricant is only necessary for the operation of the compressor, it is an unavoidable consequence that the lubricant will also circulate through the heat exchangers along with the refrigerant.

Consequently, the effect of the lubricant on the relevant heat transfer mechanisms must be considered.

It is well known that the solubility of refrigerant in lubricant, or of lubricant in refrigerant, can have strong effects on the performance of the evaporator or condenser. According to Lottin et al. (2003), the presence of lubricant is linked to three distinct, but simultaneous phenomena:

- A change in the resistance to thermal transfer in the liquid phase: it is difficult to predict whether the heat transfer coefficient will increase or decrease, but it has been observed that in some cases, a slight amount of lubricant could improve the thermal transfer resistance while high quantities of lubricant seem to always reduce the heat transfer coefficient (Thome, 1995).
- A modification of the thermodynamic equilibrium between the vapor and liquid phases of the refrigerant–lubricant mixture.
- An increase in the pressure drop, the viscosity of lubricant being higher than that of the liquid refrigerant.

Historically, lubricant was treated as a contaminant and the pure refrigerant saturation temperature was typically used to reduce the data for calculation of the heat transfer coefficient. However, as pointed out by Thome (1995), this simple approach is not correct. It ignores the fact that the lubricant-refrigerant combination behaves as a zeotropic mixture whose properties are dependent on the equilibrium compositions of the coexisting

phases. Additionally, it precludes the type of lubricant and its properties from being introduced into the calculations.

The dissertation uses the approach by Thome (1995) and also uses the properties of refrigerant-lubricant mixture to calculate the heat transfer coefficient. A detailed discussion is presented in later part of this dissertation.

1.9 Text Organization

In Chapter 2, a literature review of studies conducted on flow boiling heat transfer is given with particular attention to parameters, such as tube geometry, lubricant concentration, thermodynamic quality, etc. In Chapter 3, the experimental rig used in the heat transfer coefficient investigation is described. The uncertainties associated with basic measurements of pressure, temperature and mass flow rate is presented. Also presented are uncertainties of mass flux of refrigerant, heat flux of refrigerant, two-phase Reynolds number, Nusselt number and thermodynamic quality. The general results of various experimental tests are further discussed in Chapter 4. The effect of quality on the heat transfer coefficient of R-410A and R-410A/POE mixture is discussed. The influence of lubricant on the flow boiling of R-410A is investigated and the results are presented. Chapter 5 reviews the available relevant models and correlations for predicting heat transfer coefficients with R-410A and R-410A-lubricant mixtures in a micro-fin tube. These available methods proposed for estimating heat transfer coefficients are reviewed critically and compared to the experimental data. In particular, the Ding et al. (2008) correlation is reviewed and analyzed, as it is the only available study with influence of

lubricant on heat transfer characteristics of R-410A in a micro-fin tube. None of the methods produced agreement with the data. The modeling and correlation for flow boiling of R-410A/POE in a micro-fin tube using fluid-heating technique is the subject of Chapter 6. Conclusions and future work are discussed in Chapters 7 and 8, respectively.

Chapter 2

LITERATURE REVIEW

The studies in the past have attempted to provide a source of heat transfer information for boiling of refrigerants, refrigerant-mixtures and refrigerant-lubricant mixtures. The need to study the contribution of pool boiling, nucleate boiling and convective boiling to understand the fundamental heat transfer mechanisms and refrigerant/lubricant interaction has been the driving force for research in HVAC&R industry.

Several questions have motivated researchers to examine flow boiling of refrigerants. A few of them are:

- What are advantages and disadvantages of heat transfer augmentation using internally or externally enhanced tubes as compared to smooth tubes?
- Is it critical to know if nucleate boiling is suppressed?
- Are there any unique mechanisms which occur with near-azeotropic mixtures?
- Is it possible for refrigerants with their relatively low thermal conductivity, to be vaporized by an entirely evaporative mechanism in annular flow?
- Can the correlations of annular film condensation be applied to evaporative case, in the absence of nucleate boiling?
- How does refrigerant/lubricant interaction fundamentally affect the heat transfer mechanism inside an evaporator as compared to the effect of pure refrigerant flowing in the evaporator?

In an effort to understand these problems, the past literature has resolved to the following techniques of either visual evidence or experimental evidence: (a) two-phase fluid-flow patterns, vapor generation without bubble presence, or bubble presence with thin films, lubricant excess layer, etc.); (b) dependence of the heat transfer coefficient on heat fluxes and mass fluxes; (c) effect of pressure and pressure drop on heat transfer coefficient; (d) dependence of heat transfer coefficient on thermodynamic quality; (e) predictive ability of evaporative or pool boiling models to flow boiling data; (f) enhancement in heat transfer due to different tube geometry; (g) types of lubricant and effect of thermophysical and transport properties of refrigerant-lubricant mixtures on heat transfer coefficient; and (h) presence of hysteresis.

The following discussion critically analyzes the literature for pure refrigerants, refrigerant mixtures and refrigerant-lubricant mixtures. The type of test rigs typically used for research on flow boiling is presented. Studies on both visual and experimental evidences are cited. The literature review is later categorized into four different subsections.

2.1 Test Rigs for Boiling Heat Transfer

This section reviews the types of experimental test rigs which have appeared in the literature. Most experimental rigs described in the literature have been designed to be consisting of either a compressor or a pump to circulate the working fluid, an evaporator or a test section, and a condenser for bringing back the working fluid to a subcooled state, as

shown in Fig. 2-1. Preheaters and afterheaters and sometimes pressurizers were employed to control entering or exiting conditions.

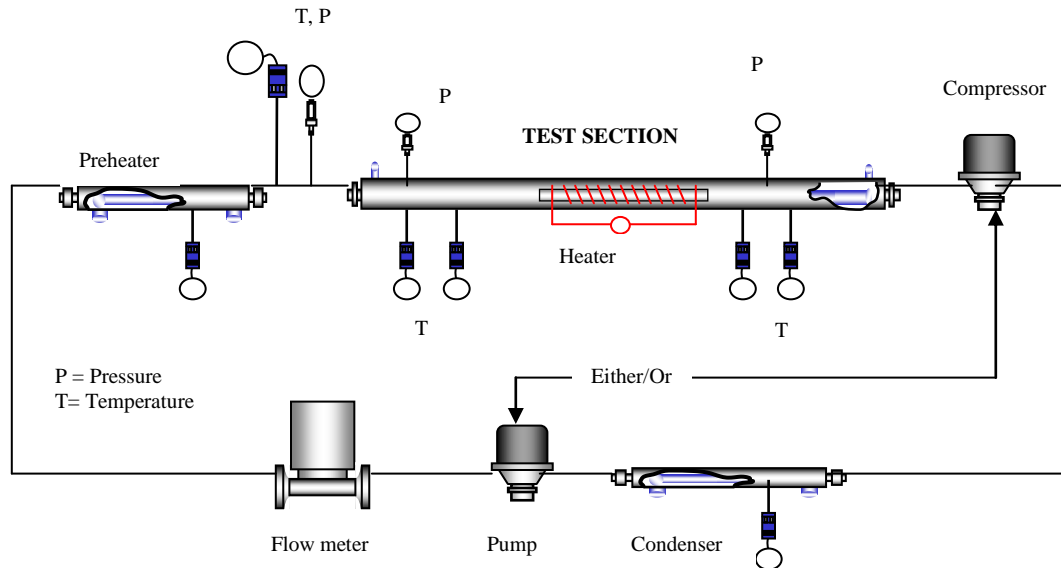


Fig. 2-1: Typical Test Rig in Literature

Pressure taps were installed along the test section, and these pressure readings were used to determine the local saturation temperature of the moving fluid. Wall temperatures were determined by a series of thermocouples attached to the tube wall by solder (Altman, et al., 1959, Sami et al., 1993, Kim et al., 2010), spot weld (Mishra et al., 1981, Singal et al., 1983, Lim and Kim, 2004), braze (Sa61) or mechanical clip (Dickson and Gouse, 1967, Radermacher et al., 1983). The test section itself was electrically heated (Staub and Zuber, 1966, Mishra et al., 1981, Kim et al., 2002, Ding. et al., 2008) or heated isothermally by fast flowing water (Altman et al., 1959, Kedzierski and Kaul, 1993, Zurcher et al., 1998) or

by a condensing fluid surrounding the tube (Baker et al., 1953). In any case, the heat flux was considered well-known and the local or average heat transfer coefficient was then appropriately determined by Newton's law of cooling.

The test section in some investigations was made of glass so that visual observation of flow patterns could be made (Staub and Zuber, 1966, Dickson and Gouse, 1967). However, the use of glass had a serious deficiency, forcing its eventual abandonment. A plating process was used to provide a continuous metal film on the inside of the glass test section. The metal film served as an excellent electrical resistance heater, however nonuniformities in its surface caused the surface roughness to cavitate and swirl the flow and augment the heat transfer. The variable surface thickness also caused nonuniform heat generation. Most studies instead used thin wall metal tubes in which the temperature drop through the wall is quite small. 'Flow visualization' with metal tubes can be attempted through deduction, either from void fraction measurements, or from the appearance of large differences between top and bottom wall temperature measurements indicating stratified flow (Chen, 1966).

2.2 Summary of Visual Evidence

Several visual evidence studies of flow boiling of pure fluids have been done to determine flow pattern and bubble existence. In the 1960s and 1970s, most of the studies were conducted with water, and some with refrigerants (Hewitt et al., 1963, Ti62, Mesler (1976), and Tippets (1962)). These studies employed transparent metal coating, heater strips on one side, or glass tubes. Often the surfaces had been milled smooth to ensure

uniform heat generation; however, this process removes potential nucleation sites, preventing generalization of results. Nearly all visualization studies show some isolated bubbles within the liquid film and the number of sited bubbles diminishes with increasing quality.

The study by Hewitt et al. (1984) showed activation of a site whenever heat transfer through the film was inhibited by wave passage, suggesting film thickness was an important though not solely definitive criterion. The authors also observed that vapor velocity had a strong influence on the observation of nucleation. The heat transfer characteristics of horizontal nucleate flow boiling of R-12, R-134a, and R-134a/ester lubricant mixture were investigated both visually and calorimetrically by Kedzierski and Kaul (1993) in a roughened quartz tube test section. The high speed motion picture images of the boiling process were obtained. The rate of bubble production of R-134a was observed to be 38 % greater than that of R-12. The addition of lubricant to R-134a caused a significant reduction in the diameter of the bubbles. A more phenomenological approach incorporating the local two-phase flow structure as a function of the local flow pattern was proposed by Kattan et al. (1998a). The authors suggested use of a new flow pattern map for small diameter tubes typical of heat exchangers for predicting local flow boiling coefficients based on local flow pattern. The study included a method for predicting the onset of dryout at the top of the tube in evaporating annular flows.

2.3 Classification of Literature Review – Experimental Evidence

This section will attempt to concentrate primarily on flow boiling related studies with micro-fin tube geometry and lubrication effects. The literature review also serves as an interaction to the data base developed for this dissertation. To understand the experimental evidence of the approach adopted by several researchers, the following literature review is organized into four sections: (1) Enhancement, (2) Comparison with Correlations/Models, (3) Geometric effects, and (4) Lubricant effects.

2.3.1 Enhancement

Singh et al. (1996) presented results of an experimental study for forced convection evaporative heat transfer coefficients of R-134a inside a horizontal micro-fin tube. The heat transfer coefficients were reported as a function of mass flux, quality, and heat flux. The test section was a micro-fin copper tube with a 12.7 mm OD, 60 fins, and 18⁰ helix angle. The nominal inside diameter of the tube was 11.78 mm with ridge height of 0.3 mm. Experiments were conducted at 575 kPa, corresponding to a saturation temperature of 20.15 °C. For a mass flux of 50 kg/m²s, as the heat flux increased, the heat transfer coefficient increased due to increased nucleate boiling associated with the higher heat flux. For a fixed thermodynamic quality of 0.3, with an increase in the mass flux in the range of 50 kg/m²s to 150 kg/m²s, the heat transfer coefficient increased for the heat flux range (10 kW/m², 20 kW/m², and 30 kW/m²). It was also observed that for a given mass flux, a higher heat flux resulted in a higher heat transfer coefficient. For a mass flux of 100 kg/m²s, the heat transfer coefficient showed marked increase, which indicated the

influence of stratification at low flow rates in horizontal tubes. For low mass fluxes ($< 100 \text{ kg/m}^2\text{s}$) the flow was predominantly stratified, but as mass flux increased, the flow transitioned to the annular regime.

The micro-fin tube reported by Schlager et al. (1989d) was compared to a low-fin tube (21 fins per tube, 30° spiral angle, 0.38 mm fin height, and a 1.8 area ratio) in Schlager et al. (1989e). For evaporation of pure refrigerant, the heat transfer enhancement factor was similar for both tubes, varying from 1.8 to 2.3. However, the pressure drop penalty factors were about 10 % to 30 % smaller for the micro-fin tube (this was also the case for condensation). The higher pressure drops in the low-fin tube could have been caused by the larger spiral angle, the larger area ratio, or a combination of both. For condensation, the enhancement factor for the micro-fin tube was 2.3 compared to 1.9 for the low-fin tube. Of special note, the addition of lubricant degraded the performance of the low-fin tube significantly more so than that of the micro-fin tube for evaporation.

Manwell and Bergles (1990) provide insight into how micro-fin tubes improve heat transfer. Specifically, the authors investigated flow patterns in micro-fin tubes by using still photography to record typical flow patterns. By comparing flow-pattern maps for a smooth tube with photographs of a micro-fin tube, they concluded that the presence of a spiral flow reduces the stratified flow region. In other words, at low flow rates, where stratified flow might otherwise occur, the spiraled fins caused the upper surface to be wetted, thus producing a thin liquid film on the grooved wall. Since the upper wall is normally dry in a smooth tube during stratified flow, the presence of the liquid film enhances heat transfer.

Khanpara et al. (1987) used the Dittus-Boelter/McAdams correlation to analyze their single-phase data for a micro-fin tube for R-113 and R-22. In the region of established turbulent flow ($Re > 10,000$), the micro-fin heat transfer coefficients are 50 to 150 % higher than those of the smooth tube, which corresponds to enhancement factors of 1.5 to 2.5. The enhancement factors for both refrigerants decreased as the mass velocity increased. Specifically, as the mass velocity approximately doubled, the enhancement factor decreased from 2.2 to 1.3 for R-113 and from 2.0 to 1.2 for R-22.

Tables 2-1 and 2-2, taken from Eckels and Pate (1994), show the enhancement factors (EF) and penalty factors (PF) for heat transfer and pressure drop, respectively, at similar mass fluxes and similar cooling (heating) capacities for determining the relative performance of micro-fin tubes operating with R-134a and R-12.

Table 2-1 Comparison of Heat Transfer Enhancement Factors (EF) for R-134a and R-12 (Eckels and Pate, 1994)

		Enhancement Factor (Heat Transfer)			
		Similar Mass Flux Comparison		Similar Cooling (Heating) Capacity Comparison	
		R-134a	R-12	R-134a	R-12
Evaporation $T = 10\text{ }^{\circ}\text{C}$	Low mass flux $150\text{ kg/m}^2\text{s}$	2.3	2.6	2.3	2.3
	High mass flux $300\text{ kg/m}^2\text{s}$	1.7	1.9	1.7	1.8
Condensation $T = 40\text{ }^{\circ}\text{C}$	Low mass flux $150\text{ kg/m}^2\text{s}$	2.2	2.2	2.2	2.2
	High mass flux $300\text{ kg/m}^2\text{s}$	1.9	2.0	1.9	1.8

The EF for the evaporation of R-134a is slightly lower than that of R-12, being 2.3 compared to 2.6 at low mass fluxes and 1.7 compared to 1.9 at higher mass fluxes. With regards to penalty factors for pressure drop (Table 2-2) for evaporation, the micro-fin tube performs better relative to the smooth tube for R-134a, and less so with R-12. For R-134a, the PF is 1.3 compared to an R-12 value of 2.0 at the same mass flux, and 1.8 at an equivalent cooling capacity. For condensation at low mass fluxes, R-134a has higher values of PF, indicating a potential reduction in performance. At high mass fluxes during condensation and evaporation, the penalty factors are similar for both refrigerants.

Table 2-2 Comparison of Pressure Drop Penalty Factors (PF) for R-134a and R-12 (Eckels and Pate, 1994)

		Penalty Factor (Pressure Drop)			
		Similar Mass Flux Comparison		Similar Cooling (Heating) Capacity Comparison	
		R-134a	R-12	R-134a	R-12
Evaporation T = 10 °C	Low mass flux 150 kg/m ² s	1.3	2.0	1.3	1.8
	High mass flux 300 kg/m ² s	1.3	1.5	1.3	1.5
Condensation T = 40 °C	Low mass flux 150 kg/m ² s	1.8	1.3	1.8	1.4
	High mass flux 300 kg/m ² s	1.4	1.4	1.4	1.3

2.3.2 Comparison with Correlations/Models

In the past few decades, numerous correlations have been developed to study heat transfer related to different alternative refrigerants and refrigerant-mixtures. Given the large quantity of papers in the literature, only studies related to the area of the current research are presented in this section. In addition, special emphasis is placed on understanding the effects of parameters such as mass velocity, quality, and heat flux on evaporation heat transfer.

In their study on evaporation heat transfer in a 7 mm micro-fin tube, Kuo et al. (1995) reported measurements of the local heat transfer coefficient and frictional pressure gradient at three different evaporation temperatures (2 °C, 6 °C, and 10 °C, respectively) and mass fluxes in the range of 100 kg/m²s to 300 kg/m²s, and heat fluxes in the range of 7 kW/m² to 12.4 kW/m². Their 1.2 m long micro-fin tube had a fin height of 0.15 mm with 60 fins, and a helix angle of 18°. For a fixed mass flux of 200 kg/m²s and a saturation temperature of 6 °C, the heat transfer coefficients increased with increasing heat flux and increasing quality. The experimental data over-predicted the correlation proposed by Kandlikar (1990). The heat transfer coefficient for evaporation is approximately proportional to $q^{0.45}$. For fixed heat flux of 7 kW/m² and a saturation temperature of 2 °C, the heat transfer coefficient increased for increasing mass flux and increasing quality. The flow quality was varied in the range of 0.1 to 0.9. For a fixed mass flux of 200 kg/m²s and a fixed heat flux of 8.4 kW/m², the heat transfer coefficient increased for increasing saturation temperatures and increasing quality. This may be due to the increase in the nucleate boiling heat transfer component. The authors also show that the pressure drop per

unit length between pressure taps increases significantly with the mass velocity and with quality. For a given quality, the pressure drop was approximately proportional to $G^{1.48}$. A correlation developed by Friedel (1979), for both horizontal flow and vertical up flow with a data bank of more than 25,000 points, was compared with the experimental data. The comparison showed their data to be 20 % to 30 % lower than the correlation proposed by Friedel.

Oh and Bergles (1998) measured the evaporation heat transfer coefficient of R-134a in a smooth tube and five micro-fin tubes (spiral angles of 6° , 12° , 18° , 25° , and 44°) of constant mean diameter of 8.71 mm and number of fins, 60. The heat transfer coefficients of the smooth tube were compared with four correlations: Shah (1982), Kandlikar (1993), Wattelet et al. (1994), and Yoshida et al. (1993). The study primarily focused on determining the optimum spiral angle, that is, where the evaporative heat transfer coefficient is maximum. For smooth tubes, all the correlations, except the Yoshida correlation, under-predicted the heat transfer coefficient. The mean deviations were 27.0 %, 20.0 %, 26.8 %, and 19.1 % for the Shah, Kandlikar, Wattelet and Yoshida correlations, respectively. In the stratified flow region (mass flux of $50 \text{ kg/m}^2\text{s}$), the heat transfer coefficient did not change greatly with quality. The Shah and Wattelet predictions worsened as the heat flux increased. The Yoshida and Kandlikar correlations contradict each other. In the annular region (mass flux of $100 \text{ kg/m}^2\text{s}$), for smooth tubes, the heat transfer coefficient increased rapidly with quality. The Shah and Kandlikar correlations failed to predict this trend. The Yoshida correlation outperformed the other correlations with a mean deviation of 8.9 % (mass flux of $200 \text{ kg/m}^2\text{s}$). The Wattelet correlation under-

predicts the trend with a mean deviation of 20.8 %. For micro-fin tubes, the quality was approximately fixed at 0.5, while the heat flux varied in the range of 5 to 20 kW/m². The spiral angle at which the maximum heat transfer coefficient occurs is mainly dependent on the mass flux, G . At $G = 50$ kg/m²s, the maximum occurred at a spiral angle of 18°, and at $G = 100$ kg/m²s, it occurred at 6°.

Khanpara et al. (1987) carried out a comparison of in-tube evaporation heat transfer in a smooth tube and a micro-fin tube, both of 9.52 mm OD. Two different test facilities, one for each type of refrigerant (R-22 and R-113), were used to obtain local evaporation heat transfer data. The main difference between the R-113 and R-22 rigs was in the pressure control. The R-113 facility utilized a surge/degassing tank open to the atmosphere, whereas pressurization by an accumulator was required in the R-22 facility. In the evaporation heat transfer analysis for the smooth tube, the heat transfer coefficients were observed to be not strongly dependent on quality, at least for the quality range considered in these experiments. The heat transfer coefficient increased with increasing mass velocity. At low mass velocity, the heat transfer coefficient is almost independent of heat flux. However, the heat transfer coefficient was more sensitive to changes in heat flux at intermediate mass velocity. According to the authors, this may have been due to the nucleate boiling regime prevailing at even higher qualities for higher mass velocity test runs. The experimental data was also compared to two correlations, namely Shah (1982) and Kandlikar (1983). The Shah correlation predicts the data for both R-22 and R-113 to within 0 to -30 % whereas the Kandlikar correlation predicts the data for both refrigerants to within ± 20 %.

Chamra et al. (2003) evaluated three different evaporative heat transfer models for micro-fin tubes. The heat transfer coefficients predicted by these three models are compared to 371 experimental data points for pure refrigerants. Tables 2-3 and 2-4 show the collected experimental data for flow inside micro-fin tubes. Table 2-3 lists the flow conditions.

Table 2-3 Flow Conditions for Pure Refrigerants Flowing Inside Micro-fin Tubes
(Chamra et. al., 2003)

Reference	Runs	Fluid	Q (kW/m ²)	G (kg/m ² /s)	x (mean)
Bogart and Thors (1994)	57	R-22	10.5-35.5	120-410	0.10–0.80
Bogart and Thors (1999)	50	R-22 R-134a	10.5-35.5	25-275	0.10–0.95
Eckels and Pate (1991)	25 23	R-134a R-12	13.6-64.3	130-400	0.05-0.88
Eckels et al. (1994)	11	R-134a	18.5-59.3	83-375	0.05-0.88
Eckels et al. (1998a)	8	R-134a	18.2-54.5	125-375	0.05-0.88
Eckels et al. (1998b)	9	R-134a	12.8-42.2	85-250	0.05-0.88
Hitachi Cable (1987)	22	R-22	10.0	100-300	0.60
Kido et al. (1995)	90/80	R-22	9.3	86-345	0.10-0.90
Kuo and Wang (1996a)	24	R-22	6.0-14.0	100-300	0.10-0.80
Kuo and Wang (1996b)	5	R-22	10.0	200	0.10-1.00
Murata and Hashizume (1993)	31	R-123	0-30.0	93-278	0.10-1.00
Muzzio et al. (1998)	26	R-22	5.4-24.1	90-400	0.35-0.75
Schlager (1998)	25	R-22	15.4-51.7	125-400	0.10-0.90
Shinohara and Tobe (1985)	9	R-22	10.0	120-300	0.60
Yasuda et al. (1990)	16	R-22	10.0	80-300	0.60

Table 2-4 delineates the tube geometries (outer tube diameter D_o , minimum wall thickness t_h , fin height e , number of fins n_f , heated test length L , and helix angle, γ). The experimental data were collected from graphs given in published papers.

Table 2-4 Tube Geometries for Pure Refrigerants Flowing Inside Micro-fin Tubes
(Chamra et. al., 2003)

Reference	D_o (mm)	t_h (mm)	e (mm)	n_f	L (mm)	γ ($^\circ$)
Bogart and Thors (1994)	9.53	0.33	0.2	60	3.66	18
	15.88	0.51	0.3	75		23
Bogart and Thors (1999)	15.88	0.51	0.3	75	4.88	23
Eckels and Pate (1991)	9.52	0.40	0.2	60	3.67	17
Eckels et al. (1994)	9.52	0.30	0.2	60	3.67	17
Eckels et al. (1998a)	9.52	0.30	0.2	60	3.66	18
Eckels et al. (1998b)	12.70	0.40	0.2	60	3.66	17
Hitachi Cable (1987)	9.50-9.52	0.28	0.2-0.21	60	0.50	17
		0.29				18
Kido et al. (1995)	7.00	0.30-0.35	0.15-0.21	60-100	0.30	3-18
Kuo and Wang (1996a)	9.52	0.30	0.2	60	1.30	18
Kuo and Wang (1996b)	9.52	0.30	0.2	60	1.30	18
Murata and Hashizume (1993)	12.70	1.00	0.3	60	0.73	30
Muzzio et al. (1998)	9.52	0.30	0.20	60	2.24	18
		0.34	0.15	65		25
Schlager (1998)	9.52	0.40	0.20	60	3.67	18
		0.50	0.38	21		30
Shinohara and Tobe (1985)	9.52	0.30	0.12-0.20	60 65	0.50	7-25
Yasuda et al. (1990)	9.52	0.30	0.20-0.25	60	3.05	18
	7.94			50		30

The three correlations studied are from Kido et al. (1995), Cavallini et al. (1999), and Murata and Hashizume (1993). The mean absolute deviation for all evaluated pure refrigerants (R-123, R-12, R-134a, and R-22) is 23.1 % for 371 data points. The Kido et al. (1995) model failed to provide accurate prediction for most of the experimental data sets. The Murata and Hashizume (1993) correlation provided good prediction for the R-22, R-12, and R-123 data sets, but predicted a higher mean absolute deviation for the R-134a data. Overall, the Cavallini et al. (1999) heat-transfer model for pure refrigerants was considered relatively successful in predicting the R-22 experimental data sets. However, the model failed to predict the R-134a experimental data. The Cavallini et al. (1999) model was concluded to be a better predictive model than the one of Kido et al. (1995), and also is applicable to a wider range of flow conditions and flow parameters.

2.3.3 Geometric Effects

Khanpara et al. (1987a) studied the evaporation of R-113 in micro-fin tubes in both electrically heated tubes (3.8 m long) and fluid-heated tubes (1.0 m long). The authors observed that for electrically heated tubes, which provided local heat transfer coefficients, the heat transfer enhancement factor for the micro-fin tube varied in the range of 1.18 to 2.72, depending on heat flux and mass flux. In contrast, the maximum increase in pressure drop was about 30 %, which corresponds to a pressure drop penalty factor of 1.3. The heat transfer coefficients for the micro-fin tube were comparable for fluid and electrical resistance heating. However, for a smooth tube tested under similar conditions, differences

of as much as 20 % to 50 %, with the electrical heating values being higher, were observed.

Reid et al. (1987) used R-113 to compare the evaporation performance of an electrically heated micro-fin tube to the performance of several other types of enhanced tubes. The heat transfer enhancement factors for the micro-fin tube varied in the range of 1.3 to 1.7, while comparable values were also observed for a low-fin tube (21 fins compared to 65 fins for the micro-fin tube). However, the difference in the performance of the two tubes was especially evident for the pressure drop penalty factors, which were twice as large for the low-fin tube: 1.3 for the micro-fin tube as compared to 2.6 for the low-fin tube.

The performance of different micro-fin tube geometries during evaporation and condensation of R-22 was evaluated in several studies by Schlager et al (1989a, b, c, d and e). For example, three different 9.5 mm OD micro-fin tubes were compared by Schlager et al. (1989a), while three different 12.7 mm OD tubes were compared by Schlager et al. (1989b). This latter study also compared the heat transfer performance of two tubes of different diameters, 9.5 mm and 12.7 mm, at similar mass fluxes. For each tube, an average heat transfer coefficient was obtained for a 90 % quality change in a 3.7 m tube. In the first study, the main difference between the three 9.5 mm tubes was that the spiral angles were varied: 15°, 18°, and 25°. The heat transfer enhancement factors varied from 1.4 to 1.9, while pressure drop penalty factors varied from 1.0 to 1.4. The performances of the three tubes were similar, falling within the band of experimental uncertainties. However, the

tube with a 25° spiral angle appeared to be slightly better for evaporation and the 18° spiral angle tube was slightly better for condensation.

The second study (Schlager et al. 1989b), for the 12.7 mm-diameter tube, produced results that were similar to those for the smaller 9.5 mm-diameter tube. In fact, a general conclusion made by Schlager et al. (1989) is that enhancement factors measured for one particular diameter might then be applied to other diameters. Another observation was that the heat transfer enhancement factors exceeded the area ratios (the ratio of the micro-fin tube's surface area to the area of a smooth tube of equivalent diameter), which varied from 1.38 to 1.55 for nearly all test conditions. Interestingly, as the mass flux was increased, the heat transfer enhancement factor values approached the area ratio. A possible explanation is that at high mass fluxes, the enhancement in heat transfer in the micro-fin tube is due to the increase in the area, with the turbulence being so high that additional disturbances caused by the fins do not significantly add to the heat transfer. In contrast, at low flow rates, the presence of the fins causes large disturbances in the flow, which, in turn, results in significant heat transfer enhancement over that caused by the area increase.

2.3.4 Lubricant Effects

A series of publications resulted from an ASHRAE-sponsored research project, RP-469, which dealt with heat transfer and pressure drop of R-22 and lubricant mixtures in both smooth and micro-fin tubes. The results of this work were reported by Schlager et al. (1989c through 1989e). The heat transfer data reported in each case were for a 9.52 mm OD tube of 3.67 m in length, with the quality varying from 15 % to 85 % from the inlet to

exit, respectively (or from 85 % to 15 % for condensation studies). The micro-fin tube had an 18° spiral angle, 60 fins, a fin height of 0.2 mm, and an area ratio of 1.5.

In Schlager et al. (1989c), the performance of the micro-fin tube was evaluated for a mixture of R-22 and naphthenic oil with a viscosity of 150 SUS. Small quantities of the lubricant, about 1.5 %, increased the evaporative heat transfer coefficient by about 11 %. This enhancement decreased as the mass flux increased and as additional lubricant was added. For example, at one mass flux, the enhancement factor varied from 2.4 for pure refrigerant to 1.9 for 5 % lubricant concentration. For condensation, lubricant addition decreased the heat transfer coefficient in the micro-fin tube by as much as 16 %. However, the heat transfer enhancement factor for condensation was not affected by the lubricant. Depending on the mass flux, the heat transfer enhancement factor varied from 1.9 to 2.4.

Schlager et al. (1989d) reported the results of a study of lubricant viscosity effects on heat transfer in a micro-fin tube. Unlike the 150 SUS lubricant reported in the previous paragraph, a higher viscosity 300 SUS naphthenic oil did not enhance heat transfer during evaporation, rather the heat transfer decreased for all lubricant concentrations, with the maximum decrease being 30 % at a 5 % lubricant concentration. For condensation, the micro-fin tube performance was similar for both lubricant viscosities.

A series of papers by Schlager et al. (1990a, b) focused on an approach for predicting the performance of micro-fin tubes when operating with refrigerant-lubricant mixtures. Because a detailed study evaluating the effects of geometrical parameters has not been performed, it was not possible to derive a general equation that can be used to design

micro-fin tubes. Instead, geometry-specific equations for heat transfer and pressure drop were developed for both pure refrigerants and refrigerant-lubricant mixtures.

Zurcher et al. (1998) reported in-tube evaporation tests for R-407C and R-407C/lubricant in a micro-fin tube. The tests were run at a nominal pressure of 645 kPa and at mass velocities of 100, 200, and 300 kg/m²s over nearly the entire vapor quality range. The test sections were commercial copper micro-fin tubes with internal diameters of 11.90 mm at the root of the micro-fin with outside diameters of 12.70 mm. The micro-fin tubes had 70 fins with a helix angle of 18⁰, a fin height of 0.25 mm, and an internal wetted area per unit length of 0.065 m²/m. Each of the two test sections were 3.013 m in length and were divided into 3 test zones. All the heat transfer test data reported were obtained using zones 5 and 6 for the following reasons: (a) inlet effects on the first refrigerant zone in the first test section; (b) influence of two 90⁰ elbows on the heat transfer coefficients measured in the fourth zone at the beginning of the test section; and (c) a drop in the hot water temperature in zones 2 and 3 in the first test section was usually too small to accurately determine the boiling coefficients. Since the modified Wilson-plot approach was applied to each zone for changes in vapor qualities of about 3-10 % in the individual test zones, the heat transfer data presented are mean values over a narrow change of vapor quality and can be considered as quasi-local values. The authors also presented thermodynamic methods for calculating temperature-enthalpy-vapor quality tables for R-407C and R-407C/lubricant mixtures that were applicable from -5 °C to +50 °C.

At the lowest mass velocity tested, Zurcher et al. (1998) showed that the micro-fin heat transfer coefficients with oil were nearly equal to those for pure R-407C over the

vapor quality range from 0.13 to 0.8. Increasing lubricant mass fraction had a detrimental effect on heat transfer. Also, at high vapor quality, $x > 0.8$, the local coefficients fell sharply with increased vapor quality. At the intermediate mass velocities tested, the micro-fin heat transfer coefficients with lubricant were nearly identical to those for pure R-407C over the vapor quality range from 0.1 to 0.7. Instead, at high vapor quality the heat transfer coefficient for a given vapor quality decreased with increasing local lubricant mass fractions up to 0.5. At the highest mass velocity tested, the micro-fin heat transfer coefficients with lubricant are approximately equal to those for pure R-407C over the vapor quality range from 0.1 to 0.45 and thereafter the scatter larger.

Similarly, Zurcher et al. (1998, Part 1 and Part 2) measured the heat transfer coefficient and two-phase pressure drop for R-407C/lubricant mixtures for plain and micro-fin tubes for the same mass flux range and nearly the entire quality range. Irrespective of its concentration, the addition of lubricant tends to decrease the local R-407C micro-fin heat transfer performance, especially at high vapor qualities where degradation as much as 50 % or more occurred. Lubricant holdup was yet again observed in micro-fin tubes together with slowly flowing viscous liquid films, especially at lower mass fluxes. For the plain tube, at vapor qualities higher than 0.7, the local boiling coefficients dramatically decreased by as much as 80-90 %, even with low traces of lubricant. For vapor velocities lower than 0.7, the lubricant had little effect on the boiling coefficients. Two-phase pressure drops increased in the presence of lubricant in plain as well as micro-fin tubes.

Hambraeus (1995) tested the evaporation heat transfer of R-134a in a horizontal evaporator using three different ester-based lubricants, varying heat flux, mass flux, and the saturation temperature. Lubricant concentration was varied in the range of 0 to 4.5 % by mass. He argued that the decrease in the heat transfer coefficient he observed was a function of the viscosity grade of the lubricant. He did observe an enhancement in heat transfer for the special case of low mass flux in combination with a low viscosity grade lubricant, where increased surface tension led to better tube wetting and thus increased heat transfer.

Eckels and Pate (1994) conducted an experimental in-tube evaporation and pressure drop study of refrigerant-lubricant mixtures (lubricant mass concentrations ranging from 0 % to 5.4 %) of R-134a and R-12 in an 8 mm ID, 3.67 m in length smooth tube. Both refrigerants, R-134a and R-12, showed improved heat transfer (5 % to 15 %) for lubricant concentrations up to 2.5 % but showed significant decrease (40 % to 50 %) the evaporative heat transfer performance at concentration of 5.3 %. The pressure drops increased as the lubricant concentration increased.

Nidegger et al. (1997) reported in-tube flow boiling experiments for refrigerant R-134a with lubricant. The tests were run at a nominal pressure of 340 kPa over a wide range of vapor qualities at mass velocities of 100, 200, and 300 kg/m²s for inlet lubricant concentrations of 0.0, 0.5, 1.0, 3.0 and 5.0 mass % lubricant. The inlet lubricant concentration in the subcooled liquid before the preheater was measured with an online measurement system that used a calibrated, vibrating tube density flowmeter. The test sections were commercial copper micro-fin tubes. They had internal diameters of 11.90

mm at the root of the micro-fins, and outside diameters of 12.70 mm. The authors used a modified Wilson plot approach for measuring the heat transfer coefficients; tube wall temperatures were not measured. The log-mean-temperature difference (LMTD) was obtained from the four terminal temperatures of the zone and the heat transfer rate was determined from the water side. The range of heat flux in the tests was 5 to 10 kW/m².

At the lowest mass velocity tested, the micro-fin heat transfer coefficients with lubricant were only about half those of pure R-134a over the vapor quality range from 0.45 to 0.80. Increasing lubricant concentration had a detrimental effect on heat transfer. At high vapor quality, $x > 0.8$, the local coefficients fell sharply with respect to vapor quality. At the intermediate mass velocities tested, the micro-fin heat transfer coefficients with lubricant were again noticeably below those for pure R-134a over the vapor quality range from 0.26 to 0.80. At $x = 0.30$ to 0.35, the 0.5 % lubricant concentration had the lowest local coefficient while the 3.0 % and 5.0 % mixtures had higher values than 0.5 % lubricant but below that of pure R-134a; instead, at $x = 0.80$ the falloff in the heat transfer coefficient was monotonic, with increasing inlet or local lubricant concentration. At the highest mass velocity tested, the micro-fin heat transfer coefficients with lubricant were about equal to or greater than those for pure R-134a over the vapor quality range from 0.18 to 0.90. At a fixed vapor quality, it was found that small concentrations of lubricant were detrimental to heat transfer while higher concentrations such as 5 % lubricant could be beneficial, depending on the vapor quality. At $x > 0.95$, the falloffs in the heat transfer coefficients for pure R-134a and 0.5 % lubricant were very steep.

The vapor quality locations of the heat transfer peaks were similar to those in pressure drop but were of different magnitudes, most likely because three heat transfer zones were used together to obtain the pressure drop. The effect of lubricant on two-phase pressure drop was found to be most evident at high vapor qualities where the local lubricant concentrations were the highest, with higher local lubricant concentrations giving higher-pressure drops. It is very likely that the peak in pressure drop with vapor quality correspond to the location where partial tube dryout begins. The pressure drops with lubricant continued to increase to high vapor qualities, suggesting that the lubricant retards tube dryout. The authors also suggested further study on mass velocity threshold below which lubricant holdup begins to be significant as it is an important design and operational limit of direct-expansion evaporators utilizing micro-fin tubes.

Ha and Bergles (1993) obtained experimental data of the local heat transfer coefficient for refrigerant R-12/lubricant mixtures for mass fluxes in the range of 25 kg/m²s to 100 kg/m²s, heat fluxes in the range of 5 kW/m² to 10 kW/m², and an evaporating pressure of 0.32 MPa for 0 % to 5 % lubricant (by mass) and pure vapor qualities in the range of 0.2 to 1.0. A 1.2 m long, horizontally oriented copper micro-fin tube with an outside diameter of 9.5 mm, having 60 fins with fin height of 0.18 mm and an 18⁰ spiral angle, was tested with indirect electrical wire heating. Circumferential and axial wall temperatures were measured, and exit flow visualization was carried out to understand the local heat transfer mechanism. The lubricant fraction was controlled manually by the needle valve in the test lubricant circulating system.

The uncertainties were reported for measurements as follows: wall superheat (± 0.1 °C); mass flux (± 1 %); heat flux (± 2 %); initial lubricant fraction (± 5 %); and average heat transfer coefficient (± 4 %). In one of the flow pattern figures for a quality of 0.5 and a mass flux of $100 \text{ kg/m}^2\text{s}$, a lubricant-rich viscous film at the top was observed for all lubricant fractions whereas, heavier and wrinkled film over the whole tube perimeter was observed for lubricant fractions of 3 % and 5 %. Foaming was suppressed, with the result that the fine grooves dampen the wavy structure of the interface in the micro-fin tube, and very thin bubbles were observed.

Bubble formation during horizontal flow boiling of R-12, R-134a and two R-134a/polyol ester mixtures were investigated both visually and calorimetrically by Kedzierski and Kaul (1993). The addition of the low viscosity lubricant to R-134a increased the sensitivity of the heat transfer coefficient to an increase in the Reynolds number at the highest heat flux. The authors used visual observations of the bubble density to explain the heat transfer trends. The addition of a high viscosity lubricant to R-134a resulted in a smaller enhancement of the heat transfer coefficient over pure R-134a. This may have resulted from the canceling effects of a drastic reduction in the diameter of the bubbles and a significant increase in the site density.

Schlager et al. (1988) studied evaporation and condensation of refrigerant-lubricant mixtures inside a smooth tube and inside a micro-fin tube. The refrigerant used was R-22 and the lubricant was a naphthenic base mineral oil with a viscosity of 150 SUS. The lubricant and refrigerant were completely miscible for the entire range of test conditions. The test section was straight and horizontal with a 9.52 mm OD tube and a length of 3.67

m. The lubricant mass concentration was varied from 0 % to 5 % and mass fluxes were tested in the range of $125 \text{ kg/m}^2\text{s}$ to $400 \text{ kg/m}^2\text{s}$, for an evaporation temperature of $3 \text{ }^\circ\text{C}$ with inlet and outlet qualities of approximately 0.15 and 0.85.

The results for pure refrigerant heat transfer were in good agreement with previous work for both smooth and micro-fin tubes. For a mass flux of $200 \text{ kg/m}^2\text{s}$, small quantities of lubricant enhanced the average heat transfer coefficient for both smooth and micro-fin tubes. The authors defined the following: $Ef_{s'/s}$ – smooth tube lubricant enhancement factor, defined as the ratio of the smooth tube heat transfer coefficient with lubricant added to the heat transfer coefficient of the smooth tube with pure refrigerant; $Ef_{a'/a}$ – micro-fin tube lubricant enhancement factor, defined as the ratio of micro-fin heat transfer coefficient with lubricant added to the micro-fin heat transfer coefficient with pure refrigerant; $Ef_{a/s}$ – micro-fin tube enhancement factor of pure refrigerant, defined as the ratio of the heat transfer coefficient of the micro-fin tube to the heat transfer coefficient of the smooth tube with pure refrigerant; and $Ef_{a'/s'}$ – micro-fin tube enhancement factor for refrigerant-lubricant mixture, defined as the ratio of the heat transfer coefficient of the micro-fin tube to the heat transfer coefficient of the smooth tube, with both tubes being tested at the same lubricant concentration.

The magnitude of the enhancement factor $Ef_{s'/s}$ was higher than $Ef_{a'/a}$ (1.36 vs. 1.11), and the peak occurred at a higher lubricant concentration (2.5 % vs. 1.5 %) for the smooth tube as compared to the micro-fin tube. Increasing mass velocity diminished the effect of lubricant enhancement. For the smooth tube at 2.5 % lubricant, $Ef_{s'/s}$ decreased from 1.36 to 1.25 as the mass flux increased from $200 \text{ kg/m}^2\text{s}$ to $400 \text{ kg/m}^2\text{s}$. At the same

lubricant concentration and respective mass fluxes, $E_{f_{a'/a}}$ for the micro-fin tube decreased from 1.1 to 1.05. The combined lubricant and micro-fin enhancement factor ($E_{f_{a'/s'}}$) decreased as the lubricant concentration was increased, but remained greater than the increase in surface area of the micro-fin tube for all conditions tested. $E_{f_{a'/s'}}$ at 1.2 % lubricant was 2.25 and decreased to 1.9 as the lubricant concentration increased to 5 %.

Thome et al. (1997; Part 1 and Part 2) reported in-tube flow boiling experiments for refrigerant R-134a mixed with lubricant for plain and a micro-fin tube for mass fluxes in the range of $100 \text{ kg/m}^2\text{s}$ to $300 \text{ kg/m}^2\text{s}$, inlet lubricant concentration in the range of 0 to 5 % (by mass) and refrigerant vapor quality in the range of 0 to 1. Up to vapor qualities of 0.6, the local boiling coefficient showed a tendency to increase at a mass flux of $300 \text{ kg/m}^2\text{s}$, whereas the boiling performance degraded at the two lower mass fluxes. For micro-fin tubes, at the lowest mass flux of $100 \text{ kg/m}^2\text{s}$, lubricant holdup caused a sharp falloff in performance thus indicating a lower mass velocity limit for efficient use of the tubes. There was no lubricant holdup in the plain tube. Also, at high vapor qualities, the local heat transfer coefficient indicated a rapid drop with increasing lubricant concentrations.

A total of 749 data points including refrigerants R-22, R-113, R-123, R-134a, and R-410A were used by Yun et al. (2002) to develop a correlation, which had a mean deviation of 20.5 % from 11 other correlations compared. The modifications included in the correlations were based upon effects of turbulence, surface tension, fin height, liquid film thickness, evaporating temperature and fluid properties. Among several non-dimensional parameters included in the correlation was a modified Reynolds number,

which was used to accommodate the turbulence effect generated from the micro-fin tube geometry. The correlation of Cavallini et al. (1999) yielded good agreement with the data.

Lottin et al. (2003) used a theoretical model to explain the effect synthetic lubricant would have on the performance of an R-410A compression refrigeration system. In the evaporator, optimum performance was observed with a 0.1 % lubricant mass fraction.

Cremaschi et al. (2005) conducted measurements on lubricant retention characteristics in the condenser, evaporator, and liquid and suction lines of air-conditioning systems employing refrigerants R-22, R-134a, and R-410A along with miscible and non-miscible lubricants. The lubricant retention was shown to depend on several parameters such as lubricant mass fraction, vapor refrigerant mass flux, mixture viscosity ratio, and orientation of the tube. At lubricant mass fraction of 5 %, the poorly miscible and soluble R-410A/mineral oil combination retained oil in the suction line by approximately 31 % more by mass than that of the miscible R-410A/POE combination.

Ding et al. (2008) presented a new correlation to predict the local flow boiling behavior of R-410A-lubricant mixtures inside a straight micro-fin tube based on the local properties of the refrigerant-lubricant mixture. The study also revealed that the presence of lubricant enhances heat transfer at low vapor qualities ($x < 0.4$), whereas at higher vapor qualities ($x > 0.4$) the heat transfer coefficient drops sharply with the increase of nominal lubricant concentration. Based on the Gungor and Winterton (1986) model, the new correlation is the sum of the convective contribution and the nucleate boiling contribution and accounts for mixture properties of refrigerant-lubricant. The convection multiplier and boiling suppression numbers were redefined for micro-fin tube geometry. The

experimental data was compared with correlations of Cavallini et al. (1998), Yun et al. (2002), Thome et al. (1997), Goto et al. (2001), and Kandlikar and Raykoff (1997). Because none of the correlations could predict the experimental data of R-410A/lubricant satisfactorily, a new correlation was developed, which agreed with 89 % of the experimental data with a deviation of ± 30 %.

Chapter 3

EXPERIMENTAL SETUP AND MEASUREMENTS

This chapter describes in detail the experimental apparatus, instrumentation, and part of the data reduction methods used in this dissertation. It also displays the tests done and includes uncertainty analysis that provides some assurance of the quality of the data. The importance and preference of using fluid heating technique rather than using electrical resistance heating technique is argued. A problem encountered in measurement of refrigerant saturation temperature is discussed in Section 3.7. As a solution, experimental vapor-liquid equilibrium data for the commercial R-410A used in the tests were established.

3.1 Apparatus

Convective boiling heat transfer data for pure R-410A and for R-410A/lubricant mixtures were measured using the Flow Boiling Apparatus of the Two Phase Laboratory at the National Institute of Standards and Technology (NIST) in Gaithersburg, Maryland. The boiling heat transfer of R-410A was carried out in a concentric tube-in-tube heat transfer test apparatus. Both tubes were copper. The experimental setup consisted of two major flow loops: a refrigerant loop which included the test section and a water loop for heating the refrigerant in the test section to the desired test conditions. The test section was a counter-flow heat exchanger with refrigerant R-410A flowing through the inner Turbo-AII™ micro-fin tube and the heating water flowing in the annulus. The outside diameter

of the inner tube was 9.5 mm and the outside diameter of the outer tube was 15.9 mm. The annulus gap was 2.2 mm.

A schematic of the test apparatus is shown in Figure 3-1. The setup consisted of an evaporator (test section), condenser, preheater, and magnetic gear pump, which delivered R-410A to the entrance of the test section in a subcooled state. Another magnetically coupled gear pump supplied a steady flow of distilled water to the annulus of the test section. The refrigerant and water flow rates were controlled by varying the pump speeds with frequency inverters.

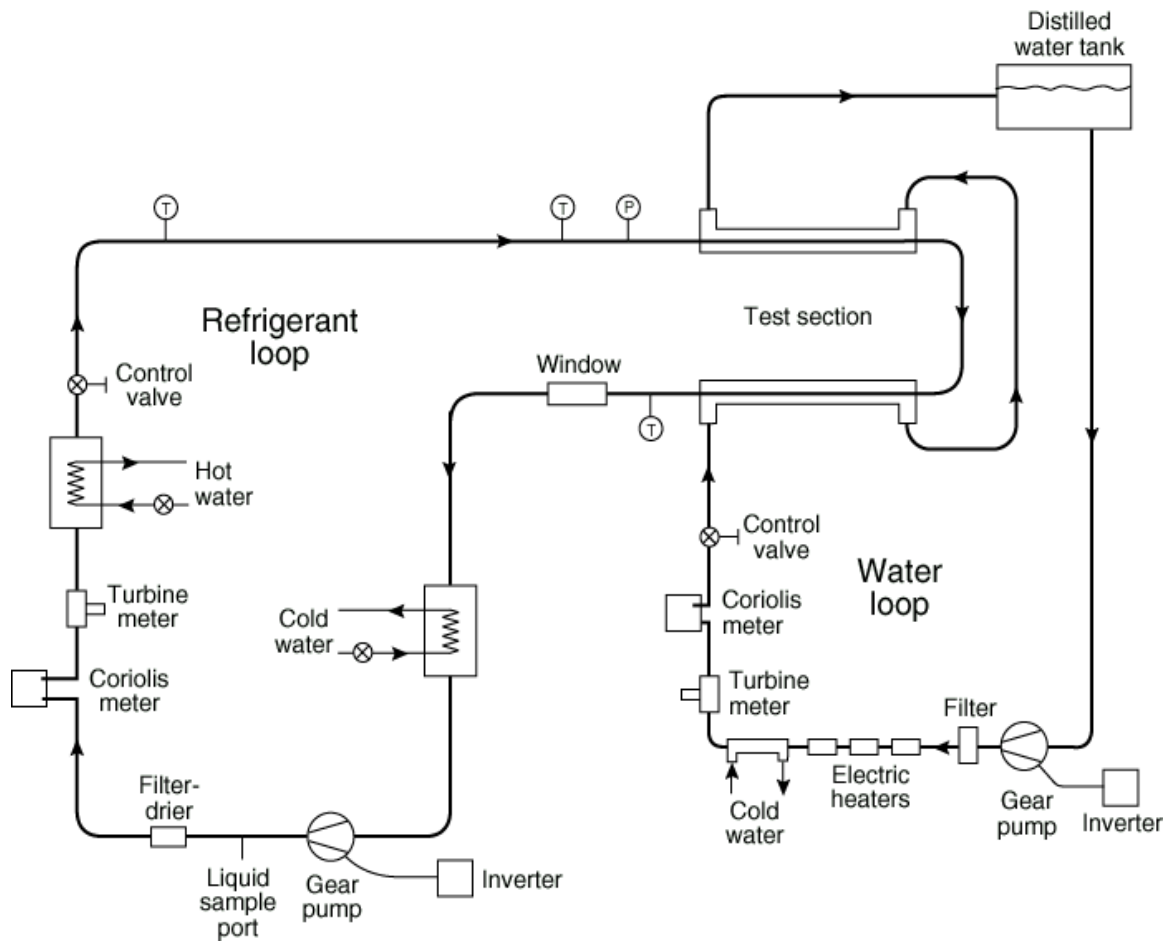


Figure 3-1: Schematic of Test Rig (Kedzierski et al., 1999)

For the water flow loop, distilled water was fed to the gear pump by gravity from an elevated tank to partially ensure that there were no air pockets or air bubbles present in the test section annulus. The water was then conditioned and fed to two redundant flow meters (Coriolis and turbine) before entering the annulus of the test section. Conditioning of the water provided the desired R-410A heat duty.

R-410A in a subcooled liquid state leaves the pump, flows through the flow meters (Coriolis and turbine) and enters the preheater. The preheater conditioned the refrigerant in such a way that the refrigerant was available at approximately 1 K of subcooling at the test section inlet. The refrigerant then entered the evaporator (test section) and began to vaporize by absorbing heat from the water flowing in the annulus of the test section. Two-phase or slightly superheated refrigerant exits the test section. The state of refrigerant (two-phase or superheated) can be visualized with the help of the transparent quartz tube that was conveniently placed at the exit of the test section. The refrigerant was then condensed in the condenser to return to subcooled state and thus complete the cycle.

3.2 Test Section

Figure 3-2 provides a detailed description of the test section. The test section consisted of a pair of 3.34 m long, horizontal tubes connected by a U-bend, which is a typical configuration for many evaporators and condensers used in the HVAC&R industry. The test section consisted of ten subsections, where for each subsection the inlet and exit temperatures were measured using type-T thermocouples on the refrigerant side and ten-junction thermopiles on the water side.

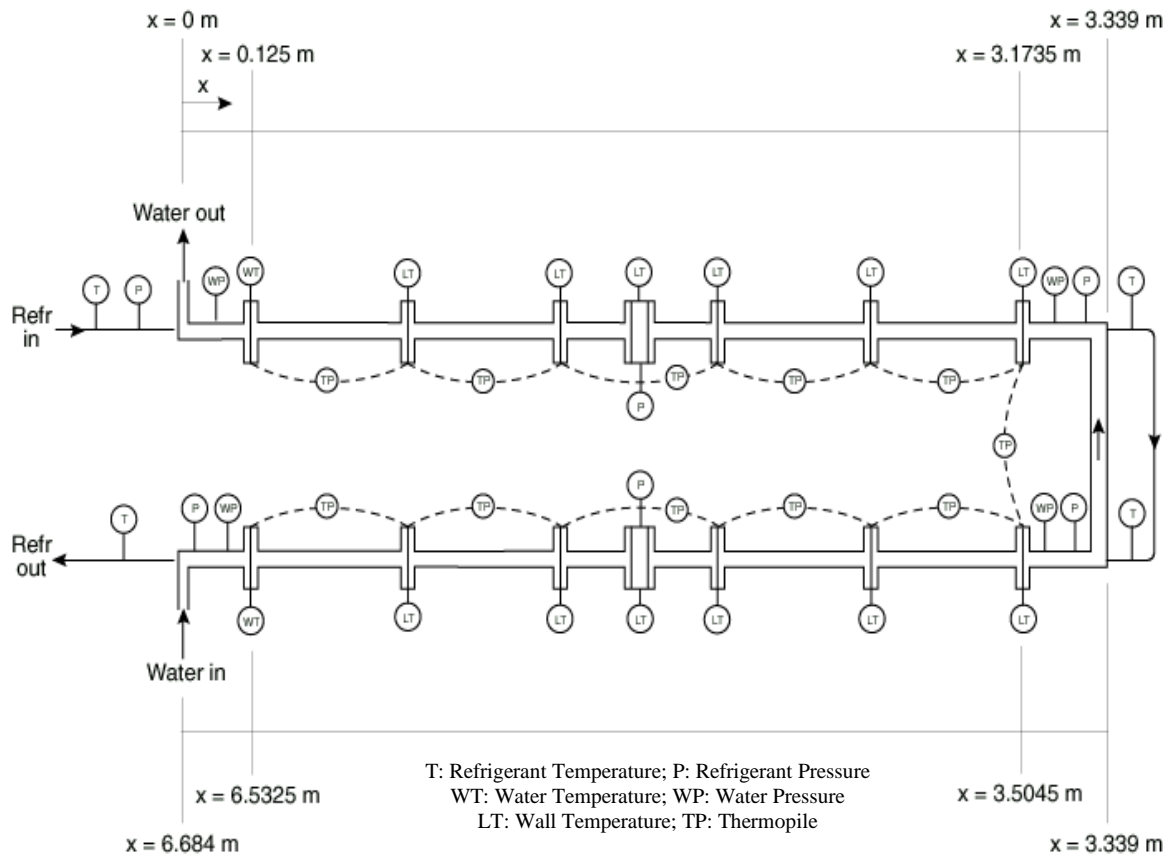


Figure 3-2: Test Section Detail (Kedzierski et al., 1999)

A fixed test pressure was maintained by balancing the refrigerant heat duty between the heat exchanger on the refrigerant side, the test section, and the heat exchanger on the water side. The annulus was constructed by connecting a series of tubes with 14 pairs of stainless steel flanges. This construction permitted the measurement of both the outer micro-fin wall temperature and the water temperature drop. The design also avoided abrupt discontinuities such as unheated portions of the test section and tube-wall “fins” between thermopile ends.

Figure 3-2 shows that the thermocouple wires pass between 12 of the gasketed flange pairs. These thermocouples measured the refrigerant-tube wall temperature at ten locations on the top, side, and bottom of the tube wall. These locations were separated by 0.6 m on average, and they were located near the intersection of the shell flanges. In addition to these, type-T thermocouples were also mounted next to the pressure taps near the middle of each test section length. The thermocouples had an expanded uncertainty of 0.1 K. The thermocouple junction was soldered to the outside surface and was sanded to a thickness of 0.5 mm for good thermal contact. The leads were strapped to a thin non-electrically-conducting epoxy layer on the wall for a distance of 14.3 mm before they passed between a pair of the shell flanges. The wall temperature was corrected for a heat-flux dependent fin effect. The correction was typically 0.05 K.

Figure 3-2 also shows that a chain of thermopiles was used to measure the water temperature drop between each flange location. Each thermopile consisted of 10 thermocouples in series, with ten junctions at each end evenly spaced around the circumference of the annulus. Because the upstream junctions of one thermopile and the downstream junctions of another tend to enter the annulus at the same axial location (except at the water inlet and outlet), the junctions of the adjacent piles were alternated around the circumference. A series of Teflon half rings attached to the inner refrigerant tube centered the tube in the annulus. The half-rings were circumferentially baffled to mix the water flow (Kedzierski et al., 1999). Mixing was further ensured by a high water Reynolds number (Kattan et al., 1995).

As shown in Figure 3-2, six refrigerant pressure taps along the test section allowed the measurement of the upstream absolute pressure and five pressure drops along the test section. Differential pressure transducers with an expanded uncertainty of 1 % of the reading were used to measure the pressure drops. Two sets of two water pressure taps were used to measure the water pressure drop along each tube. Also, a sheathed thermocouple measured the refrigerant temperature at each end of the refrigerant tubes, with the junction of each centered radially; however, only the thermocouple at the inlet of the first tube was used in the calculations. The entire test section was wrapped with 5 cm of foam insulation to minimize heat transfer between the water and the ambient.

3.3 Micro-fin Tube Details

Micro-fin tubes come in various tube sizes with different tube thickness, helix angles and number of fins. Table 3-1 provides the geometrical parameters of the Turbo-AII™ micro-fin tube used in this study.

Table 3-1: Geometric Parameters of Turbo-AII™ Micro-fin Tube

Parameter	Dimension	Parameter	Dimension
D_o	9.52 mm	β	18^0
t_w	0.3 mm	α	50^0
D_r	8.91 mm	N_f	60
A_c	60.8 mm^2	S_p	0.707 mm
e	0.2 mm	D_h	5.45 mm
P	0.47 mm	Distance between pressure taps	1.587 m, 1.588 m

Figure 3-3 shows a cross sectional view of the test section, including detail of the micro-fin tube. The annulus gap was 2.2 mm, and the micro-fin tube wall thickness was 0.3 mm. The micro-fin tube has 60 evenly spaced 0.2 mm high fins with a 18° helix angle. For this geometry, the cross sectional flow area was 60.8 mm^2 yielding an equivalent smooth diameter (D_e) of 8.8 mm. The root diameter of the micro-fin tube was 8.91 mm. The inside-surface area per unit length of the tube was estimated to be 44.6 mm.

The hydraulic diameter (D_h) of the micro-fin tube was estimated to be 5.45 mm. The ratio of the inner surface area of the micro-fin tube to the surface area of a smooth tube of the same D_e was 1.6. The fins rifled down the axis of the tube at a helix angle of 18° with respect to the tube axis (Kedzierski et al., 1999).

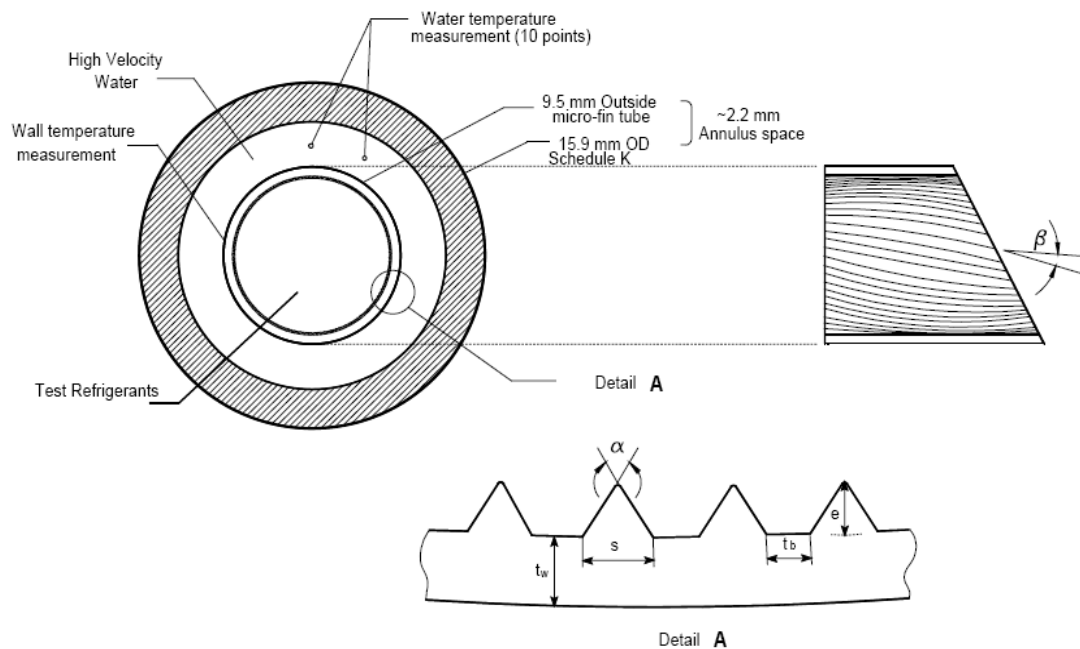


Figure 3-3: Cross Sectional View of Test Section and Micro-fin Tube Details
(Kedzierski et al., 1999)

3.4 Charging the Refrigerant

The system charging procedure ensured the purity of the R-410A. The procedure consisted of charging the loop, initially filled with air at atmospheric conditions, with pressurized R-410A gas until the saturation pressure of the R-410A supply canister was reached. The mixture of air and R-410A was then vented to a pressure slightly above atmosphere, preventing back filling the test section with air. This procedure was performed a minimum of three times. Assuming uniform mixing of the initial charge and the R-410A during each fill, this reduced the air concentration to a volume fraction of less than 1×10^{-6} .

After thorough evacuation of the test rig to 26 in.Hg at full vacuum, commercial R-410A was charged in a liquid state into the test rig. The R-410A charging canister was placed upside down to ensure liquid-only charging.

3.5 Measurements

The three basic measurements of this study were pressure, temperature and mass flow rate on both the refrigerant-side and the water-side. The thermocouples, pressure transducers (absolute and differential) and mass flow meters were thoroughly calibrated prior to taking data. The measurement of these variables and other critical variables are discussed in detail below.

3.5.1 Measurements for Temperature

Type-T copper-constantan thermocouples were used to record all temperature measurements. The thermocouples were all from the same manufacturer's batch. The thermocouples were calibrated against a glass-rod standard platinum resistance thermometer (SPRT) and a reference voltage to a residual deviation in the range of 0.005 K to 0.01 K. A quartz thermometer, which was calibrated with a distilled ice bath, agreed with the SPRT temperature to within approximately 0.003 K. On a given day, the first step was to compare the thermocouples to the SPRT and Quartz Thermometer. The temperatures of SPRT, Quartz thermometer, and the thermocouples matched within 0.5 % or less of each other.

The measurements of wall temperatures on the refrigerant side and thermopiles on the water side are described in detail in Section 3.2.

3.5.2 Measurements for Pressure

Pressure measurements were made using absolute and differential pressure transducers. The pressure transducers were calibrated using dead weight tester and a mercury manometer. The voltage output for the transducer was recorded to obtain a relation between pressure and voltage. The calibration could only be done at atmospheric pressure. Any errors which might develop by the use of the transducers at higher absolute pressure could not be quantified.

3.5.3 Measurements for Mass Flow Rate

Though mass flow rate is not necessary to determine the local heat transfer coefficient, it is required to calculate local thermodynamic quality. A coriolis flowmeter and a turbine flowmeter measured the mass flow rate for the refrigerant loop and for the water loop. The flow meters were calibrated with water at near room temperature using the scale and electronic stopwatch technique. The response of all the flow meters was flat over a wide range of Reynolds numbers so that a viscosity correction was unnecessary.

3.5.4 Single Phase Heating Tests for Energy Balance

In order to verify temperature measurements and thus the capabilities of the test apparatus, several initial single phase liquid heating tests were made. For this purpose, single-phase R-134a was used since its heat transfer characteristics are well known and considerable amounts of experimental data are available. In order to assure that the instrumentation was behaving correctly, an energy balance was made between temperature rise on the water side and temperature rise on the refrigerant side. The results of those tests are shown in Fig. 3-4. The difference between heat transfer of R-134a and water is plotted versus R-134a mass flow rate.

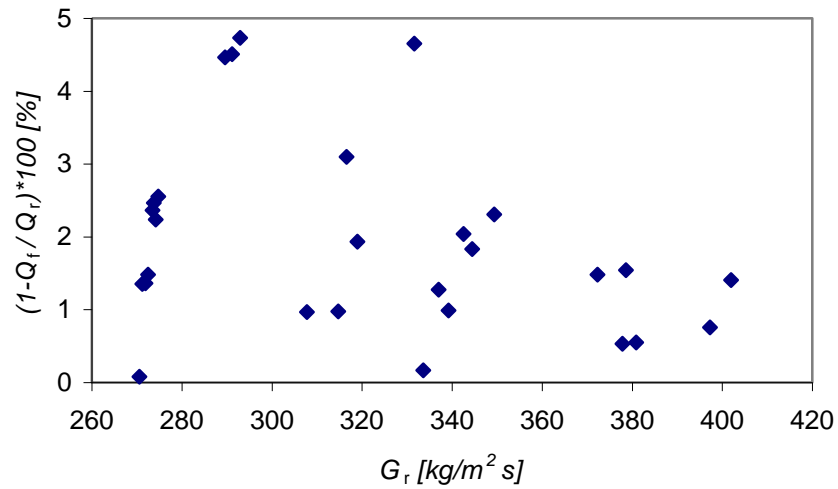


Fig. 3-4: Single-phase Energy Balance with R-134a

The single-phase tests had mass fluxes in the range of 100 to 400 kg/m²s and heat fluxes in the range of 5 kW/m² to 25 kW/m². The inlet and outlet subcooling for the entire test section was controlled, ensuring single-phase flow. The heat duty for the R-134a loop compared very closely to the heat duty for the water loop, mostly to within 3 % for all the single-phase measurements. (Note: $Q_r = m_r c_{p_r} (T_{in} - T_{out})$ and $Q_f = m_f c_{p_f} (T_{out} - T_{in})$.)

3.5.5 Testing Protocol

The step-by-step procedure for physically operating the test rig is provided in Appendix E. With the test rig, a series of tests were performed at conditions as shown in Table 3-2.

Table 3-2: Tested Range of Measurements

Parameter	Range
Saturation Pressure (MPa)	1.034 to 1.103
Saturation Temperature (°C)	7.2 to 10
Mass Flux (kg/m ² s)	150 to 400
Heat Flux (kW/m ²)	3 to 20
Thermodynamic Quality	0.02 to 0.6

For a given test, the refrigerant inlet pressure and the refrigerant mass flow rate were fixed. The refrigerant flow rate was measured with redundant flow meters (Coriolis and turbine). Also held constant were the water inlet temperature and water mass flow rate through the use of a water-chilled heat exchanger and variable electric heaters. On reaching steady state, one specific data set was thus recorded.

For the next data set, while keeping the rest of parameters constant, a new fixed value of inlet water temperature was achieved to yield different heat flux and a change in quality.

The variation of mass flow rate of refrigerant produced different mass flux values. Similarly, the variation of water flow rate produced different values of heat flux. In this manner, several data sets were obtained for the range of parameters shown in Table 3-2.

Data were obtained for three different saturation pressures of 1.034 MPa, 1.068 MPa, and 1.103 MPa. The average refrigerant saturation temperature, T_s , was varied between 7.2 °C and 10 °C with approximately 1 K of subcooling at the test section inlet. The water inlet temperature and flow rate established the overall refrigerant quality change

in the test section. The water temperature drop, the tube wall temperature, the refrigerant temperature, pressure, and pressure drop were all measured at ten axial locations along the test section. These measurements were used to determine the local heat transfer coefficient for the micro-fin tube. A FORTRAN program (Appendix D) was used to calculate the boiling heat transfer parameters. (Note: All saturated refrigerant properties were evaluated at the measured saturation pressure using REFPROP 7.1 (Lemmon et al., 2006).)

For two-phase tests, a mixture of naphthenic mineral oil and POE lubricant (1 % and 99 % by mass, respectively) was chosen for the study. The POE employed in this study had a nominal kinematic viscosity of $68 \mu\text{m}^2/\text{s}$ at 297.8 K. The nominal concentration of the lubricant was 0.4 %.

3.5.6 Data Acquisition System

All DC voltages from the thermocouples, pressure transducers and flow meters were recorded by a data logger. Data collection and control for all measurements involved the use of a dedicated data acquisition system (Hewlett Packard, HP 3497A) and Labview program. Automatic scanning of all thermocouples, thermopiles, pressure transducers and flow meters was done. Data was saved when steady-state was reached, i.e., when instream temperatures and pressure variations dissipated. This requirement was satisfied typically one hour after a change in mass flux or heat flux or both was made. A typical single scan of all thermocouples, thermopiles, pressure transducers, and mass flow rates took approximately 45 seconds. Steady-state data for a single-run (fixed mass flux and fixed saturation temperature and fixed water inlet temperature) was recorded for anywhere

between five to ten minutes. The data were recorded in an ASCII data file, which was then manipulated in Excel.

3.5.7 Problems

Measurements for two-phase heat transfer of R-410A and R-410A/POE involved recording data for fifty thermocouples, four mass flow meters, and ten pressure transducers. Two problems occurred during the data collection.

First, three thermocouples measuring the outer wall of the micro-fin tube were recording skewed voltage readings. In a resulting manner, the temperature values of these three thermocouples were skewed. The speculation is that during high heat flux tests involving relatively higher mass flow rates of water in the annulus of the test section, either part of or the entire epoxy on these three thermocouples had come off, thus exposing the soldered thermocouple with an unreliable thermal contact with the outer wall of micro-fin tube.

Second, just about at the end-phase of taking two-phase tests with pure R-410A, the third and fourth differential pressure transducers of the test section showed discrepancy in their measurements. These pressure transducers had the range of 0 – 10 psid. During early mornings, before starting the pumps on the refrigerant and/or water side, when data for ambient temperatures were recorded, they compared within 0.1 K of the SPRT and quartz thermometer. The pressure inside the test section matched closely with what Refprop 7.0 would calculate for the respective ambient temperature. Therefore, the discrepancy in

measurements of third and fourth differential pressure transducers of the test section could not be understood. It was decided that all differential pressure transducers be re-calibrated.

3.5.8 Summary of Experimental Data

A total of 230 data points were collected with R-410A and 85 data points with R-410A/POE to measure the local two-phase flow boiling heat transfer coefficient. Approximately all of the data is in the annular flow regime. The data base then provides a strong basis for analysis the heat transfer coefficient.

3.6 Uncertainty in Measurements

The standard uncertainty (u_i) is the positive square root of the estimated variance u_i^2 . The individual standard uncertainties are combined to obtain the combined standard uncertainty by the law of propagation of uncertainty (Taylor and Kuyatt, 1994). The standard uncertainty becomes an expanded uncertainty when it is multiplied by a coverage factor to correspond to a particular confidence interval. All of the measurement uncertainties reported in this study are expanded uncertainties with a coverage factor of two yielding a 95 % confidence interval.

Table 3-3 shows the range and 95 % relative uncertainty of the installed instrumentation. Table 3-4 shows the expanded measurement uncertainty (U_m) of the various measurements along with the range of each parameter.

Table 3-3: Instrumentation Range and Uncertainty

Instrument	Range	95 % Relative Uncertainty
T-type Thermocouples ($^{\circ}\text{C}$)	0 to 100	0.20
10-junction Thermopiles ($^{\circ}\text{C}$)	0.5 to 5	0.21
Absolute Pressure Transducer (kPa)	0 to 3500	2.0 % of the value
Differential Pressure Transducer (kPa)	0 to 172	1.0 % of the value
Coriolis Mass Flow Meter (kg/h)	0 to 544	2.1 % of full scale
Turbine Mass Flow Meter (kg/h)	0 to 544	2.1 % of full scale

Table 3-4: Median Estimated 95 % Relative Expanded Uncertainties and Range for Measurements (Sawant et al., 2007)

Parameter	Minimum	Maximum	U %
G_r [$\text{kg}/\text{m}^2 \cdot \text{s}$]	57	552	2.0
T_r [K]	293.0	323.0	0.1 (0.3 K)
P [kPa]	600	2000	1.5
T_w [K]	288.0	318.0	0.1 (0.25 K)
\dot{m}_f [kg/s]	0.0150	0.0450	2.0
T_f [K]	278.0	313.0	0.1
q'' [kW/m^2]	1.5	43.8	5.1
dT_f/dz [K/m]	0.009	0.45	5.2
Nu	78	410	16.4
Re	5300	16500	4.0
x_q	0.001	0.72	8.0
ΔT_s [K]	0.8	6.0	15.2 (0.44 K)

3.7 Equilibrium Refrigerant Temperature

The Air Conditioning and Refrigeration Institute (ARI) approved of stringent refrigerant purity standards to limit the levels of unsaturated impurities. The new ARI Standard 700-2006 contains specification to limit unsaturated impurities in R-410A and other alternative refrigerants to a maximum level of 40 ppm (ARI-700, 2006). Since the R-410A used in this study was a commercially prepared mixture, its pressure and the temperature relationship is likely different than that of an ideal R-410A mixture since the composition and purity of the commercially prepared sample is likely different than that of an ideal R-410A mixture.

Depending on the manufacturing process used to prepare the commercial sample, unsaturated impurities or stray components such as R-115 (byproduct of R-125 manufacturing process) may be present in the mixture which would cause a deviation from the "standard" properties of R-410A (Bivens, 2006). For example, the measured saturation temperature of the R-410A test fluid used in this study differed from that obtained using REFPROP 7.1 by approximately 1 K over the pressure range tested. The difference was confirmed to be equal to 0.85 K after the measured saturation temperature was compared to the study by Weber (2000). To alleviate this discrepancy, vapor equilibrium measurements were carried out for the test fluid of this study for temperatures between 280 K and 300 K and pressures between 1.0 MPa and 1.2 MPa.

A precisely controlled temperature liquid bath was used with a glass standard platinum resistance thermometer calibrated to within ± 0.005 K. As shown in Fig. 3-5, a constant volume vessel instrumented with a pressure transducer with an uncertainty of

± 0.01 kPa was charged with the test fluid and fully immersed in the bath. The mass quality of the charge was calculated from the known volume and the charged mass. The densities of the vapor and the liquid were obtained from REFPROP 7.1 (Lemmon et al., 2006) at the measured temperature.

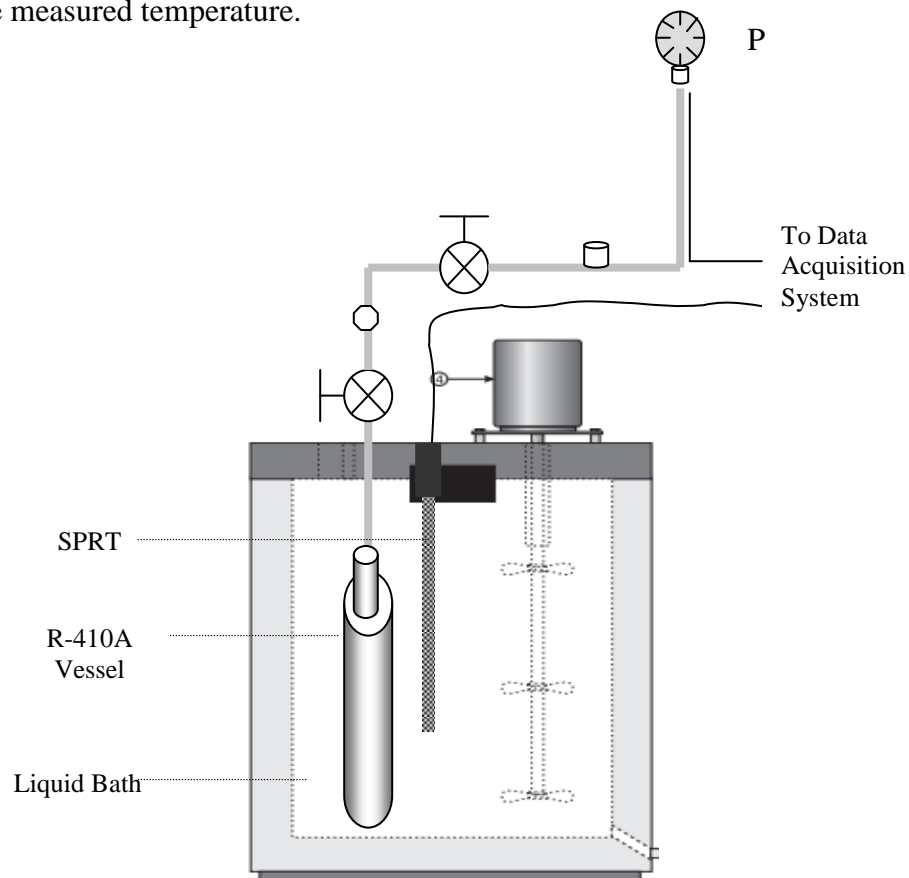


Fig. 3-5: Vapor-Liquid Equilibrium Measurements of R-410A

The saturation temperature (T_r), refrigerant pressure (P_r) and thermodynamic mass quality (x_q) were correlated for the R-410A used in this study, absent the lubricant, resulting in:

$$\frac{1}{T_r} = A_0 + A_1 \ln(P_r) + A_2 x_q \quad (3-1)$$

where T_r is in K and P_r is in kPa. The constants are $A_0 = 0.658452 \times 10^{-2} \text{ K}^{-1}$; $A_1 = -0.434741 \times 10^{-3} \text{ K}^{-1}$; $A_2 = -0.129204 \times 10^{-5} \text{ K}^{-1}$ with the temperature residuals being between -0.005 K and 0.01 K . Figure 3-6 shows that eq. (3-1) represents the measured temperature to within $\pm 0.01 \text{ K}$ for pressures between 1 MPa and 1.2 MPa. Equation 3-1, the locally measured pressure, and the calculated thermodynamic quality were used to calculate the saturation temperature for all of the measurements reported in this study.

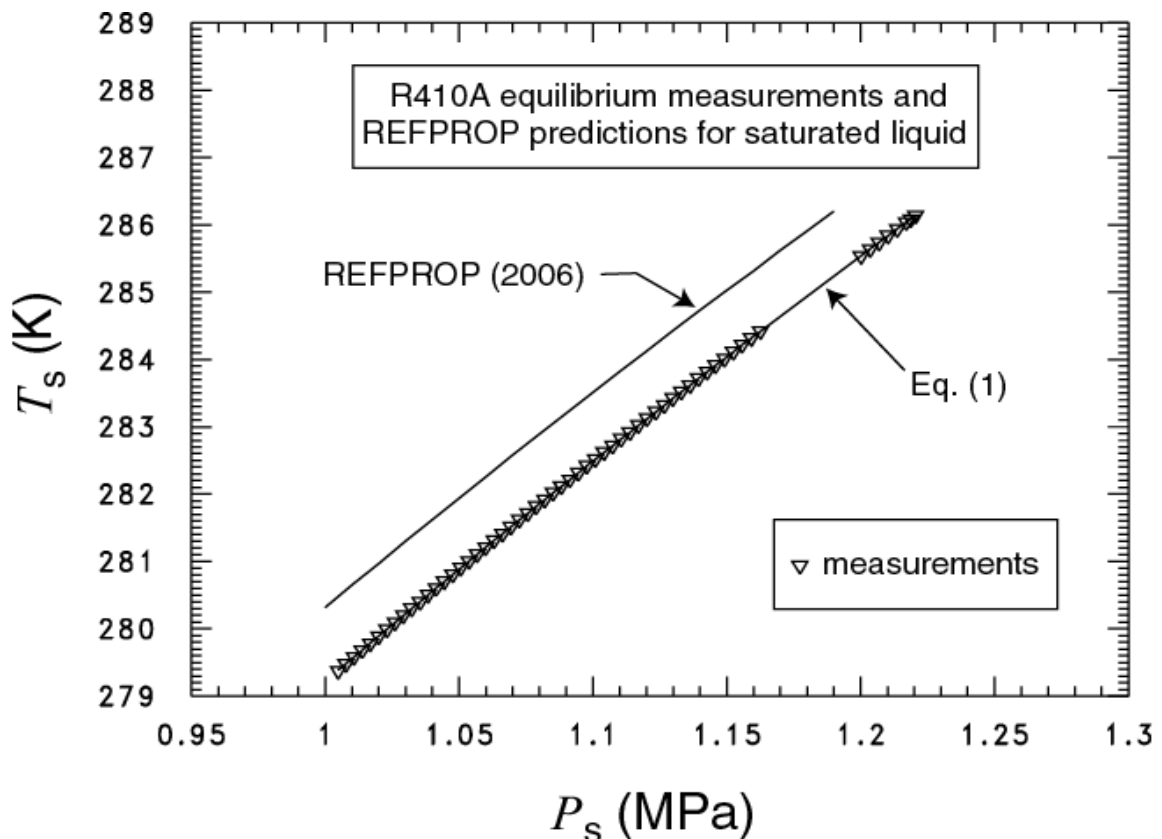


Figure 3-6: Comparison of Measurements with REFPROP 7.1 (Lemmon et al., 2006)

The constants in eq. (3-1) were modified to predict the saturated conditions of R-410A/lubricant mixtures following the procedure of Thome (1995):

$$\frac{1}{T_r} = \frac{\ln(P_r) - b + \frac{A_2}{A_1} x_q}{a} \quad (3-2)$$

where a and b are fourth degree polynomials in the local lubricant mass fraction in the refrigerant liquid (w_1):

$$\begin{aligned} a &= -2300.2K + 182.5Kw_1 - 724.2Kw_1^2 + 3868.0Kw_1^3 - 5268.9w_1^4 \\ b &= 15.146 - 0.722w_1 + 2.391w_1^2 - 13.779w_1^3 + 17.066w_1^4 \end{aligned} \quad (3-3)$$

where the local lubricant mass fraction was obtained from the quality and the all-liquid ($x_q = 0$) lubricant mass fraction (w_b) as:

$$w_1 = \frac{1}{\frac{1 - x_q}{w_b} - 1} \quad (3-4)$$

All of the coefficients of the a and b polynomials, with the exception of the constant terms, were taken from Thome (1995). The constant terms of the polynomials were adjusted to reproduce the lubricant-free R-410A expression given in eq. (3-1) when $w_1 = 0$.

Figure 3-7 illustrates the magnitude of the effect that 0.4 % mass fraction of lubricant has on the saturation temperature of R-410A for a saturation pressure of 1.1 MPa and various qualities. In general, the lubricant increases the saturation temperature by less than 0.025 K for qualities less than 0.5.

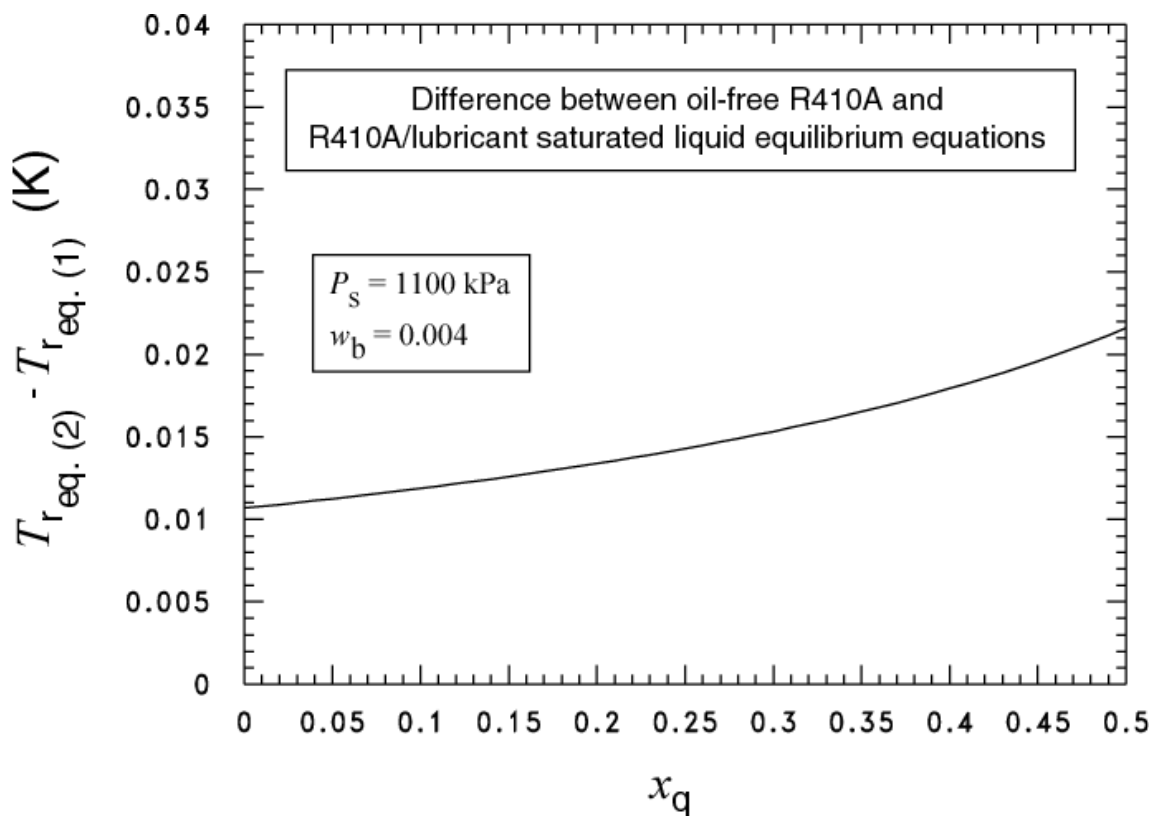


Figure 3-7: Difference between R-410A and R-410A/POE at Saturated Liquid Equilibrium Equations

3.8 Fluid Heating and Electrical Resistance Heating

For in-tube boiling and condensation experimental measurements, the two most common methods to condition the working fluid is to externally supply electrical resistance heating or to externally supply heating via a secondary fluid. For all stratified flow types, fluid heating induces a nearly uniform temperature boundary condition around the tube perimeter, which is similar to actual operating conditions in the HVAC&R industry, while electrical resistance heating creates circumferential heat conduction around the tube from the hot, dry-wall condition at the top to the colder, wet-wall condition at the bottom, yielding an unknown boundary condition (Wolverine Tube Inc., 2004).

Most of the experimental studies for flow boiling of refrigerants and refrigerant-lubricant mixtures reported in the literature are with electrical resistance heating applied as the boundary condition, where the electrical resistance heating is realized by direct resistance heating of the tube itself or by wrapping heating tape around the tube. While this is a convenient experimental method, it is not representative of many industrial applications where a secondary fluid stream is used as the heating medium. Concerns have been expressed in the flow boiling heat transfer literature related to the applicability for practical equipment design of heat transfer data generated with an electrically heated boundary condition, e.g., see Kedzierski (1995), Kandlikar et al. (1997) and Ohadi et al. (1999).

Kedzierski (1995) investigated the difference between electrical resistance heating and fluid heating during a pool boiling study of R-123 on four commercial enhanced surfaces at a saturation temperature of 277.6 K. The comparison was direct and unbiased

because of the measurements of heat flux and wall superheat that were independent of the type of heating used. The heat fluxes using the fluid heating technique were as much as 32 % higher than those obtained by using the electrical resistance heating technique. The author believed that the heat flux showed dependency on the boundary condition by: (a) boiling on the enhancement, (b) conduction in the copper and (c) single phase or electric resistance heating at the heated surface. For the same time-averaged heat flux, Kedzierski (1995) speculated that a larger part of the heat flux was used to superheat liquid for electrical resistance heating than for fluid heating. In conclusion, it was argued that an interaction between the fluctuating wall temperature and the fixed electrical heat flux induced a higher degree of superheated liquid on the electrically heated surface than on the fluid heated surface.

Another direct comparison between fluid heating and electrical resistance heating was conducted on two identical stainless steel tubes in pool boiling with water at atmospheric pressure by Kandlikar et al. (1997). The electrical resistance heating boundary condition was achieved by using direct current from a power supply to generate high amperage, whereas pure ethylene glycol was used for fluid heating. The results of this study were in agreement with Kedzierski (1995). For the range of parameters tested, the heat fluxes measured via the fluid heating technique were higher than the heat fluxes measured via the electrical resistance heating technique by 30 to 100 %. A further numerical analysis - based on a steady-state heat conduction model in the heater plate in the vicinity of a bubble - implied that the differences between the fluid heating and

electrical resistance heating methods would be smaller at higher heat fluxes when large regions of the heater would be occupied by bubbles.

The comparisons between fluid and electric heating boundary conditions were made for identical surfaces and heat fluxes by Ohadi et al. (1999). The overall average heat transfer coefficient for the water heating method was higher than that of the electrical resistance heating method for the same superheat for the Turbo-BII tube. The authors also showed that the temperature profile at the heated wall influenced local boiling heat transfer for two fluid heated surfaces.

Electrical resistance heating is not a physically realistic boundary condition for refrigerant applications. For annular flow with partial dryout on the top perimeter of the tube, electrical resistance heating is also not advisable because of axial heat conduction along the test section (Wolverine Tube Inc., 2004). Therefore, the most pertinent and useful data are local measurements obtained from a fluid heated rig.

Based on the above, one can conclude that the fluid heating boundary condition is a more realistic approximation of actual boundary conditions seen in practical applications and thus is the experimental technique that should be implemented when possible.

Chapter 4

HEAT TRANSFER: RESULTS AND DISCUSSION

4.1 Background

The most common explanation of the physical mechanism of heat transfer in annular flow boiling is that of a superposition of a forced convection evaporative process and a nucleate boiling process. With increasing vapor quality the liquid film thins and the core vapor accelerates. Heat transfer to the core is improved by this acceleration and the thinning of the liquid film also serves to lessen its conductive resistance. Heat transfer is thought to improve sufficiently and to occur with such rapidity that bubble growth disappears. At this point, the nucleate boiling is said to be suppressed, and vapor generation is due strictly to evaporation from the vapor-liquid interface.

A large number of studies on pure refrigerants and refrigerant-mixtures in smooth tubes have been published in the literature to reliably predict heat transfer rates. On studies related to convective vaporization in tubes and tube banks, Webb and Gupte (1992) reviewed a series of correlations and provided commentary on all the listed correlations. An experimental study on flow boiling of pure and mixed refrigerants was conducted and documented in a state-of-the-art review by Thome (1996). The author called for an improvement in the prediction methodologies for refrigerant-mixtures and refrigerant-lubricant mixtures flow boiling heat transfer. A bubble-point temperature must be used to determine the heat transfer coefficient of a refrigerant-lubricant mixture. Greco (2006)

studied pure refrigerants and refrigerant mixtures in a horizontal stainless steel smooth tube with electrical heating. In the nucleate boiling dominated region, the heat transfer coefficient is a strong function of heat flux with an influence index in the range of 0.53 to 0.74. In a study to compare CO₂ and R-410A in horizontal smooth tubes, it was observed by Hrnjak and Park (2007) that at every identical test condition, CO₂ exhibited higher heat transfer coefficients than R-410A mainly due to a higher nucleate boiling contribution.

The effect of lubricant on the boiling heat transfer coefficient of refrigerants has been extensively studied in an empirical manner. In a survey, Schlager et al. (1987) cite studies that highlight the effect of lubricant on the heat transfer and pressure drop of condensing and evaporating refrigerants with emphasis on refrigerant-lubricant mixtures flowing in tubes. A similar study was later conducted by Groll and Shen (2003). Ding et al. (2008) used existing experimental data to develop a model, which included micro-fin tube parameters and refrigerant-lubricant mixture properties to predict micro-fin heat transfer enhancement.

4.2 Thermodynamic Approach (Thome, 1995)

Thome (1995) advocated a thermodynamic approach where the lubricant-refrigerant mixture is treated as a zeotropic mixture with a temperature glide. On the basis of this method the local boiling heat transfer coefficient (h) is defined as:

$$h = \frac{q''}{(T_w - T_{bub})} \quad (4-1)$$

where T_w is the wall temperature and T_{bub} is the local bubble point temperature of the bulk liquid mixture and q'' is the heat flux defined as the ratio of heat duty to surface area (Q/A). The use of the mixture bubble point temperature, as opposed to the previous use of the pure refrigerant saturation temperature, allows for the correct thermodynamic definition of the local heat transfer coefficient but also requires knowledge of the local refrigerant-lubricant liquid composition. It is assumed that no appreciable amount of lubricant enters the vapor phase. To determine the liquid composition at some point in a typical evaporator, the heat absorbed by the refrigerant up to that point must be known. This is usually portrayed in a temperature-enthalpy plot or heat release curve. The task of evaporator design for a given refrigerant-lubricant combination can be accomplished with knowledge of the heat transfer coefficient from a pure fluid correlation and the actual bubble temperature of the mixture from a temperature-enthalpy plot. A detailed description of this thermodynamic approach by Thome (1995) is given in Chapter 6.

4.3 Experimental Methodology and Data Reduction

The system was charged with commercially available R-410A. Its composition was maintained by thoroughly evacuating the test rig and by charging only liquid from the cylinder. Experiments were conducted for various heat fluxes, mass fluxes, and saturation temperatures of lubricant-free R-410A and R-410A/lubricant mixture. Flow boiling heat transfer measurements were taken for three different average refrigerant pressures of 1.034 MPa, 1.068 MPa, and 1.103 MPa. The refrigerant mass flow rate was varied to achieve mass fluxes in the range from 100 kg/m²s to 400 kg/m²s. The average refrigerant

saturation temperature, T_r , was varied between 7.2 °C and 10 °C with approximately 1 K subcooling at the test section inlet. The heat flux was varied from 2 kW/m² to 20 kW/m².

A data acquisition system (Hewlett Packard, HP 3497A) and a tailored software program (LabView) were used to record all the conditions in a data file. All saturated refrigerant properties, with the exception of the equilibrium mixture temperature, were evaluated at the measured saturation pressure using version 7.1 of REFPROP (Lemmon et al., 2006) mixture property routines. Data were recorded once steady state conditions had been achieved. The details of the measurement techniques are discussed in Chapter 3. These measurements were then used to calculate the flow boiling heat transfer of R-410A in the absence of and in the presence of lubricant. Appendix C contains a summary of the measured results which can be used by other researchers.

The local convective boiling two-phase heat transfer coefficient based on the actual inner surface area ($h_{2\phi}$) was calculated as:

$$h_{2\phi} = \frac{q''}{T_w - T_r} \quad (4-2)$$

The refrigerant temperature (T_r) is obtained from eq. (3-1) for pure R-410A and from eq. (3-2) for R-410A/lubricant mixtures. The wall temperatures were measured on the top, side and bottom of the micro-fin tube wall using type-T copper-constantan thermocouples. The top, side and bottom wall temperatures were averaged to a single value. Inside wall temperatures (T_w) were calculated from the measured outside wall temperatures by use of the steady-state radial, one dimensional conduction equation with uniform heat generation and assuming adiabatic conditions on the outside of the tube.

The wall temperatures (T_w) were fitted to their axial positions (z) to reduce the uncertainty in the measurement. The measured wall temperatures were fitted to:

$$T_w = A_0 + A_1z + A_2z^2 \quad (4-3)$$

The water temperature (T_f) was determined from the measured temperature change obtained from each thermopile and the inlet water temperature measurement. In addition, the water temperature at the exit of the test section was measured. The water temperature was regressed to the axial location of the thermopiles along the z -coordinate (see Fig. 3-2). The water temperatures were fitted to:

$$T_f = A_0 + A_1z + A_2z^2 + A_3z^3 \quad (4-4)$$

For a counter-flow configuration, the temperature distribution of R-410A and water along the test section for one of the data sets is shown in Fig. 4-1.

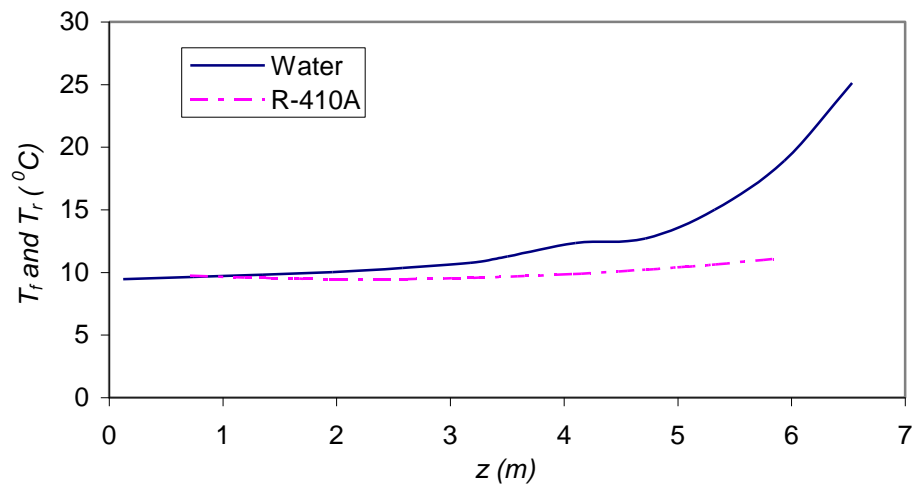


Figure 4-1: Refrigerant and Water-side Temperature Profiles

The profiles for the water and wall temperatures illustrate the need for separate regression equations. These are fitted temperature profiles as explained in eq. (4-3) and eq. (4-4). The x-axis is the length of the entire test section. The water temperature fits, the measured water mass flow rate (m_f), and the properties of the water were used to calculate the local heat flux (q'') of the micro-fin tube based on the actual inner surface area:

$$q'' = \frac{m_f}{p} \left(c_{p_f} \frac{dT_f}{dz} + v_f \frac{dP_f}{dz} \right) \quad (4-5)$$

The wetted perimeter of the inside of the micro-fin tube is p . The specific heat (c_{pf}) and the specific volume (v_f) of the water were calculated locally as a function of the water temperature. The local axial water temperature gradient (dT_f/dz) was calculated from a derivative of eq. (4-4). The water pressure gradient (dP_f/dz) was linearly interpolated between the pressure taps to the location of the wall thermocouples. The pressure gradient term was typically less than 3 % of the temperature gradient term.

4.4 Results and Discussion

The enthalpy of the refrigerant at the inlet of the test section was calculated from its equilibrium refrigerant temperature and measured pressure. The subsequent change in the refrigerant enthalpy along the test section was calculated from the local heat flux and the measured refrigerant mass flow rate. The refrigerant pressures were measured at six pressure taps along the test section. The pressure was linearly interpolated between the taps. The refrigerant entered the test section as nearly saturated liquid having

approximately 1 K of subcooling. The average saturation temperature, T_r , at the inlet varied between 7.2 °C and 10 °C. Figure 4-2 shows an example of the local heat flux for lubricant-free R-410A and the R-410A/lubricant mixture as calculated from eq. (4-5) versus thermodynamic quality for counterflow configuration and a fixed inlet test section pressure of 1.1 MPa. For a given quality, the heat flux for the lubricant-free R-410A is roughly 3 kW/m² greater than that of the R-410A/POE (99.6/0.4) mixture, but has approximately the same nearly constant rate of increase with respect to quality.

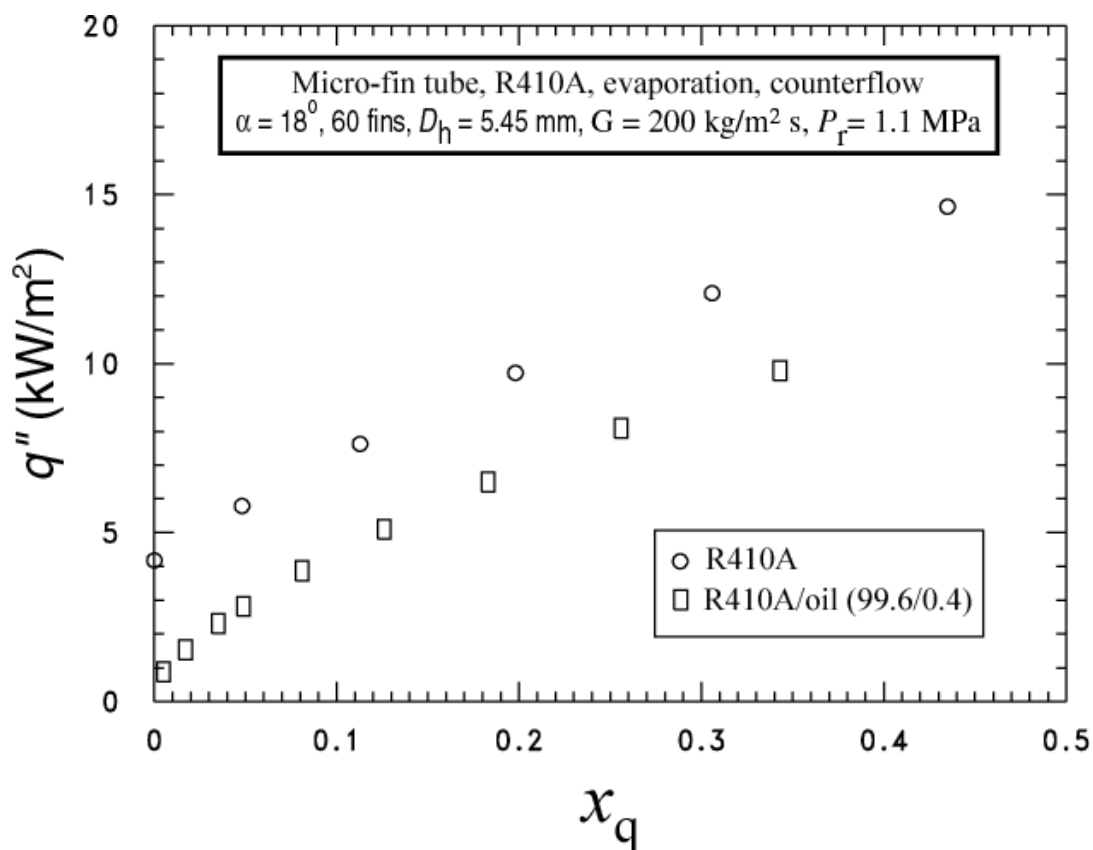


Fig. 4-2: Heat flux distribution for R-410A and R-410A/POE
 (Sawant et al., 2007)

Figure 4-3 shows a plot of the local heat flux as calculated from eq. (4-5) versus thermodynamic quality for lubricant-free R-410A and a R-410A/lubricant mixture for mass fluxes ranging from 200 kg/m²s to 225 kg/m²s. It can be seen that the heat flux of the R-410A/lubricant mixture is consistently less than the heat flux of pure R-410A. In the low mass quality region, heat flux has a tendency to increase as quality increases. This is because, as quality increases, void fraction increases and the liquid film thickness thins and accordingly the wall superheat decreases. During horizontal in-tube evaporation, the liquid film at the top of the tube thins as the refrigerant evaporates, eventually disappearing all together.

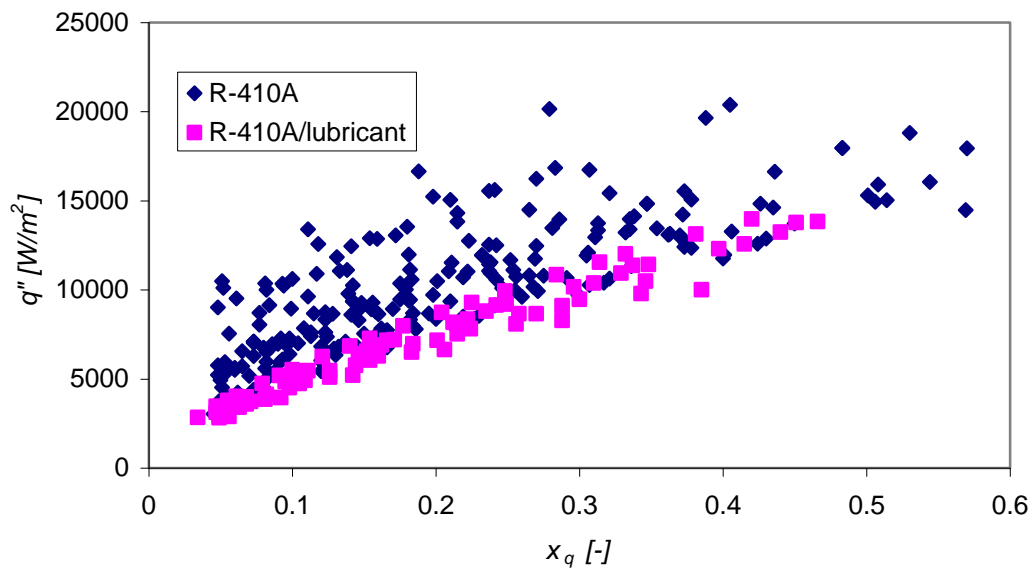


Fig. 4-3: Heat Flux Distribution for Tests with R-410A and R-410A/POE

Figure 4.4 shows variation of heat flux with respect to thermodynamic quality for three different saturation temperatures of 7.2 °C, 8.5 °C, and 9.8 °C. As saturation temperature increases, the ratio of the specific volume of vapor to liquid decreases. As a result, the decrease of bubble buoyancy prevents nucleate boiling. At higher saturation temperatures, heat flux is reduced because a decrease in bubble buoyancy prevents bubble departure and eventually deactivates nucleate boiling.

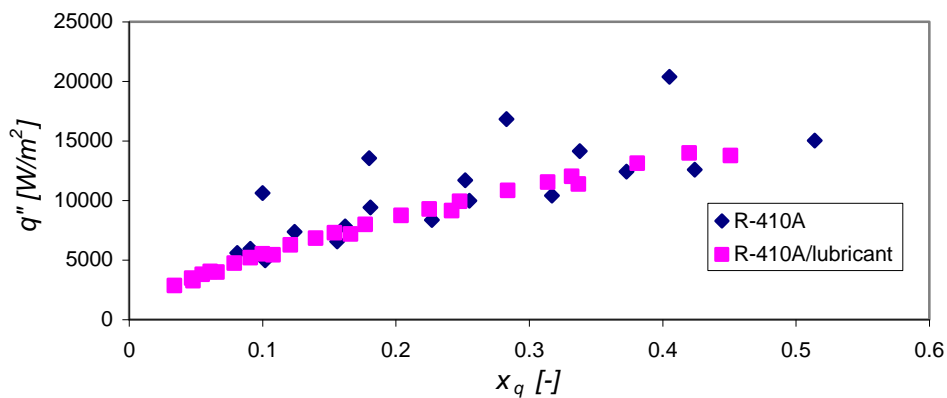
The local Nusselt number (Nu) was calculated using the hydraulic diameter (D_h) and the heat transfer coefficient based on the actual inner surface area of the tube (A_i) as:

$$Nu = \frac{h_{2\phi} D_h}{k_l} \quad (4-6)$$

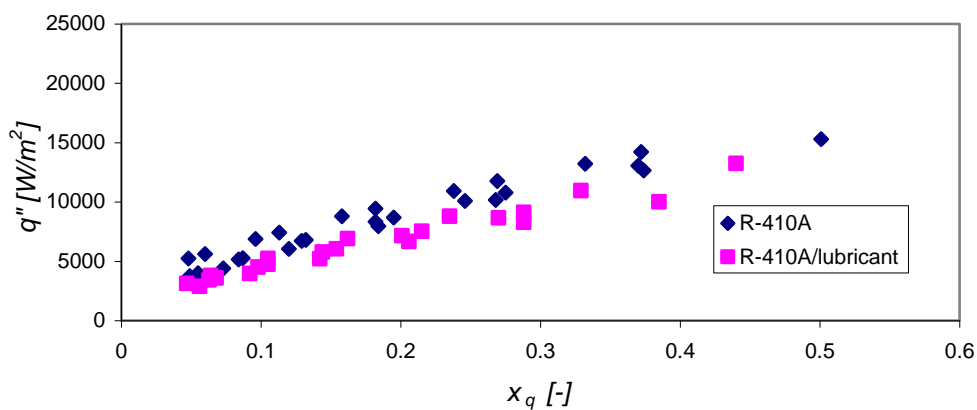
where k_l is the thermal conductivity of the liquid.

The hydraulic diameter was measured with a polar planimeter from a scaled drawing of the tube cross section, but it can be approximated for other tube geometries with fin parameters by expanding on the expression that was given for D_h in Kedzierski and Goncalves (1999):

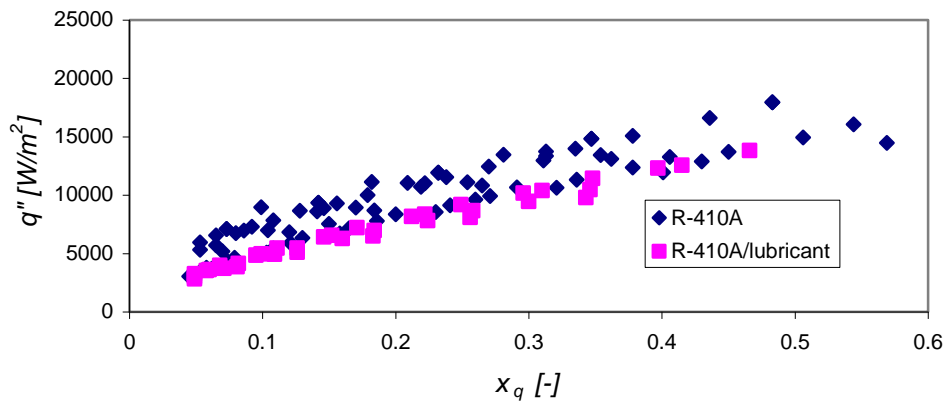
$$D_h = \frac{4A_c \cos \alpha}{N_f S_p} = \frac{(\pi D_r^2 - 2N_f t_b e) \cos \alpha}{s + \frac{2e}{\cos(\beta/2)}} \quad (4-7)$$



a) Saturation Temperature = 7.2 °C



b) Saturation Temperature = 8.5 °C



c) Saturation Temperature = 9.8 °C

Fig. 4-4: Effect of Saturation Temperature on Heat Flux

Figure 3-3 of Chapter 3 shows the fin parameters that are used in eq. (4-7) where S_p is the perimeter of one fin and channel taken perpendicular to the axis of the fin, s is the spacing between the fins, β is the fin-tip angle, e is the fin height, α is the twist angle of the fins, t_b is the thickness of the fin at its base, N_f is the total number of fins, and D_r is the diameter of the tube at the fin root, i.e., fin base.

The hydraulic diameter of the present tube geometry of this study as estimated from eq. (4-7) is 5.2 mm, while that obtained from the planimeter and used in the data reduction was 5.45 mm (Kedzierski et al., 1999). Figure 4-5 illustrates the various fin parameters that were used in the calculation of D_h .

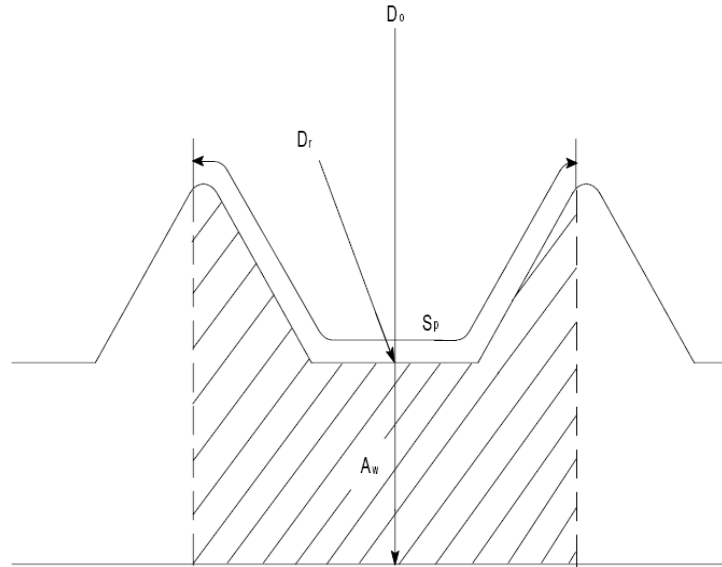


Figure 4-5: Detail Cross Section of Micro-fin Tube

The internal surface area of the fin per unit length (A_i/L) can be estimated from:

$$\frac{A_i}{L} = N_f \left(\frac{s}{\cos \alpha} + \frac{2e}{\cos \alpha \cos(\beta/2)} \right) \quad (4-8)$$

The A_i/L estimated from eq. (4-8) is 46.8 mm, while that obtained from the planimeter and used in the data reduction was 44.6 mm.

Figure 4-6 shows a comparison of the R-410A heat transfer coefficient versus quality to that for the R-410A/POE (99.6/0.4) mixture for a mass flux of approximately 200 kg/m²s.

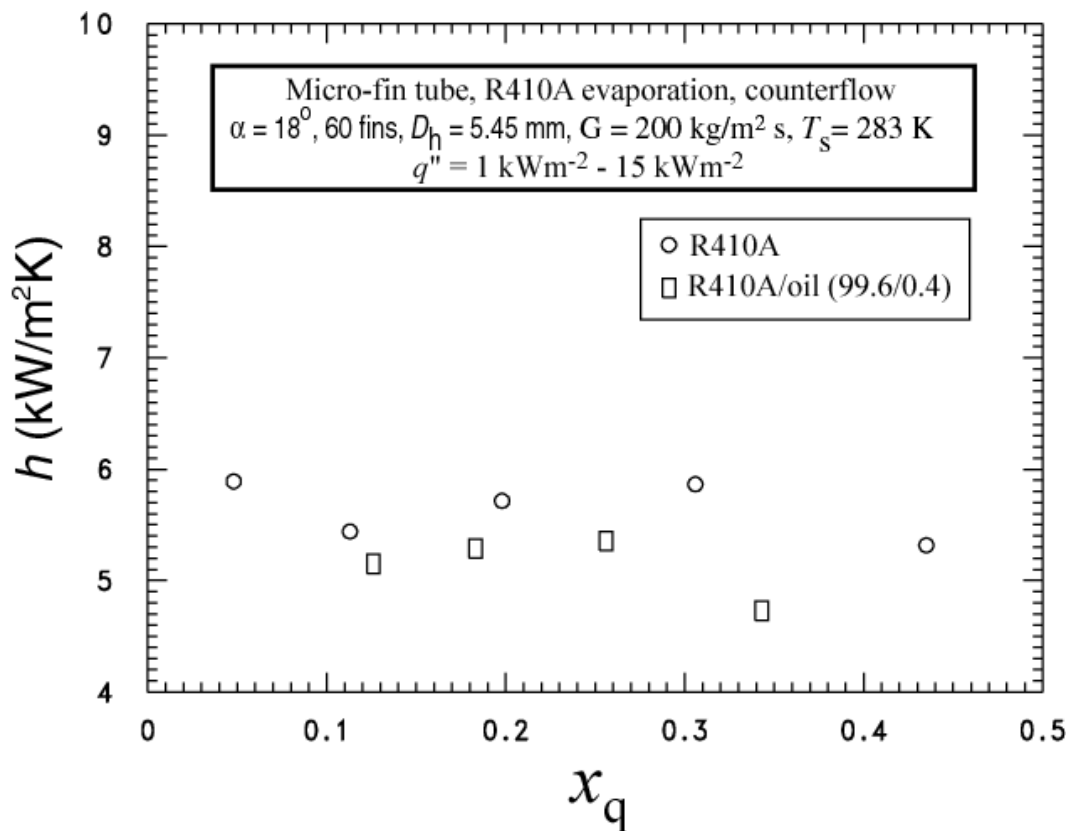


Fig. 4-6: Comparison of the Two-phase Heat Transfer Coefficient for R-410A and R-410A/POE (Sawant et al., 2007)

In general, the measured boiling heat transfer coefficients are nearly constant with respect to quality over the range tested. Thinning of the liquid film on the wall for larger qualities is expected to induce an increase in the heat transfer coefficient. I conjecture that the actual heat transfer increase is not evident because the increase is within the uncertainty of the heat transfer measurement. On an average, the refrigerant-lubricant mixture heat transfer coefficient is approximately $300 \text{ W/m}^2\text{-K}$ less than the pure R-410A heat transfer coefficient, which represent an approximately 6 % degradation in heat transfer due to the lubricant for those particular conditions.

The variation of the two-phase heat transfer coefficient of R-410A versus mass quality is shown in Fig. 4-7. At lower thermodynamic quality, the slight increase in the two-phase heat transfer coefficient is due to activation of nucleate boiling. Cooper (1984) proposed that nucleate boiling heat transfer coefficient is a function of reduced pressure. The figure shows that 0.4 % of lubricant degrades the heat transfer performance of R-410A.

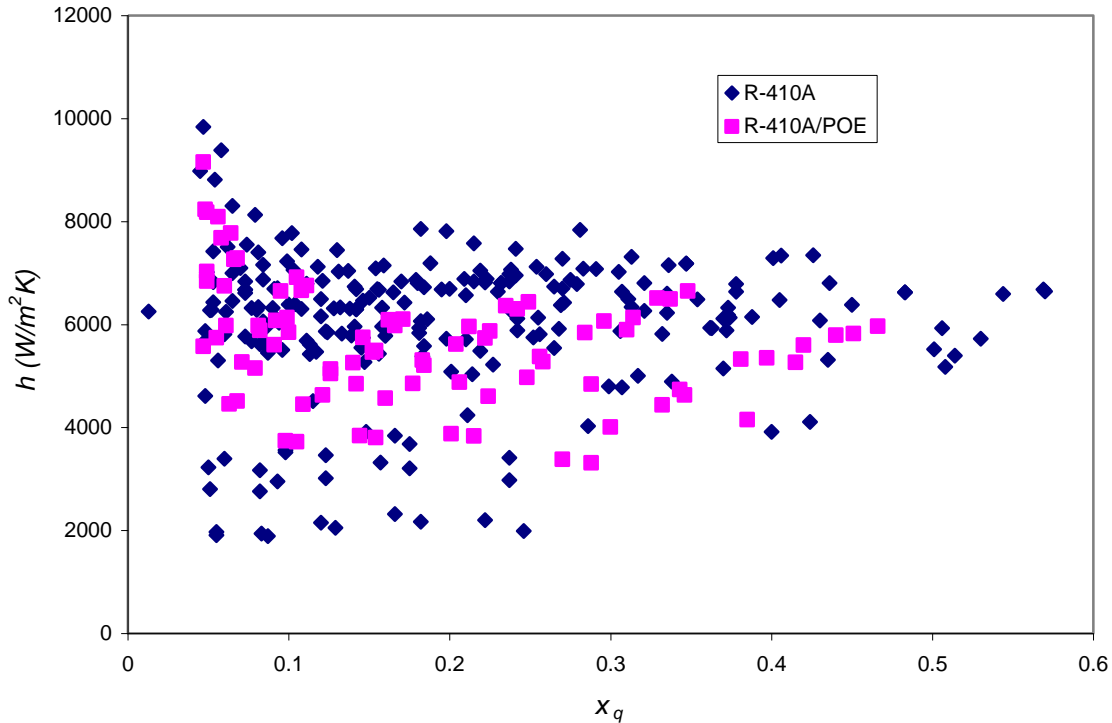


Fig. 4-7: Effect of Lubricant on Two-Phase Heat Transfer Coefficient of R-410A

According to convective boiling heat transfer theory, convective heat transfer characteristics are not directly affected by boiling temperature, but the boiling temperature has an influence through changes in the thermophysical properties of refrigerants as a function of temperature.

The next chapter focuses on comparing my data with several two-phase in-tube boiling heat transfer correlations.

Chapter 5

COMPARISON WITH CORRELATIONS

Since flow boiling is an important mode of heat transfer encountered in many heat exchangers, accurate estimation of the heat transfer coefficient can help lead to economic savings in the design and operation of HVAC&R systems. With an aim to improve the design of heat exchangers, researchers in the HVAC&R industry have proposed a large number of correlations for flow boiling. Prior to listing correlations relevant to this study, some of the dimensionless numbers that impact flow boiling will be discussed.

5.1 Principal Dimensionless Numbers

During in-tube convective boiling heat transfer, the heat transfer coefficient consists of contributions from nucleate and convective boiling. The boiling number is a non-dimensional number introduced to relate the effects of heat flux and mass velocity in the flow boiling process. It can be thought of as the ratio of mass of vapor generated per unit area of heat transfer surface to the mass flow rate per unit flow cross-sectional area. This dimensionless group was first used by Davidson et al. (1943). They argued that it represented the stirring effect of the bubbles upon the flow. Regardless, it may be thought of as a measure of the nucleate boiling contribution. As heat flux increases, nucleation is increased. Also, increased mass velocity results in a higher convective heat transfer coefficient.

The boiling number is given by:

$$Bo = \frac{q}{Gh_{fg}} \quad (5-1)$$

The Lockhart-Martinelli parameter, X_{tt} , is a second important non-dimensional parameter defined as the ratio of the pressure drops from a liquid-only flow to that of a gas-only flow (Lockhart and Martinelli, 1947).

$$X_{tt} = \sqrt{\frac{\left(\frac{dP}{dz}\right)_l}{\left(\frac{dP}{dz}\right)_g}} \approx \left(\frac{1-x}{x}\right)^{0.9} \left(\frac{\rho_g}{\rho_l}\right)^{0.5} \left(\frac{\mu_l}{\mu_g}\right)^{0.1} \quad (5-2)$$

Shah (1976) defined the Convection number as a replacement to the Lockhart-Martinelli parameter since viscosity effects were found to be unimportant.

$$Co = \left(\frac{1-x}{x}\right)^{0.8} \left(\frac{\rho_g}{\rho_l}\right)^{0.5} \quad (5-3)$$

The Froude number, Fr , is the ratio of inertia forces to gravitational forces and is given in eq. (5-4). In horizontal flow, it can be considered as a measure of the wall wetness or a definition of whether part of the tube circumference is dry. It accounts for partial wall wetting, which may occur in horizontal channels (Webb and Gupte, 1992).

$$Fr_l = \frac{G^2}{\rho_l^2 gD} \quad (5-4)$$

Researchers in the HVAC&R industry have attempted to represent convective vaporization in terms of three types of models: the superposition, asymptotic, and enhancement models (Webb and Gupte, 1992). These terms describe techniques for combining the nucleate boiling and convective contributions. The “superposition” model assumes that the total heat flux is the sum of the nucleate boiling component and the convective evaporation component. The “asymptotic” model is descriptive of the asymptotes that the model possesses. In the “enhancement” model, an enhancement factor is utilized. In this type of model, the two-phase heat transfer coefficient has the form of an enhancement to single-phase heat transfer coefficient of a flowing liquid by a two-phase enhancement factor. Appendix B lists correlations for each of these types of models.

The following sections consider three studies by Kim et al. (2002), Ding et al. (2008), and Hamilton et al. (2005). All of these studies employed micro-fin tubes in their research with R-410A. While Hamilton et al. (2005) used fluid heating for their research, Kim et al. (2002) and Ding et al. (2008) used the electrical resistance heating method. The correlations from these three studies are compared to the heat transfer measurements.

Much more work has been done on in-tube flow boiling with pure refrigerants and refrigerant-mixtures in smooth tubes than for tubes with enhanced surfaces. However, the representation of the effect of lubricant on in-tube flow boiling with pure refrigerants and refrigerant-mixtures in terms of correlation is not well understood or studied. Schlager et al. (1990), Eckels et al. (1994 and 1998a), Usmani and Ravigururajan (1999), and Ding et al. (2008) are the studies that provide correlations for refrigerant-lubricant mixture flow boiling inside horizontal micro-fin tubes. Ding et al. (2008) is the only study that uses

properties of the lubricant to arrive at their correlation. Wei et al (2007b) and Hambraeus (1995) used properties of refrigerant-lubricant mixtures in their studies on smooth tubes by considering a thermodynamic approach, which resembles Thome's (1995) approach. The mixture properties were used to replace the pure refrigerant properties to address the influence of lubricant on heat transfer.

5.2 Correlation by Kim et al. (2002)

Kim et al. (2002) developed a model using non-dimensional parameters that account for the heat transfer enhancement of micro-fin tubes over smooth ones. Their model attempts to capture the physics of the physical phenomena in a basic form used for smooth tube correlations. In addition to the non-dimensional parameters Boiling number and Lockhart-Martinelli parameter, Kim et al. (2002) also included other parameters such as surface tension, fin height, liquid film thickness, evaporating temperature and fluid properties. A modified Reynolds number was included in their correlation to capture the turbulent flow effects caused by the micro-fins.

This correlation for micro-fin tubes has essentially had the form of a smooth tube correlation. The authors argued that, during two-phase heat transfer, as the surface tension of the thin liquid film changes, the wetting characteristic of the micro-fin tube surface is affected. They included the non-dimensional parameter, S , to account for effects related to surface tension and turbulence during nucleate boiling that improved evaporation heat transfer at low qualities. Another non-dimensional parameter of the ratio of liquid film

thickness to fin height was introduced to account for maximizing thermal fin efficiency during convective boiling.

The final proposed correlation of Kim et al. (2002) is:

$$\frac{h_{tp}}{h_l} = \left[C_1 x^{Bo} C_2 \left(\frac{P_{sat} x D_i}{\sigma} \right)^{C_3} + C_4 x \left(\frac{1}{X_{tt}} \right)^{C_5} \left(\frac{Gf}{\mu_l} \right)^{C_6} \right] Re_l^{C_7} Pr_l^{C_8} \left(\frac{\delta}{f} \right)^{C_9} \quad (5.5)$$

P_{sat} is the saturation pressure, D_i is the maximum inside diameter of microfin tube; D_r is the diameter of microfin tube at fin root; f is the fin height; and σ is the surface tension of the thin liquid film. The values for coefficients C1 through C9 for the correlation (eq. 5.5) are given in Table 5-1. The liquid film thickness, δ , is calculated as:

$$\delta = \frac{D_r(1-\varepsilon)}{4} \quad (5.6)$$

where the void fraction, ε , is given by:

$$\varepsilon = \left(\frac{x}{\rho_g} \right) \left[(1 + 0.12(1-x)) \left(\frac{x}{\rho_g} + \left(\frac{(1-x)}{\rho_g} \right) \right) + \left(\frac{1.18(1-x)(g\sigma(\rho_l - \rho_g))^{0.25}}{G\rho_l^{0.5}} \right) \right]^{-1} \quad (5.7)$$

Table 5-1: Coefficients of Correlation by Kim et al. (2002)

Coefficient	Value	Coefficient	Value
C1	0.009622	C6	-0.7360
C2	0.1106	C7	0.2045
C3	0.3814	C8	0.7452
C4	7.6850	C9	-0.1302
C5	0.5100		

The database of Kim et al. (2002) included a wide range of inner tube diameters from 8.82 to 14.66 mm, fin heights from 0.12 to 0.381 mm, spiral angles from 16° to 30° , mass fluxes from 50 to 637 kg/m²s, heat fluxes from 5 to 39.5 kW/m², and evaporating temperatures from -15 to 70 °C. The five different refrigerants considered were R-22, R-113, R-123, R-134a, and R-410A.

To seek validation, the proposed correlation was then compared with studies that involved augmentation techniques, especially micro-fin tubes. Kim et al. (2002) showed 90 % of their experimental data to correlate with eq. (5-5) within a deviation of ± 30 %. The authors showed that, for their proposed correlation, the mean deviation was 20.5 % and the average deviation was -11.7 % when compared with eleven studies from the literature in the past, including Thome et al. (1997) and Cavallini et al. (1999). The authors compared correlation by Thome et al. (1997) with the same eleven studies from the literature in the past. The Thome et al. (1997) correlation yielded a mean deviation of 64.4 % and an average deviation of 51.5 %. Similarly, the correlation by Cavallini et al. (1999) yielded a mean deviation of 36.4 % and an average deviation of -16.1 %.

Figure 5-1 compares the measured two-phase heat transfer coefficient of R-410A/lubricant mixtures of the current study with the two-phase heat transfer coefficients calculated using the correlation of Kim et al. (2002). The correlation predicted approximately 30 % of the experimental data to within ± 30 %. The correlation of Kim et al. (2002) did not provide satisfactory prediction of the experimental data. One of the primary reasons is that the correlation of Kim et al. (2002) does not consider the influence of either refrigerant-mixtures or the effect of lubricant on the evaporation heat transfer of

the refrigerants studied. The correlation does not consider the influence of mixture properties. In addition, most of the heat transfer coefficients provided in the literature were based on micro-fin tube equivalent diameter or the root-diameter.

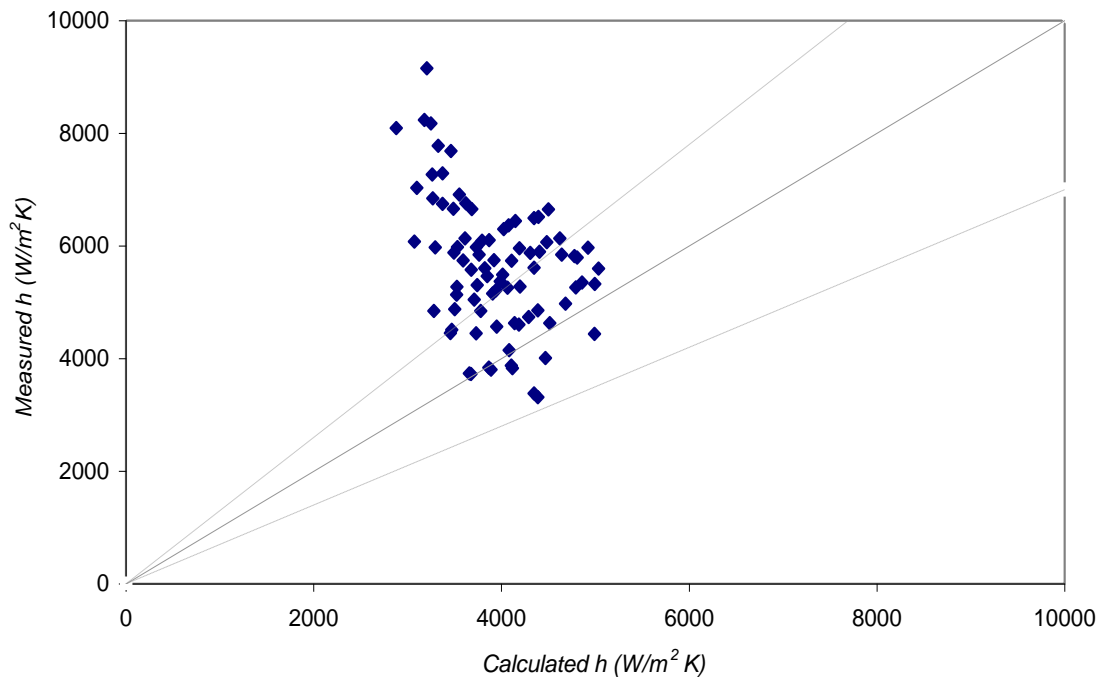


Fig. 5-1: Comparison of Experimental Data with Correlation of Kim et al. (2002)

The poor predictability can also be attributed to not knowing what effect the presence of lubricant will have on the non-dimensional parameters such as S and the ratio of film thickness to fin height, which are a primary contribution of the Kim et al. (2002) correlation. The use of electrical resistance heating instead of fluid heating may also play a part in the discrepancy.

5.3 Correlation by Ding et al. (2008)

Ding et al. (2008) presented a new correlation to predict the local flow boiling behavior of R-410A-lubricant mixtures inside a straight micro-fin tube based on the local properties of the refrigerant-lubricant mixture. The study also revealed that the presence of lubricant enhances heat transfer at low vapor qualities ($x < 0.4$); whereas, at higher vapor qualities ($x > 0.4$) the heat transfer coefficient drops sharply with increase in the nominal lubricant concentration. Based on the Gungor and Winterton (1986) model, the new correlation is the sum of a convective contribution and a nucleate boiling contribution and accounts for mixture properties of the refrigerant-lubricant. The convection multiplier and boiling suppression numbers were redefined for micro-fin tube geometry.

The test section employed a straight micro-fin tube with outside diameter of 7 mm. The lubricant used was ester-based with commercial ISO grade 68 with density of 964 kg/m³. The local flow boiling heat transfer coefficient for refrigerant-lubricant mixtures was calculated as per Thome (1995). Ding et al. (2008) reported heat transfer data for two of their six subsections so that they were considering only fully developed thermal and momentum boundary layers. For refrigerant-lubricant mixtures, the local vapor quality was defined as the total mass of vapor divided by the total mass of fluid (refrigerant plus lubricant). The local lubricant concentration was calculated as:

$$\omega_{local} = \frac{m_o}{m_o + m_{r,L}} = \frac{\omega_{no}}{1 - x_{r,o}} \quad (5-8)$$

where the nominal lubricant concentration, ω_{no} , is given by:

$$\omega_{no} = \frac{m_o}{(m_o + m_r)} \quad (5-9)$$

The experimental data was compared with correlations of Cavallini et al. (1998), Yun et al. (2002), Thome et al. (1997), Goto et al. (2001), and Kandlikar and Raykoff (1997). Because none of the correlations could predict the experimental data of R-410A/lubricant satisfactorily, a new correlation was developed which used the refrigerant-lubricant mixture properties.

The heat transfer coefficient of R-410A-lubricant mixtures, $\alpha_{r,o,tp}$, is the sum of the convective contribution ($E\alpha_{r,o,L}$) and the nucleate boiling contribution ($S\alpha_{r,o,nb}$), similar to Gungor and Winterton (1986).

$$\alpha_{r,o,tp} = E\alpha_{r,o,L} + S\alpha_{r,o,nb} \quad (5-10)$$

where $\alpha_{r,o,L}$ is the heat transfer coefficient of the liquid component flowing alone inside a microfin tube which incorporated the ribbed tube enhancement factor E_{RB} ; $\alpha_{r,o,nb}$ is the nucleate boiling coefficient recommended by Gungor and Winterton (1986); E and S are the two-phase convection multiplier and the two-phase boiling suppression factor, respectively.

$$\alpha_{r,o,L} = E_{RB}\alpha_{r,o,DB} \quad (5-11)$$

$$\alpha_{r,o,DB} = 0.023 \frac{\lambda_{r,o,L}}{d_f} \text{Re}_{r,o,L}^{0.8} \text{Pr}_{r,o,L}^{0.4} \quad (5-12)$$

$$\alpha_{r,o,nb} = 55 P_{re}^{0.12} (-\log_{10} P_{re})^{-0.55} M^{-0.5} q_{im}^{0.67} \quad (5-13)$$

$$E_{RB} = \left\{ 1 + \left[2.64 \text{Re}_{r,o,L}^{0.036} \text{Pr}_{r,o,L}^{-0.024} \left(\frac{e_f}{d_f} \right)^{0.212} \left(\frac{l_f}{d_f} \right)^{-0.21} \left(\frac{\beta_f}{90} \right)^{0.29} \right]^7 \right\}^{1/7} \quad (5-14)$$

where $\alpha_{r,o,DB}$ is the heat transfer coefficient of the liquid component flowing alone inside a smooth tube calculated using the Dittus-Boelter correlation (Dittus and Boelter, 1930); E_{RB} is the ribbed tube enhancement factor for single-phase turbulent tube flow (Ravigururajan and Bergles, 1985); $\lambda_{r,o,L}$ is the thermal conductivity of the R-410A-lubricant mixture liquid component; P_{re} is the reduced pressure; d_f is the diameter at fin root; e_f is the microfin height; l_f is the axial pitch from fin to fin; β_f is the helix angle of the microfin; $\text{Re}_{r,o,L}$ is the liquid-phase Reynolds number; and $\text{Pr}_{r,o,L}$ is the liquid Prandtl number. The Reynolds number and Prandtl number are calculated as:

$$\text{Re}_{r,o,L} = \frac{G(1-x_{r,o})d_f}{\mu_{r,o,L}} \quad (5-15)$$

$$\text{Pr}_{r,o,L} = \frac{c_{p,r,o,L} \mu_{r,o,L}}{\lambda_{r,o,L}} \quad (5-16)$$

where $c_{p,r,o,l}$ and $\mu_{r,o,L}$ are the isobaric specific heat and dynamic viscosity of the R-410A/lubricant mixture liquid component, respectively.

The two-phase convection multiplier E and boiling suppression factor S were redefined for microfin tubes as:

$$E = 1 + 33,686.87 Bo^{1.16} + 1.169 X_{tt}^{-0.86} \quad (5.17)$$

$$S = 1 + 2.53 \times 10^{-6} E^{1.489} Re_{r,o,L}^{1.17} \quad (5.18)$$

where the Boiling number (Bo) and Lockhart-Martinelli's parameter (X_{tt}) are given by:

$$Bo = \frac{q}{G h_{fg}} \quad (5.19)$$

$$X_{tt} = \left(\frac{(1 - x_{r,o})}{x_{r,o}} \right)^{0.9} \left(\frac{\rho_{r,V}}{\rho_{r,o,L}} \right)^{0.5} \left(\frac{\mu_{r,V}}{\mu_{r,o,L}} \right)^{0.1} \quad (5.20)$$

In eqs. 5-19 and 5-20, h_{fg} is the latent heat of evaporation, q is the heat flux; G is mass flux; $\rho_{r,V}$ and $\mu_{r,V}$ are the vapor-phase density and the vapor-phase dynamic viscosity of R-410A, respectively; $\rho_{r,o,L}$ is the density of the R-410A/lubricant mixture liquid component.

The proposed correlation by Ding et al. (2008) for the local heat transfer coefficient agreed with 89 % of their experimental data with a deviation of ± 30 %.

Figure 5-2 shows the comparison of the measured two-phase local heat transfer coefficient of my study versus the calculated two-phase local heat transfer coefficient as correlated by Ding et al. (2008). The comparison was expected to yield satisfactory results because both studies employed R-410A/lubricant mixtures in micro-fin tubes. However, as seen from the figure, the results do not agree well. Approximately 10 % of the experimental data fit the correlation of Ding et al. (2008) with a deviation of $\pm 30\%$.

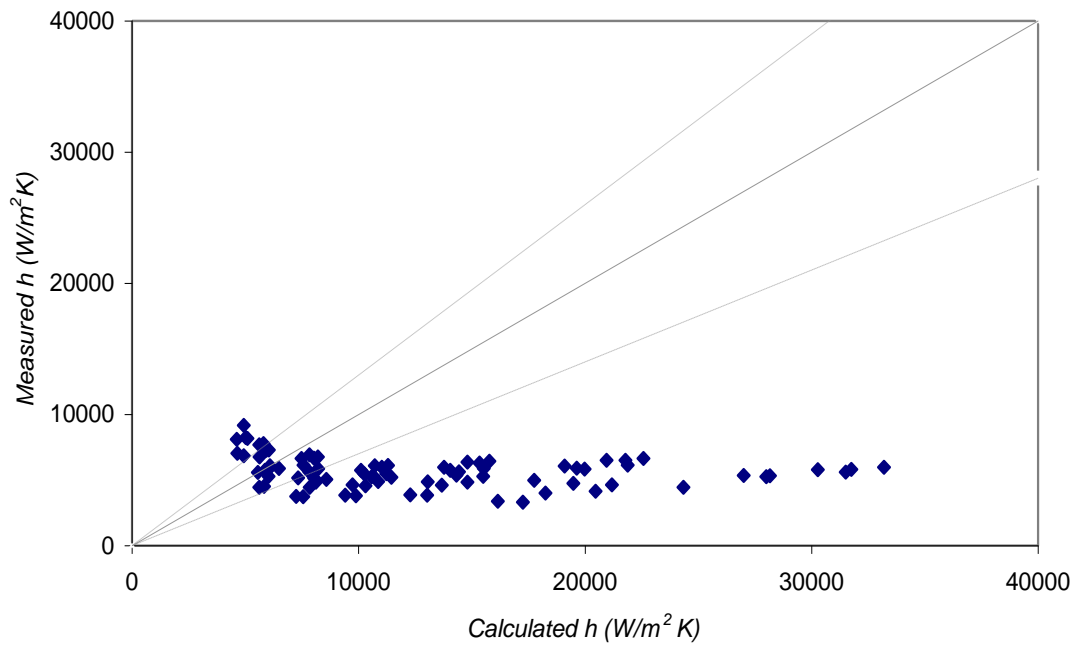


Fig. 5-2: Comparison of Experimental Data with Correlation of Ding et al. (2008)

5.4 Correlation by Hamilton et al. (2005)

Hamilton et al. (2005) correlated micro-fin-tube-convective boiling Nusselt numbers for four pure refrigerants: R-22, R-32, R-125, and R-134a; and four refrigerant mixtures: R-410B (R-32/R-125 (45/55)), R-32/R-134a (27/73 and 30/70) and R-407C (R-32/R-125/R-134a (25/23/52)) to a single expression consisting of a product of dimensionless properties: (Note: the numbers in parenthesis represent mass percentages of the refrigerants contained in the blends.)

$$Nu = 482.18 Re^{0.3} Pr^{C_1} \left(\frac{P_r}{P_c} \right)^{C_2} Bo^{C_3} \left(-\log_{10} \frac{P_r}{P_c} \right)^{C_4} M_r^{C_5} 1.1^{C_6} \quad (5-21)$$

where

$$C_1 = 0.51 x_q$$

$$C_2 = 5.57 x_q - 5.21 x_q^2$$

$$C_3 = 0.54 - 1.56 x_q + 1.42 x_q^2$$

$$C_4 = -0.81 + 12.56 x_q - 11.00 x_q^2$$

$$C_5 = 0.25 - 0.035 x_q^2$$

$$C_6 = 1/T_s ((T_{LV} - T_{MV})\{279.8(x_v - x_l) - 4298(T_d - T_b)/T_s\})$$

The limits of applicability for the correlation are:

$$70 \text{ kg/m}^2\text{s} < G_r < 370 \text{ kg/m}^2\text{s} \quad \text{and} \quad 0 < x_q < 0.7$$

The correlation was shown by Hamilton et al. (2005) to predict some of the existing data from the literature (Nidegger et al., 1997, Zurcher et al., 1997, Kim et al., 2002, Seo and Kim (2000), and Chamra and Webb (1995)) to within ± 20 %. Cooper (1984) suggested that the fluid properties that govern nucleate pool boiling can be well represented by a product of the reduced pressure (P_r/P_c), the acentric factor ($-\log_{10}(P_r/P_c)$),

and other dimensionless variables. The all-liquid Reynolds number (Re), the Boiling number (Bo), the liquid Prandtl number (Pr), the reduced pressure (P_r/P_c), and the quality (x_q) were all evaluated locally at the saturation temperature. M_r is the molar mass of the refrigerant in g/mol.

The all-liquid Reynolds number and the Nusselt number are based on the hydraulic diameter. Also, the Nusselt number is based on the actual inner surface area of the tube. The T_d and T_b are the dew point temperature and the bubble point temperature of the mixture, respectively, evaluated at the local saturation pressure and overall composition. The T_{LV} and the T_{MV} are the saturation temperatures of the least volatile (pure) component and the most volatile component, respectively, evaluated at the saturation pressure of the mixture. The mass fraction of the vapor (x_v) and that of the liquid (x_l) are evaluated at the saturation pressure and the local thermodynamic quality, while the overall composition is the all-liquid or all-vapor value. The constant C_6 is zero for pure refrigerants.

Figure 5-3 provides a comparison of the Nusselt numbers predicted with eq. (5-21) for the micro-fin tube to those measured in this study for lubricant-free R-410A and the R-410A/POE mixture. Approximately 71 % of the measured, lubricant-free data fall within ± 20 % of the predicted data. The lubricant-free measurements that fell outside the ± 20 % region of the predicted data were for conditions that were very close to those of the measurements that were well predicted. No justifiable reason was found to identify these points as outliers. Figure 5-3 also shows that eq. (5-21) predicts 83 % of the R-410A/POE Nusselt numbers to within ± 20 %. The R-410A/POE predictions were made using the R-410A/POE mixture liquid viscosity and liquid density evaluated at the local lubricant mass

fraction to calculate the Re and Pr in eq. (5-15). Use of the lubricant properties in the correlation caused between a 0.3 % and a 0.8 % reduction in the Nusselt number as compared to results using the lubricant-free R-410A properties alone.

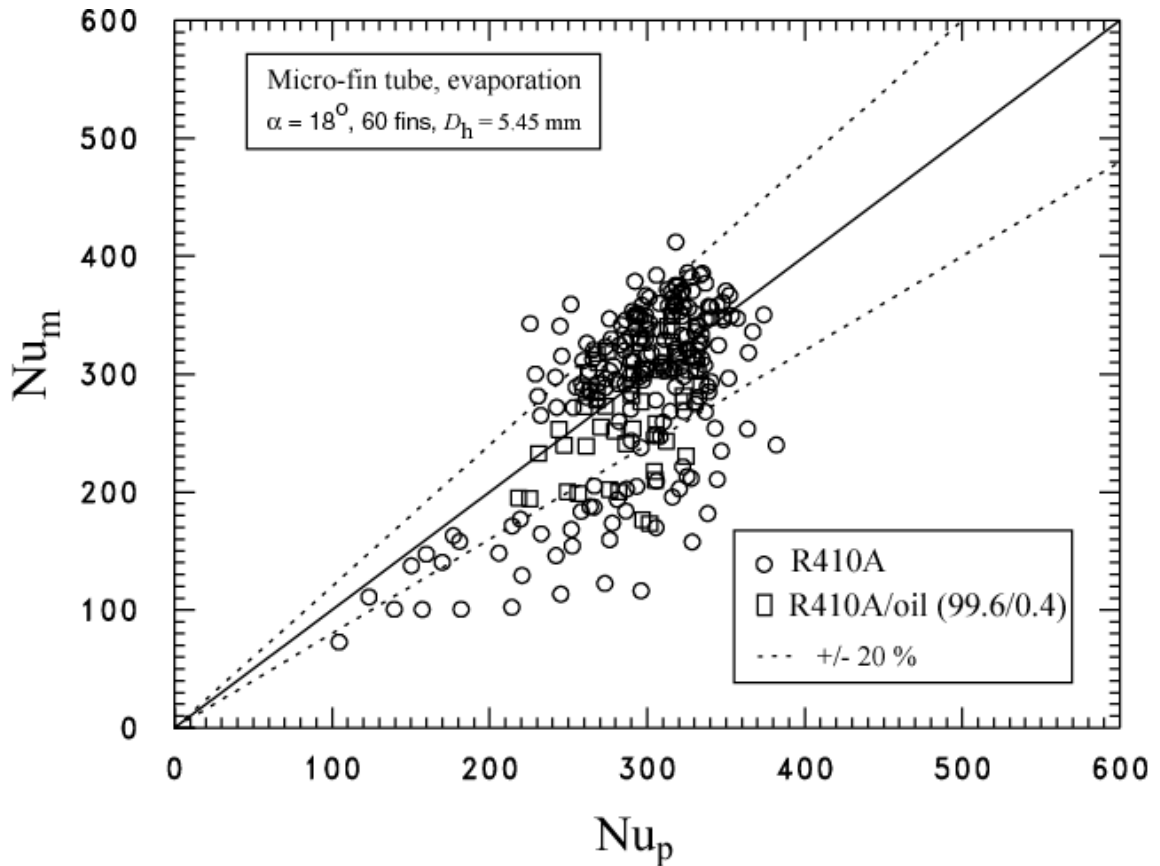


Fig. 5-3 Comparison of Experimental Data with Correlation of Hamilton et al. (2005)

The heat transfer degradation due to lubricant, ΔNu_d was calculated as:

$$\Delta Nu_d = 100 \left(\frac{Nu_p - Nu_m}{Nu_p} \right) \quad (5-22)$$

where Nu_p is the Nusselt number obtained from the lubricant-free correlation (eq. (5-21)) using the lubricant-free R-410A properties, while Nu_m is the Nusselt number obtained from the measured refrigerant/lubricant mixture heat transfer data.

Figure 5-4 shows the heat transfer degradation due to the lubricant (ΔNu_d) as a function of the thermodynamic quality for all of the measured R-410A/POE data. The figure shows that the degradation in heat transfer due to the addition of 0.4 % mass fraction is between -20 % and +42 % exhibiting no apparent relationship with respect to quality.

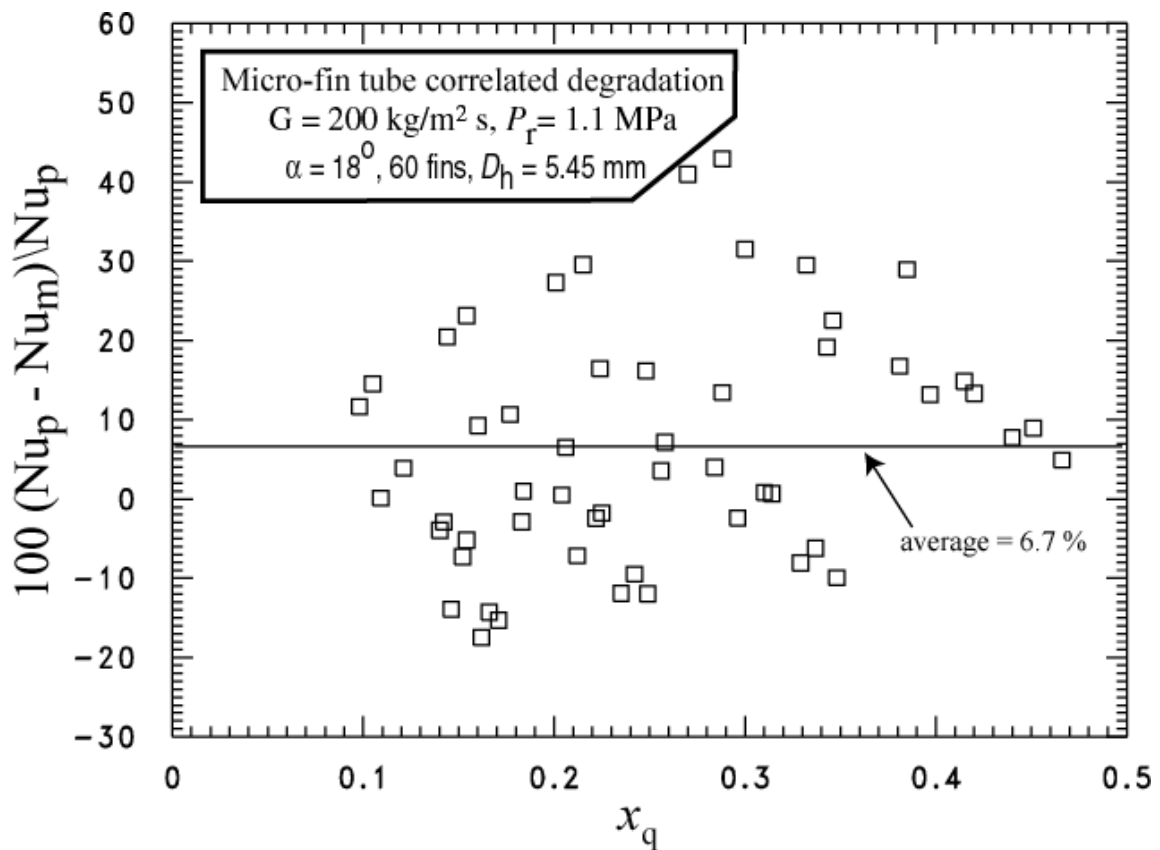


Fig. 5-4 Apparent Heat Transfer Degradation due to Lubricant with Correlation of Hamilton et al. (2005)

The average degradation due to the presence of the lubricant was approximately 6.7 %, which is within the uncertainty of both the measurements and the predictions.

Of the three correlations considered here when compared with experimental data, the correlation of Hamilton et al. (2005) was the one that captured most of the physics and was able to correlate the data the best, whereas, the correlations of Kim et al. (2002) and Ding et al. (2008) were less able to predict the measured data.

Thus, I chose to develop a new model to predict the experimental behavior of the flow boiling of R-410A-lubricant mixtures in micro-fin tubes since some of the correlations is fully capable of describing the data adequately. The objective for the model is to be able to predict behavior of lubricant-free refrigerants, refrigerant-mixtures, and refrigerant-lubricant mixtures for flow boiling studies. The results can then be used to design efficient heat exchangers for the air conditioning, heating and refrigeration industry.

Chapter 6

MODEL DEVELOPMENT

6.1 Introduction

In nearly all HVAC&R systems, the compressor uses lubricant to prevent the wear and tear of moving parts. Some amount of the lubricant migrates and circulates together with the refrigerant through the system. The circulating lubricant has an effect on the boiling performance of the refrigerant due to accumulation of lubricant on the heat transfer surfaces. Several researchers have investigated how lubricant affects the flow boiling heat transfer process. Some examples include Worsoe-Schmidt (1960), Green and Furse (1963), Chaddock and Mathur (1979), Tichy et al. (1986), Schlager et al. (1990), Kedzierski and Kaul (1993), Hambraeus (1995), Nidegger et al. (1997), Lottin et al. (2003), Cremaschi et al. (2005) and Ding et al. (2008). (See Chapter 2 for more detailed discussion.)

Most of the studies emphasized the role lubricant concentration plays on the performance of refrigerant flow boiling heat transfer, with Jensen and Jackman (1984) concluding that high lubricant concentration reduces the overall heat transfer coefficient. As the volatile refrigerant evaporates quickly at the vapor-liquid interface, the liquid layer close to the interface becomes lubricant-rich, which increases surface tension. As a result, the lubricant layer suppresses the growth of bubbles, thereby reducing the heat transfer coefficient. On the other hand, some studies attributed an observed enhancement of flow

boiling heat transfer to the phenomenon of foaming. Stephan (1963) was one of the first researchers to connect foaming and refrigerant-lubricant evaporation and to note that a lubricant-rich layer exists near the wall. Burkhardt and Hahne (1979), however, contradict these hypotheses by concluding that the lubricant must affect pool boiling other than through only foaming or liquid-vapor surface tension effects. They concluded this because lubricant influences flow boiling through factors such as the saturation pressure, lubricant concentration, tube geometry, range of heat flux, refrigerant-lubricant mixture properties, properties of lubricant (viscosity, miscibility, surface tension, etc), etc.

For example, Sauer et al. (1978) concluded that lubricant viscosity and surface tension effects were important in determining the magnitude of the nucleate boiling of refrigerants, but were unable to correlate these effects.

6.2 Thome's Model (1995)

Thome (1995) pointed out that the historical approach of using the saturation temperature of pure refrigerant to reduce the data for calculation of the heat transfer coefficient was inadequate. This approach ignored the fact that the refrigerant-lubricant combination behaves as a zeotropic mixture whose properties are dependent on the equilibrium compositions of the coexisting phases. Additionally, it does not allow for the type of lubricant and its properties to be included in the calculations.

According to Thome (1996), the flow boiling heat transfer coefficient of a refrigerant-lubricant mixture can be affected by the lubricant in three ways: (a) the increase of nucleate boiling due to the presence of lubricant can enhance flow boiling; (b) the

higher viscosity of the refrigerant-lubricant mixture can cause degradation in heat transfer; and (c) the mass diffusion occurring during nucleate boiling due to addition of lubricant may decrease the convective heat transfer coefficient.

Since most of the lubricants have good solubility with the refrigerants, Thome (1995) advocated a thermodynamic approach where the refrigerant-lubricant mixture is treated as a zeotropic mixture with a temperature glide. The lubricant should be considered as a component in the mixture that changes the bubble temperature, temperature-enthalpy relationship, etc. Therefore, in the approach of Thome (1995), the properties of the refrigerant-lubricant mixture were used instead of the properties of pure refrigerant. On the basis of this method the local boiling heat transfer coefficient (h) becomes:

$$h = \frac{q''}{(T_w - T_{bub})} \quad (6-1)$$

In Equation (6-1), T_w is the wall temperature and T_{bub} is the local bubble point temperature of the bulk liquid mixture. The use of the mixture bubble point temperature, as opposed to the previous use of the pure refrigerant saturation temperature, not only allows for the correct thermodynamic definition of the local heat transfer coefficient but also requires knowledge of the local refrigerant-lubricant liquid composition. Thome assumed that no appreciable amount of lubricant entered the vapor phase. To determine the liquid composition at some point in a typical evaporator, the heat absorbed by the refrigerant up to that point must be known. This is usually portrayed in a temperature-

enthalpy plot or heat release curve. The task of evaporator design for a given refrigerant-lubricant combination can be accomplished with knowledge of the heat transfer coefficient from a pure fluid correlation and the actual bubble temperature of the mixture from a temperature-enthalpy plot.

Thome (1995) introduced the empirical equation proposed by Takaishi and Oguchi (1987) to obtain the local bubble point temperature.

$$T_{bub} = \frac{A(\omega_{oil})}{\ln(P_{sat}) - B(\omega_{oil})} \quad (6-2)$$

where $A(\omega_{oil}) = a_0 + a_1\omega_{oil} + a_2\omega_{oil}^3 + a_3\omega_{oil}^5 + a_4\omega_{oil}^7$ (6-3)

and $B(\omega_{oil}) = b_0 + b_1\omega_{oil} + b_2\omega_{oil}^3 + b_3\omega_{oil}^5 + b_4\omega_{oil}^7$ (6-4)

P_{sat} is the saturation pressure; ω_{oil} is the lubricant mass fraction, where the coefficients in eq. (6-3) and eq. (6-4) are given in Table 6-1.

Table 6-1: Values of Empirical Constants

$a_0 = -2394.5$	$a_1 = 182.52$	$a_2 = -724.21$	$a_3 = 3868.0$	$a_4 = -5268.9$
$b_0 = 9.0736$	$b_1 = -0.72212$	$b_2 = 2.3914$	$b_3 = -13.779$	$b_4 = 17.066$

The values for a_0 and b_0 were replaced in order to generalize eq. (6-2) for refrigerants other than HCFC-22 and for a broader range of temperatures. The values of a_1 , a_2 , a_3 , a_4 , b_1 , b_2 , b_3 , and b_4 were fitted to experimental data to account for the partial pressure of lubricant. However, because the partial pressure of lubricant is negligible, the

effect of the type of lubricant on constants $a1$, $a2$, $a3$, $a4$, $b1$, $b2$, $b3$, and $b4$ was found to be negligible.

Due to the variation of bubble temperature, the heat required to evaporate a mixture from some starting condition up to the desired local condition is determined not only by the latent change, but also sensible heat transfer is involved in the evaporation of refrigerant-lubricant mixtures. Thome (1995) recommended the following equation to obtain the local change in enthalpy:

$$dH = h_{LV}dx + (1-x)dT_{bub}(C_p)_L + dT_{bub}(C_p)_V \quad (6-5)$$

where, h_{LV} is the latent heat of vaporization of the refrigerant, x is the local vapor quality, $(c_p)_L$ is the specific heat of the liquid refrigerant-lubricant mixture, $(c_p)_V$ is the specific heat of the pure refrigerant vapor. The values of $(c_p)_L$ and $(c_p)_V$ are a function of the local lubricant concentration and bubble point temperature, while h_{LV} is a function of the bubble point temperature only.

The author emphasized that the local lubricant concentration in the liquid phase is a key factor to obtain local mixture properties.

$$\omega_{local} = \frac{\omega_{inlet}}{(1-x)} \quad (6-6)$$

6.3 Semi-theoretical model by Kedzierski (2003)

Heat exchanger designers are interested in knowing the effect of lubricant on the performance of the evaporator. In recent years, research emphasis has focused on

investigating the effects of lubricant-refrigerant phase separation, lubricant viscosity, and lubricant mass fraction on flow boiling heat transfer. Kedzierski (2000) stressed the importance of determining which lubricant properties are important and how they influence heat transfer. Based on this he developed a mechanistic model to explain the interactions of a lubricant with a refrigerant. Most of the work in refrigerant-lubricant mixture pool boiling has been carried out with these goals in mind.

The semi-theoretical model of Kedzierski (2003) was developed in a series of studies: Kedzierski (1993), Kedzierski and Kaul (1993), Kedzierski (1999), and Kedzierski (2000a). Kedzierski's approach is applicable to refrigerant-lubricant mixtures. Kedzierski's research for more than a decade helped to gain a clearer idea of the interactions of lubricant with refrigerant in an evaporator. His approach accurately predicts his experimental data as well as other low pressure refrigerant-lubricant pool boiling data from the literature. The mathematical form of his semi-theoretical model is simple, and yet easy to use by practitioners and theoreticians, alike. For these reasons, my dissertation follows Kedzierski's approach. Therefore, Kedzierski's (2003) model is discussed in more detail in the following paragraphs.

According to Kedzierski, the pool boiling enhancement/degradation mechanism associated with the addition of lubricant to refrigerant is due to an accumulation of lubricant at the boiling surface. The enhancement mechanism of lubricants is analogous to the action of surfactants in that both enhancements arise from the creation of an excess layer. Kedzierski (1999) used the Gibbs adsorption equation (Rosen, 1978) and the Young and Dupre equation (Adamson, 1967) to speculate that the boiling heat transfer

enhancement of R-123 by the addition of hexane was caused by an accumulation of hydrocarbon at the boiling surface. The greater concentration of hydrocarbon or “excess layer” at the heat transfer surface caused a reduction of surface energy between the solid surface and the liquid. This action further caused a reduction in the bubble departure diameter, consequently increasing the active site density. A heat transfer enhancement exists when a favorable balance between an increase in site density and a reduction in bubble size occurs.

The lubricant excess layer exists as a region of liquid near a heated wall with a lubricant concentration that is greater than that of the bulk fluid. As outlined in Kedzierski (2000a), the excess layer causes a reduction in the liquid-solid surface energy (σ_{ls}) that results in a simultaneous reduction in the bubble departure diameter and an increase in the site density. This was illustrated with the Gibbs adsorption equation (Rosen, 1978):

$$d\sigma_{ls} = -RT_i\Gamma d \ln c \quad (6-7)$$

R is the universal gas constant and T_i is the temperature of the interface. Eq. (6-7) shows that a greater surface energy reduction results for increases in the surface excess concentration (Γ) and/or increases in the bulk lubricant concentration (c). A heat transfer enhancement exists when the increase in site density compensates for reduction in bubble size. However, as the lubricant mass fraction increases, the bubble size decreases while the site density increases.

6.3.1 Basis of the Model by Kedzierski (2003)

The predictive model (Kedzierski, 2003) is based on describing the mechanisms involved in the formation of the lubricant excess layer. Stephan (1963) was one of the first researchers to note that a lubricant-rich layer exists near the tube wall. The excess concentration or excess surface density arises from the low vapor pressure of the lubricant relative to the refrigerant. The refrigerant-lubricant liquid mixture travels to the heated wall, and the refrigerant preferentially evaporates from the surface leaving behind a liquid phase rich in lubricant. In reality, however, there is lubricant that is removed along with refrigerant, while the remaining lubricant is deposited on the surface. A balance between deposition and removal of the lubricant establishes the thickness of the excess lubricant layer at the surface. The excess lubricant resides in a thin layer on the surface and influences the boiling performance resulting in an enhancement or degradation in heat transfer. The lubricant excess layer controls the bubble size, the site density, and in turn, the magnitudes of the heat transfer.

Given the fact that the model relies on the existence of a lubricant excess layer, the model is valid for refrigerant-lubricant mixtures, which is one of the main reasons I chose to apply this model in my dissertation.

The critical solution temperature is one of the parameters used in determining whether the lubricant and refrigerant are miscible or not. The proximity of the bulk fluid temperature to the critical solution temperature (CST) of the mixture benefits pool boiling heat transfer by the formation of additional excess liquid films that draw superheated liquid onto the bubble sites.

Figure 6-1 shows a bubble on a heated wall. As the bubble begins to form, the state of refrigerant liquid in the vicinity of the bubble transitions to a two-phase state due to evaporation at the vapor-liquid interface. Two thin layers of different soluble solutions rest on the vapor-liquid interface of the bubble. Of course, only a partial separation is likely because of the short time available before the bubble temperature equilibrates with the bulk liquid.

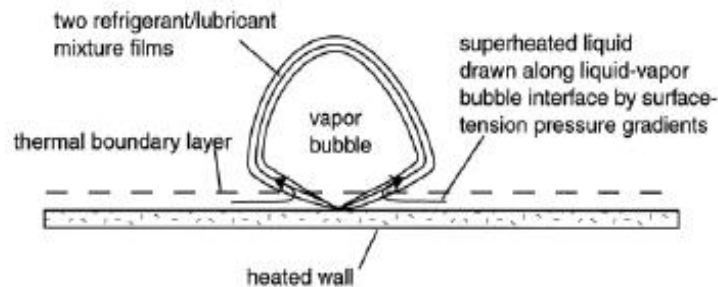


Fig. 6-1: Bubble on a heated wall (Kedzierski, 2000)

The interfaces of the two liquid films are drawn in Fig. 6-1 to have large curvature gradients, which results in large film pressure gradients. These pressure gradients help transport the superheated liquid to the sides of the bubble. The additional bubble superheat causes the pool boiling heat transfer enhancement.

At a nucleation site a bubble of refrigerant vapor will begin to form. At the vapor-liquid interface of the bubble, the concentration of the refrigerant is depressed below that of the bulk due to the mass transfer process which must take place to move the refrigerant to the bubble surface, and at the same time, the concentration of the lubricant increases

above that of the bulk as required by continuity. This effect would be uniform around the bubble if these processes were controlled simply by diffusion of mass and energy. However, because the process takes place at a surface and therefore in a boundary layer in a gravitational field, convection affects the boiling process, and the temperature and species concentrations will vary around the bubble.

6.3.2 Excess Surface Density

The excess surface density (Γ) represents the mass of lubricant per unit surface area within the layer (l_e) at the wall that is in excess of the lubricant that would have been within the layer l_e had the layer not existed; however, there is strong evidence to suggest that the excess layer is nearly pure lubricant (Kedzierski, 2001a). The excess surface density is defined as:

$$\Gamma = l_e(\rho_L - \rho_b x_b) \quad (6-8)$$

where l_e is the thickness of the excess layer, x_b is the bulk lubricant mass fraction, and ρ_b and ρ_L are the densities of the refrigerant-liquid mixture at the bulk composition and the liquid lubricant, respectively. For a dilute solution of lubricant, Γ may be thought of as simply the mass of lubricant per unit surface area.

6.3.3 Derivation of model by Kedzierski (2003)

Figure 6-2 shows a schematic of three bubbles on a heated wall in a pool of liquid with corresponding thermal boundary layer temperature profiles and lubricant excess layer

thickness at a wall heat flux of 39 kW/m^2 . Each bubble in the refrigerant-lubricant mixture is at a different bulk lubricant mass fraction. As the lubricant mass fraction increases, the average departure bubble diameter decreases.

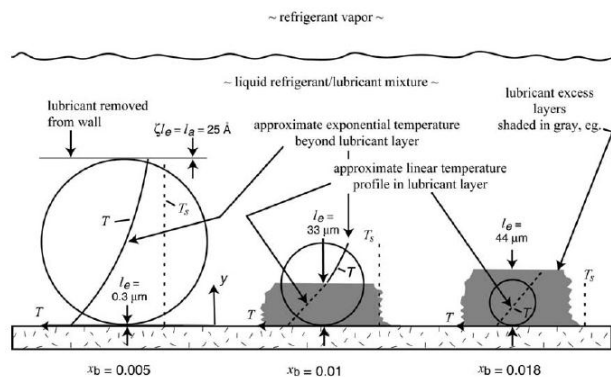


Fig. 6-2: Schematic of the Average Departure Bubble for Three R-123/lubricant Mixtures with Corresponding Excess Layers (Kedzierski, 2003)

The bulk temperature of the refrigerant-lubricant mixture varies over the diameter of the bubble; the heat transfer varies over the surface of the bubble; the mass concentration of the bulk fluid varies due to presence of the wall and the convective heat and mass transfer rates at the surface of the bubble vary around its circumference due to the buoyancy created by the variations in temperature and species concentration.

The model by Kedzierski (2003) assumes that nearly pure lubricant resides on the heat transfer surface within the thickness l_e . It also assumes that all of the lubricant carried to the wall by the bulk liquid-lubricant mixture is deposited on the wall while the entire refrigerant leaves the wall as refrigerant vapor.

For a spherical bubble of radius r_b , the mass of refrigerant vapor (M_{rv}) leaving the wall in a single bubble is:

$$M_{rv} = \frac{4}{3} \pi r_b^3 \rho_{rv} \quad (6-9)$$

where ρ_{rv} is the density of refrigerant vapor. The mass lubricant (ML) deposited on the surface due to the evaporation of the refrigerant for a single bubble can be calculated from eq. (6-9) and the definition of lubricant mass fraction as:

$$M_L = \frac{4}{3} \pi r_b^3 \rho_{rv} \frac{x_b}{(1-x_b)} \quad (6-10)$$

where the lubricant mass fraction is defined as:

$$x_b = \frac{M_L}{M_r + M_L} \quad (6-11)$$

The present model assumes that diffusion is of secondary importance because there is insufficient time for diffusion to establish an excess layer at the bubble vapor-liquid interface. Rather, the bubble lifts the existing lubricant excess layer from the wall by boiling through the lubricant. The thickness of the lubricant removed by the bubble that is removed is limited by that which van der Waals forces hold the bubble. Thus the thickness is independent of the bulk lubricant mass fraction. Typically the thickness of an adiabatic or a van der Waals excess layer (l_a) is approximately 2 monolayers thick (Adamson, 1967), which is approximately 25 Å for lubricants (Laesecke, 2001).

As illustrated in Fig. 6-2 for the $x_b = 0.005$ bubble, the removed lubricant resides in the vicinity of the top of the bubble in the thickness of an adiabatic excess layer (l_a) and represents a fraction (ζ) of the excess layer thickness (l_e). The mass of the lubricant “cap” on the bubble (M_L) was approximated as a disk with a radius equal to the departure bubble radius (r_b) and thickness equal to l_a :

$$M_L = \pi r_b^2 \rho_L l_a = \pi r_b^2 \rho_L \zeta l_e \quad (6-12)$$

where ρ_L is the density of the liquid lubricant.

The refrigerant bubble radius was evaluated by conducting a mass balance between lubricant deposition and removal (setting eqs. (6-10) and (6-12) equal and then rearranging to solve).

$$r_b = \frac{0.75 \zeta l_e \rho_L (1 - x_b)}{x_b \rho_{rv}} = \frac{18.75 A \rho_L (1 - x_b)}{x_b \rho_{rv}} \quad (6-13)$$

where 25 \AA was substituted for ζl_e .

Analogous to turbulent flow boundary layer theory, a linear temperature profile was assumed for the excess layer, while an exponential temperature profile was assumed for the field outside the excess layer. The dimensionless form of the temperature profile valid outside the excess layer (θ) is:

$$\theta = \frac{T - T_s}{T_w - T_s} = e^{-\lambda y / r_b} \quad (6-14)$$

where T is the local temperature of the fluid, y is the perpendicular distance measured from the wall, and λ is a constant for each mixture obtained from fitting the measured pool boiling curve using eq. (6-15).

The wall superheat (ΔT_s) valid for $x_b > 0$ is:

$$\Delta T_s = T_w - T_s = \frac{q'' l_e}{k_L (1 - e^{-\lambda l_e / r_b})} = \frac{q'' \Gamma}{k_L (1 - e^{-\lambda l_e / r_b}) (\rho_L - \rho_b x_b)} \quad (6-15)$$

where Fourier's Law of Heat Conduction is used to determine the heat flux:

$$q'' = \frac{k_L \Delta T_e}{l_e} \quad \text{and} \quad (6-16)$$

$$\Delta T_e = T_w - T_e \quad (6-17)$$

In an effort to generalize the constant λ based on refrigerant and lubricant properties such as viscosity, miscibility, and composition, the excess surface density measurements were modified and the following expression for Γ was derived:

$$\Gamma = \frac{8(\rho_l - \rho_b x_b) x_b T_s \sigma}{3\zeta (1 - x_b) \rho_L h_{fg} \Delta T_s} \quad (6-18)$$

The same surface density measurements and eq. (6-18) was statistically regressed to obtain a non-dimensional excess surface density group for refrigerant-lubricant pool boiling and expressed as:

$$\frac{x_b T_s \sigma}{l_e (1 - x_b) \rho_L h_{fg} \Delta T_s} = \frac{(\rho_l - \rho_b x_b) x_b T_s \sigma}{(1 - x_b) \rho_L h_{fg} \Delta T_s \Gamma} = 5.9 \times 10^{-7} \quad (6-19)$$

Solving for l_e yields:

$$l_e = \frac{\Gamma}{\rho_L - \rho_b x_b} = \frac{x_b T_s \sigma}{5.9 \times 10^{-7} (1 - x_b) \rho_L h_{fg} \Delta T_s} \quad (6-20)$$

Another modification to the model was to introduce the influence of lubricant properties on the heat transfer. Consequently, a correlation of the effects of lubricant mass fraction, viscosity (ν_L) and the lower critical solution temperature (CST) on R-134a pool boiling on a Turbo-BIITM-HP surface was integrated in the modified model. After regressing the data to include excess surface density measurements, the following correlation gave the ratio of refrigerant-lubricant heat flux to that of pure refrigerant heat flux for the same superheat (Kedzierski, 2001c):

$$\frac{q_m''}{q_p''} = 1.27 - x_b \left\{ 99.1 - \left(\frac{\nu_L - \nu_r}{\nu_r} \right) \left[0.578 - 2.09 \left(\frac{T_s - T_c}{T_s} \right) \right] - 226 \left(\frac{T_s - T_c}{T_s} \right) \right\} \quad (6-21)$$

The heat transfer data for the three R-123/York-CTM mixtures and corresponding excess surface densities were used to obtain new values for the thermal boundary layer parameter, λ .

$$\lambda = 0.27 + r_b \frac{q_m''}{q_p''} 10700 / m \quad (6-22)$$

Eqs. (6-15) and (6-20) was simultaneously solved for the refrigerant-lubricant mixture heat transfer coefficient valid for $x_b > 0$:

$$h = \frac{q''}{T_w - T_s} = \frac{5.9 \times 10^{-7} (1 - x_b) \rho_L h_{fg} \Delta T_s k_L (1 - e^{-\lambda_e / r_b})}{x_b T_s \sigma} \quad (6-23)$$

6.4. Basis of Proposed Model

One motivation for this dissertation is that there is no significant documentation of the effect of lubricant on the convective boiling heat transfer of R410A in the open literature. Heat exchanger manufacturers would like to be able to predict how refrigerant-lubricant phase separation, lubricant viscosity, and lubricant mass fraction affect the performance of the evaporator so that better and more efficient heat exchangers can be designed. In modeling of refrigerant/lubricant flow boiling heat transfer, it is important to determine what lubricant properties are important and how they influence heat transfer. It is also important to develop a model that explains, during heat transfer, the interaction of lubricant with the refrigerant.

In nucleate pool boiling, heat transfer is a strong function of heat flux. In forced convective evaporation, the heat transfer is less dependent on heat flux while its dependence on the local vapor quality and mass velocity appear as new and important parameters. Thus, both nucleate boiling and convective heat transfer must be taken into account to predict heat transfer data. Nucleate boiling tends to be dominant at low vapor qualities and high heat fluxes while convection tends to dominate at high vapor qualities and mass velocities and low heat fluxes.

6.5 Model Development

A new heat transfer correlation is proposed based on the superposition type of models (see Chapter 5). The new correlation is based on the mechanisms of nucleate and convective dominated boiling heat transfer. The new correlation resembles the format proposed by Gungor and Winterton (1986), which is discussed in Appendix B. The Gungor and Winterton (1986) model is based on saturated and subcooled vaporization data of pure refrigerants and other fluids in smooth tubes. The present study employs a micro-fin tube and includes data for pure R-410A and R-410A-lubricant mixture. A mixture of naphthenic mineral oil and POE lubricant (1/99, percentage by mass, respectively) were chosen for the study. The POE employed had a nominal kinematic viscosity of $68 \mu\text{m}^2/\text{s}$ at 297.8 K.

The measured local two-phase heat transfer coefficient of R-410A-lubricant mixture, $h_{2\phi}$, is defined as the sum of contributions of convective boiling and nucleate boiling as follows:

$$h_{2\phi} = Eh_c + Sh_{nb} \quad (6-24)$$

where h_c and h_{nb} represent heat transfer contributions from convection and nucleate boiling, respectively. The factors E and S are commonly known as the two-phase convection multiplier and the suppression factor, respectively.

The convective contribution was calculated using the conventional Dittus-Boelter correlation (Dittus and Boelter, 1930).

$$h_c = \frac{0.023k}{D_h} \text{Re}^{0.8} \text{Pr}^{0.4} \quad (6-25)$$

In eq. (6-25), the Reynolds number (Re) and Prandtl number (Pr) was calculated using the properties of the refrigerant-lubricant mixture. The hydraulic diameter was used in all heat transfer calculations.

For the nucleate boiling contribution, I elected to use the Kedzierski (2003) model and hence h_{nb} was represented by eq. (6-23). This choice was accepted mainly because the Kedzierski model discusses in detail the lubricant's effect on heat transfer. There are several models that depict nucleate boiling heat transfer. For instance, after investigating a number of literature expressions for h_{pool} , Gungor and Winterton (1986) used the model by Cooper (1984). The Cooper (1984) model, however, does not include the influence of lubricant on heat transfer.

$$h_{nb} = \frac{q''}{T_w - T_s} = \frac{5.9 \times 10^{-7} (1 - x_b) \rho_L h_{fg} \Delta T_s k_L (1 - e^{-\lambda_e / r_b})}{x_b T_s \sigma} \quad (6-23)$$

Along with the measured two-phase heat transfer coefficient, $h_{2\phi}$, in eq. (6-24), h_c and h_{nb} were calculated from eqns. (6-25) and (6-23), respectively. Thus the proposed model in eq. (6-24) has two unknowns: the two-phase convection multiplier, E , and the suppression factor, S .

The factor, E , reflects much higher velocities and hence forced convective heat transfer in the overall two-phase flow relation compared to the single-phase liquid-only flow. Gungor and Winterton (1986) therefore correlated E against the Lockhart-Martinelli

parameter. The authors argued that in two-phase flow, even for low qualities, the velocities are higher, the void fraction is high and the boundary layer next to the heat transfer surface is thin. The enhancement of heat transfer is achieved by including quality and the vapor to liquid density ratio. To account for quality, vapor to liquid density ratio, and higher velocities, the two-phase multiplier, E , was chosen to have the following functional form:

$$E = \frac{A_1}{X_{tt} \text{Re } x_q} \quad (6-27)$$

where A_1 is a constant to be determined.

The suppression factor, S , reflects the lower effective superheat available in forced convection as opposed to pool boiling, due to the thinner boundary layer (Gungor and Winterton, 1986). For this reason, the authors correlated the suppression factor, S , against a two-phase Reynolds number to take into account the fact that the boundary layer of superheated liquid in which the bubble grows is thinner during forced convection. Based on this analogy, the suppression factor, S , was chosen to have the following functional form:

$$S = e^{-A_0 \text{Re } x_q} \quad (6-28)$$

where A_0 is a second constant to be determined.

An iterative procedure was used to calculate the two-phase multiplier, E , and the suppression factor, S . Initially, E was equated to unity in eq. (6-24), which was then solved for S as:

$$S = \frac{h_{2\phi} - h_c}{h_{nb}}$$

The best fit of the value of S was obtained after repeated iterations. This value of S was then plugged into eq. (6-24) and E was determined as:

$$E = \frac{h_{2\phi} - Sh_{nb}}{h_c}$$

To obtain the best estimates for E repeated iterations were carried out. The obtained values of E and S yielded the final correlation as:

$$h_{2\phi} = 13.7e^{-0.00132\text{Re}x_q} h_{nb} + 1.685 \times 10^{13} \left(\frac{1}{X_{tt} \text{Re}x_q} \right)^{4.419} h_c \quad (6-29)$$

6.6 Discussion

Figure 6-3 compares my measured two-phase heat transfer coefficients for R-410A/POE mixtures (h_{meas}) and the heat transfer coefficients predicted by eq. (6-29) (h_{calc}). Eq. (6-29) predicts approximately 70 % of the experimental data within a deviation of ± 30 %.

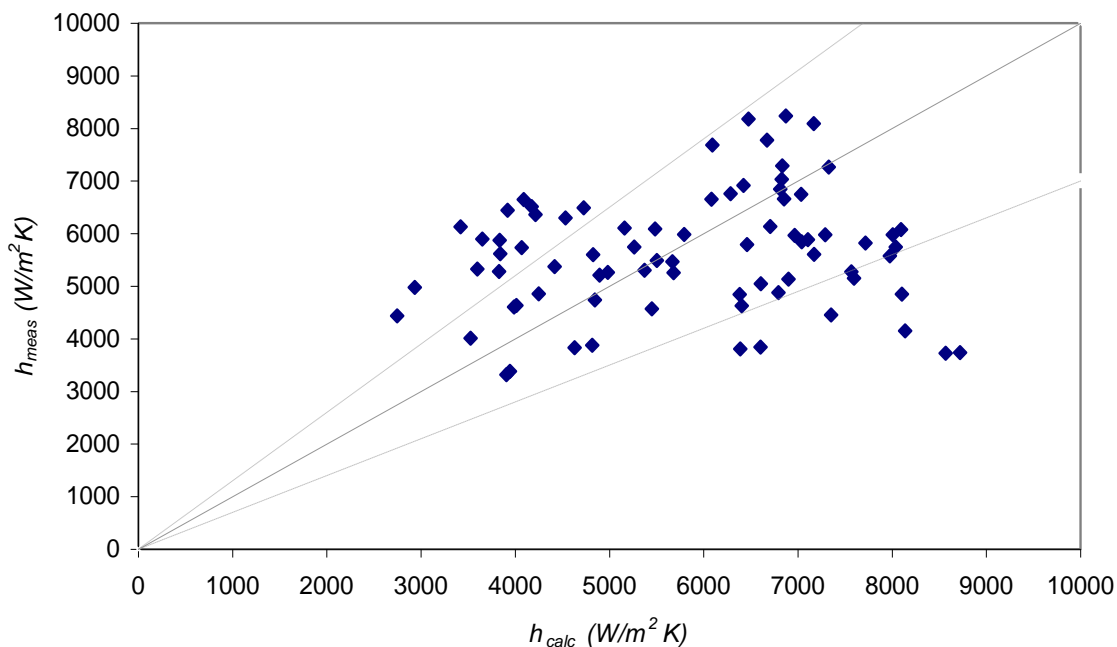


Fig. 6-3: Comparison of Experimental Data with the New Correlation for R-410A/POE

Figure 6-4 compares h_{meas} and h_{calc} as a function of thermodynamic quality. The present correlation overpredicts the heat transfer coefficient for qualities less than 0.1 by 45 %. At qualities between about 0.2 to 0.3, eq. (6-29) underpredicts the experimental values of the heat transfer coefficient by 35%.

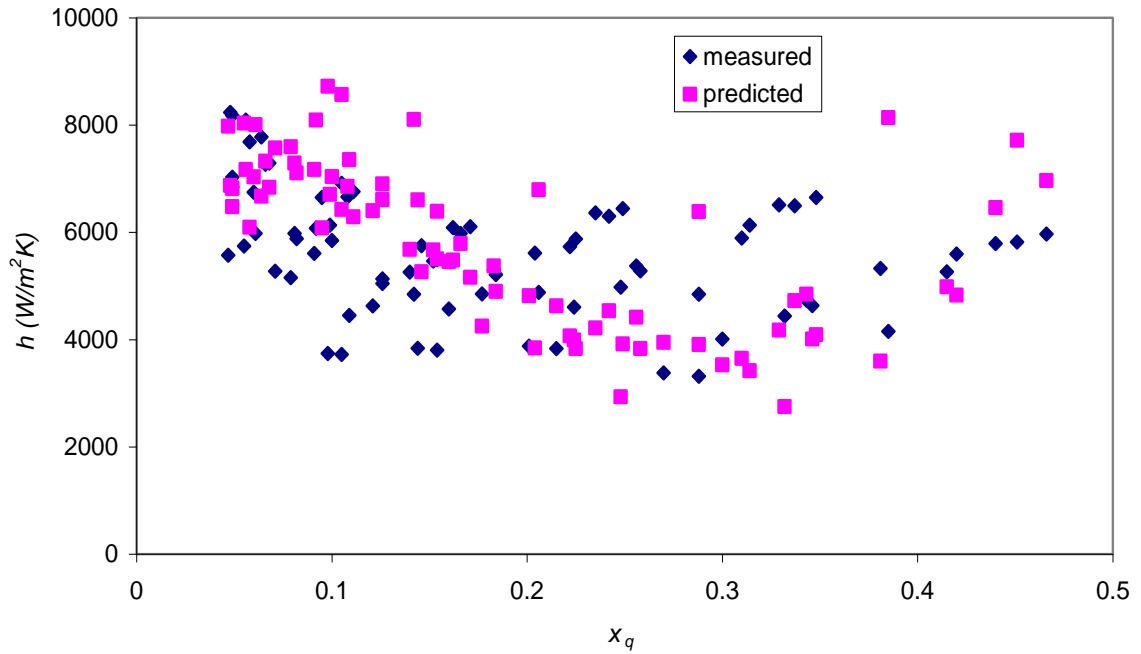


Figure 6-4: Measured and Predicted Heat Transfer Coefficients of R-410A/POE

The average deviation and absolute average deviation are defined as follows:

$$\text{Average deviation (\%)} = \left[\sum \frac{h_{calc} - h_{meas}}{h_{calc}} \right] \times 100 \quad (6-30)$$

$$\text{Absolute average deviation (\%)} = \left[\sum \left| \frac{h_{calc} - h_{meas}}{h_{calc}} \right| \right] \times 100 \quad (6-31)$$

The average and absolute average deviations of the present correlation are -3 % and 25.4 %, respectively.

Figure 6-5 shows average deviations as a function of thermodynamic mass quality. The average and absolute average deviation of the present correlation was -3 % and 25.4 %, respectively. The measured and calculated values of Nusselt number are represented by:

$$Nu_{meas} = \frac{h_{meas} D_h}{k} \quad \text{and} \quad Nu_{pred} = \frac{h_{pred} D_h}{k} \quad (6-32)$$

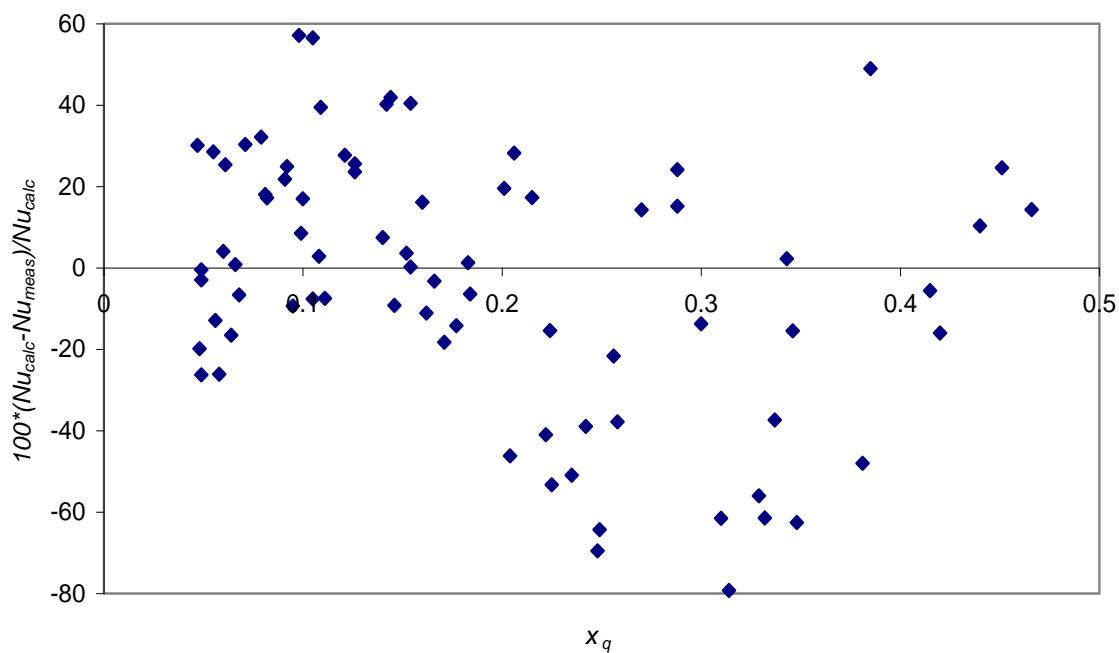


Fig. 6-5: Average Deviation versus Quality for New Correlation of R-410A/POE

Chapter 7

CONCLUSIONS AND RECOMMENDATIONS FOR FURTHER RESEARCH

7.1 Concluding Remarks

The research described in this dissertation involved determining experimental heat transfer coefficients, examining the phenomena involved in the physical process, and analyzing the predictive ability of available models and correlations. A new correlation is established to predict the influence of lubricant on flow boiling heat transfer of a R-410A/POE mixture in a micro-fin tube. Over 300 data points were used for analysis, covering a range of pressure, thermodynamic quality, heat and mass flux, which is generally used in heat exchangers of refrigeration industry.

Several data collection factors were shown to influence the experimental heat transfer coefficient. High mass flux tests developed the risk of unreliable wall temperature measurements for three out of the fifty thermocouples used. My study cautions manufacturers and researchers about the purity of R-410A and cites that possible presence of unsaturated impurities or stray components can alter the vapor equilibrium measurements of refrigerant blend such as R-410A. Using vapor equilibrium measurements, correlations to calculate saturation temperature of pure R-410A and R-410A/POE mixture were developed (Chapter 3). A mass fraction of 0.4 % by mass of lubricant increased the saturation temperature by less than 0.025 K for thermodynamic mass qualities less than 0.5. The use of equilibrium temperature in the definition of heat transfer coefficient may itself cause a quality dependence to appear in the results.

The heat transfer rates of pure R-410A and R-410A/POE mixtures in a micro-fin tube through application of the fluid heating technique were measured in counter-flow configuration. The measured heat transfer coefficients were proportional to both heat flux and thermodynamic quality. The dependence of heat flux required the existence of nucleate boiling. The measured boiling heat transfer coefficients exhibited little variation with increasing qualities. An average degradation of 6.7 % was observed in the heat transfer coefficient of the R-410A/POE mixture when compared with pure R-410A (Chapter 4). This may be due to mass transfer resistance restricting bubble growth in the nucleate boiling mode. In the forced convection/evaporation mode, it may be due to mass transfer resistance suppressing the nucleate boiling for the refrigerant-lubricant mixture, but not for pure R-410A. The relative heat transfer of the R-410A/POE mixture was between -20 % and +42 % of that of pure R-410A.

Three correlations were examined: only one of them explained the influence of refrigerant-lubricant mixture whereas the other two were for lubricant-free refrigerants (Chapter 5). The R-410A/POE predictions were made using R-410A/POE mixture liquid viscosity and liquid density evaluated at the local lubricant mass fraction to calculate the Reynolds number and Prandtl number of the refrigerant-lubricant mixture. The experimental data was compared to the existing NIST database of alternative refrigerants to determine the effect of the axial bulk lubricant concentration gradient on evaporative heat transfer. The Kim et al. (2002) and Ding et al. (2008) poorly predicted my experimental data. This result, while disappointing, illustrates the difficulty with the prediction of refrigerant-lubricant mixture behavior. It also suggests the wide need for

more experiments in this area. The use of lubricant properties in the Hamilton et al. (2005) correlation caused between a 0.3 % and a 0.8 % reduction in the Nusselt number as compared to results using pure R-410A properties alone.

A new heat transfer coefficient correlation based on Kedzierski's (2000) simple and yet easy mechanistic model applicable to refrigerant-lubricant mixtures was proposed and validated with my experimental data (Chapter 6). The new model attempts to explain the influence of a lubricant with a refrigerant by simultaneously taking into account the contributions of both, nucleate boiling and convective boiling. The newly developed heat transfer model predicts 70 % of my experimental data within a deviation of ± 30 %. The average and absolute average deviations of the model are -3 % and 25.4 %, respectively.

7.1.1 Originality and Contribution

The originality and contributions of this dissertation are:

- (1) The presentation of local convective boiling measurements for lubricant-free R-410A and an R-410A/POE lubricant mixture (99.6/0.4 by mass) in a fluid heated micro-fin tube. This study represents the first, and only, study of the effects of lubricant on the heat transfer rate of R-410A during flow boiling using the fluid heating technique. (Note: all of the other studies apply the electrical-heating technique, which has been shown by Kedzierski (1995) to strongly influence the heat transfer results.)
- (2) The development of a new heat transfer model for flow boiling of refrigerants and refrigerant-mixtures in the presence of lubricants.

7.2 Future Work

Continuation of the work of this dissertation would further enhance the scientific understanding of evaporation heat transfer and would have practical industrial benefit and application. Additional data for a variety of pure fluids and mixtures of pure fluids and lubricants should be collected so that the present correlation could be compared against a larger range of working fluids.

Moreover, the development of a better pressure drop model flow boiling of refrigerant-lubricant mixtures could help the HVAC&R industry to design better, more energy efficient, evaporators.

7.2.1 Two-phase Flow Patterns

The test apparatus comprised of a transparent quartz tube (window) conveniently located at the exit of the test section to visualize flow patterns of the two-phase flow of lubricant-free and refrigerant-lubricant mixtures, thereby demonstrating the suppression of nucleate boiling with increasing thermodynamic quality for flow boiling. Although similar studies have been conducted in the past by several researchers, developing a reliable flow pattern map for refrigerant-lubricant mixtures and combining this experimental evidence with existing flow boiling correlations for various flow patterns would help in improving the accuracies of correlations. A high speed video camera could be employed, in conjunction with flow pattern maps, to calculate the thickness of the lubricant excess layer. Moreover, this flow visualization technique could be used to study refrigerant dryout and its effects on heat transfer performance during flow boiling.

7.2.2 Fluorescence Technique

The bulk lubricant concentration of the localized lubricant excess layer can be measured using a fluorescence measurement technique that can also aid in exploring the effect of heat flux on the lubricant surface density. The work would involve the design of a fluorescence setup to observe fluorescence for identification of and location of the lubricant in the convective flow. The technique would rely on the relative fluorescent properties of the lubricant and the refrigerant. The amount of lubricant in the mixture can be calculated from the intensity of the fluorescence emission. The lubricant excess layer could also be measured for a non-adiabatic boiling surface with a bifurcated optical bundle probe. A source lamp with a greater intensity, a lens to focus the source onto the tube, and interference filters with wider band widths would all likely improve the observation of the fluorescence intensity.

7.2.3 Effect of Lubricant Concentration

This dissertation studied one refrigerant-lubricant (R-410A/POE) mixture. The lubricant concentration (by mass) was 0.4 %. The next logical step would be to investigate the effect of different lubricant concentrations (1 % to 10 %) on flow boiling heat transfer of R-410A. Further addition of lubricant to the test rig to increase lubricant concentration of the refrigerant-lubricant mixture would also invite build up of lubricant in the test section. The transparent quartz tube at the exit of the test section could help determine how viscous the two-phase flow is. A density flowmeter could help record the mass fraction of the lubricant in the refrigerant-lubricant mixture, which circulates in the

refrigerant loop. The density flowmeter could thus indicate the severity of lubricant buildup. Based on calculations of the lubricant excess layer for different lubricant concentrations, the contribution of nucleate boiling could help decipher the threshold boundary at which lubricant holdup begins to dominate. Foaming may occur at higher lubricant concentrations. As a result, the phenomenon of foaming in flow boiling could be investigated to know at what lubricant concentrations foaming begins to occur and how foaming affects the performance of the evaporator (test section).

7.2.4 Model using Refrigerant-Lubricant Mixture Properties

The correlation that I developed as part of this study and other existing correlations discussed in this study use empirical expressions to identify the flow boiling characteristics of pure refrigerants and refrigerant mixtures or refrigerant-lubricant mixtures. One of the future objectives would be to use properties of refrigerant-lubricant mixtures only and avoid empirical coefficients while developing a heat transfer model. This objective could be accomplished by collecting experimental data from a large number of refrigerant-lubricant mixtures. A calibrated density meter if installed in the refrigerant loop could lead to accurate online measurements of density of the refrigerant-lubricant mixture.

7.2.5 Apparatus Modifications

With the implementation of any or all of the above mentioned items, the test apparatus would require significant modification. For example, to be able to measure the

refrigerant-lubricant mixture properties, instrumentation such as a density flowmeter and a viscometer could be installed in the refrigerant loop.

Appendix A

General Description of Boiling

A combination of liquid and vapor refrigerant exists in commonly used evaporators (tube-in-tube, air-cooled, brazed and gasketed plate evaporators, etc.) in the air-conditioning, heating and refrigeration industries. Unlike single-phase flow systems, the heat transfer coefficient for a two-phase mixture depends on the flow regime, the thermodynamic and transport properties of the refrigerant vapor and liquid refrigerant, the roughness of the heating surface, the wetting-characteristics of the surface-liquid pair, the technique of heating and the boundary condition associated with it and other parameters.

When evaporation occurs at a solid-liquid interface, it is termed as boiling (Incropera and DeWitt, 1996). The process occurs when the difference, between the temperature of the surface and the saturation temperature corresponding to the liquid pressure, is positive. During the process, latent heat effects associated with the phase change are significant. Boiling is characterized by the formation of bubbles, which grow and subsequently detach from the surface. The parameters that affect vapor bubble growth are many, among which are included the excess temperature, the nature of the surface, and thermophysical properties of the fluid, such as its surface tension, thermal conductivity, viscosity, etc. It is very important to study evaporation because the dynamics of vapor bubble formation affect fluid motion near the surface and therefore strongly influence the heat transfer coefficient.

Appendix A

Boiling can be classified in different ways because it may occur under various conditions. In 'pool boiling' the liquid is quiescent and its motion near the surface is due to free convection and due to mixing induced by bubble growth and detachment. In contrast, for 'forced convection boiling', the fluid motion is induced by external means, as well as by free convection and bubble-induced mixing.

Boiling may also be classified as 'subcooled' or 'saturated'. In subcooled boiling, the temperature of the liquid is below saturation temperature and bubbles formed at the surface may condense in the liquid. In contrast, the temperature of the liquid slightly exceeds the saturation temperature in saturated boiling. Bubbles formed at the surface are then propelled through the liquid by buoyancy forces, eventually escaping from a free surface.

A1 Regimes of Boiling

Nukiyama (1934) was the first to identify the regimes of boiling, which are illustrated in Fig. 1-2. When the temperature of the heating surface is near the fluid saturation temperature, heat is transferred by convection currents to the free surface where evaporation occurs (Region I). Transition to nucleate boiling occurs when the surface temperature exceeds saturation by a few degrees (Region II). In nucleate boiling (Region III), a thin layer of superheated liquid is formed adjacent to the heating surface. In this layer, bubbles nucleate and grow from spots on the surface. The thermal resistance of the

Appendix A

superheated liquid film is greatly reduced by bubble-induced agitation, and vaporization. Increased wall temperature increases bubble population, causing a large increase in heat flux.

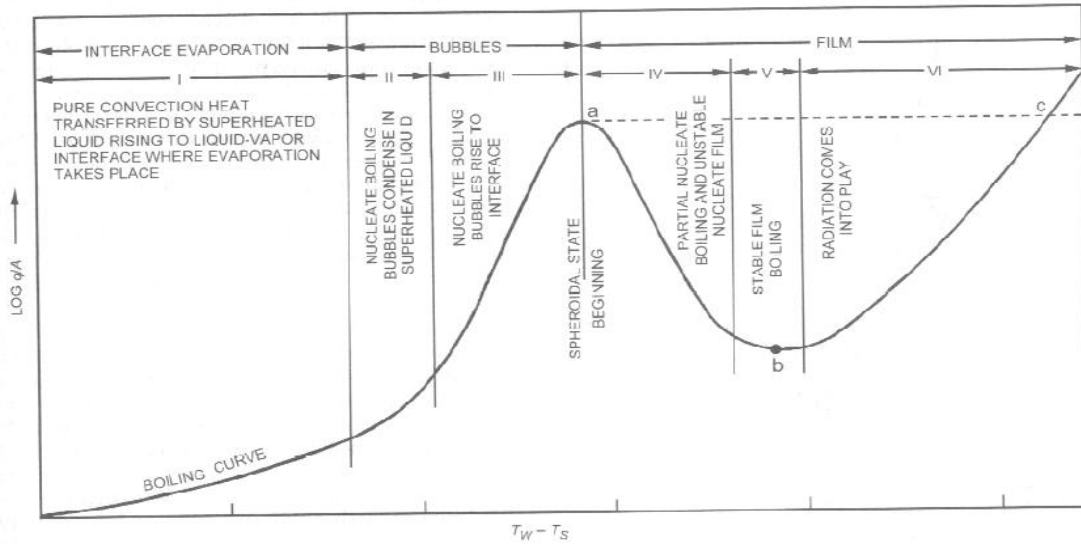


Fig. A-1: Regimes of Flow Boiling (ASHRAE, 2001)

In the transition boiling regime (Region IV), or unstable film boiling, bubble formation is so rapid that a vapor film or blanket begins to form on the surface. The heat flux density decreases in this regime because the thermal conductivity of the vapor is much less than that of the liquid. In film boiling (Regions V and VI), heat flux reaches the minimum and the surface is completely covered by a vapor blanket. Heat transfer from the surface to the liquid occurs by conduction (and some radiation) through the vapor.

Appendix A

A2 Horizontal Convective Boiling Heat Transfer

Horizontal convective boiling heat transfer with a uniform heat flux condition usually occurs as shown in Fig. 1-3, which illustrates the various flow patterns at different thermodynamic qualities. In most of the applications for refrigerants, the annular flow pattern is one of interest, as refrigerants commonly enter the evaporator at a vapor quality of about twenty percent and quickly develop into annular flow.

Subcooled liquid enters the test section and boiling takes place on the wall along the tube. While the liquid is being heated to the saturation temperature and the wall temperature remains below the temperature necessary for nucleation, single-phase convective heat transfer to the liquid phase is occurring. During single-phase, the heat transfer coefficient is approximately constant; it changes only as the thermodynamic and transport properties of the liquid change with temperature.

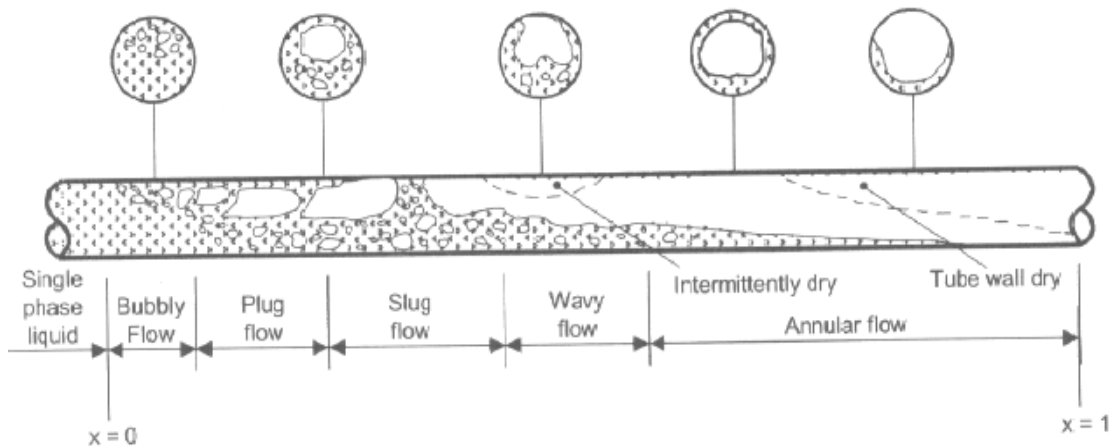


Fig. A-2: Two-phase Flow Patterns in a Horizontal Tube
(taken from Collier and Thome, 1996)

Appendix A

At a certain point along the tube, the condition at the wall is such that the vapor is formed by nucleation. Vapor formation takes place in the subcooled liquid and this heat transfer mechanism is called subcooled convective boiling. At low thermodynamic qualities, the flow contains many bubbles and hence it is called bubbly flow. The main heat transfer in this region is nucleate boiling. The heat transfer coefficient owing to developing turbulence increases linearly.

As the liquid keeps absorbing heat, the thermodynamic quality is increased through the saturated nucleate boiling region. The flow pattern changes from bubbly or slug flow to annular flow. In the annular flow region, the thickness of the liquid film on the heating surface is such that the effective thermal conductivity is sufficient to prevent the liquid in contact with the wall from being superheated to a temperature which would allow nucleation. Heat is carried away from the wall by forced convection in the film to the liquid-vapor interface, where evaporation occurs. The region beyond transition has been referred to as the two-phase convective evaporation region. If nucleate boiling is completely absent, “suppression of nucleate boiling” is said to have taken place. Since the liquid film becomes thinner and thinner with increasing quality and since the vapor core velocity increases sharply, heat is conducted more readily through the liquid, and the heat transfer coefficient increases.

Appendix A

At some point, the liquid film is entirely evaporated and dryout (also known as boiling crisis) occurs: since vapor is a much poorer thermal conductor than liquid, the heat transfer is suddenly and severely diminished. In a horizontal geometry, the wall dryout occurs more frequently at the top position of the tube since the liquid film is thinner at the top position of the tube due to gravity. Beyond this point the wall temperatures rise suddenly.

The heat transfer coefficient depends not only on quality, but on mass and heat flux. As in single-phase flow, an increase in mass velocity causes an increase in turbulence and may cause a consequent increase in heat transfer coefficient. It should also be noted that at higher mass flux the dependence on quality becomes stronger. For the case of increased heat flux, nucleate boiling at the wall may occur in more locations, increasing the heat transfer coefficient. For very high heat flux, no annular flow may be established and sudden reductions in heat transfer coefficient values may occur at low quality or even in the subcooled boiling regime (Collier and Thome, 1996). This phenomenon is known as a sudden departure from nucleate boiling and is caused by sudden flashing of vapor all along the tube wall (i.e. film boiling).

Appendix B

Correlations

Many heat transfer correlations related to flow boiling have been published by several researchers. However, it is difficult to pin point at a particular correlation that is applicable to all refrigerants, pure and mixed. According to Webb and Gupte (1992), examination of existing correlations has shown them correlations to fall into one of the three model categories: ‘superposition’, ‘asymptotic’, and ‘enhancement’. These models are discussed in detail below.

B1 Superposition model

In this model, the total heat transfer coefficient is the sum of contributions from nucleate boiling and bulk convection.

Rohsenow model (1952)

The first true correlation model for flow boiling heat transfer coefficient was proposed by Rohsenow in 1952 as a simple addition of the nucleate and convective coefficients.

$$h_{tp} = h_{nb} + h_{cb} \quad (\text{B-1})$$

Appendix B

Chen's correlation (1966)

The model by Rohsenow (1952) was used in principle by Chen, who formulated the first cohesive flow boiling method in 1966. Chen (1966) found it necessary to introduce a nucleate boiling suppression factor to the nucleate boiling term, in order to account for diminished contribution of nucleate boiling as quality increases, and increased convective boiling effects for higher vapor fraction by adding an enhancement factor.

$$h_{tp} = h_{nb} + h_{cb} \quad (\text{B-2})$$

The nucleate pool boiling correlation (h_{nb}) was based on Foster and Zuber's pool boiling equation (1955) and the bulk convective contribution (h_{cb}) was based on Dittus-Boelter's equation (1930). The suppression factor, S , was correlated with a two-phase Reynolds number to account for the thinner boundary layer at the higher quality. The enhancement factor, F , was correlated with the Martinelli parameter to account for higher vapor velocities at the higher quality.

$$h_{cb} = 0.023 \left(\frac{k_l}{D} \right) \text{Re}_{tp}^{0.8} \text{Pr}_l^{0.4} \quad (\text{B-3})$$

$$\text{Re}_{tp} = \frac{G(1-x)D}{\mu_l} F(X_{tt})^{1.25}$$

$$X_{tt} = \left(\frac{1-x}{x} \right)^{0.9} \left(\frac{\rho_v}{\rho_l} \right)^{0.5} \left(\frac{\mu_v}{\mu_l} \right)^{0.1}$$

$$h_{nb} = 0.00122 \left(\frac{k_l^{0.79} C_{p_l}^{0.45} \rho_l^{0.49}}{\sigma^{0.5} \mu_l^{0.29} h_{lv}^{0.24} \rho_v^{0.24}} \right) \{T_w - T_{sat}(P_l)\}^{0.24} \{P_{sat}(T_w) - P_l\}^{0.75} S \quad (\text{B-4})$$

Appendix B

$$S(\text{Re}_{tp}) = (1 + 2.56 \times 10^{-6} \text{Re}_{tp}^{1.17})^{-1} \quad (\text{B-5})$$

The correlation was based on vertical axial flow and was developed to fit flow boiling of water and organic fluids like methanol, cyclohexane, and pentane.

Bennett and Chen's correlation (1980)

Bennett and Chen (1980) modified the Chen (1966) correlation to account for the model analysis on nucleate boiling near the wall and for the effects of liquid Prandtl number in the term of bulk convection.

$$h_{tp} = h_{nb} + h_{cb} \quad (\text{B-2})$$

$$h_{cb} = h_l F(X_{tt}) \text{Pr}_l^{0.296} \quad (\text{B-6})$$

$$S = \frac{1 - \exp\{-F(X_{tt})h_l X_o / k_l\}}{F(X_{tt})h_l X_o / k_l} \quad (\text{B-7})$$

$$h_l = 0.023 \left(\frac{k_l}{D} \right) \text{Re}_l^{0.8} \text{Pr}_l^{0.4} \quad (\text{B-8})$$

$$X_o = 0.041 \left(\frac{\sigma}{g(\rho_l - \rho_v)} \right)^{0.5} \quad (\text{B-9})$$

As can be seen, the correlation includes the surface tension and density difference between liquid and vapor phase in the nucleate boiling suppression factor (S). The heat transfer enhancement factor (F) includes thermal characteristics of the fluid.

Appendix B

Gungor and Winterton's correlation (1986)

Gungor and Winterton (1986) modified the Chen (1966) correlation keeping the same additive form. They proposed the following correlation for heat transfer during flow boiling inside horizontal and vertical tubes and annuli.

$$h = Eh_l + Sh_{pool} \quad (\text{B-10})$$

$$h_{pool} = 55 \text{Pr}^{0.12} (-\log_{10} \text{Pr})^{-0.55} M^{-0.5} q^{0.67} \quad (\text{B-11})$$

$$E = 1 + 24000 \text{Bo}^{1.16} + 1.37 X_{tt}^{-0.86} \quad (\text{B-12})$$

$$S = (1 + 1.15 \times 10^{-6} E^2 \text{Re}_l^{1.17})^{-1} \quad (\text{B-13})$$

The authors used the Cooper correlation (1984) for the pool boiling heat transfer coefficient. The enhancement factor was correlated using not only the Lockhart-Martinelli parameter but also the Boiling number. The inclusion of Boiling number accounts for the enhanced heat transfer due to a significant disturbance of the liquid layer due to boiling. This means that the enhancement factor does not only affect the pure convective evaporation contribution but also the nucleate boiling contribution. The correlation covered seven different fluids, including water and ethylene glycol.

The authors recommended that if the tube is horizontal and the Froude number is less than 0.05, then E and S should be multiplied by:

$$e_E = Fr_l^{(0.1-2Fr_l)} \quad (\text{B-14})$$

$$e_S = \sqrt{Fr_l} \quad (\text{B-15})$$

Appendix B

where Fr_l is the Froude number defined by:

$$Fr_l = \frac{G^2}{\rho_l^2 g D} \quad (\text{B-16})$$

Correlation by Jung et al. (1989)

Jung et al. (1989) proposed the evaporative heat transfer correlation for pure refrigerants using the original form of Chen (1966). A pool boiling heat transfer coefficient obtained by Stephan and Abdelsalam's correlation (1980) and a single phase heat transfer coefficient for liquid-only flow obtained by the Dittus-Boelter's correlation (1930).

$$h_p = N.h_{nb} + F.h_l \quad (\text{B-17})$$

$$N = 4048X^{1.22}Bo^{1.13} \quad (X < 1.0) \quad (\text{B-18})$$

$$N = 2.0 - 0.1X^{-0.28}Bo^{-0.33} \quad (1.0 < X < 5.0) \quad (\text{B-19})$$

$$h_{nb} = 207 \frac{k_l}{bd} \left(\frac{qbd}{k_l T_{sat}} \right)^{0.745} \left(\frac{\rho_g}{\rho_l} \right)^{0.581} Pr_l^{0.533} \quad (\text{B-20})$$

$$bd = 0.0146\beta \left[\frac{2\sigma}{g(\rho_l - \rho_g)} \right]^{0.5} \quad \beta = 35^0 \quad (\text{B-21})$$

$$F = 2.37 \left(0.29 + \frac{1}{X} \right)^{0.85} \quad (\text{B-22})$$

$$h_l = 0.023 \left(\frac{k_l}{D} \right) Re_l^{0.8} Pr_l^{0.4} \quad (\text{B-23})$$

Appendix B

B2 Asymptotic Model

In this type of model, the total heat transfer coefficient the form of Kutateladze's (1961) power-type addition.

Kutateladze's model (1961)

Kutateladze (1961) proposed a power-type addition model for the two boiling components.

$$h_{tp} = [h_{nb}^n + h_{cb}^n]^{1/n} \quad (\text{B-24})$$

Liu and Winterton's correlation (1991)

Liu and Winterton (1991) introduced the following correlation for flow boiling inside tube and annuli based on Kutateladze's (1961) power-type addition model:

$$h_{tp} = [(S.h_{nb})^2 + (E.h_l)^2]^{1/2} \quad (\text{B-25})$$

$$h_{nb} = 55 \text{Pr}^{0.12} (-\log_{10} \text{Pr})^{-0.55} M^{-0.5} q^{0.67} \quad (\text{B-26})$$

$$h_l = 0.023 \left(\frac{k_l}{D} \right) \text{Re}_l^{0.8} \text{Pr}_l^{0.4} \quad (\text{B-27})$$

$$S = (1 + 0.055 E^{0.1} \text{Re}_l^{0.16})^{-1} \quad (\text{B-28})$$

$$E = \left[1 + x \text{Pr}_l \left(\frac{\rho_l}{\rho_g} - 1 \right) \right]^{0.35} \quad (\text{B-29})$$

Appendix B

The advantage of this method compared with the simple addition model is that nucleate boiling is further suppressed as vapor quality increases. In this correlation, refrigerants, water and ethylene glycol were studied. The Cooper (1984) correlation was used to provide for pool boiling heat transfer coefficient.

B3 Enhancement Model

In this type of model, the two-phase heat transfer coefficient has the form of an enhancement to single-phase heat transfer coefficient of a flowing liquid by two-phase enhancement factor.

Shah's Correlation (1976)

A different approach to flow boiling was proposed by Shah in 1976 where the nucleate boiling component is represented by the Boiling number, Bo , while a convection number, Co , is used for the convective boiling component. For selection between the two components, the method uses a graphical chart, later curve-fitted as the greater of the two. The method is easy to use because nucleate boiling is represented by Bo alone, rather than appropriate correlations. However, this restricts the range of applicability and accuracy, especially for pressure effects.

$$\frac{h_p}{h_l} = \max[f_1(Bo), f_2(Co), f_3(Fr)] \quad (\text{B-30})$$

$$Bo = \frac{q}{Gh_{fg}} \quad (\text{B-31})$$

Appendix B

$$Co = \left(\frac{1-x}{x} \right)^{0.8} \left(\frac{\rho_g}{\rho_l} \right)^{0.5} \quad (\text{B-32})$$

$$Fr_l = \frac{G^2}{\rho_l^2 g D} \quad (\text{B-33})$$

Shah's correlation (1982)

In his study, Shah (1976 and 1982) categorized the flow boiling regime into three regions by using three dimensionless parameters as given by equations (A-31), (A-32), and (A-33). They were nucleate boiling regime (*nb*), bubble suppression regime (*bs*), and convective boiling regime (*cb*). In 1982, Shah incorporated more data points and test fluids to arrive at a correlation represented as follows:

$$Ns = Co \text{ for } Fr_l \geq 0.04$$

$$Ns = 0.38 Fr_l^{-0.3} Co \text{ for } Fr_l < 0.04$$

$$Fs = 14.7 \text{ for } Bo \geq 11 \times 10^{-4}$$

$$Fs = 15.4 \text{ for } Bo < 11 \times 10^{-4}$$

$$h_{cb} = 1.8 Ns^{-0.8}$$

$$\text{for } Ns > 1.0 \quad h_{nb} = 230 Bo^{0.5} \text{ for } Bo > 0.3 \times 10^{-4}$$

$$h_{nb} = 1 + 46 Bo^{0.5} \text{ for } Bo \leq 0.3 \times 10^{-4}$$

$$\text{for } Ns \leq 1.0 \quad h_{bs} = Fs Bo^{0.5} \exp(2.74 Ns^{-0.1}) \text{ for } 0.1 < Ns \leq 1.0$$

$$h_{bs} = Fs Bo^{0.5} \exp(2.47 Ns^{-0.15}) \text{ for } Ns \leq 0.1$$

Appendix B

for $Ns > 1.0$, $h_{tp} = \text{larger of } h_{nb} \text{ and } h_{cb}$

for $Ns \leq 0.1$, $h_{tp} = \text{larger of } h_{bs} \text{ and } h_{cb}$

Schrock and Grossman's Correlation (1959)

Via their study on flow boiling in a vertical tube, Schrock and Grossman (1959) proposed the following correlation:

$$\frac{h}{h_l} = 7.39 \times 10^{-3} \left[Bo + 1.5 \times 10^{-4} X_{tt}^{-0.66} \right] \quad (\text{B-34})$$

Kandlikar's Correlation (1990)

Kandlikar's correlation (1990) is a modification of Shah's correlation. The data for the correlation was divided into two regions as convective boiling region ($Co < 0.65$) and nucleate boiling region ($Co > 0.65$).

$$h_{tp} = h_l \left(C_1 Co^{C_2} (25 Fr_l) \right)^{C_5} + C_3 Bo^{C_4} F_{fl} \quad (\text{B-35})$$

$$h_l = 0.023 \left(\frac{k_l}{D} \right) Re_l^{0.8} Pr_l^{0.4} \quad (\text{B-36})$$

Kandlikar added an empirical 'fluid-dependent parameter', F_{fl} , which is multiplied to the nucleate boiling term. However, for all fluids in stainless steel tubes, $F_{fl} = 1.0$ (Kandlikar, 1998). For convective boiling region, $C_1=1.1360$; $C_2=-0.9$; $C_3=667.2$; $C_4=0.7$;

Appendix B

and $C_5=0.3$. For nucleate boiling region, $C_1=0.6683$; $C_2=-0.2$; $C_3=1058.0$; $C_4=0.7$; and $C_5=0.3$. For vertical tubes, $C_5=0$ and for horizontal tubes, $C_5=0$ for $Fr_1 > 0.04$.

Appendix C

Experimental Data

C1 Pure R410A Data

Nu	Re	xq	Bo	Pr/Pc	Tr/Tc	MW	Pr
292	7369	0.085	1.51E-04	0.215	0.816	72.59	2.28
300.3	7361	0.16	1.94E-04	0.215	0.816	72.59	2.29
302.5	7347	0.256	2.41E-04	0.214	0.816	72.59	2.29
268.3	7333	0.37	2.92E-04	0.214	0.816	72.59	2.3
351.1	6871	0.073	1.46E-04	0.204	0.811	72.59	2.3
295.3	6868	0.146	1.93E-04	0.204	0.811	72.59	2.3
303.3	6860	0.242	2.46E-04	0.204	0.811	72.59	2.31
306.1	6846	0.363	3.07E-04	0.204	0.811	72.59	2.31
267.9	6831	0.508	3.72E-04	0.203	0.811	72.59	2.32
301.6	7105	0.048	1.30E-04	0.205	0.811	72.59	2.3
278.9	7102	0.113	1.71E-04	0.205	0.811	72.59	2.3
294.7	7093	0.198	2.19E-04	0.204	0.811	72.59	2.3
302.8	7078	0.306	2.73E-04	0.204	0.811	72.59	2.31
274.5	7063	0.435	3.31E-04	0.203	0.811	72.59	2.32
271.8	10773	0.056	1.11E-04	0.203	0.81	72.59	2.3
291.8	10762	0.111	1.42E-04	0.203	0.81	72.59	2.3
304.8	10743	0.181	1.77E-04	0.202	0.81	72.59	2.31
285.1	10724	0.265	2.14E-04	0.202	0.81	72.59	2.31
288.4	13366	0.082	1.19E-04	0.203	0.81	72.59	2.3
306	13345	0.141	1.48E-04	0.202	0.81	72.59	2.3
293.5	13323	0.21	1.79E-04	0.202	0.81	72.59	2.31
297.7	7543	0.139	2.07E-04	0.205	0.811	72.59	2.3
315.1	7534	0.242	2.65E-04	0.204	0.811	72.59	2.31
326.7	7518	0.373	3.30E-04	0.204	0.811	72.59	2.31
296.5	7502	0.53	4.01E-04	0.203	0.811	72.59	2.32
310.8	10519	0.094	1.56E-04	0.207	0.812	72.59	2.3
331.4	10508	0.172	2.00E-04	0.207	0.812	72.59	2.3
346	10489	0.27	2.49E-04	0.206	0.812	72.59	2.3
318.2	10470	0.388	3.02E-04	0.206	0.812	72.59	2.31
329.8	10589	0.1	1.62E-04	0.209	0.813	72.59	2.29
351.7	10578	0.18	2.07E-04	0.209	0.813	72.59	2.3
366.8	10559	0.283	2.58E-04	0.208	0.813	72.59	2.3
336	10539	0.405	3.13E-04	0.208	0.813	72.59	2.31
323	13859	0.051	1.22E-04	0.207	0.812	72.59	2.29
350	13846	0.111	1.55E-04	0.206	0.812	72.59	2.3
370.6	13824	0.188	1.93E-04	0.206	0.812	72.59	2.3
350.4	13801	0.279	2.34E-04	0.205	0.812	72.59	2.31
281.2	7385	0.087	1.17E-04	0.209	0.813	72.59	2.29
286.5	7377	0.145	1.50E-04	0.208	0.813	72.59	2.3

Appendix C

Nu	Re	xq	Bo	Pr/Pc	Tr/Tc	MW	Pr
283.7	7364	0.219	1.86E-04	0.208	0.813	72.59	2.3
247.1	7350	0.307	2.26E-04	0.207	0.812	72.59	2.3
297.5	11258	0.073	1.01E-04	0.208	0.813	72.59	2.29
302.7	11240	0.123	1.25E-04	0.208	0.813	72.59	2.3
277.9	11221	0.183	1.52E-04	0.207	0.812	72.59	2.3
312.5	14201	0.084	1.04E-04	0.208	0.813	72.59	2.29
300.3	14179	0.133	1.26E-04	0.207	0.812	72.59	2.3
345.8	6806	0.091	1.41E-04	0.21	0.814	72.59	2.29
306.8	6803	0.162	1.87E-04	0.21	0.814	72.59	2.29
317.7	6795	0.255	2.39E-04	0.209	0.814	72.59	2.3
321	6781	0.373	2.98E-04	0.209	0.813	72.59	2.3
280.7	6767	0.514	3.61E-04	0.208	0.813	72.59	2.31
326.2	10040	0.077	1.30E-04	0.209	0.813	72.59	2.29
345.5	10030	0.142	1.66E-04	0.209	0.813	72.59	2.29
356.1	10013	0.223	2.06E-04	0.208	0.813	72.59	2.3
324.5	9995	0.321	2.50E-04	0.208	0.813	72.59	2.3
346	12595	0.093	1.33E-04	0.209	0.813	72.59	2.29
369.2	12575	0.159	1.65E-04	0.209	0.813	72.59	2.3
361	12555	0.237	2.00E-04	0.208	0.813	72.59	2.3
395.3	7342	0.096	1.02E-04	0.207	0.812	72.59	2.3
271.6	7340	0.147	1.34E-04	0.207	0.812	72.59	2.3
259.7	7331	0.214	1.71E-04	0.206	0.812	72.59	2.3
247.8	7317	0.299	2.13E-04	0.206	0.812	72.59	2.31
202.7	7303	0.4	2.59E-04	0.205	0.812	72.59	2.31
401.3	7479	0.102	1.08E-04	0.209	0.813	72.59	2.29
280.6	7477	0.156	1.42E-04	0.209	0.813	72.59	2.3
270.2	7469	0.227	1.82E-04	0.209	0.813	72.59	2.3
259.3	7454	0.317	2.26E-04	0.208	0.813	72.59	2.3
213.2	7439	0.424	2.74E-04	0.208	0.813	72.59	2.31
382.9	10583	0.081	8.61E-05	0.212	0.814	72.59	2.29
302.7	10580	0.124	1.14E-04	0.212	0.814	72.59	2.29
302.5	10570	0.181	1.45E-04	0.211	0.814	72.59	2.29
298	10551	0.252	1.81E-04	0.211	0.814	72.59	2.3
254	10532	0.338	2.19E-04	0.21	0.814	72.59	2.3
154.2	7520	0.093	1.36E-04	0.222	0.819	72.59	2.28
173.5	7517	0.157	1.65E-04	0.222	0.819	72.59	2.28
187.5	7635	0.098	1.45E-04	0.231	0.823	72.59	2.27
202.4	7625	0.166	1.76E-04	0.231	0.823	72.59	2.27
100.6	9987	0.055	5.61E-05	0.231	0.823	72.59	2.26
102.2	9985	0.083	7.40E-05	0.231	0.823	72.59	2.27
113.4	9978	0.12	9.45E-05	0.231	0.823	72.59	2.27
122.4	9967	0.166	1.18E-04	0.231	0.823	72.59	2.27
116.2	9955	0.222	1.42E-04	0.23	0.823	72.59	2.27
237.7	8202	0.115	1.83E-04	0.231	0.823	72.59	2.27

Appendix C

Nu	Re	xq	Bo	Pr/Pc	Tr/Tc	MW	Pr
268.3	8191	0.201	2.22E-04	0.231	0.823	72.59	2.27
243.4	10703	0.048	1.47E-04	0.234	0.825	72.59	2.26
289.1	10690	0.117	1.78E-04	0.234	0.825	72.59	2.26
102.6	10405	0.055	6.38E-05	0.218	0.818	72.59	2.28
98.4	10403	0.087	8.43E-05	0.218	0.818	72.59	2.28
106.7	10395	0.129	1.08E-04	0.218	0.818	72.59	2.28
113	10382	0.182	1.34E-04	0.218	0.817	72.59	2.28
103.8	10369	0.246	1.62E-04	0.217	0.817	72.59	2.29
148.2	12721	0.051	6.24E-05	0.236	0.825	72.59	2.26
146	12719	0.082	8.24E-05	0.236	0.825	72.59	2.26
159.6	12710	0.123	1.05E-04	0.236	0.825	72.59	2.26
169.9	12695	0.175	1.31E-04	0.235	0.825	72.59	2.26
157.8	12680	0.237	1.59E-04	0.235	0.825	72.59	2.27
171.2	14060	0.05	6.27E-05	0.241	0.827	72.59	2.25
168.3	14057	0.082	8.28E-05	0.241	0.828	72.59	2.26
183.9	14048	0.123	1.06E-04	0.241	0.827	72.59	2.26
195.8	14032	0.175	1.32E-04	0.24	0.827	72.59	2.26
181.7	14016	0.237	1.59E-04	0.24	0.827	72.59	2.26
177	12235	0.06	7.56E-05	0.221	0.819	72.59	2.28
183.5	12232	0.098	9.98E-05	0.221	0.819	72.59	2.28
204.7	12224	0.148	1.27E-04	0.221	0.819	72.59	2.28
221.5	12209	0.211	1.59E-04	0.22	0.819	72.59	2.28
210.7	12193	0.286	1.92E-04	0.22	0.818	72.59	2.29
365.1	8958	0.049	7.00E-05	0.219	0.818	72.59	2.28
358.1	8956	0.084	9.60E-05	0.219	0.818	72.59	2.28
330.1	8953	0.132	1.27E-04	0.219	0.818	72.59	2.28
348.6	8946	0.195	1.62E-04	0.219	0.818	72.59	2.28
358.7	8935	0.275	2.02E-04	0.218	0.818	72.59	2.29
320	8922	0.37	2.45E-04	0.218	0.817	72.59	2.29
391.4	8218	0.062	8.64E-05	0.22	0.818	72.59	2.28
373.5	8216	0.084	1.05E-04	0.22	0.818	72.59	2.28
367.6	8213	0.137	1.45E-04	0.22	0.818	72.59	2.28
343.3	8210	0.21	1.91E-04	0.22	0.818	72.59	2.28
367.9	8202	0.305	2.44E-04	0.22	0.818	72.59	2.29
385.5	8190	0.426	3.05E-04	0.22	0.818	72.59	2.29
349.6	8176	0.57	3.70E-04	0.219	0.818	72.59	2.3
329.9	8976	0.09	1.31E-04	0.221	0.819	72.59	2.28
349.4	8966	0.155	1.67E-04	0.221	0.819	72.59	2.28
357.4	8949	0.237	2.08E-04	0.22	0.818	72.59	2.28
326.2	8932	0.335	2.52E-04	0.219	0.818	72.59	2.29
370.5	8922	0.07	9.75E-05	0.222	0.819	72.59	2.28
339.5	8920	0.12	1.29E-04	0.222	0.819	72.59	2.28
351.8	8910	0.184	1.65E-04	0.221	0.819	72.59	2.28
352.8	8894	0.265	2.05E-04	0.221	0.819	72.59	2.28

Appendix C

Nu	Re	xq	Bo	Pr/Pc	Tr/Tc	MW	Pr
311.2	8877	0.362	2.48E-04	0.22	0.819	72.59	2.29
329.1	9313	0.08	1.23E-04	0.225	0.821	72.59	2.27
353.4	9306	0.141	1.58E-04	0.225	0.821	72.59	2.27
370	9294	0.219	1.96E-04	0.225	0.82	72.59	2.28
341.6	9282	0.311	2.38E-04	0.224	0.82	72.59	2.28
514	7973	0.047	6.86E-05	0.223	0.82	72.59	2.27
433.8	7971	0.065	8.37E-05	0.223	0.82	72.59	2.27
390.2	7969	0.108	1.15E-04	0.223	0.82	72.59	2.28
346.8	7966	0.165	1.52E-04	0.223	0.82	72.59	2.28
364.6	7960	0.241	1.94E-04	0.223	0.82	72.59	2.28
375.5	7949	0.336	2.41E-04	0.222	0.819	72.59	2.29
336	7938	0.45	2.93E-04	0.222	0.819	72.59	2.29
490.5	7768	0.058	8.26E-05	0.223	0.82	72.59	2.27
425.1	7766	0.079	1.01E-04	0.223	0.82	72.59	2.27
389.9	7764	0.13	1.38E-04	0.223	0.82	72.59	2.28
350.9	7760	0.2	1.83E-04	0.223	0.82	72.59	2.28
371.7	7753	0.291	2.33E-04	0.223	0.82	72.59	2.28
386.1	7742	0.406	2.91E-04	0.223	0.82	72.59	2.29
347.7	7730	0.544	3.53E-04	0.222	0.82	72.59	2.29
469.6	7856	0.045	6.55E-05	0.223	0.82	72.59	2.27
404.5	7854	0.062	7.99E-05	0.223	0.82	72.59	2.27
369.6	7852	0.103	1.10E-04	0.223	0.82	72.59	2.27
331.3	7849	0.158	1.45E-04	0.223	0.82	72.59	2.28
348.1	7843	0.23	1.85E-04	0.223	0.82	72.59	2.28
357.6	7832	0.321	2.30E-04	0.223	0.82	72.59	2.28
320	7820	0.43	2.79E-04	0.222	0.82	72.59	2.29
460.8	7787	0.054	7.68E-05	0.224	0.82	72.59	2.27
395.1	7785	0.074	9.37E-05	0.224	0.82	72.59	2.27
358.7	7783	0.121	1.29E-04	0.224	0.82	72.59	2.28
320	7780	0.186	1.70E-04	0.224	0.82	72.59	2.28
337.5	7773	0.271	2.17E-04	0.224	0.82	72.59	2.28
349.1	7762	0.378	2.71E-04	0.223	0.82	72.59	2.29
312.7	7750	0.506	3.28E-04	0.223	0.82	72.59	2.29
366.3	5755	0.065	1.69E-04	0.224	0.82	72.59	2.27
341.8	5752	0.15	2.23E-04	0.224	0.82	72.59	2.28
366.6	5746	0.26	2.85E-04	0.224	0.82	72.59	2.28
383.8	5736	0.401	3.55E-04	0.224	0.82	72.59	2.29
352.9	5725	0.569	4.31E-04	0.223	0.82	72.59	2.29
378.6	9044	0.099	1.68E-04	0.225	0.821	72.59	2.27
412.1	9033	0.182	2.10E-04	0.224	0.82	72.59	2.28
411.9	9021	0.281	2.54E-04	0.224	0.82	72.59	2.28
348.4	8687	0.073	1.37E-04	0.222	0.819	72.59	2.28
329.3	8683	0.142	1.82E-04	0.222	0.819	72.59	2.28
356.3	8675	0.232	2.32E-04	0.221	0.819	72.59	2.28

Appendix C

Nu	Re	xq	Bo	Pr/Pc	Tr/Tc	MW	Pr
377	8663	0.347	2.89E-04	0.221	0.819	72.59	2.29
348.6	8649	0.483	3.51E-04	0.221	0.819	72.59	2.29
348.4	8687	0.073	1.37E-04	0.222	0.819	72.59	2.28
329.3	8683	0.142	1.82E-04	0.222	0.819	72.59	2.28
356.3	8675	0.232	2.32E-04	0.221	0.819	72.59	2.28
377	8663	0.347	2.89E-04	0.221	0.819	72.59	2.29
348.6	8649	0.483	3.51E-04	0.221	0.819	72.59	2.29
356.9	8923	0.053	1.01E-04	0.224	0.82	72.59	2.27
334.8	8920	0.104	1.33E-04	0.224	0.82	72.59	2.27
358.4	8913	0.17	1.70E-04	0.224	0.82	72.59	2.28
374	8902	0.254	2.12E-04	0.224	0.82	72.59	2.28
341.3	8890	0.354	2.57E-04	0.223	0.82	72.59	2.28
311.4	9717	0.086	1.21E-04	0.224	0.82	72.59	2.27
338.6	9709	0.146	1.55E-04	0.223	0.82	72.59	2.28
357.4	9697	0.222	1.93E-04	0.223	0.82	72.59	2.28
333	9683	0.313	2.34E-04	0.223	0.82	72.59	2.28
320.6	9536	0.092	1.30E-04	0.224	0.82	72.59	2.27
349.7	9529	0.156	1.65E-04	0.224	0.82	72.59	2.28
370.8	9517	0.238	2.06E-04	0.224	0.82	72.59	2.28
346.8	9504	0.335	2.50E-04	0.223	0.82	72.59	2.28
336.6	9244	0.053	1.09E-04	0.224	0.82	72.59	2.27
329.9	9241	0.108	1.44E-04	0.224	0.82	72.59	2.27
360	9234	0.179	1.84E-04	0.224	0.82	72.59	2.28
382.2	9222	0.27	2.29E-04	0.223	0.82	72.59	2.28
356.9	9209	0.378	2.78E-04	0.223	0.82	72.59	2.29
337.5	8931	0.065	1.24E-04	0.223	0.82	72.59	2.27
330.6	8927	0.128	1.64E-04	0.223	0.82	72.59	2.28
361	8920	0.209	2.10E-04	0.223	0.82	72.59	2.28
383.9	8907	0.313	2.61E-04	0.222	0.82	72.59	2.28
358	8894	0.436	3.17E-04	0.222	0.819	72.59	2.29
324.8	11121	0.061	1.42E-04	0.218	0.817	72.59	2.28
365.9	11107	0.131	1.77E-04	0.218	0.817	72.59	2.28
395.1	11092	0.215	2.15E-04	0.217	0.817	72.59	2.29
327.4	12473	0.052	1.36E-04	0.22	0.818	72.59	2.28
371.5	12458	0.118	1.69E-04	0.219	0.818	72.59	2.28
407.8	12443	0.198	2.05E-04	0.219	0.818	72.59	2.28
330.5	11731	0.081	1.48E-04	0.22	0.818	72.59	2.28
370.4	11717	0.154	1.84E-04	0.22	0.818	72.59	2.28
390.7	11702	0.241	2.24E-04	0.22	0.818	72.59	2.28
296	11861	0.077	1.23E-04	0.22	0.818	72.59	2.28
329.3	11853	0.138	1.57E-04	0.22	0.818	72.59	2.28
357.4	11838	0.215	1.96E-04	0.22	0.818	72.59	2.28
347.3	11823	0.307	2.37E-04	0.219	0.818	72.59	2.29
295.8	9164	0.048	9.53E-05	0.22	0.818	72.59	2.28

Appendix C

Nu	Re	xq	Bo	Pr/Pc	Tr/Tc	MW	Pr
287	9161	0.096	1.26E-04	0.22	0.818	72.59	2.28
311	9153	0.158	1.61E-04	0.219	0.818	72.59	2.28
327.6	9141	0.238	2.00E-04	0.219	0.818	72.59	2.29
304.4	9128	0.332	2.43E-04	0.219	0.818	72.59	2.29
302.4	8929	0.06	1.05E-04	0.218	0.817	72.59	2.28
292.1	8926	0.113	1.38E-04	0.218	0.817	72.59	2.28
316.2	8919	0.182	1.76E-04	0.218	0.817	72.59	2.28
333	8906	0.269	2.20E-04	0.217	0.817	72.59	2.29
307.6	8893	0.372	2.66E-04	0.217	0.817	72.59	2.29
386.6	7932	0.053	7.62E-05	0.22	0.818	72.59	2.28
344.6	7930	0.073	9.30E-05	0.22	0.818	72.59	2.28
321.4	7928	0.12	1.28E-04	0.22	0.818	72.59	2.28
291.5	7925	0.184	1.69E-04	0.22	0.818	72.59	2.28
309.3	7918	0.268	2.15E-04	0.219	0.818	72.59	2.29
321.5	7906	0.374	2.68E-04	0.219	0.818	72.59	2.29
289.7	7893	0.501	3.25E-04	0.219	0.818	72.59	2.3

C2 R410-A/POE Data

Nu	Re	xq	Bo	Pr/Pc	Tr/Tc	MW	Pr
275.3	8184	0.071	7.68E-05	0.222	0.819	72.59	2.28
232.6	8182	0.109	1.01E-04	0.222	0.819	72.59	2.28
238.9	8176	0.16	1.30E-04	0.221	0.819	72.59	2.28
241	8166	0.224	1.61E-04	0.221	0.819	72.59	2.28
210.2	8155	0.3	1.95E-04	0.221	0.819	72.59	2.29
357.5	7900	0.049	6.45E-05	0.222	0.819	72.59	2.27
307.5	7898	0.082	8.84E-05	0.222	0.819	72.59	2.28
264	7896	0.126	1.17E-04	0.222	0.819	72.59	2.28
272.8	7890	0.184	1.49E-04	0.222	0.819	72.59	2.28
276.7	7880	0.258	1.86E-04	0.222	0.819	72.59	2.28
243.1	7869	0.346	2.25E-04	0.221	0.819	72.59	2.29
352.6	7913	0.06	7.72E-05	0.223	0.82	72.59	2.27
320.8	7911	0.099	1.06E-04	0.223	0.82	72.59	2.28
286.1	7908	0.152	1.40E-04	0.223	0.82	72.59	2.28
300.6	7902	0.222	1.79E-04	0.222	0.82	72.59	2.28
309.4	7891	0.31	2.23E-04	0.222	0.819	72.59	2.28
276.6	7880	0.415	2.70E-04	0.222	0.819	72.59	2.29
427	7768	0.049	7.09E-05	0.222	0.819	72.59	2.27
380.8	7766	0.068	8.65E-05	0.222	0.819	72.59	2.27
353.2	7764	0.111	1.19E-04	0.222	0.819	72.59	2.28
319.5	7761	0.171	1.57E-04	0.222	0.819	72.59	2.28
337.6	7755	0.249	2.00E-04	0.222	0.819	72.59	2.28
349.1	7744	0.348	2.49E-04	0.222	0.819	72.59	2.29

Appendix C

Nu	Re	xq	Bo	Pr/Pc	Tr/Tc	MW	Pr
313.9	7732	0.466	3.03E-04	0.221	0.819	72.59	2.29
288.1	9099	0.047	6.19E-05	0.211	0.814	72.59	2.29
266.5	9097	0.079	8.49E-05	0.211	0.814	72.59	2.29
239.5	9095	0.121	1.12E-04	0.211	0.814	72.59	2.29
251.4	9087	0.177	1.43E-04	0.211	0.814	72.59	2.29
257.9	9074	0.248	1.78E-04	0.21	0.814	72.59	2.3
230.3	9060	0.332	2.16E-04	0.21	0.814	72.59	2.3
296.7	8675	0.055	7.09E-05	0.211	0.814	72.59	2.29
289.8	8673	0.091	9.73E-05	0.211	0.814	72.59	2.29
272.1	8670	0.14	1.28E-04	0.211	0.814	72.59	2.29
290.9	8663	0.204	1.64E-04	0.21	0.814	72.59	2.3
303.1	8650	0.284	2.04E-04	0.21	0.814	72.59	2.3
276.6	8638	0.381	2.48E-04	0.21	0.814	72.59	2.3
309	8373	0.061	7.82E-05	0.211	0.814	72.59	2.29
302.3	8371	0.1	1.07E-04	0.211	0.814	72.59	2.29
284.2	8368	0.154	1.42E-04	0.211	0.814	72.59	2.29
304.5	8361	0.225	1.81E-04	0.21	0.814	72.59	2.3
318.2	8348	0.314	2.25E-04	0.21	0.814	72.59	2.3
291	8336	0.42	2.73E-04	0.21	0.814	72.59	2.31
421.8	6747	0.056	7.15E-05	0.22	0.818	72.59	2.28
317	6745	0.092	9.82E-05	0.22	0.818	72.59	2.28
253	6743	0.142	1.30E-04	0.22	0.818	72.59	2.28
254.9	6737	0.206	1.66E-04	0.22	0.818	72.59	2.28
253.4	6728	0.288	2.06E-04	0.219	0.818	72.59	2.29
217.5	6717	0.385	2.50E-04	0.219	0.818	72.59	2.29
231.8	8220	0.063	6.93E-05	0.218	0.817	72.59	2.28
194.7	8218	0.098	9.14E-05	0.218	0.817	72.59	2.28
200	8212	0.144	1.17E-04	0.218	0.817	72.59	2.28
202.1	8202	0.201	1.45E-04	0.217	0.817	72.59	2.29
176.5	8192	0.27	1.76E-04	0.217	0.817	72.59	2.29
235.1	8136	0.068	7.39E-05	0.219	0.818	72.59	2.28
194.2	8134	0.105	9.76E-05	0.219	0.818	72.59	2.28
198.5	8128	0.154	1.25E-04	0.219	0.818	72.59	2.28
200.1	8118	0.215	1.55E-04	0.219	0.818	72.59	2.28
173.3	8108	0.288	1.88E-04	0.218	0.818	72.59	2.29
367.4	7452	0.049	6.40E-05	0.223	0.82	72.59	2.27
312.6	7450	0.081	8.77E-05	0.223	0.82	72.59	2.27
268.7	7448	0.126	1.16E-04	0.223	0.82	72.59	2.28
277.9	7443	0.183	1.48E-04	0.223	0.82	72.59	2.28
281.8	7433	0.256	1.84E-04	0.222	0.82	72.59	2.28
248.7	7423	0.343	2.23E-04	0.222	0.819	72.59	2.29
402.4	8168	0.058	7.38E-05	0.225	0.821	72.59	2.27
348.6	8166	0.095	1.01E-04	0.225	0.821	72.59	2.27
301.5	8163	0.146	1.34E-04	0.225	0.821	72.59	2.27

Appendix C

Nu	Re	xq	Bo	Pr/Pc	Tr/Tc	MW	Pr
313	8156	0.212	1.71E-04	0.225	0.821	72.59	2.28
318.9	8146	0.296	2.13E-04	0.224	0.82	72.59	2.28
281.7	8134	0.397	2.58E-04	0.224	0.82	72.59	2.29
475.9	7746	0.047	6.70E-05	0.217	0.817	72.59	2.28
404.4	7744	0.064	8.18E-05	0.217	0.817	72.59	2.28
359.8	7742	0.105	1.12E-04	0.217	0.817	72.59	2.28
317.3	7740	0.162	1.48E-04	0.217	0.817	72.59	2.28
332	7733	0.235	1.89E-04	0.217	0.817	72.59	2.29
340.3	7722	0.329	2.36E-04	0.217	0.817	72.59	2.29
303.2	7711	0.44	2.86E-04	0.216	0.817	72.59	2.3
425.3	7696	0.048	6.87E-05	0.21	0.814	72.59	2.29
375.4	7694	0.066	8.38E-05	0.21	0.814	72.59	2.29
344.3	7692	0.108	1.15E-04	0.21	0.814	72.59	2.29
309.6	7689	0.166	1.52E-04	0.21	0.814	72.59	2.29
326.5	7682	0.242	1.94E-04	0.21	0.814	72.59	2.3
337	7671	0.337	2.42E-04	0.21	0.814	72.59	2.3
302.7	7660	0.451	2.93E-04	0.209	0.814	72.59	2.31

Appendix D

Computer Program

```

C*
C*-----MUST LINK WITH REFPRP3, REFPRP4, AND BLOCKS-----
C   PROGRAM PROCN
C
C   IMPLICIT DOUBLE PRECISION (A-H,O-Z)
C   DOUBLE PRECISION MREF,MWAT,MOLEMASS, NUAVG, JAAVG
C
C   PARAMETER (NFL = 50)
C   INTEGER NCOEF
C   INTEGER IAC !LJH
COMMON /PREFS/ NREFST,IEQN
COMMON /ESDATA/ CRIT(5,NFL)
COMMON /ERRSPN/ IERS
COMMON /ERRHPN/ IERH
COMMON /ERBUBT/ IERBT
COMMON /ERBUBP/ IERBP
COMMON /VAR/ X(100),X$(100),B(100)
COMMON /NCIR/ NC,IR
COMMON /FILE/ FILEPROF,FILEPRIN,TEST,DATE,FLOW
COMMON /GEN/ PREFPOS,MREF,TR1,PR1,HR1,TR,PR,HR,QUAL,VL,VV,HV,HL,
+CVL,CVV,CPL,CPV,VISCL,VISCV,CONDL,CONDV,HEATFLUX,TT,MOLEMASS
COMMON /GEN2/CRITTEMP,CRITPRES,CRITSVOL,CR,CRL,CRV,XMASSL,
+CTEMPL,CPRESL,
+CSVOLL,XMASSV,CTEMPV,CPRESV,CSVOLV,VOLESP,HTCOEF,TW,IAC
COMMON /RAWMEAS/ TWTR(20), XWTR(20), TWALL(20), XWALL(20),
*           XPREF(6), PREF(6), XTREF(5), TREF(5),
*           TWTRraw(20), TWALLraw(20)
C
C   CHARACTER*6 HREF,HNAME(NFL)*50
C   CHARACTER*20 HREF,HNAME(NFL)*50      !9/3/03 Nitin
C   CHARACTER*12 X$,Y$,CORR
C   CHARACTER*12
ref$,FILEPROF,FILEIN,FILEOUT,FILEPRIN,TEST,REFTYPE,NUMCYC
C   CHARACTER*30 DATE
C   CHARACTER*1 FLOW
C   CHARACTER*255 HERR
C
C   DIMENSION IR(20),CR(20),CRL(20),CRV(20), XORG(100)
C   dimension crl1(20),crv1(20)
C   DIMENSION CTW3T1(4),CTW3T2(4),CTT3T1(4),CTT3T2(4)
C   DIMENSION CTW3S1(4),CTW3S2(4),CTT3S1(4),CTT3S2(4)
C   DIMENSION CTW2T1(4),CTW2T2(4),CTT2T1(4),CTT2T2(4)
C   DIMENSION CTW2S1(4),CTW2S2(4),CTT2S1(4),CTT2S2(4)
C   DIMENSION PREFPOS(15),ZZ(12)
C   DIMENSION Y(15,100),Y$(100)
C   DIMENSION VTW(10),VDW(10),VTT(10)
C   DIMENSION NDATA(2)
C   DIMENSION GA(12), PRA(12), VM(12), XQA(12), VVA(12), REA(12),
*           HVHLA(12), XNUA(12), XJAA(12), SVA(12), PRRA(12)

```

Appendix D

```
*          TRA(12), VISCLA(12), VISCVA(12), DQDZ(12), DPDZ(12),
*          PRESS(12)      OPEN(2, FILE='DQDZ.DAT')
OPEN(14, FILE='TARAWDP.DAT')
OPEN(13, FILE='TAFRIC.DAT')
OPEN(1, FILE='NUQFLX.DAT')
OPEN(11, FILE='TAUNCERT.DAT')
OPEN(10, FILE='TAPRES4.DAT')
OPEN(4, FILE='TAPRES.DAT')
OPEN(15, FILE='BOILRANG.DAT')
OPEN(16, FILE='FRACDIFF.DAT')
OPEN(17, FILE='TAE22PRP.DAT')
OPEN(9, FILE='CORR.DAT')
C-----DEVICE 8 IS AN INPUT FILE
C      OPEN(8, FILE='FILE.DAT')
      OPEN(8, FILE='TEST.DAT')
1001 FORMAT (36(A12))
1002 FORMAT (36(E15.7))
1003 FORMAT (A28, E12.4)
1004 FORMAT (A28, A12)
1005 FORMAT (A28, A30)
1006 FORMAT (A12, A30)
1007 FORMAT (A28, E12.4)
1008 FORMAT (36(E12.4))
C      1009 FORMAT (36(A7))
1009 FORMAT (T5, A8, T13, A8, T20, A8, T31, A8, T42, A8, T49, A8, T56, A8, T65, A8,
*          T72, A8, T78, A8, T85, A8, T92, A8, T102, A8, T110, A8, T120, A8)
1010 FORMAT (2(E12.4), A12)
1011 FORMAT (2X, F6.1, 2X, F6.0, 2X, F5.3, 2X, F6.2, 2(2X, F5.3),
*          2X, F6.2, 2X, F5.2, 2X, F4.2, 2X, A1)
1012 FORMAT (2X, F7.1, 2X, F8.0, 2X, F5.3, 2X, E12.5, 2(2X, F5.3),
*          2X, F6.2, 2X, F7.2, 2X, F4.2, 2X, F4.1, 2X, F7.3, 2X, F6.0, 2X, F7.1,
*          2X, F6.0, 2X, F7.1)
1013 FORMAT (A12, A30, A1)
1014 FORMAT (2(2X, F8.4, 2X, F9.3), A20)
1015 FORMAT (2X, F6.0, 3(2X, F5.3), 2X, F7.5, 2(2X, F6.2), 2X, F7.5,
*          2X, F6.2, 3(2X, F7.5), 2X, F7.0, 2(2X, F10.8), 2X, F6.0)
1016 FORMAT (2X, F7.1, 2X, F6.0, 2X, F5.3, 2X, F3.1, 2X, F6.2, 2X, F6.3,
*          2X, F10.3, 2X, F7.3, 2X, F7.3, 2X, F7.3, 2X, F7.3, 2X, I3.1, 2(2X, F7.3))
1017 FORMAT (2X, F6.0, 2X, F7.3, 2X, F5.3, 2X, F7.5, 2X, F8.0, 2X, F7.3,
*          2(2X, F5.3, 2X, F6.3), 2X, F6.2, 2X, A1)
1018 FORMAT (3(2X, F6.0), 3(2X, F10.8), 2X, F9.0, 2X, F8.2, 2X, F6.0,
*          2X, F5.3, 2X, F6.2, 2X, F5.3, 2X, F10.8)
C      *          3(2X, F5.3), 2X, F6.2, 2X, F5.3, 2X, F10.8)
1019 FORMAT (2X, F6.0, 3(2X, F5.3), 2X, F7.5, 2(2X, F6.2), 2X, F7.5, 2X, F6.2)
1020 FORMAT (2X, F7.3, 2(2X, F5.3), 2X, F12.8, 2X, F9.1, 2X, F8.1)
1021 FORMAT (F5.3, 2X, F5.3, 2X, F5.3, 2X, F9.1, 2X, F7.0, 2X, F6.1, 2X, F6.2,
*          2X, F6.2, 2X, F6.2, 2X, F6.2, 2X, F6.4, 2X, F3.1)
1022 FORMAT (7(2X, F6.3))
1023 FORMAT (T1, A8, T10, A8, T17, A8, T26, A8, T34, A8, T42, A8, T50, A8)
1024 FORMAT (T1, A8, T8, A8, T17, A8, T24, A8, T30, A8, T38, A8, T47, A8, T58, A8,
*          T68, A8, T77, A8, T81, A8, T92, A8, T101, A8)
```

Appendix D

```
1025 FORMAT (T1,A9,T10,A8,T20,A8,T32,A8,T45,A8,T58,A8,T70,A8,T80,A8)
1026 FORMAT (F11.9,2X,F7.1,2X,F9.1,2X,E12.5,2X,E12.5,2X,F6.4,2X,E12.5,
*      2X,F6.2)
C      1 = 3rd TOGETHER
C      2 = 3rd SEPARATED
C      3 = 2nd TOGETHER
C      4 = 2nd SEPARATED
C      5 = LINEAR INT.
C
      ITW=2
      ITT=2
      NDATA(1)=55
      NDATA(2)=75
C
      PI=3.1415927
      DIAMETER=0.00882
      PAMB=101325.0
C 1st
      PREFPOS(1)=0.7120
      PREFPOS(2)=1.3250
      PREFPOS(3)=1.6340
      PREFPOS(4)=1.9385
      PREFPOS(5)=2.5500
      PREFPOS(6)=3.1475
C 2nd
      PREFPOS(7)=3.5300
      PREFPOS(8)=4.0785
      PREFPOS(9)=4.6880
      PREFPOS(10)=4.9970
      PREFPOS(11)=5.3010
      PREFPOS(12)=5.9130
C
      Z0=-0.412
      Z1=1.6585
      Z2=3.2455
      Z3=3.431
      Z4=5.019
      Z5=6.606
C-----These will be headers for CORR.DAT (file 9)-----
      Y$(1)="NUDh "
      Y$(2)="REDh "
      Y$(3)="xq "
      Y$(4)="BO "
      Y$(5)="RP "
      Y$(6)="RT "
      Y$(7)="MM "
      Y$(8)="VO "
      Y$(9)="PR "
      Y$(10)="FLOW "
      Y$(11)="ENHF "
      Y$(12)="REL "
```

Appendix D

```

Y$(13)="NUSDQ  "
Y$(14)="RELDH  "
Y$(15)="NUSDH  "
C   Y$(16)="DTSAT "
C   Y$(17)="XWTR  "
C   Y$(18)="TWTR  "
C   Y$(19)="XWALL "
C   Y$(20)="TWALL "
C   Y$(21)="HWS_CALC  "
C   Y$(22)=" ENH_FACTOR "
C   Y$(8)=" INCERT  "
C   Y$(9)=" NUX      "
C   Y$(10)=" NUXX    "
C   Y$(11)=" REX     "
C   Y$(12)=" REXX    "
C   Y$(13)=" QUX     "
C   Y$(14)=" QUXX    "
C   Y$(15)=" JAX     "
C   Y$(16)=" JAXX    "
C   Y$(17)=" RPX     "
C   Y$(18)=" RPXX    "
C   Y$(19)=" RTX     "
C   Y$(20)=" RTXX    "
C   Y$(21)=" MMX     "
C   Y$(22)=" MMXX    "
C   Y$(23)=" LRP     "
C   Y$(24)=" LRPX    "
C   Y$(25)=" LRPXX   "
C   Y$(26)=" POSITION "
C   Y$(27)=" POINT_NUM "
C   Y$(28)=" XCO1    "
C   Y$(29)=" XCO2    "
C
WRITE(9,1009) (Y$(J), J=1, 15)
WRITE(11,1024) 'NU ', 'RE ', 'QUAL ', 'FLOWN ', 'DTSAT ',
*             'XWTR ', 'QFLX ', 'TWTR ', 'XWALL ', 'TWALL ', 'IAC',
*             'TWALLraw ', 'TWTRraw'
WRITE(17,1025) 'VISCL', 'CP', 'Hfg', 'Vv', 'Vl', 'P/Pc', 'Kl', 'MW'
C   WRITE(11,1023) 'QUAL ', 'Xwtr ', 'TWraw ', 'TWfit ', 'Xwall ',
C   *             'TTraw ', 'TTfit '

READ(8,*) NUMFILE
C=====
DO 20 KKKK=1, NUMFILE
  READ(8,*) FILEIN, FILEOUT, FILEPRIN, FILEPROF, FLOW, INDREF
  OPEN(5, FILE=FILEIN)
  READ(5,1001) REFTYPE
  READ(5,*) NUMCYC
  READ(5,*) (B(I), I=1,14)
C   READ(5,*) CORR
  READ(5,*) (B(I), I=16,19)

```

Appendix D

```
      READ(5,1001) WALL
      READ(5,*) (B(I), I=20,31)
      READ(5,1001) WATER
      READ(5,*) (B(I), I=32,43)
      READ(5,1001) WALLRAW
      READ(5,*) (B(I), I=44,55)
      READ(5,1001) WATERRAW
      READ(5,*) (B(I), I=56,67)
C*****CONVERT B's to X's required by PROCN*****
      DO 51 I=1,12
          X(I)=B(I+19)
          X(I+12)=B(I+31)
          TWALLraw(I)=B(I+43)
          TWTRraw(I)=B(I+55)
51      CONTINUE
C CONVERT PSI TO KPA
      B(7)=B(7)*6.894744
      X(26)=B(3)
      X(50)=1000*B(7)
      X(53)=B(18)
      X(54)=B(19)
      X(40)=B(1)
      X(42)=B(14)
      X(45)=1000*B(9)
      X(46)=1000*B(10)
      X(47)=1000*B(11)
      X(48)=1000*B(12)
      X(49)=1000*B(13)

      OPEN(6,FILE=FILEOUT)
      DO 11 I=1, 5
          CR(I)=0.0
          CRL(I)=0.0
          CRV(I)=0.0
11      CONTINUE
C
      DO 12 I=1, 100
          Y$(I)=" Trash "
          DO 12 J=1, 15
              Y(J,I)=0.0
12      CONTINUE
C
      CALL VARNAMES(Y$)
      WRITE (6,1001) (Y$(I), I=1, 36)
C      READ(5,1006) TEST,DATE
C      READ(5,1013) TEST,DATE, FLOW
      TEST=REFTYPE
      DATE=FILEIN
C      READ(5,*) (X(I), I=1, NDATA(IDATFORM))
C      DO 1967 I = 1, NDATA(IDATFORM)
C          XORG(I) = X(I)
```

Appendix D

```
C 1967 CONTINUE
  CLOSE(5)
  CALL COEFP3T(CTT3T1,CTT3T2,CTW3T1,CTW3T2)
  CALL COEFP3S(CTT3S1,CTT3S2,CTW3S1,CTW3S2)
  CALL COEFP2T(CTT2T1,CTT2T2,CTW2T1,CTW2T2)
  CALL COEFP2S(CTT2S1,CTT2S2,CTW2S1,CTW2S2)
  DO 167 IJK=1, 4
C   WRITE(6,*) CTW3T1(IJK),"Twat fit", CTT3T1(IJK),"Twall fit"
167 CONTINUE
  ICOND=1
  IF (ICOND.EQ.1) GOTO 67
  ZZ(1)=0.7120
  ZZ(2)=1.3250
  ZZ(3)=1.6340
  ZZ(4)=1.9385
  ZZ(5)=2.5500
  ZZ(6)=3.1475
  ZZ(7)=3.5300
  ZZ(8)=4.0785
  ZZ(9)=4.6880
  ZZ(10)=4.9970
  ZZ(11)=5.3010
  ZZ(12)=5.9130
  COPPER=200.0
  WALL=0.0005
  DO 66 IJK=1, 12
    Z=ZZ(IJK)
    VTW(1)=CTW3T1(1)+CTW3T1(2)*Z+CTW3T1(3)*Z*Z+CTW3T1(4)*Z*Z*Z
    VDW(1)=CTW3T1(2)+2.0*CTW3T1(3)*Z+3.0*CTW3T1(4)*Z*Z
    VTW(2)=CTW3S1(1)+CTW3S1(2)*Z+CTW3S1(3)*Z*Z+CTW3S1(4)*Z*Z*Z
    VDW(2)=CTW3S1(2)+2.0*CTW3S1(3)*Z+3.0*CTW3S1(4)*Z*Z
    VTW(3)=CTW2T1(1)+CTW2T1(2)*Z+CTW2T1(3)*Z*Z
    VDW(3)=CTW2T1(2)+2.0*CTW2T1(3)*Z
    VTW(4)=CTW2S1(1)+CTW2S1(2)*Z+CTW2S1(3)*Z*Z
    VDW(4)=CTW2S1(2)+2.0*CTW2S1(3)*Z
    CALL WATERTEM(Z,VTW(5),VDW(5))
    TW=VTW(ITW)
    DTWDZ=VDW(ITW)
    CPW=CPWLIQ(TW)
    HEATFLUX=CPW*DTWDZ*X(42)/(PI*DIAMETER)
    DTWALL=HEATFLUX*WALL/COPPER
    X(IJK)=X(IJK)-DTWALL
66 CONTINUE
  CALL COEFP3T(CTT3T1,CTT3T2,CTW3T1,CTW3T2)
  CALL COEFP3S(CTT3S1,CTT3S2,CTW3S1,CTW3S2)
  CALL COEFP2T(CTT2T1,CTT2T2,CTW2T1,CTW2T2)
  CALL COEFP2S(CTT2S1,CTT2S2,CTW2S1,CTW2S2)
67 CONTINUE
  INTACT=1
  IEQN=2
  NREFST=2
```

Appendix D

```
IF (INDREF.EQ.0) THEN
C R407C
  NC=3
  IR(1)=9
  IR(2)=16
  IR(3)=18
C CR(1)=0.227
C CR(2)=0.245
  CR(1)=0.23
  CR(2)=0.25
  CR(3)=0.52
END IF
IF (INDREF.EQ.1) THEN
C R134A
  NC=1
  IR(1)=18
  CR(1)=1.0
END IF
IF (INDREF.EQ.2) THEN
C R410A
  NC=2
  IR(1)=9
  IR(2)=16
C CR(1)=0.45
C CR(2)=0.55
  CR(1)=0.5
  CR(2)=0.5
END IF
IF (INDREF.EQ.3) THEN
C R125
  NC=1
  IR(1)=16
  CR(1)=1.0
END IF
IF (INDREF.EQ.4) THEN
C R32
  NC=1
  IR(1)=9
  CR(1)=1.0
END IF
IF (INDREF.EQ.5) THEN
C R32/R134a
  NC=2
  IR(1)=9
  IR(2)=18
  CR(1)=0.30
END IF
IF (INDREF.EQ.6) THEN
C R32/R134a
  NC=2
  IR(1)=9
```

Appendix D

```

      IR(2)=18
      CR(1)=0.281
      CR(2)=0.729
      END IF
      IF (INDREF.EQ.7) THEN
C
      R22
      NC=1
      IR(1)=7
      END IF
      CALL BCONST(NC,IR)
      DO 14 I=1, NC
      CRL(I)=CR(I)
      CRV(I)=CR(I)
14  CONTINUE
      TR1=X(26)
      PR1=X(50)
      DPW1=X(53)
      DPW2=X(54)
      MREF=X(40)
      MWAT=X(42)
      P0=X(50)
      P1=P0-X(45)
      P2=P1-X(46)
      P3=P2-X(47)
      P4=P3-X(48)
      P5=P4-X(49)
      CALL CALCMAS(MOLEMASS,CR,1)
      CALL CRITXSI(CR,CRITTEMP,CRITPRES,CRITSVOL,IER)
      B4=5.52674000E-13
      B3=-2.56582000E-09
      B2=4.72977600E-06
      B1=-4.76298500E-03
      B0=3.04277200E+00
      PP = PR1/1000.D0
      DT = B4*PP**4.0D0 + B3*PP**3.0D0 + B2*PP**2.0D0 +
1      B1*PP + B0
      TR1 = TR1+DT
      CALL HCVCPSI(0,TR1,PR1,CR,HR1,T$,T$,T$,T$)
      VTW(1)=CTW3T1(1)
      VTW(2)=CTW3S2(1)
      VTW(3)=CTW2T1(1)
      VTW(4)=CTW2S1(1)
      Z=0
      CALL WATERTEM(Z,VTW(5),VDW(5))
      TW1=VTW(ITW)
      PW1=PAMB+DPW1*(0.0-0.1015)/(3.1975-0.1015)
C-----FIRST HALF OF HAIRPIN
      DO 60 IND=1, 6
      Z=PREFPOS(IND)
      PR=P1+(P0-P1)*(Z-Z1)/(Z0-Z1)
      IF (Z.GT.Z1) PR=P2+(P1-P2)*(Z-Z2)/(Z1-Z2)

```

Appendix D

```

VTW(1)=CTW3T1(1)+CTW3T1(2)*Z+CTW3T1(3)*Z*Z+CTW3T1(4)*Z*Z*Z
VDW(1)=CTW3T1(2)+2.0*CTW3T1(3)*Z+3.0*CTW3T1(4)*Z*Z
VTW(2)=CTW3S2(1)+CTW3S2(2)*Z+CTW3S2(3)*Z*Z+CTW3S2(4)*Z*Z*Z
VDW(2)=CTW3S2(2)+2.0*CTW3S2(3)*Z+3.0*CTW3S2(4)*Z*Z
VTW(3)=CTW2T1(1)+CTW2T1(2)*Z+CTW2T1(3)*Z*Z
VDW(3)=CTW2T1(2)+2.0*CTW2T1(3)*Z
VTW(4)=CTW2S1(1)+CTW2S1(2)*Z+CTW2S1(3)*Z*Z
VDW(4)=CTW2S1(2)+2.0*CTW2S1(3)*Z
CALL WATERTEM(Z,VTW(5),VDW(5))
TW=VTW(ITW)
DTWDZ=VDW(ITW)
CPWDT=CPWDTINT(TW,TW1)
if (flow.eq.'P'.or.flow.eq.'p') then
  DTWDZ=-1*DTWDZ
  CPWDT=-1*CPWDT
endif
VW=(VWLIQ(TW1)+VWLIQ(TW))/2.0
PW=PAMB+DPW1*(Z-0.1015)/(3.1975-0.1015)
DPWDZ=DPW1/(3.1975-0.1015)
HR=HR1+(MWAT/MREF)*(CPWDT+VW*(PW-PW1))
CALL HPINSI(HR,PR,CR,TR,QUAL,CRL,CRV,VL,VV,HL,HV)
c WRITE(*,*) CRL,CRV
CALL HCVCP2SI(1,TR,PR,CRL,T$,T$,T$,CPL,T$)
CALL HCVCP2SI(2,TR,PR,CRV,T$,T$,T$,CPV,T$)
CALL TRNSPSI(PR,TR,T$,CRL,VISCL,CONDL,1)
CALL TRNSPSI(PR,TR,T$,CRV,VISCV,CONDV,2)
CALL CALCMAS(XMMASSL,CRL,1)
CALL CRITXSI(CRL,CTEMPL,CPRESL,CSVOLL,IER)
CALL CALCMAS(XMMASSV,CRV,1)
CALL CRITXSI(CRV,CTEMPV,CPRESV,CSVOLV,IER)
C*****Calculate surface tension for use in Thome correlation
TR=TR+273.15
RHOL=1/VL
CALL SURFT(TR,RHOL,CRL,SIGMA,IERR,HERR)
TR=TR-273.15
VOLESP=VL+QUAL*(VV-VL)
CPW=CPWLIQ(TW)
C-----calculate Q/L into refr for smooth tube-----
HEATFLUX=(CPW*DTWDZ+VW*DPWDZ)*MWAT/(PI*DIAMETER)
VTT(1)=CTT3T1(1)+CTT3T1(2)*Z+CTT3T1(3)*Z*Z+CTT3T1(4)*Z*Z*Z
VTT(2)=CTT3S2(1)+CTT3S2(2)*Z+CTT3S2(3)*Z*Z+CTT3S2(4)*Z*Z*Z
VTT(3)=CTT2T1(1)+CTT2T1(2)*Z+CTT2T1(3)*Z*Z
VTT(4)=CTT2S1(1)+CTT2S1(2)*Z+CTT2S1(3)*Z*Z
VTT(5)=X(IND)
TT=VTT(ITT)
HTCOEF=HEATFLUX/(TT-TR)
c WRITE(*,*) CPW,DTWDZ,VW,DPWDZ,ITW,HEATFLUX,TT-TR,HTCOEF
CALL RECORDER(Y,IND)
Y(IND,5)=Y(IND,5)+273.15
Y(IND,7)=-Y(IND,7)
WRITE(6,1002)(Y(IND,I),I=1,36)

```

Appendix D

```
Y(IND,5)=Y(IND,5)-273.15
Y(IND,7)=-Y(IND,7)
WRITE(16,*) crv(1)-crl(1),crv(2)-crl(2),crv(3)-crl(3)
  write(22,*) 'IND',IND
  write(22,*) 'Z',Z
  WRITE(22,*) 'P1',P1
  WRITE(22,*) 'PO',P0
  WRITE(22,*) 'Z1',Z1
  WRITE(22,*) 'PR', PR
  WRITE(22,*) 'CTW3T1(1)',CTW3T1(1)
  WRITE(22,*) 'CTW3T1(2)',CTW3T1(2)
  WRITE(22,*) 'CTW3T1(3)',CTW3T1(3)
  WRITE(22,*) 'CTW3T1(4)',CTW3T1(4)
  WRITE(22,*) 'CTW3S2(1)',CTW3S2(1)
  WRITE(22,*) 'CTW3S2(2)',CTW3S2(2)
  WRITE(22,*) 'CTW3S2(3)',CTW3S2(3)
  WRITE(22,*) 'CTW3S2(4)',CTW3S2(4)
  WRITE(22,*) 'VTW(1)',VTW(1)
  WRITE(22,*) 'VDW(1)',VDW(1)
  WRITE(22,*) 'VTW(2)',VTW(2)
  WRITE(22,*) 'VDW(2)',VDW(2)
  WRITE(22,*) 'VTW(3)',VTW(3)
  WRITE(22,*) 'VDW(3)',VDW(3)
  WRITE(22,*) 'VTW(4)',VTW(4)
  WRITE(22,*) 'VDW(4)',VDW(4)
  WRITE(22,*) 'CTW2T1(1)',CTW2T1(1)
  WRITE(22,*) 'CTW2T1(2)',CTW2T1(2)
  WRITE(22,*) 'CTW2T1(3)',CTW2T1(3)
  WRITE(22,*) 'CTW2S1(1)',CTW2S1(1)
  WRITE(22,*) 'CTW2S1(2)',CTW2S1(2)
  WRITE(22,*) 'CTW2S1(3)',CTW2S1(3)
  WRITE(22,*) 'TW',TW
  WRITE(22,*) 'DTWDZ',DTWDZ
  WRITE(22,*) 'TW1',TW1
  WRITE(22,*) 'CPWDT',CPWDT
  WRITE(22,*) 'VW',VW
  WRITE(22,*) 'PW',PW
  WRITE(22,*) 'PW1',PW1
  WRITE(22,*) 'HR1',HR1
  WRITE(22,*) 'HR',HR
  WRITE(22,*) 'PR',PR
  WRITE(22,*) 'CR(1)',CR(1)
  WRITE(22,*) 'CR(2)',CR(2)
  WRITE(22,*) 'TR',TR
  WRITE(22,*) 'QUAL',QUAL
  WRITE(22,*) 'CRL(1)',CRL(1)
  write(22,*) 'CRL(2)',CRL(2)
  WRITE(22,*) 'CRV(1)',CRV(1)
  WRITE(22,*) 'CRV(2)',CRV(2)
  WRITE(22,*) 'VL',VL
  WRITE(22,*) 'VV',VV
```

Appendix D

```

WRITE (22, *) 'HL', HL
WRITE (22, *) 'HV', HV
WRITE (22, *) 'CPW', CPW
WRITE (22, *) 'DTWDZ', DTWDZ
WRITE (22, *) 'VW', VW
WRITE (22, *) 'HEATFLUX', HEATFLUX
WRITE (22, *) 'CTT3T1 (1)', CTT3T1 (1)
WRITE (22, *) 'CTT3T1 (2)', CTT3T1 (2)
WRITE (22, *) 'CTT3T1 (3)', CTT3T1 (3)
WRITE (22, *) 'CTT3T1 (4)', CTT3T1 (4)
WRITE (22, *) 'CTT3S2 (1)', CTT3S2 (1)
WRITE (22, *) 'CTT3S2 (2)', CTT3S2 (2)
WRITE (22, *) 'CTT3S2 (3)', CTT3S2 (3)
WRITE (22, *) 'CTT3S2 (4)', CTT3S2 (4)
WRITE (22, *) 'CTT2T1 (1)', CTT2T1 (1)
WRITE (22, *) 'CTT2T1 (2)', CTT2T1 (2)
WRITE (22, *) 'CTT2T1 (3)', CTT2T1 (3)
WRITE (22, *) 'CTT2S1 (1)', CTT2S1 (1)
WRITE (22, *) 'CTT2S1 (2)', CTT2S1 (2)
WRITE (22, *) 'CTT2S1 (3)', CTT2S1 (3)
WRITE (22, *) 'VTT (1)', VTT (1)
WRITE (22, *) 'VTT (2)', VTT (2)
WRITE (22, *) 'VTT (3)', VTT (3)
WRITE (22, *) 'VTT (4)', VTT (4)
WRITE (22, *) 'VTT (5)', VTT (5)
WRITE (22, *) 'ITT', ITT
WRITE (22, *) 'TT', TT
WRITE (22, *) 'TT-TR', TT-TR
WRITE (22, *) 'HTCOEF', HTCOEF
WRITE (22, *)
60 CONTINUE
CPWDTUB=0.0
Z=3.339
VTW (1)=CTW3T1 (1)+CTW3T1 (2)*Z+CTW3T1 (3)*Z*Z+CTW3T1 (4)*Z*Z*Z
VTW (2)=CTW3S2 (1)+CTW3S2 (2)*Z+CTW3S2 (3)*Z*Z+CTW3S2 (4)*Z*Z*Z
VTW (3)=CTW2T1 (1)+CTW2T1 (2)*Z+CTW2T1 (3)*Z*Z
VTW (4)=CTW2S1 (1)+CTW2S1 (2)*Z+CTW2S1 (3)*Z*Z
CALL WATERTEM (Z, VTW (5), VDW (5))
TWATOUT1=VTW (ITW)
VTW (1)=CTW3T2 (1)+CTW3T2 (2)*Z+CTW3T2 (3)*Z*Z+CTW3T2 (4)*Z*Z*Z
VTW (2)=CTW3S2 (1)+CTW3S2 (2)*Z+CTW3S2 (3)*Z*Z+CTW3S2 (4)*Z*Z*Z
VTW (3)=CTW2T2 (1)+CTW2T2 (2)*Z+CTW2T2 (3)*Z*Z
VTW (4)=CTW2S2 (1)+CTW2S2 (2)*Z+CTW2S2 (3)*Z*Z
CALL WATERTEM (Z, VTW (5), VDW (5))
TWATINL2=VTW (ITW)
CPWDTUB=CPWDTINT (TWATINL2, TWATOUT1)
C-----SECOND HALF OF HAIRPIN
DO 70 IND=7, 12
Z=PREFPOS (IND)
PR=P4+(P3-P4)*(Z-Z4)/(Z3-Z4)
IF (Z.GT.Z4) PR=P5+(P4-P5)*(Z-Z5)/(Z4-Z5)

```

Appendix D

```
VTW(1)=CTW3T2(1)+CTW3T2(2)*Z+CTW3T2(3)*Z*Z+CTW3T2(4)*Z*Z*Z
VDW(1)=CTW3T2(2)+2.0*CTW3T2(3)*Z+3.0*CTW3T2(4)*Z*Z
VTW(2)=CTW3S2(1)+CTW3S2(2)*Z+CTW3S2(3)*Z*Z+CTW3S2(4)*Z*Z*Z
VDW(2)=CTW3S2(2)+2.0*CTW3S2(3)*Z+3.0*CTW3S2(4)*Z*Z
VTW(3)=CTW2T2(1)+CTW2T2(2)*Z+CTW2T2(3)*Z*Z
VDW(3)=CTW2T2(2)+2.0*CTW2T2(3)*Z
VTW(4)=CTW2S2(1)+CTW2S2(2)*Z+CTW2S2(3)*Z*Z
VDW(4)=CTW2S2(2)+2.0*CTW2S2(3)*Z
CALL WATERTEM(Z,VTW(5),VDW(5))
TW=VTW(ITW)
DTWDZ=VDW(ITW)
CPWDT=CPWDTINT(TW,TW1)
if (flow.eq.'P' .or. flow.eq.'p') then
  DTWDZ=-1*DTWDZ
  CPWDT=-1*CPWDT
endif
VW=(VWLIQ(TW1)+VWLIQ(TW))/2.0
PW=PAMB+DPW2*(Z-3.4805)/(6.5565-3.4805)
DPWDZ=DPW2/(6.5565-3.4805)
HR=HR1+(MWAT/MREF)*(CPWDT-CPWDTUB+VW*(PW-PW1))
WRITE(22,*)
WRITE(22,*) 'ITW',ITW
WRITE(22,*) 'TWATINL2',TWATINL2
WRITE(22,*) 'TWATOUT1',TWATOUT1
WRITE(22,*) 'CPWDTUB',CPWDTUB
WRITE(22,*) 'P4',P4
WRITE(22,*) 'P3',P3
WRITE(22,*) 'Z3',Z3
WRITE(22,*) 'Z4',Z4
WRITE(22,*) 'CTW3T2(1)',CTW3T2(1)
WRITE(22,*) 'CTW3T2(2)',CTW3T2(2)
WRITE(22,*) 'CTW3T2(3)',CTW3T2(3)
WRITE(22,*) 'CTW3T2(4)',CTW3T2(4)
WRITE(22,*) 'CTW3S2(1)',CTW3S2(1)
WRITE(22,*) 'CTW3S2(2)',CTW3S2(2)
WRITE(22,*) 'CTW3S2(3)',CTW3S2(3)
WRITE(22,*) 'CTW3S2(4)',CTW3S2(4)
WRITE(22,*) 'CTW2T2(1)',CTW2T2(1)
WRITE(22,*) 'CTW2T2(2)',CTW2T2(2)
WRITE(22,*) 'CTW2T2(3)',CTW2T2(3)
WRITE(22,*) 'CTW2S2(1)',CTW2S2(1)
WRITE(22,*) 'CTW2S2(2)',CTW2S2(2)
WRITE(22,*) 'CTW2S2(3)',CTW2S2(3)
WRITE(22,*)
CALL HPINSI(HR,PR,CR,TR,QUAL,CRL,CRV,VL,VV,HL,HV)
CALL HCVCP2SI(1,TR,PR,CRL,T$,T$,T$,CPL,T$)
CALL HCVCP2SI(2,TR,PR,CRV,T$,T$,T$,CPV,T$)
CALL TRNSPSI(PR,TR,T$,CRL,VISCL,CONDL,1)
CALL TRNSPSI(PR,TR,T$,CRV,VISCV,CONDV,2)
CALL CALCMAS(XMMASL,CRL,1)
CALL CRITXSI(CRL,CTEMPL,CPRESL,CSVOLL,IER)
```

Appendix D

```
CALL CALCMAS (XMMASV, CRV, 1)
CALL CRITXSI (CRV, CTEMPV, CPRESV, CSVOLV, IER)
TR=TR+273.15
RHOL=1/VL
CALL SURFT (TR, RHOL, CRL, SIGMA, IERR, HERR)
TR=TR-273.15
VOLESP=VL+QUAL*(VV-VL)
CPW=CPWLIQ(TW)
HEATFLUX=(CPW*DTWDZ+VW*DPWDZ)*MWAT/(PI*DIAMETER)
VTT(1)=CTT3T2(1)+CTT3T2(2)*Z+CTT3T2(3)*Z*Z+CTT3T2(4)*Z*Z*Z
VTT(2)=CTT3S2(1)+CTT3S2(2)*Z+CTT3S2(3)*Z*Z+CTT3S2(4)*Z*Z*Z
VTT(3)=CTT2T2(1)+CTT2T2(2)*Z+CTT2T2(3)*Z*Z
VTT(4)=CTT2S2(1)+CTT2S2(2)*Z+CTT2S2(3)*Z*Z
VTT(5)=X(IND)
TT=VTT(ITT)
HTCOEF=HEATFLUX/(TT-TR)
CALL RECORDER(Y, IND)
Y(IND, 5)=Y(IND, 5)+273.15
Y(IND, 7)=-Y(IND, 7)
WRITE(6, 1002) (Y(IND, I), I=1, 36)
Y(IND, 5)=Y(IND, 5)-273.15
Y(IND, 7)=-Y(IND, 7)
WRITE(16, *) crv(1)-crl(1), crv(2)-crl(2), crv(3)-crl(3)
  write(22, *) 'IND', IND
  write(22, *) 'Z', Z
  WRITE(22, *) 'P1', P1
  WRITE(22, *) 'PO', P0
  WRITE(22, *) 'Z1', Z1
  WRITE(22, *) 'PR', PR
  WRITE(22, *) 'CTW3T1(1)', CTW3T1(1)
  WRITE(22, *) 'CTW3T1(2)', CTW3T1(2)
  WRITE(22, *) 'CTW3T1(3)', CTW3T1(3)
  WRITE(22, *) 'CTW3T1(4)', CTW3T1(4)
  WRITE(22, *) 'CTW3S2(1)', CTW3S2(1)
  WRITE(22, *) 'CTW3S2(2)', CTW3S2(2)
  WRITE(22, *) 'CTW3S2(3)', CTW3S2(3)
  WRITE(22, *) 'CTW3S2(4)', CTW3S2(4)
  WRITE(22, *) 'VTW(1)', VTW(1)
  WRITE(22, *) 'VDW(1)', VDW(1)
  WRITE(22, *) 'VTW(2)', VTW(2)
  WRITE(22, *) 'VDW(2)', VDW(2)
  WRITE(22, *) 'VTW(3)', VTW(3)
  WRITE(22, *) 'VDW(3)', VDW(3)
  WRITE(22, *) 'VTW(4)', VTW(4)
  WRITE(22, *) 'VDW(4)', VDW(4)
  WRITE(22, *) 'CTW2T1(1)', CTW2T1(1)
  WRITE(22, *) 'CTW2T1(2)', CTW2T1(2)
  WRITE(22, *) 'CTW2T1(3)', CTW2T1(3)
  WRITE(22, *) 'CTW2S1(1)', CTW2S1(1)
  WRITE(22, *) 'CTW2S1(2)', CTW2S1(2)
  WRITE(22, *) 'CTW2S1(3)', CTW2S1(3)
```

Appendix D

```
WRITE (22, *) 'TW', TW
WRITE (22, *) 'DTWDZ', DTWDZ
WRITE (22, *) 'TW1', TW1
WRITE (22, *) 'CPWDT', CPWDT
WRITE (22, *) 'VW', VW
WRITE (22, *) 'PW', PW
WRITE (22, *) 'PW1', PW1
WRITE (22, *) 'DPWDZ', DPWDZ
WRITE (22, *) 'HR1', HR1
WRITE (22, *) 'HR', HR
WRITE (22, *) 'PR', PR
WRITE (22, *) 'CR(1)', CR(1)
WRITE (22, *) 'CR(2)', CR(2)
WRITE (22, *) 'TR', TR
WRITE (22, *) 'QUAL', QUAL
WRITE (22, *) 'CRL(1)', CRL(1)
write (22, *) 'CRL(2)', CRL(2)
WRITE (22, *) 'CRV(1)', CRV(1)
WRITE (22, *) 'CRV(2)', CRV(2)
WRITE (22, *) 'VL', VL
WRITE (22, *) 'VV', VV
WRITE (22, *) 'HL', HL
WRITE (22, *) 'HV', HV
WRITE (22, *) 'CPW', CPW
WRITE (22, *) 'DTWDZ', DTWDZ
WRITE (22, *) 'VW', VW
WRITE (22, *) 'DPWDZ', DPWDZ
WRITE (22, *) 'HEATFLUX', HEATFLUX
WRITE (22, *) 'CTT3T1(1)', CTT3T1(1)
WRITE (22, *) 'CTT3T1(2)', CTT3T1(2)
WRITE (22, *) 'CTT3T1(3)', CTT3T1(3)
WRITE (22, *) 'CTT3T1(4)', CTT3T1(4)
WRITE (22, *) 'CTT3S2(1)', CTT3S2(1)
WRITE (22, *) 'CTT3S2(2)', CTT3S2(2)
WRITE (22, *) 'CTT3S2(3)', CTT3S2(3)
WRITE (22, *) 'CTT3S2(4)', CTT3S2(4)
WRITE (22, *) 'CTT2T1(1)', CTT2T1(1)
WRITE (22, *) 'CTT2T1(2)', CTT2T1(2)
WRITE (22, *) 'CTT2T1(3)', CTT2T1(3)
WRITE (22, *) 'CTT2S1(1)', CTT2S1(1)
WRITE (22, *) 'CTT2S1(2)', CTT2S1(2)
WRITE (22, *) 'CTT2S1(3)', CTT2S1(3)
WRITE (22, *) 'VTT(1)', VTT(1)
WRITE (22, *) 'VTT(2)', VTT(2)
WRITE (22, *) 'VTT(3)', VTT(3)
WRITE (22, *) 'VTT(4)', VTT(4)
WRITE (22, *) 'VTT(5)', VTT(5)
WRITE (22, *) 'ITT', ITT
WRITE (22, *) 'TT', TT
WRITE (22, *) 'TT-TR', TT-TR
WRITE (22, *) 'HTCOEF', HTCOEF
```

Appendix D

```
WRITE(6,1003) " CONCENTRATION FLUID 3 --> ",CR(3)
WRITE(6,1003) " CONCENTRATION FLUID 4 --> ",CR(4)
WRITE(6,1003) " CONCENTRATION FLUID 5 --> ",CR(5)
CLOSE(6)
CALL WRITER(Y,Y$)
C-----CALC THE DQ/DXQ TO DETERMINE IF ITS COUNTERFLOW OR PARALLEL FLOW
C-----IF DQDXQ > 0 ITS PARALLEL FLOW, IF DQDXQ < 0 ITS COUNTERFLOW
DQDXQ = (ABS(Y(4,7)) - ABS(Y(6,7)))/(ABS(Y(4,6)) - ABS(Y(6,6)))
IF(DQDXQ.LT.0.0)THEN
    FLOW="P"
    FLOWN = 2.0
END IF
IF(DQDXQ.GT.0.0)THEN
    FLOW="C"
    FLOWN = 1.0
END IF
write(18,1001) "quality","htcoef_meas","htcoef_corr",
1 "NU_meas","NU_corr"
DO 13 J=1, 12
    QUAL=Y(J,6)
    HEATFLUX=Y(J,7)
    HTCDEF=Y(J,8)
    VOLESF=Y(J,10)
    VL=Y(J,11)
    VV=Y(J,12)
    TT=Y(J,2)
    TR=Y(J,5)
    CONDL=Y(J,15)
    CONDV=Y(J,16)
    COND=CONDL+0.0*(CONDV-CONDL)
    VISCL=Y(J,13)
    VISCV=Y(J,14)
    VISC=VISCL+0.0*(VISCV-VISCL)
    HVHL=Y(J,9)
    CPL=Y(J,17)
    CPV=Y(J,18)
    CP=CPL+0.0*(CPV-CPL)
    PR=Y(J,3)
    DIAMH = 0.00545
C-----EQUIVALENT CROSS SECTIONAL FLOW DIA: DEQ (m)
DEQ = 0.0088
C-----convert Q/L from smooth tube value to finned tube -----
SMFLUX=HEATFLUX
HEATFLUX=HEATFLUX/1.5572
XNU=HEATFLUX*DIAMH/((TT-TR)*CONDL)
DTSAT = TR - TT
XRE=MREF*DIAMH/(((PI*DEQ**2)/4.0)*VISCL)
GA(J)=MREF/(((PI*DEQ**2)/4.0))
XJA=HVHL/(CPL*(TT-TR))
XBO=HEATFLUX/(GA(J)*HVHL)
XRP=PR/CRITPRES
```

Appendix D

```

70 CONTINUE
WRITE(6,1001) (Y$(I), I=1, 36)
WRITE(6,*) " "
WRITE(6,1004) " TEST NAME --> ",TEST
WRITE(6,1005) " DATE OF THE TEST --> ",DATE
WRITE(6,1003) " MASS FLOW RATE --> ",MREF
WRITE(6,1003) " TEMP. OF REF. INLET --> ",TR1
WRITE(6,1003) " PRES. OF REF. INLET --> ",PR1
WRITE(6,1003) " ENTHALPY REF. INLET --> ",HR1
WRITE(6,1003) " MOLECULAR MASS --> ",MOLEMASS
WRITE(6,1003) " CRITICAL TEMPERATURE --> ",CRITTEMP
WRITE(6,1003) " CRITICAL PRESSURE --> ",CRITPRES
WRITE(6,1003) " CRITICAL ESP. VOLUME --> ",CRITSVOL
WRITE(6,1003) " CONCENTRATION FLUID 1 --> ",CR(1)
WRITE(6,1003) " CONCENTRATION FLUID 2 --> ",CR(2)
XQU=QUAL
XRT=(TR+273.15)/(CRITTEMP+273.15)
XREX=XRE**XQU
XREXX=XRE**(XQU**2)
XJAX=DABS(XJA)**XQU
XJAXX=DABS(XJA)**(XQU**2)
XRPX=XRP**XQU
XRPXX=XRP**(XQU**2)
XRTX=XRT**XQU
XRTXX=XRT**(XQU**2)
XMMX=MOLEMASS**XQU
XMMXX=MOLEMASS**(XQU**2)
XLRP=-DLOG10(XRP)
XLRPX=XLRP**XQU
XLRPXX=XLRP**(XQU**2)
XNUX=DABS(XNU)**XQU
XNUXX=DABS(XNU)**(XQU**2)
XQUX=DABS(XQU+0.01)**XQU
XQUXX=DABS(XQU+0.01)**(XQU**2)
ERH=1000.0
C XCO1=(HTCOEF/CONDL)*((VISCL*VOLESP)**2)/9.81)**0.33333
C XCO2=9.81*HVHL*DIAMETER**3/(CONDL*VISCL*(TR-TT)*VOLESP**2)
XVO=(VV-VL)/VOLESP
XVOX=XVO**XQU
XVI=(VISCL-VISCV)/VISCL
XPR=VISCL*CPL/CONDL
XVL=VV/VL
C NU USING BEST CORRELATION FO THIS WORK
C W1=XRE**0.290164
C W2=XRP**(-0.689724*QUAL*QUAL)
C W3=(-DLOG10(XRP))**(-0.550395*QUAL*QUAL)
C W4=DABS(XJA)**(0.207773*QUAL)
C W5=XVO**(2.61904*QUAL)
C W6=XPR**0.358903
C XNU1=5.6521*W1*W2*W3*W4*W5*W6
c Correlation of Hamilton, Kezierski, and Kaul from NISTIR 7243

```

Appendix D

```
C1 = 0.51*XQU
C2 = 5.57*XQU-5.21*XQU**2.
C3 = 0.54-1.56*XQU+1.42*XQU**2.
C4 = -0.81+12.56*XQU-11*XQU**2.
C5 = 0.25-.035*XQU**2.
XMW = 72.585
XPRTL = CPL*VISCL/CONDL
CALL BCONST(NCC, IR(2))
P=PR/1000
lbub=.true.
crl1=crl
crv1=crv
CALL BUBLP (P, crl1, crv1, Tlv, vldum, vvdum, lbub, lcrit)
CALL BCONST(NCC, IR(1))
P=PR/1000
lbub=.true.
crl1=crl
crv1=crv
CALL BUBLP (P, crl1, crv1, Tmv, vldum, vvdum, lbub, lcrit)
call bconst(nc, ir)
p=pr/1000
lbub=.true.
crl1=crl
crv1=crv
call bublp(p, crl1, crv1, tbub, vldum, vvdum, lbub, lcrit)
p=pr/1000
lbub=.false.
crl1=crl
crv1=crv
call bublp(p, crl1, crv1, tdew, vldum, vvdum, lbub, lcrit)
dx = dabs(crl(1)-crv(1))
c6 = (tlv-tmv)*(278.9*(dx)-4298*(tdew-tbub)/(tr+273.15))
1 / (tr+273.15)
XNU1 = 482.18*XRE**0.3*XPRTL**C1*XRP**C2*XBO**C3*(-LOG10(XRP))**C4
1 *XMW**C5*1.1**C6
XHTC = (CONDL/DIAMH)*XNU1
xhtc2 = xhtc*.0446/(pi*diameter)
write(18,1002) xqu,htcoef*(pi*diameter)/.0446,xhtc,xnu,xnu1
CC1=2.6494816
CC2=0.290156
CC3=-0.689786
CC4=-0.550372
CC5=0.207769
CC6=2.61893
CC7=0.358894
W1=XRE**CC2
W2=XRP**(CC3*QUAL*QUAL)
W3=(-DLOG10(XRP))**(CC4*QUAL*QUAL)
W4=DABS(XJA)**(CC5*QUAL)
W5=XVO**(CC6*QUAL)
W6=XPR**CC7
```

Appendix D

```

XNU1=CC1*W1*W2*W3*W4*W5*W6
C WATER SIDE HEAT TRANSFER COEFFICIENT COMPARATION
TW=Y (J, 36)
HEATF=-HEATFLUX*11.735/9.525
WHTCEXP=HEATF/(TT-TW)
DD1=0.009525
DD2=0.013925
DDE=DD2-DD1
ATR=PI*(DD2**2-DD1**2)/4.0
COND=CONDWLIQ(TW)
VISC=VISCWLIQ(TW)
CP=CPWLIQ(TW)
W1=DABS(MWAT*DDE/(VISC*ATR))**0.8
W2=(CP*VISC/COND)**0.4
W3=(DD2/DD1)**0.45
WHTCCALC=0.023*(COND/DDE)*W1*W2*W3
C-----USING THE EQUIVALENT DIAMETER IN THE REYNOLDS NUMBER XREQ
XREQ = XRE*DEQ/DIAMH
XREV=DABS(XREQ*XQU*(VV/VL)**0.5)
XREL=DABS(XREQ*(1.0-XQU))
XREM=XREV+XREL
NUSDQ=XNU4
IF (FRD.LE.0.05) THEN
    E=E*FRD** (0.1-2*FRD)
    S=S*FRD**0.5
    HLIQ=HLIQ*E
    HPOOL=HPOOL*S
ELSE
HSMOOTHG= ((E*HLIQ)**2+(S*HPOOL)**2)**0.5
END IF
END IF
TM1=(1+0.12*(1-QUAL))*(VV*QUAL+VL*(1-QUAL))
TM2=(1.18*(1-QUAL)*(9.81*SIGMA*(1/VL-1/VV))**0.25)/(GA(J)/VL**0.5)
IF (QUAL.LE.0) ALPHA=0
IF (QUAL.GE.1) ALPHA=1
IF ((QUAL.GT.0).AND.(QUAL.LT.1)) ALPHA = VV*QUAL/(TM1+TM2)
THETAS = 2*(PI-ACOS(2*ALPHA-1))
THETAD = ALPHA*THETAS
HNB=HPOOL
DEL=PI*DIAMETER*(1-ALPHA)/(2*(2*PI-THETAD))
LFRE=4*MREF*(1-QUAL)*DEL/(1-ALPHA)/VISCL/PI/DIAMETER**2
HCB=0.0133*XREL**0.69*XPR**0.4*CONDL/DEL
HWET=(HNB**3+HCB**3)**.3333
KREV=4*MREF*QUAL/PI/DIAMETER/ALPHA/VISCV
PRV=CPV*VISCV/CONDV
HVAP=0.023*KREV**0.8*PRV**0.4*CONDV/DIAMETER
HTPK=(THETAD*HVAP+(2*PI-THETAD)*HWET)/2/PI
QTH=1/((0.291*(VL/VV)**-0.571*(VISCL/VISCV)**-0.143)+1)
IF (QUAL.LE.QTH) HSMOOTH=HWET
IF (QUAL.GE.1) HSMOOTH=HVAP
IF ((QUAL.GT.QTH).AND.(QUAL.LT.1)) HSMOOTH=HTPK

```

Appendix D

```

IF (QUAL.LE.QTH) THEN
    IAC = 0.0
ELSE
    IAC = 1.0
END IF
NUSDQ = HSMOOTHG*DEQ/CONDL
NUSDH = HSMOOTHG*DIAMH/CONDL
XRELDH = XREL*DIAMH/DEQ
    HMICRO=XNU*CONDL/DIAMH
    AMICRO=0.013735
    ASMOOTH=0.00882
    ENHF=HMICRO*1.6/HSMOOTHG
VM(J) = XQU*VV + (1-XQU)*VL
PRA(J) = XPR
XQA(J) = XQU
VVA(J) = VV
REA(J) = XRE
HVHLA(J) = HVHL
XNUA(J) = XNU
XJAA(J) = XJA
SVA(J) = XVO
PRRA(J) = XRP
TRA(J) = TR
VISCLA(J) = VISCL
VISCVA(J) = VISCV
WRITE(9,1012) XNU,XRE,XQU,XBO,XRP,XRT,MOLEMASS,XVO,XPR,FLOWN,
* ENHF, XREL, HSMOOTH*DEQ/CONDL, XRELDH, HSMOOTH*DIAMH/CONDL
PREFPOS(J),XQU,TR,PR,XRE,XNU,ENHF,MOLEMASS,XPR,XVO,
    QFLX = DABS(HEATFLUX)
    WRITE(11,1016) XNU, XRE, XQU, FLOWN, DTSAT, XWTR(J), QFLX,
* TWTR(J), XWALL(J), TWALL(J), IAC,
* TWALLraw(J), TWTRraw(J)
    WRITE(1,1017) QFLX, DTSAT, XQU, MREF, PR, TR, XWTR(J),
* TWTR(J), XWALL(J), TWALL(J), MOLEMASS, FLOW
13 CONTINUE
C-----END OF J-LOOP
    CALL DYDX1(XQA,XWALL,12,DQDZ)
    CALL DYDX1(PRESS,XWALL,12,DPDZ)
    DO 125 J=1, 12
        FTOT = DPDZ(J)*DIAMH/(GA(J)**2*VM(J))
        WRITE(2,1020) DQDZ(J), XQA(J), XWALL(J), FTOT, DPDZ(J)
* ,XNUA(J)
125 CONTINUE
C-----WRITE FRICTION FACTOR TO FILE (LIMIT TO TWO CENTER PORTION OF
C-----THE TEST SECTION TO ENSURE NO SINGLE PHASE ASSOCIATED WITH dp
    CALL INTRP(XQA(3),XQA(4),XWALL(3),XWALL(4),Z1,XQ1)
    CALL INTRP(XQA(6),XQA(7),XWALL(6),XWALL(7),Z2,XQ2)
    XQAVG = (XQ1 + XQ2)/2.D0
    DXQ = XQ2 - XQ1
    CALL INTRP(VM(3),VM(4),XQA(3),XQA(4),XQ1,VM1)
    CALL INTRP(VM(6),VM(7),XQA(6),XQA(7),XQ2,VM2)

```

Appendix D

```

CALL INTRP (175.D0,130.D0, .424D0, .242D0, .358D0,ANSW)
CALL INTRP (XNUA (4),XNUA (6),XQA (4),XQA (6),XQAVG,NUAVG)
CALL INTRP (GA (4),GA (6),XQA (4),XQA (6),XQAVG,GAVG)
CALL INTRP (VVA (4),VVA (6),XQA (4),XQA (6),XQAVG,VVAVG)
CALL INTRP (HVHLA (4),HVHLA (6),XQA (4),XQA (6),XQAVG,HFG)
CALL INTRP (REA (4),REA (6),XQA (4),XQA (6),XQAVG,REAVG)
CALL INTRP (VISCLA (4),VISCLA (6),XQA (4),XQA (6),XQAVG,VISLA)
CALL INTRP (VISCVA (4),VISCVA (6),XQA (4),XQA (6),XQAVG,VISVA)
CALL INTRP (TRA (3),TRA (4),XWALL (3),XWALL (4),Z1,TRA1)
CALL INTRP (TRA (6),TRA (7),XWALL (6),XWALL (7),Z2,TRA2)
CALL INTRP (PRA (4),PRA (6),XQA (4),XQA (6),XQAVG,PRAVG)
TRA1 = TRA1 + 273.15D0
TRA2 = TRA2 + 273.15D0
DL = Z2 - Z1
DP = X(46)
PRT2 = DIAMH/(XQAVG*DL)
PRT1 = 2.D0*DIAMH/(VM2 + VM1)*DL
FM = PRT1*(DP/GAVG**2 - VM2 + VM1)
FBO = PRT2*(DP/(GAVG**2*VVAVG) - DXQ)
BO = DABS(DXQ*HFG/(9.801D0*DL))
FNEW = 0.00456D0*BO**0.211/(REAVG**0.062)
DPNEW = (FNEW + (VM2 - VM1)*PRT1)*GAVG**2/PRT1
FBOP = 0.0185*(BO/REAVG)**0.25
PRTA1 = DXQ*DIAMH/(XQAVG*DL)
PRTB2 = DL*GAVG**2*XQAVG*VVAVG/DIAMH
DPBO = (FBOP + PRTA1)*PRTB2
FTOT = DP*DIAMH/(GAVG**2*DL*0.5D0*(VM2+VM1))
WRITE(13,1018) DP, DPBO, DPNEW, FM, FBO, FNEW, BO, NUAVG, REAVG,
*           XQAVG, MOLEMASS, PRAVG, FTOT
WRITE(14,1019) DP, DL, XQ1, XQ2, MREF, TRA1, TRA2, FM, MOLEMASS
WRITE(10,1015) DP, DL, XQ1, XQ2, MREF, TRA1, TRA2, FM, MOLEMASS,
*           VM1, VM2, VVAVG, HFG, VISLA, VISVA, REAVG
CALL INTRP (XQA (6),XQA (7),XWALL (6),XWALL (7),Z3,XQ3)
CALL INTRP (XQA (10),XQA (11),XWALL (10),XWALL (11),Z4,XQ4)
XQAVG = (XQ3 + XQ4)/2.D0
DXQ = XQ4 - XQ3
CALL INTRP (VM (6),VM (7),XQA (6),XQA (7),XQ3,VM3)
CALL INTRP (VM (10),VM (11),XQA (10),XQA (11),XQ4,VM4)
C-----CALC AVERAGE QUANTIES PER TEST SECTION QUARTER
CALL INTRP (XNUA (7),XNUA (9),XQA (7),XQA (9),XQAVG,NUAVG)
CALL INTRP (GA (7),GA (9),XQA (7),XQA (9),XQAVG,GAVG)
CALL INTRP (VVA (7),VVA (9),XQA (7),XQA (9),XQAVG,VVAVG)
CALL INTRP (HVHLA (7),HVHLA (9),XQA (7),XQA (9),XQAVG,HFG)
CALL INTRP (REA (7),REA (9),XQA (7),XQA (9),XQAVG,REAVG)
CALL INTRP (TRA (6),TRA (7),XWALL (6),XWALL (7),Z3,TRA3)
CALL INTRP (TRA (10),TRA (11),XWALL (10),XWALL (11),Z4,TRA4)
CALL INTRP (VISCLA (7),VISCLA (9),XQA (7),XQA (9),XQAVG,VISLA)
CALL INTRP (VISCVA (7),VISCVA (9),XQA (7),XQA (9),XQAVG,VISVA)
CALL INTRP (PRA (7),PRA (9),XQA (7),XQA (9),XQAVG,PRAVG)
TRA3 = TRA3 + 273.15D0
TRA4 = TRA4 + 273.15D0

```

Appendix D

```

PRT2 = DIAMH/(XQAVG*DL)
PRT1 = 2.D0*DIAMH/((VM4 + VM3)*DL)
C-----MODIFIED BO PIERRE FRICTION FACTOR W/O APPROX FOR SPECIFIC VOL
FM = PRT1*(DP/GAVG**2 - VM4 + VM3)
C-----BO PIERRE FRICTION FACTOR
FBO = PRT2*(DP/(GAVG**2*VVAVG) - DXQ)
C-----CALC BO PIERRE BOILING #
BO = DABS(DXQ*HFG/(9.801D0*DL))
C-----CALC CORRELATED FRICTION FACTOR FROM FM DATA
FNEW = 0.00456D0*BO**0.211/(REAVG**0.062)
C-----CALC PRESS DROP (Pa) USING CORRELATION FOR FM
DPNEW = (FNEW + (VM4 - VM3)*PRT1)*GAVG**2/PRT1
C-----CALC BO PIERRE PRESSURE DROP
FBOP = 0.0185*(BO/REAVG)**0.25
PRTA1 = DXQ*DIAMH/(XQAVG*DL)
PRTB2 = DL*GAVG**2*XQAVG*VVAVG/DIAMH
DPBO = (FBOP + PRTA1)*PRTB2
C-----CALC THE TOTAL FRICTION FACTOR INCLDING WALL FRIC AND ACC LOSSES
FTOT = DP*DIAMH/(GAVG**2*DL*0.5D0*(VM2+VM1))
WRITE(13,1018) DP, DPBO, DPNEW, FM, FBO, FNEW, BO, NUAVG, REAVG,
*           XQAVG, MOLEMASS, PRAVG, FTOT
WRITE(14,1019) DP, DL, XQ3, XQ4, MREF, TRA3, TRA4, FM, MOLEMASS
WRITE(10,1015) DP, DL, XQ3, XQ4, MREF, TRA3, TRA4, FM, MOLEMASS,
*           VM3, VM4, VVAVG, HFG, VISLA, VISVA, REAVG
DO 2121 I=1, 5
  WRITE(4,1014) XPREF(I), PREF(I), XTREF(I), TREF(I), FILEIN
2121 CONTINUE
  WRITE(4,1014) XPREF(6), PREF(6), XTREF(5), TREF(5), FILEIN
20  CONTINUE
C-----SHOULD CLOSE 8 AND 9 HERE
CLOSE(2)
CLOSE(9)
CLOSE(4)
CLOSE(8)
CLOSE(10)
CLOSE(1)
CLOSE(13)
CLOSE(14)
CLOSE(15)
CLOSE(16)
CLOSE(17)
IF (INDREF .EQ. 2 .or. INDREF .EQ. 5
&   .or. INDREF .EQ. 6) THEN
  IF (INDREF .EQ. 1) THEN
    IR(1) = IR(1)
    IR(2) = IR(3)
  ENDIF
  CALL PROB2B(NUMFILE)
ENDIF
STOP
END

```

Appendix D

```
C This is the end of the main program
C*****
      SUBROUTINE WATERTEM(Z,TTTT,DTDZ)
      IMPLICIT DOUBLE PRECISION (A-H, O-Z)
      COMMON /VAR/ X(100),X$(100)
      CHARACTER*12 X$
      DIMENSION ZZ(12),TT(12)
      ZZ(1)=0.1250
      ZZ(2)=0.7375
      ZZ(3)=1.3520
      ZZ(4)=1.9640
      ZZ(5)=2.5770
      ZZ(6)=3.1735
      ZZ(7)=3.5045
      ZZ(8)=4.1035
      ZZ(9)=4.7140
      ZZ(10)=5.3250
      ZZ(11)=5.9380
      ZZ(12)=6.5325
      DO 11 I=1, 12
         TT(I)=X(12+I)
11      CONTINUE
         IND=12
         DO 10 I=2, 12
            IF (ZZ(I).GT.Z) THEN
               IND=I
               GOTO 20
            END IF
10      CONTINUE
20      CONTINUE
         IF (IND.EQ.7) THEN
            IND=6
            IF (Z.GT.3.339) IND=8
         END IF
         I0=IND-1
         I1=IND
         TTTT=TT(I0)+(TT(I1)-TT(I0))*(Z-ZZ(I0))/(ZZ(I1)-ZZ(I0))
         DTDZ=(TT(I1)-TT(I0))/(ZZ(I1)-ZZ(I0))
         RETURN
      END
C*****
      SUBROUTINE WALLTEMP(Z,TTTT)
      IMPLICIT DOUBLE PRECISION (A-H,O-Z)
      COMMON /VAR/ X(100),X$(100)
      CHARACTER*12 X$
      DIMENSION ZZ(12),TT(12)
      ZZ(1)=0.7120
      ZZ(2)=1.3250
      ZZ(3)=1.6340
      ZZ(4)=1.9385
      ZZ(5)=2.5500
```

Appendix D

```
ZZ(6)=3.1475
ZZ(7)=3.5300
ZZ(8)=4.0785
ZZ(9)=4.6880
ZZ(10)=4.9970
ZZ(11)=5.3010
ZZ(12)=5.9130
DO 11 I=1, 12
    TT(I)=X(12)
11 CONTINUE
IND=12
DO 10 I=2, 12
    IF (ZZ(I).GT.Z) THEN
        IND=I
        GOTO 20
    END IF
10 CONTINUE
20 CONTINUE
IF (IND.EQ.7) THEN
    IND=6
    IF (Z.GT.3.339) IND=8
END IF
I0=IND-1
I1=IND
TTTT=TT(I0)+(TT(I1)-TT(I0))*(Z-ZZ(I0))/(ZZ(I1)-ZZ(I0))
RETURN
END
SUBROUTINE REFPRESS(Z,PPPP)
IMPLICIT DOUBLE PRECISION (A-H,O-Z)
COMMON /VAR/ X(100),X$(100)
CHARACTER*12 X$
DIMENSION ZZ(12),PP(12)
ZZ(1)=-0.412
ZZ(2)=1.6585
ZZ(3)=3.2455
ZZ(4)=3.4310
ZZ(5)=5.0190
ZZ(6)=6.6060
PP(1)=X(50)
PP(2)=PP(1)-X(45)
PP(3)=PP(2)-X(46)
PP(4)=PP(3)-X(47)
PP(5)=PP(4)-X(48)
PP(6)=PP(5)-X(49)
IND=6
DO 10 I=2, 6
    IF (ZZ(I).GT.Z) THEN
        IND=I
        GOTO 20
    END IF
10 CONTINUE
```

Appendix D

```
20 CONTINUE
   IF (IND.EQ.4) THEN
       IND=3
       IF (Z.GT.3.339) IND=5
   END IF
   I0=IND-1
   I1=IND
   PPPP=PP(I0)+(PP(I1)-PP(I0))*(Z-ZZ(I0))/(ZZ(I1)-ZZ(I0))
   RETURN
END
SUBROUTINE PROFILE(NCOEF,C,NP,AA,BB,FIT)
IMPLICIT DOUBLE PRECISION (A-H,O-Z)
DIMENSION AA(20),BB(20)
DIMENSION C(4),G1(4),G2(4,4)
DIMENSION A(4,4),B(4),XX(4)
CHARACTER*2 FIT
NCOEF=NCOEF+1
C(1)=1.0
C(2)=1.0
C(3)=1.0
C(4)=1.0
11 CONTINUE
   DO 321 I=1, NCOEF
       B(I)=0.0
       DO 322 J=1, NCOEF
           A(I,J)=0.0
322 CONTINUE
321 CONTINUE
   DO 432 I=1, NP
       IF(FIT.EQ."CB".OR.FIT.EQ."PW") THEN
           G=C(1)+C(2)*BB(I)+C(3)*BB(I)**2-AA(I)
           IF (NCOEF.EQ.4) G=G+C(4)*BB(I)**3
           G1(1)=1.D0
           G1(2)=BB(I)
           G1(3)=BB(I)**2
           G1(4)=BB(I)**3
       END IF
       IF(FIT.EQ."CW") THEN
           G = C(1) + C(2)*BB(I)**2 + C(3)*BB(I)**3 - AA(I)
           G1(1) = 1.D0
           G1(2) = BB(I)**2
           G1(3) = BB(I)**3
       END IF
       IF(FIT.EQ."CT") THEN
           G = C(1) + C(2)*BB(I)**2 - AA(I)
           G1(1) = 1.D0
           G1(2) = BB(I)**2
       END IF
       IF(FIT.EQ."PT") THEN
           G = C(1) + C(2)*BB(I) + C(3)*BB(I)**2 - AA(I)
           G1(1) = 1.D0
```

Appendix D

```

        G1(2) = BB(I)
        G1(3) = BB(I)**2
    END IF
    DO 122 J=1, NCOEF
    DO 123 K=1, NCOEF
        G2(J,K)=0.0
123     CONTINUE
122     CONTINUE
    DO 323 J=1, NCOEF
    B(J)=B(J)+2.0*G*G1(J)
        DO 324 K=1, NCOEF
            A(J,K)=A(J,K)+2.0*G*G2(J,K)+2.0*G1(J)*G1(K)
324     CONTINUE
323     CONTINUE
432     CONTINUE
        CALL GAUSSY(A,B,XX,NCOEF)
        VT=0.0
        DO 157 I=1, NCOEF
            C(I)=C(I)-XX(I)
            VT=VT+DABS(100*XX(I)/(C(I)+1.0E-30))
157     CONTINUE
        IF (VT/NCOEF>0.0001) GOTO 11
        IF (FIT.EQ."CW") THEN
            C(4) = C(3)
            C(3) = C(2)
            C(2) = 0.D0
        END IF
        IF (FIT.EQ."CT") THEN
            C(4) = 0.D0
            C(3) = C(2)
            C(2) = 0.D0
        END IF
        IF (FIT.EQ."PT") THEN
            C(4) = 0.D0
        END IF
    RETURN
    END
    SUBROUTINE GAUSSY(A,B,XX,N)
    IMPLICIT DOUBLE PRECISION (A-H,O-Z)
    DIMENSION A(4,4),B(4),XX(4)
c    INTEGER CCOEF      ! - 09/02/03
    DO 28 K=1, N
        AMAX=0.0
        DO 4 I=K, N
            IF (DABS(A(I,K))-DABS(AMAX)) 3,3,2
2             AMAX=A(I,K)
            IMAX=I
3             CONTINUE
4             CONTINUE
        IF (DABS(AMAX)-0.1E-13) 10,10,14
10         WRITE(*,*) K,' SISTEMA LINEARMENTE DEPENDENTE '

```

Appendix D

```

        STOP
14      CONTINUE
        BTEMP=B(K)
        B(K)=B(IMAX)
        B(IMAX)=BTEMP
        DO 18 J=K, N
            ATEMP=A(K,J)
            A(K,J)=A(IMAX,J)
            A(IMAX,J)=ATEMP
18      CONTINUE
        KPLUS=K+1
        IF (K-N) 22,27,27
22      CONTINUE
        DO 24 I=KPLUS, N
            B(I)=B(I)-B(K)*A(I,K)/A(K,K)
            ACON=A(I,K)
            DO 25 J=K,N
                A(I,J)=A(I,J)-A(K,J)*ACON/A(K,K)
25      CONTINUE
24      CONTINUE
27      CONTINUE
28      CONTINUE
        L=N
32      SUM=0.0
        IF (L-N) 34,38,38
34      LPLUS=L+1
            DO 36 J=LPLUS, N
                SUM=SUM+A(L,J)*XX(J)
36      CONTINUE
38      CONTINUE
        XX(L)=(B(L)-SUM)/A(L,L)
        IF (L-1) 42,42,40
40      L=L-1
            GOTO 32
42      CONTINUE
        RETURN
        END
        SUBROUTINE COEFP3T(CWAL1,CWAL2,CWAT1,CWAT2)
        IMPLICIT DOUBLE PRECISION (A-H,O-Z)
        COMMON /VAR/ X(100),X$(100)
        COMMON /FILE/ FILEPROF,FILEPRIN,TEST,DATE,FLOW
        COMMON /RAWMEAS/ TWTR(20),XWTR(20),TWALL(20),XWALL(20),
*          XPREF(6),PREF(6),XTREF(5),TREF(5)
        INTEGER CODE
        CHARACTER*12 X$,FILEPRIN,FILEPROF,TEST
        CHARACTER*30 DATE
        CHARACTER*1 FLOW
        CHARACTER*2 FIT
        DIMENSION CWAL1(4),CWAL2(4),CWAT1(4),CWAT2(4)
        DIMENSION YYY(20),XXX(20)
        OPEN(3,FILE=FILEPROF)
```

Appendix D

```
1001 FORMAT (2(E12.4),A12)
      NUMPOINT=12
      YYY(1)=X(1)
      XXX(1)=0.7120
      YYY(2)=X(2)
      XXX(2)=1.3250
      YYY(3)=X(3)
      XXX(3)=1.6340
      YYY(4)=X(4)
      XXX(4)=1.9385
      YYY(5)=X(5)
      XXX(5)=2.5500
      YYY(6)=X(6)
      XXX(6)=3.1475
      DO 10 I=1, 6
         WRITE(3,1001) XXX(I),YYY(I)+273.15," TT.-.1st  "
10    CONTINUE
      YYY(7)=X(7)
      XXX(7)=3.5300
      YYY(8)=X(8)
      XXX(8)=4.0785
      YYY(9)=X(9)
      XXX(9)=4.6880
      YYY(10)=X(10)
      XXX(10)=4.9970
      YYY(11)=X(11)
      XXX(11)=5.3010
      YYY(12)=X(12)
      XXX(12)=5.9130
      DO 11 I=7, 12
         WRITE(3,1001) XXX(I),YYY(I)+273.15," TT.-.2nd  "
11    CONTINUE
C-----RETAIN THE RAW WALL TEMPERATURE (TWALL) MEASUREMENTS
      DO 1956 I = 1, 12
         XWALL(I) = XXX(I)
         TWALL(I) = YYY(I)
1956 CONTINUE
      IF(FLOW.EQ."P") THEN
         FIT = "PT"
         CODE = 2
      END IF
      IF(FLOW.EQ."C") THEN
         FIT = "CT"
         CODE = 1
      END IF
      CALL PROFILE(CODE,CWAL2,NUMPOINT,YYY,XXX,FIT)
      DO 19 I=1, 4
         CWAL1(I)=CWAL2(I)
19    CONTINUE
      YYY(1)=X(13)
      XXX(1)=0.1250
```

Appendix D

```

    YYY(2)=X(14)
    XXX(2)=0.7375
    YYY(3)=X(15)
    XXX(3)=1.3520
    YYY(4)=X(16)
    XXX(4)=1.9640
    YYY(5)=X(17)
    XXX(5)=2.5770
    YYY(6)=X(18)
    XXX(6)=3.1735
    DO 12 I=1, 6
        WRITE(3,1001) XXX(I),YYY(I)+273.15," TW.-.1st  "
12  CONTINUE
    YYY(7)=X(19)
    XXX(7)=3.5045
    YYY(8)=X(20)
    XXX(8)=4.1035
    YYY(9)=X(21)
    XXX(9)=4.7140
    YYY(10)=X(22)
    XXX(10)=5.3250
    YYY(11)=X(23)
    XXX(11)=5.9380
    YYY(12)=X(24)
    XXX(12)=6.5325
    DO 13 I=7, 12
        WRITE(3,1001) XXX(I),YYY(I)+273.15," TW.-.2nd  "
13  CONTINUE
C-----RETAIN THE RAW WATER TEMPERATURE (TWTR) MEASUREMENTS
    DO 1967 I = 1, 12
        XWTR(I) = XXX(I)
        TWTR(I) = YYY(I)
1967 CONTINUE
    IF(FLOW.EQ."P") THEN
        FIT = "PW"
        CODE = 3
    END IF
    IF(FLOW.EQ."C") THEN
        FIT = "CW"
        CODE = 2
    END IF
    CALL PROFILE(CODE,CWAT2,NUMPOINT,YYY,XXX,FIT)
    DO 18 I=1, 4
        CWAT1(I)=CWAT2(I)
18  CONTINUE
    YYY(1)=0
    XXX(1)=-0.412
    YYY(2)=-X(45)
    XXX(2)=1.6585
    YYY(3)=-X(46)
    XXX(3)=3.2455
```

Appendix D

```
YYY(4)=-X(47)
XXX(4)=3.431
YYY(5)=-X(48)
XXX(5)=5.019
YYY(6)=-X(49)
XXX(6)=6.606
DO 14 I=1, 6
    WRITE(3,1001) XXX(I),YYY(I)," PRES_REF  "
    XPREF(I) = XXX(I)
    PREF(I) = YYY(I)
14 CONTINUE
YYY(1)=X(25)
XXX(1)=-1.0
YYY(2)=X(26)
XXX(2)=-0.6375
YYY(3)=X(27)
XXX(3)=3.339
YYY(4)=X(28)
XXX(4)=3.339
YYY(5)=X(29)
XXX(5)=6.8635
DO 15 I=1, 5
    WRITE(3,1001) XXX(I),YYY(I)+273.15," TEMP_REF  "
    XTREF(I) = XXX(I)
    TREF(I) = YYY(I)
15 CONTINUE
C    WRITE(3,*) " TTCOEF 1st  TTCOEF 2nd  WATCOEF 1st WATCOEF 2nd"
C    DO 16 I=1, 4
C        WRITE (3,1002) CWAL1(I),CWAL2(I),CWAT1(I),CWAT2(I)
C 16 CONTINUE
C    CLOSE(3)
RETURN
END
SUBROUTINE COEFP3S(CWAL1,CWAL2,CWAT1,CWAT2)
IMPLICIT DOUBLE PRECISION (A-H,O-Z)
COMMON /VAR/ X(100),X$(100)
COMMON /FILE/ FILEPROF,FILEPRIN,TEST,DATE,FLOW
INTEGER CODE          !9/3/03
CHARACTER*12 X$,FILEPRIN,FILEPROF,TEST
CHARACTER*30 DATE
CHARACTER*1 FLOW
DIMENSION CWAL1(4),CWAL2(4),CWAT1(4),CWAT2(4)
DIMENSION YYY(20),XXX(20)
NUMPOINT=6
YYY(1)=X(1)
XXX(1)=0.7120
YYY(2)=X(2)
XXX(2)=1.3250
YYY(3)=X(3)
XXX(3)=1.6340
YYY(4)=X(4)
```

Appendix D

```
XXX(4)=1.9385
YYY(5)=X(5)
XXX(5)=2.5500
YYY(6)=X(6)
XXX(6)=3.1475
IF (FLOW.EQ."C") THEN      !9/2/03
  CODE = 3                  !9/2/03
END IF                      !9/2/03
CALL PROFILE (CODE,CWAL1,NUMPOINT,YYY,XXX,"CB")
YYY(1)=X(7)
XXX(1)=3.5300
YYY(2)=X(8)
XXX(2)=4.0785
YYY(3)=X(9)
XXX(3)=4.6880
YYY(4)=X(10)
XXX(4)=4.9970
YYY(5)=X(11)
XXX(5)=5.3010
YYY(6)=X(12)
XXX(6)=5.9130
IF (FLOW.EQ."C") THEN      !9/2/03
  CODE = 3                  !9/2/03
END IF                      !9/2/03
code=3
CALL PROFILE (CODE,CWAL2,NUMPOINT,YYY,XXX,"CB")
YYY(1)=X(13)
XXX(1)=0.1250
YYY(10)=X(13)
XXX(10)=0.1250
YYY(11)=X(13)
XXX(11)=0.1250
YYY(12)=X(13)
XXX(12)=0.1250
YYY(2)=X(14)
XXX(2)=0.7375
YYY(3)=X(15)
XXX(3)=1.3520
YYY(4)=X(16)
XXX(4)=1.9640
YYY(5)=X(17)
XXX(5)=2.5770
YYY(6)=X(18)
XXX(6)=3.1735
YYY(7)=X(18)
XXX(7)=3.1735
YYY(8)=X(18)
XXX(8)=3.1735
YYY(9)=X(18)
XXX(9)=3.1735
IF (FLOW.EQ."C") THEN      !9/2/03
```

Appendix D

```
CODE = 3                                !9/2/03
END IF                                  !9/2/03
code=2
CALL PROFILE (CODE, CWAT1, NUMPOINT, YYY, XXX, "CB")
YYY (1) = X (19)
XXX (1) = 3.5045
YYY (10) = X (19)
XXX (10) = 3.5045
YYY (11) = X (19)
XXX (11) = 3.5045
YYY (12) = X (19)
XXX (12) = 3.5045
YYY (2) = X (20)
XXX (2) = 4.1035
YYY (3) = X (21)
XXX (3) = 4.7140
YYY (4) = X (22)
XXX (4) = 5.3250
YYY (5) = X (23)
XXX (5) = 5.9380
YYY (6) = X (24)
XXX (6) = 6.5325
YYY (7) = X (24)
XXX (7) = 6.5325
YYY (8) = X (24)
XXX (8) = 6.5325
YYY (9) = X (24)
XXX (9) = 6.5325
IF (FLOW.EQ. "C") THEN                 !9/2/03
CODE = 3                                !9/2/03
END IF                                  !9/2/03
code=3
CALL PROFILE (CODE, CWAT2, NUMPOINT, YYY, XXX, "CB")
RETURN
END
SUBROUTINE COEFP2T (CWAL1, CWAL2, CWAT1, CWAT2)
IMPLICIT DOUBLE PRECISION (A-H, O-Z)
COMMON /VAR/ X (100), X$ (100)
COMMON /FILE/ FILEPROF, FILEPRIN, TEST, DATE, FLOW
INTEGER CODE                            !9/3/03
CHARACTER*12 X$, FILEPRIN, FILEPROF, TEST
CHARACTER*30 DATE
CHARACTER*1 FLOW
DIMENSION CWAL1 (4), CWAL2 (4), CWAT1 (4), CWAT2 (4)
DIMENSION YYY (20), XXX (20)
NUMPOINT=12
YYY (1) = X (1)
XXX (1) = 0.7120
YYY (2) = X (2)
XXX (2) = 1.3250
YYY (3) = X (3)
```

Appendix D

```
XXX(3)=1.6340
YYY(4)=X(4)
XXX(4)=1.9385
YYY(5)=X(5)
XXX(5)=2.5500
YYY(6)=X(6)
XXX(6)=3.1475
YYY(7)=X(7)
XXX(7)=3.5300
YYY(8)=X(8)
XXX(8)=4.0785
YYY(9)=X(9)
XXX(9)=4.6880
YYY(10)=X(10)
XXX(10)=4.9970
YYY(11)=X(11)
XXX(11)=5.3010
YYY(12)=X(12)
XXX(12)=5.9130
IF(FLOW.EQ."C") THEN      !9/2/03
  CODE = 2                 !9/2/03
END IF                     !9/2/03
CALL PROFILE(CODE,CWAL2,NUMPOINT,YYY,XXX,"CB")
DO 19 I=1, 4
  CWAL1(I)=CWAL2(I)
19 CONTINUE
YYY(1)=X(13)
XXX(1)=0.1250
YYY(2)=X(14)
XXX(2)=0.7375
YYY(3)=X(15)
XXX(3)=1.3520
YYY(4)=X(16)
XXX(4)=1.9640
YYY(5)=X(17)
XXX(5)=2.5770
YYY(6)=X(18)
XXX(6)=3.1735
YYY(7)=X(19)
XXX(7)=3.5045
YYY(8)=X(20)
XXX(8)=4.1035
YYY(9)=X(21)
XXX(9)=4.7140
YYY(10)=X(22)
XXX(10)=5.3250
YYY(11)=X(23)
XXX(11)=5.9380
YYY(12)=X(24)
XXX(12)=6.5325
IF(FLOW.EQ."C") THEN      !9/2/03
```

Appendix D

```
      CODE = 2                      !9/2/03
      END IF                          !9/2/03
      CALL PROFILE (CODE, CWAT2, NUMPOINT, YYY, XXX, "CB")
c    CALL PROFILE (3, CWAT2, NUMPOINT, YYY, XXX, "CB")      !9/2/03
      DO 18 I=1, 4
          CWAT1 (I) = CWAT2 (I)
18    CONTINUE
      RETURN
      END
      SUBROUTINE COEFP2S (CWAL1, CWAL2, CWAT1, CWAT2)
      IMPLICIT DOUBLE PRECISION (A-H, O-Z)
      COMMON /VAR/ X(100), X$(100)
      COMMON /FILE/ FILEPROF, FILEPRIN, TEST, DATE, FLOW
      INTEGER CODE                      !9/3/03
      CHARACTER*12 X$, FILEPRIN, FILEPROF, TEST
      CHARACTER*30 DATE
      CHARACTER*1 FLOW
      DIMENSION CWAL1 (4), CWAL2 (4), CWAT1 (4), CWAT2 (4)
      DIMENSION YYY (20), XXX (20)
      NUMPOINT=6
      YYY (1) = X (1)
      XXX (1) = 0.7120
      YYY (10) = X (1)
      XXX (10) = 0.7120
      YYY (11) = X (1)
      XXX (11) = 0.7120
      YYY (12) = X (1)
      XXX (12) = 0.7120
      YYY (2) = X (2)
      XXX (2) = 1.3250
      YYY (3) = X (3)
      XXX (3) = 1.6340
      YYY (4) = X (4)
      XXX (4) = 1.9385
      YYY (5) = X (5)
      XXX (5) = 2.5500
      YYY (6) = X (6)
      XXX (6) = 3.1475
      YYY (7) = X (6)
      XXX (7) = 3.1475
      YYY (8) = X (6)
      XXX (8) = 3.1475
      YYY (9) = X (6)
      XXX (9) = 3.1475
      IF (FLOW.EQ. "C") THEN          !9/2/03
          CODE = 2                    !9/2/03
      END IF                          !9/2/03
      CALL PROFILE (CODE, CWAL1, NUMPOINT, YYY, XXX, "CB")
      YYY (1) = X (7)
      XXX (1) = 3.5300
      YYY (10) = X (7)
```

Appendix D

```
XXX(10)=3.5300
YYY(11)=X(7)
XXX(11)=3.5300
YYY(12)=X(7)
XXX(12)=3.5300
YYY(2)=X(8)
XXX(2)=4.0785
YYY(3)=X(9)
XXX(3)=4.6880
YYY(4)=X(10)
XXX(4)=4.9970
YYY(5)=X(11)
XXX(5)=5.3010
YYY(6)=X(12)
XXX(6)=5.9130
YYY(7)=X(12)
XXX(7)=5.9130
YYY(8)=X(12)
XXX(8)=5.9130
YYY(9)=X(12)
XXX(9)=5.9130
IF (FLOW.EQ."C") THEN      !9/2/03
  CODE = 2                  !9/2/03
END IF                      !9/2/03
CALL PROFILE (CODE,CWAL2,NUMPOINT,YYY,XXX,"CB")
NUMPOINT=6
YYY(1)=X(13)
XXX(1)=0.1250
YYY(2)=X(14)
XXX(2)=0.7375
YYY(3)=X(15)
XXX(3)=1.3520
YYY(4)=X(16)
XXX(4)=1.9640
YYY(5)=X(17)
XXX(5)=2.5770
YYY(6)=X(18)
XXX(6)=3.1735
IF (FLOW.EQ."C") THEN      !9/2/03
  CODE = 2                  !9/2/03
END IF                      !9/2/03
CALL PROFILE (CODE,CWAT1,NUMPOINT,YYY,XXX,"CB")
YYY(1)=X(19)
XXX(1)=3.5045
YYY(2)=X(20)
XXX(2)=4.1035
YYY(3)=X(21)
XXX(3)=4.7140
YYY(4)=X(22)
XXX(4)=5.3250
YYY(5)=X(23)
```

Appendix D

```

XXX(5)=5.9380
YYY(6)=X(24)
XXX(6)=6.5325
IF (FLOW.EQ."C") THEN      !9/2/03
  CODE = 2                  !9/2/03
END IF                      !9/2/03
CALL PROFILE (CODE,CWAT2,NUMPOINT,YYY,XXX,"CB")
C CALL PROFILE (3,CWAT2,NUMPOINT,YYY,XXX,"CB")      !9/2/03
RETURN
END
DOUBLE PRECISION FUNCTION CPWDTINT (T2,T1)
IMPLICIT DOUBLE PRECISION (A-H,O-Z)
  N=20
  DT=(T2-T1)/(N-1)
  CPT1=CPWLIQ(T1)
  T=T1
  SCP=0.0
  DO 10 I=2, N
    T=T+DT
    CPT=CPWLIQ(T)
    CP=(CPT1+CPT)/2.0
    SCP=SCP+CP
    CPT1=CPT
10  CONTINUE
    CPWDTINT=SCP*DT
RETURN
END
C*****
DOUBLE PRECISION FUNCTION VWLIQ(T)
DOUBLE PRECISION AUX,T
  AUX=1000.5-4.2826D-4*T-5.8712D-3*T*T+1.7797D-5*T*T*T
  AUX=AUX-2.3462/T+2.3390D-2/(T*T)
  VWLIQ=1/AUX
RETURN
END
C*****
DOUBLE PRECISION FUNCTION CPWLIQ(T)
IMPLICIT DOUBLE PRECISION (A-H,O-Z)
  AUX=4.1625+1.0523D-3*T-2.4682D-5*T*T+2.0130D-7*T*T*T
  AUX=AUX+0.1652/T-1.6453D-3/(T*T)
  CPWLIQ=1000.0*AUX
RETURN
END
C*****
DOUBLE PRECISION FUNCTION VISCWLIQ(T)
IMPLICIT DOUBLE PRECISION (A-H,O-Z)
  AUX=(0.4536*T*T-46.662*T+1767.3)/1000000.0
  VISCWLIQ=AUX
RETURN
END
DOUBLE PRECISION FUNCTION CONDWLIQ(T)

```

Appendix D

```

IMPLICIT DOUBLE PRECISION (A-H,O-Z)
  AUX=(-0.0077*T*T+2.0469*T+560.71)/1000.0
  CONDWLIQ=AUX
  RETURN
  END
C*****
SUBROUTINE CONVQUAL (QUAL, QUALrp, CL, CV, INDCOMP, INDCONV, NC, IR)
IMPLICIT DOUBLE PRECISION (A-H,O-Z)
PARAMETER (NFL = 50)
COMMON /ESDATA/ CRIT(5,NFL)
DIMENSION CL(20), CV(20), IR(20)
CLM=1.0D-40
CVM=1.0D-40
QUAL1=QUAL+1.0D-40
QUALrp1=QUALrp+1.0D-40
IF (INDCOMP.EQ.1) THEN
  DO 10 I=1, NC
    CLM=CLM+CL(I)/CRIT(1, IR(I))
    CVM=CVM+CV(I)/CRIT(1, IR(I))
10  CONTINUE
  IF (INDCONV.EQ.1) QUAL=1.0/(1.0+(CVM/CLM)*(1.0/QUALrp1-1.0))
  IF (INDCONV.EQ.2) QUALrp=1.0/(1.0+(CLM/CVM)*(1.0/QUAL1-1.0))
END IF
IF (INDCOMP.EQ.2) THEN
  DO 20 I=1, NC
    CLM=CLM+CL(I)*CRIT(1, IR(I))
    CVM=CVM+CV(I)*CRIT(1, IR(I))
20  CONTINUE
  IF (INDCONV.EQ.1) QUAL=1.0/(1.0+(CLM/CVM)*(1.0/QUALrp1-1.0))
  IF (INDCONV.EQ.2) QUALrp=1.0/(1.0+(CVM/CLM)*(1.0/QUAL1-1.0))
END IF
RETURN
END
SUBROUTINE CONVCOMP (COMP, COMPrp, INDCONV, NC, IR)
IMPLICIT DOUBLE PRECISION (A-H,O-Z)
PARAMETER (NFL = 50)
COMMON /ESDATA/ CRIT(5,NFL)
DIMENSION COMP(20), COMPrp(20), IR(20)
CM=0.0
IF (INDCONV.EQ.1) THEN
  DO 20 I=1, NC
    CM=CM+COMPrp(I)*CRIT(1, IR(I))
20  CONTINUE
  DO 30 I=1, NC
    COMP(I)=COMPrp(I)*CRIT(1, IR(I))/(CM+1.0D-40)
30  CONTINUE
END IF
IF (INDCONV.EQ.2) THEN
  DO 40 I=1, NC
    CM=CM+COMP(I)/CRIT(1, IR(I))
40  CONTINUE

```

Appendix D

```

        DO 50 I=1, NC
            COMPrp(I)=COMP(I)/CRIT(1,IR(I))/(CM+1.0D-40)
50      CONTINUE
        END IF
        RETURN
        END
C*****
SUBROUTINE CALCMAS (XMMAS,COMP,INDCOMP)
IMPLICIT DOUBLE PRECISION (A-H,O-Z)
COMMON /NCIR/ NC,IR
PARAMETER (NFL = 50)
COMMON /ESDATA/ CRIT(5,NFL)
DIMENSION IR(20),COMP(20)
CM=1.0D-40
DO 10 I=1, NC
    IF (INDCOMP.EQ.1) CM=CM+COMP(I)/CRIT(1,IR(I))
    IF (INDCOMP.EQ.2) CM=CM+COMP(I)*CRIT(1,IR(I))
10  CONTINUE
IF (INDCOMP.EQ.1) XMMAS=1.0/CM
IF (INDCOMP.EQ.2) XMMAS=CM
RETURN
END
SUBROUTINE CRITXSI (X,TC,PC,VC,IER)
IMPLICIT DOUBLE PRECISION (A-H,O-Z)
COMMON /NCIR/ NC,IR
DIMENSION X(20),Xrp(20),IR(20)
TTC=300.0
CALL CONVCOMP(X,Xrp,2,NC,IR)
CALL CRITX(Xrp,TTC,PC,VC)
TC=TTC-273.15
PC=PC*1000.0
RETURN
END
C*****
SUBROUTINE HCVCP2SI (NPH,T,P,X,H,S,CV,CP,VS)
IMPLICIT DOUBLE PRECISION (A-H,O-Z)
COMMON /NCIR/ NC,IR
DIMENSION X(20),Xrp(20),IR(20)
Trp=T+273.15
Prp=P/1000.0
CALL CONVCOMP(X,Xrp,2,NC,IR)
CALL HCVCP2(NPH,Trp,Prp,Xrp,Hrp,Srp,CVrp,CPrp,VSrp)
CALL CALCMAS(XMMAS,X,1)
H=1000.0*Hrp/XMMAS
S=1000.0*Srp/XMMAS
CV=1000.0*CVrp/XMMAS
CP=1000.0*CPrp/XMMAS
VS=VSrp
RETURN
END
C*****

```

Appendix D

```

SUBROUTINE HPINSI (H, P, X, T, XQ, XL, XV, VL, VV, HL, HV)
IMPLICIT DOUBLE PRECISION (A-H, O-Z)
COMMON /NCIR/ NC, IR
DIMENSION X(20), XL(20), XV(20), Xrp(20), XLrp(20), XVrp(20), IR(20)
CALL CALCMMAS (XMMASS, X, 1)
CALL CONVCOMP (X, Xrp, 2, NC, IR)
Hrp=XMMASS*H/1000.0
Prp=P/1000.0
CALL HPIN (Hrp, Prp, Xrp, Trp, XQrp, XLrp, XVrp, VLrp, VVrp, HLrp, HVrp)
CALL CONVCOMP (XL, XLrp, 1, NC, IR)
CALL CONVCOMP (XV, XVrp, 1, NC, IR)
CALL CONVQUAL (XQ, XQrp, XL, XV, 1, 1, NC, IR)
CALL CALCMMAS (XMMASSL, XL, 1)
CALL CALCMMAS (XMMASSV, XV, 1)
A0=0.574512D-2
A1=-0.434742D-3
A2=-0.129206D-5
Trp=(A0+A1*Log((Prp/6.895))+A2*XQ)**(-1.0d0)
T=Trp-273.15
VL=VLrp/XMMASSL
VV=VVrp/XMMASSV
HL=1000.0*HLrp/XMMASSL
HV=1000.0*HVrp/XMMASSV
RETURN
END
SUBROUTINE TRNSPSI (P, T, V, X, VISC, COND, NPH)
IMPLICIT DOUBLE PRECISION (A-H, O-Z)
COMMON /NCIR/ NC, IR
DIMENSION X(20), Xrp(20), IR(20)
Prp=P/100000.0
Trp=T+273.15
CALL CONVCOMP (X, Xrp, 2, NC, IR)
CALL TRNSP (Prp, Trp, Vrp, Xrp, VISCrp, CONDRp, NPH)
CALL CALCMMAS (XMMASS, X, 1)
V=1.0/(Vrp*XMMASS)
VISC=VISCrp*1.0D-6
COND=CONDRp
RETURN
END
C*****
SUBROUTINE VARNAMES (Y$)
IMPLICIT DOUBLE PRECISION (A-H, O-Z)
DIMENSION Y$(100), CRL$(5), CRV$(5)
CHARACTER*12 Y$, CRL$, CRV$
CRL$(1)=" CR1 (LIQ.)  "
CRL$(2)=" CR2 (LIQ.)  "
CRL$(3)=" CR3 (LIQ.)  "
CRL$(4)=" CR4 (LIQ.)  "
CRL$(5)=" CR5 (LIQ.)  "
CRV$(1)=" CR1 (VAP.)  "
CRV$(2)=" CR2 (VAP.)  "

```

Appendix D

```

CRV$(3)=" CR3 (VAP.)  "
CRV$(4)=" CR4 (VAP.)  "
CRV$(5)=" CR5 (VAP.)  "
Y$(1)=" PREFPOS (I)  "
Y$(2)=" TT           "
Y$(3)=" PR           "
Y$(4)=" HR           "
Y$(5)=" TR           "
Y$(6)=" QUAL         "
Y$(7)=" HEATFLUX     "
Y$(8)=" HTCOEF       "
Y$(9)=" HV-HL        "
Y$(10)=" VOLESP      "
Y$(11)=" VL          "
Y$(12)=" VV          "
Y$(13)=" VISCL       "
Y$(14)=" VISCV       "
Y$(15)=" CONDL       "
Y$(16)=" CONDV       "
Y$(17)=" CPL         "
Y$(18)=" CPV         "
Y$(19)=" XMMASSL     "
Y$(20)=" XMASSV      "
Y$(21)=" CTEMPL      "
Y$(22)=" CTEMPV     "
Y$(23)=" CPRESL     "
Y$(24)=" CPRESV     "
Y$(25)=" CSVOLL     "
Y$(26)=" CSVOLV     "
II=26
DO 20 I=1, 5
    Y$(II+1)=CRL$(I)
    Y$(II+2)=CRV$(I)
    II=II+2
20 CONTINUE
RETURN
END
SUBROUTINE RECORDER(Y,IND)
IMPLICIT DOUBLE PRECISION (A-H,O-Z)
DOUBLE PRECISION MREF,MOLEMASS
DIMENSION PREFPOS(15),CR(20),CRL(20),CRV(20),Y(15,100)
COMMON /GEN/ PREFPOS,MREF,TR1,PR1,HR1,TR,PR,HR,QUAL,VL,VV,HV,HL,
+CVL,CVV,CPL,CPV,VISCL,VISCV,CONDL,CONDV,HEATFLUX,TT,MOLEMASS
COMMON /GEN2/CRITTEMP,CRITPRES,CRITSVOL,CR,CRL,CRV,XMMASSL,
+CTEMPL,CPRESL,
+CSVOLL,XMASSV,CTEMPV,CPRESV,CSVOLV,VOLESP,HTCOEF,TW,IAC
CHARACTER*6 HREF,HNAME(50)*50
CHARACTER*12 X$,Y$,CORR
CHARACTER*12
ref$,FILEPROF,FILEIN,FILEOUT,FILEPRIN,TEST,REFTYPE,NUMCYC
CHARACTER*30 DATE

```

Appendix D

```
CHARACTER*1 FLOW
CHARACTER*255 HERR
DIMENSION XORG(100)
DIMENSION CTW3T1(4),CTW3T2(4),CTT3T1(4),CTT3T2(4)
DIMENSION CTW3S1(4),CTW3S2(4),CTT3S1(4),CTT3S2(4)
DIMENSION CTW2T1(4),CTW2T2(4),CTT2T1(4),CTT2T2(4)
DIMENSION CTW2S1(4),CTW2S2(4),CTT2S1(4),CTT2S2(4)
DIMENSION ZZ(12)
DIMENSION Y$(100)
DIMENSION VTW(10),VDW(10),VTT(10)
DIMENSION NDATA(2)
DIMENSION GA(12), PRA(12), VM(12), XQA(12), VVA(12), REA(12),
*       HVHLA(12), XNUA(12), XJAA(12), SVVA(12), PRRA(12),
*       TRA(12), VISCLA(12), VISCVA(12), DQDZ(12), DPDZ(12),
*       PRESS(12)
I=IND
Y(I,1)=PREFPOS(IND)
Y(I,2)=TT
Y(I,3)=PR
Y(I,4)=HR
Y(I,5)=TR
Y(I,6)=QUAL
Y(I,7)=HEATFLUX
Y(I,8)=HTCOEF
Y(I,9)=HV-HL
Y(I,10)=VOLESP
Y(I,11)=VL
Y(I,12)=VV
Y(I,13)=VISCL
Y(I,14)=VISCV
Y(I,15)=CONDL
Y(I,16)=CONDV
Y(I,17)=CPL
Y(I,18)=CPV
Y(I,19)=XMMASSL
Y(I,20)=XMMASSV
Y(I,21)=CTEMPL
Y(I,22)=CTEMPV
Y(I,23)=CPRESL
Y(I,24)=CPRESV
Y(I,25)=CSVOLL
Y(I,26)=CSVOLV
II=26
DO 20 J=1, 5
    Y(I,II+1)=CRL(J)
    Y(I,II+2)=CRV(J)
    II=II+2
20 CONTINUE
Y(I,36)=TW
RETURN
END
```

Appendix D

```

SUBROUTINE WRITER(Y,Y$)
  IMPLICIT DOUBLE PRECISION (A-H,O-Z)
  DOUBLE PRECISION MREF,MOLEMASS
  DIMENSION PREFPOS(15),CR(5),CRL(5),CRV(5)
  COMMON /FILE/ FILEPROF,FILEPRIN,TEST,DATE,FLOW
  COMMON PREFPOS,MREF,TR1,PR1,HR1,TR,PR,HR,QUAL,VL,VV,HV,HL,
+CVL,CVV,CPL,CPV,VISCL,VISCV,CONDL,CONDV,HEATFLUX,TT,MOLEMASS,
+CRITTEMP,CRITPRES,CRITSVOL,CR,CRL,CRV,XMMASSL,CTEMPL,CPRESL,
+CSVOLL,XMMASSV,CTEMPV,CPRESV,CSVOLV,VOLESP,HTCOEF,TW,IND
  DIMENSION Y(15,100),Y$(100)
  CHARACTER*12 Y$
  CHARACTER*12 FILEPROF,FILEPRIN,TEST
  CHARACTER*30 DATE
  CHARACTER*1 FLOW
  OPEN(7,FILE=FILEPRIN)
  WRITE(7,*) " "
  WRITE(7,*) " "
  WRITE(7,1004) " TEST NAME           --> ",TEST
  WRITE(7,1005) " DATE OF THE TEST           --> ",DATE
  WRITE(7,1003) " MASS FLOW RATE             --> ",MREF
  WRITE(7,1003) " TEMP. OF REF. INLET        --> ",TR1
  WRITE(7,1003) " PRES. OF REF. INLET        --> ",PR1
  WRITE(7,1003) " ENTHALPY REF. INLET       --> ",HR1
  WRITE(7,1003) " MOLECULAR MASS           --> ",MOLEMASS
  WRITE(7,1003) " CRITICAL TEMPERATURE      --> ",CRITTEMP
  WRITE(7,1003) " CRITICAL PRESSURE        --> ",CRITPRES
  WRITE(7,1003) " CRITICAL ESP. VOLUME     --> ",CRITSVOL
  WRITE(7,1003) " CONCENTRATION FLUID 1    --> ",CR(1)
  WRITE(7,1003) " CONCENTRATION FLUID 2    --> ",CR(2)
  WRITE(7,1003) " CONCENTRATION FLUID 3    --> ",CR(3)
  WRITE(7,1003) " CONCENTRATION FLUID 4    --> ",CR(4)
  WRITE(7,1003) " CONCENTRATION FLUID 5    --> ",CR(5)
  WRITE(7,*) " "
  WRITE(7,*) " "
  WRITE(7,*) " "
  JWIDTH=5
  JCONT=2
  DO 10 K=1, 7
    WRITE(7,*) " "
    WRITE(7,1001) Y$(1),(Y$(J), J=JCONT, JCONT+JWIDTH-1)
    DO 20 I=1, 15
      WRITE(7,1002) Y(I,1),(Y(I,J), J=JCONT, JCONT+JWIDTH-1)
20    CONTINUE
    WRITE(7,1001) Y$(1),(Y$(J), J=JCONT, JCONT+JWIDTH-1)
    JCONT=JCONT+JWIDTH
    WRITE(7,*) " "
    WRITE(7,*) " "
10  CONTINUE
1001 FORMAT (A12,5(A12))
    1002 FORMAT (E12.4,5(E12.4))
1003 FORMAT (A28,E12.4)

```

Appendix D

```

1004 FORMAT (A28,A12)
1005 FORMAT (A28,A30)
WRITE(7,*) " "
WRITE(7,*) " "
WRITE(7,1004) " TEST NAME           --> ",TEST
WRITE(7,1005) " DATE OF THE TEST       --> ",DATE
WRITE(7,1003) " MASS FLOW RATE         --> ",MREF
WRITE(7,1003) " TEMP. OF REF. INLET      --> ",TR1
WRITE(7,1003) " PRES. OF REF. INLET       --> ",PR1
WRITE(7,1003) " ENTHALPY REF. INLET     --> ",HR1
WRITE(7,1003) " MOLECULAR MASS         --> ",MOLEMASS
WRITE(7,1003) " CRITICAL TEMPERATURE  --> ",CRITTEMP
WRITE(7,1003) " CRITICAL PRESSURE     --> ",CRITPRES
WRITE(7,1003) " CRITICAL ESP. VOLUME   --> ",CRITSVOL
WRITE(7,1003) " CONCENTRATION FLUID 1  --> ",CR(1)
WRITE(7,1003) " CONCENTRATION FLUID 2  --> ",CR(2)
WRITE(7,1003) " CONCENTRATION FLUID 3  --> ",CR(3)
WRITE(7,1003) " CONCENTRATION FLUID 4  --> ",CR(4)
WRITE(7,1003) " CONCENTRATION FLUID 5  --> ",CR(5)
WRITE(7,*) " "
WRITE(7,*) " "
WRITE(7,*) " "
CLOSE(7)
RETURN
END
SUBROUTINE INTRP(F1,F2,X1,X2,X,F)
IMPLICIT REAL*8(A-Z)
C-----INTERPOLATE FOR F BETWEEN TWO X'S
F = (X - X1)*(F2 - F1)/(X2 - X1) + F1
RETURN
END
SUBROUTINE DYDX1(Y,X,NPTS,DYDX)
IMPLICIT REAL*8 (A-Z)
INTEGER I, NPTS
DIMENSION Y(200), X(200), DYDX(200)
C-----ASSUME THE DATA IS SORTED; OTHERWISE USE SORTED SUB IN REGR.FOR
C-----FORWARD DIFFERENCE METHOD
DYDX(1) = (Y(2) - Y(1))/(X(2) - X(1))
C-----CENTRAL DIFFERENCE METHOD
DO 10 I=2, NPTS-1
D1 = X(I+1) - X(I)
D2 = X(I) - X(I-1)
A = D2/(D1**2 + D1*D2)
B = -D1/(D2**2 + D1*D2)
DYDX(I) = A*Y(I+1) + B*Y(I-1) - (A + B)*Y(I)
10 CONTINUE
C-----BACKWARD DIFFERENCE METHOD
DYDX(NPTS) = (Y(NPTS) - Y(NPTS-1))/(X(NPTS) - X(NPTS-1))
RETURN
END

```

Appendix E

Test Rig Operation

E1 Labview Program on computer

- a) Double click on Labview 7.0 icon.
- b) Make sure your DAQ is on.
- c) Open d:\nitin\experiments\twophase\2phase_R410A.vi
- d) Name the voltage and temperature files (.dat extension).
- e) In order to take equilibrium data (Thermocouples and pressure at room temperature) when no pumps or brine is running through the system, hit RUN (arrow button on Labview). You might have to hit the CLEAR button on the DAQ system since the DAQ will get stuck trying to read the counter, corresponding to water and refrigerant side flow rates (at this time the pumps are not running).

E2 Test Rig Startup

- a) Start the water side pump by hitting the RUN button on the E-TRAC AC inverter. Set the frequency to the desired value. I have it set at 14 Hz to start with.
- b) Start the refrigerant side pump by hitting the FWD button on inverter and setting the frequency to 14.0 Hz.
- c) Open the brine flow to the test rig by opening the reservoir valve. This will help drop the pressure in the system. Adjust the valve to the pressure (and thus the corresponding saturation temperature) that you desire.
- d) Plug the Variable Heater cord and monitor the water outlet temperature on the Labview program. If the temperature is approaching close to 4 deg. C, then boost the heater setting by increasing the blue knob next to the inverter.

E3 Recording Data

- a) The Labview program displays graphs for saturation pressure, inlet water temperature, flow rates on refrigerant and water side, etc. For the desired saturation temperature, if the graphs for the parameters stated above are steady, you are ready to collect data.
- b) Stop the program by hitting the STOP button. Change the filename to what you'd like. I try to name files according to the date. For instance, if it is April 7th, 2006, my first voltage and temperature files would be 060407v1.dat and 060407t1.dat respectively. My next data files would be 060407v2.dat and 060407t2.dat. And so on ...
- c) I collect the data for about 10-15 minutes. Once finished, I hit the STOP button. I change the filenames to trialv1.dat and trialt1.dat.
- d) For next set of data, I do necessary changes (like higher refrigerant mass flux or higher heat flux, or higher saturation temperature, etc.). I wait to get steady conditions again.
- e) Follow step 3b again.

Appendix E

E4 At the End of the Day

- a) Stop the refrigerant side pump. Hit the down arrow button and get the frequency to zero. Hit STOP on the inverter.
- b) Unplug the Variable Heater cord. Turn the blue knob counterclockwise all the way.
- c) Stop the chiller.
- d) Stop the water side pump by hitting the STOP button.

Appendix F

Calculation of RCL and ATEL for R-410A

The Refrigerant Concentration Limit (RCL) for each refrigerant shall be the lowest value of the three values of Acute-Toxicity Exposure Limit (ATEL), Oxygen Deprivation Limit (ODL), and Flammable Concentration Limit (FCL). RCL is determined using assumptions of complete vaporization with no removal by ventilation, dissolution, reaction, or decomposition and complete mixing of the refrigerant in the space to which it is released.

F1 Acute-Toxicity Exposure Limit (ATEL)

The ATEL shall be the lowest of the four blend acute toxic concentration factors (TCFs): (a) Mortality; (b) Cardiac Sensitization; (c) Anesthetic or Central Nervous System Effects; and (d) Other Escape-Impairing Effects and permanent Injury.

a) Mortality: 28.3% of the 4-hour LC50 for rats. If not determined, 28.3% of the 4-hour ALC for rats. If neither has been determined, 0 ppm. The following equations shall be used to adjust LC50 or ALC values that were determined with 15-minute to 8-hour tests for refrigerants for which 4-hour test data are not available:

b) Cardiac Sensitization: 100% of the NOEL for cardiac sensitization in unanesthetized dogs. If not determined, 80% of the LOEL for cardiac sensitization in dogs. If neither has been determined, 1000 ppm. The cardiac sensitization term is omitted from ATEL determination if the LC50 or ALC in (a) is less than 10,000

Appendix F

ppm by volume or if the refrigerant is found, by toxicological review, not to cause cardiac sensitization.

- c) Anesthetic or Central Nervous System Effects: 50% of the 10-minute EC50 in mice or rats for loss of righting ability in a rotating apparatus, or 80% of NOEL in mice or rats for loss of righting ability in a rotating apparatus, whichever is higher. If not determined, 50% of the LOEL for signs of any anesthetic or CNS effect in rats during acute toxicity studies. If neither has been determined, 80% of the NOEL for signs of any anesthetic or CNS effect in rats during an acute, subchronic, or chronic toxicity study in which clinical signs are documented.
- d) Other Escape-Impairing Effects and Permanent Injury: 80% of the lowest concentration, for human exposures of 30 minutes, that is likely to impair ability to escape or to cause irreversible health effects.

Each blend acute TCF quantity is calculated from the acute TCF values of its individual components, following the Additivity Method for Mixtures. The blend acute toxicity calculation shall be done as follows:

$$\text{Blend Mortality Indicator } (a)_{\text{blend}} = \frac{1}{\frac{mf_1}{a_1} + \frac{mf_2}{a_2} + \dots + \frac{mf_n}{a_n}} \quad (\text{F-1})$$

Where a is the mortality indicator for component n in the blend (i.e., the four-hour LC₅₀) and mf_n is the mole fraction of the component n .

Appendix F

In a similar fashion, Blend Cardiac Sensitization Indicator (b)_{blend} can be calculated from $1/(\sum mf_n/b_n)$, where b_n is the cardiac sensitization indicator for component n in the blend (i.e., 100% of the NOEL or, if not determined, 80% of the LOEL), and from the mole fraction mf_n of component n , and so forth.

Each acute TCF for a blend can be expressed in ppm if the acute TCFs for each component n are expressed in ppm and mf_n is expressed as the mole fraction of component n in the blend.

F2 Example: ATEL Calculation for R-410A

R-410A composition expressed in mole fraction is (0.698 mole fraction R-32 and 0.302 mole fraction R-125).

$$\text{Mortality Indicator of R-410A} = \frac{1}{\frac{0.698}{215,000 \text{ ppm}} + \frac{0.302}{218,000 \text{ ppm}}} = 216,000 \text{ ppm}$$

where $(a)_{R-32}$ = the LC50 of R-32 or $760,000 \text{ ppm} * 0.283 = 215,000 \text{ ppm}$ and $(a)_{R-125}$ = the LC50 of R-125 or $769,000 \text{ ppm} * 0.283 = 218,000 \text{ ppm}$.

$$\text{Cardiac Sensitization Indicator of R-410A} = \frac{1}{\frac{0.698}{200,000 \text{ ppm}} + \frac{0.302}{75,000 \text{ ppm}}} = 133,000 \text{ ppm}$$

where $(b)_{R-32}$ is Cardiac Sensitization Indicator NOEL for R-32 or 200,000 ppm and $(b)_{R-125}$ is Cardiac Sensitization Indicator NOEL for R-125 or 75,000 ppm.

Appendix F

$$\text{Anesthetic Effect Indicator for R-410A} = \frac{1}{\frac{0.698}{200,000 \text{ ppm}} + \frac{0.302}{567,000 \text{ ppm}}} = 249,000 \text{ ppm}$$

where $(c)_{R-32}$ is Anesthetic Effect Indicator NOEL for R-32 or $250,000 \text{ ppm} * 0.8 = 200,000 \text{ ppm}$ and $(c)_{R-125}$ is Anesthetic Effect Indicator NOEL for R-125 or $709,000 \text{ ppm} * 0.8 = 567,000 \text{ ppm}$. (Note: EC_{50} was not used because there was no value for R-32 or R-125, and LOEL was not used because the values for R-32 and R-125 affected more than half (10/10 and $>5/10$) of the animals.) Had legitimate EC_{50} , LOEL, or NOEL values been available, it would have been possible to use a EC_{50} for one blend component, a LOEL for a second, and a NOEL for a third, etc.

There are no pertinent escape-impairing or permanent injury effect indicators (d) known for R-410A. Therefore, the ATEL for R-410A is set on the Cardiac Sensitization Effect (b), 133,000 ppm, which is the lowest of acute TCFs in Section 7.1.1 (a) through (c) for the blend. Rounding to two significant figures gives 130,000 ppm as the ATEL of R-410A.

F3 RCL for R-410A

Since the blend is nonflammable and the ATEL is less than the oxygen deprivation level of 140,000 ppm, the RCL is also 130,000 ppm.

Appendix G

Refrigeration History and Refrigerants

Refrigeration is the artificial withdrawal of heat, producing in a substance or within a space a temperature lower than that which would exist under the natural influence of the surroundings. Alternatively, refrigeration is essentially the process of cooling by removing and transferring heat or keeping an item below room temperature by storing the item in a system or substance designed to cool or freeze. Air-conditioning is the process of treating air to control simultaneously its temperature, humidity, cleanliness, and distribution to meet the comfort requirements of the occupants of the conditioned space. Refrigeration and air-conditioning are interconnected. The largest application of refrigeration, which is the process of cooling, is for air-conditioning (Stoecker and Jones, 2001). Industrial refrigeration embraces processing and preservation of food; removing heat from substances in chemical, petroleum, and petrochemical plants; and numerous special applications such as those in the manufacturing and construction industries.

G1 Refrigeration History

In ancient times, around 2500 years B.C., in order to produce ice, Indians, Egyptians, and others kept water in porous pots and left them open to cold atmosphere during the night. The evaporation of water in almost cool dry air accompanied with radiation heat transfer in the clear night caused the formation of ice even when the ambient temperature was above the freezing temperature.

Appendix G

There are further references that support the use of ice in China 1000 years B.C. During the early 4th century A.D., another method used to produce refrigeration involved dissolving salt in water (Prasad, 2005).

Because the amount of ice production was so small, many of these methods were not feasible for commercial usage. As a result, numerous investigators across the world studied phase changes in the 1600s and 1700s to overcome challenges of limited ice usage. These studies set the foundation for and the development of “artificial” refrigeration. Thomas Harris and John Long got the earliest British patent in 1790. Oliver Evans first proposed the use of a volatile fluid in a closed cycle to freeze water into ice (Evans, 1805). Jacob Perkins and Richard Trevithick expanded Oliver Evans’ study to propose an air-cycle system for refrigeration in 1828, but did not build a system. In 1834 Jacob Perkins developed a hand operated refrigeration system using volatile ether as the working fluid. The ether vapor was sucked via a hand operated compressor and then the high temperature, high pressure ether vapor was condensed in a water cooled chamber (condenser). Liquid ether was finally throttled to the lower pressure and thus evaporation of this liquid in an evaporator lowered the temperature of water surrounding the vessel (Perkins, 1834). Finally ice was formed. The mechanical vapor-compression methodology is nowadays often called the *Perkins Cycle*.

Appendix G

In the 19th century, there was tremendous development of refrigeration systems to replace natural ice by artificial ice producing machines. In 1851, John Gorrie, a physician, obtained the first American patent of a cold air machine to produce ice in order to cure people suffering from high fever. In Australia, James Harrison used sulphuric ether to record the world's first installation of a refrigeration machine for use in a brewery, where a steam engine worked as a power source to drive the compressor (Prasad, 2005).

During the early 20th century, significant focus was placed on developing large sized refrigeration machines. The most common working fluids (refrigerants) were familiar solvents and other volatile fluids, effectively including whatever worked and was available. Very little consideration was given to aspects related to flammability, toxicity, reactivity, etc. By 1904, an approximately 450-ton cooling system was installed for air-conditioning at the New York Stock Exchange. In Germany, people used air-conditioning in theatres for comfort purposes. Around 1911 or so, innovations in compressor technology boosted compressor speeds from 100 rpm to 300 rpm. The first modern two-stage compressor was built and brought into use in 1915 (Prasad, 2005). The first documented, systematic search for a refrigerant came in the 1920s (Carrier and Waterfill, 1924). The authors investigated a range of candidate refrigerants (including carbon dioxide, ammonia, water, sulphur dioxide, carbon tetrachloride, and dielene) for suitability in centrifugal and positive-displacement compression machines.

Appendix G

G2 Refrigerants

Refrigerants employed during the early part of the development of artificial refrigeration were ones that were readily available, such as ammonia, carbon dioxide, hydrocarbons, ethers, methyl chloride, and sulfur dioxide (Calm, 2008). These refrigerants were often flammable, toxic, and/or had poor thermodynamic performance. These issues led to focus being placed on halocarbon refrigerants (Calm, 2008). In particular, in 1928, Thomas Midgley Jr. and his associates Albert L. Henne and Robert R. McNary consulted property tables and the Periodic Table of Elements to find chemicals with the desired boiling point temperature, focusing their search on stable, non-toxic and non-flammable chemicals. Based on their analysis, eight elements remained, namely, carbon, nitrogen, oxygen, sulfur, hydrogen, fluorine, chlorine, and bromine (Midgley, 1937). Through their research, Midgley and his associates showed that when one varies the chlorination and fluorination of hydrocarbons, one can strongly influence boiling point, flammability and toxicity of the molecules (Midgley and Henne, 1930). Their early work led to the commercial introduction of R-12 in 1931 followed by R-11 in 1932 (Downing, 1966, 1984). The use of CFCs and HCFCs during the mid-20th century dominated in residential and small commercial air-conditioners and heat pumps. Ammonia continued as, and remains today, the most popular refrigerant in large, industrial systems especially for food and beverage processing and storage (Calm, 2008).

Appendix G

A shift away from CFC and HCFC refrigerants toward more “eco-friendly” refrigerants happened beginning in the 1970s and 1980s with the discovery that refrigerants containing chlorine contribute to the depletion of stratospheric ozone. The shift was triggered primarily by two international agreements: of the Montreal protocol (1987) and the Kyoto Protocol (1997). A renewed interest in natural refrigerants, such as water and carbon dioxide, was sparked. Public and private organizations undertook research programs to examine and search for new candidate refrigerants, but yielding few promising options.

More recently, there has been considerable activity in the HVAC&R industry related to systems, such as solar powered vapor-absorption system, vortex tube, pulse tubes, steam-jet refrigeration, thermoelectric devices, magnetic refrigeration, cryogenics, etc. Moreover, the world energy crisis has led to the utilization of waste heat, solar energy, bio-energy, wind energy, etc. as alternative sources for powering refrigeration systems. There continues to be an ongoing and concerted effort by various governments and private agencies to develop commercial systems which can address growing environmental regulations and to reduce these systems’ dependence on conventional energy resources.

BIBLIOGRAPHY

Adamson, A. W., 1967, "Physical chemistry of surfaces," Interscience Publ., New York, 2nd edition, p. 353.

Altman, M., Norris, R. H., and Staub, F. N., 1959, "Local and average heat transfer and pressure drop for refrigerants evaporating in horizontal tubes," *J. Heat Transfer*, p. 189-198.

ARI, 1997, "Soft-optimized system tests conducted with several possible R-22 and R-502 alternatives," *Air Conditioning and Refrigeration Institute*, Arlington, VA, USA.

ARI-700, 2006, "Specifications for fluorocarbon refrigerants," *Air Conditioning and Refrigeration Institute*, Arlington, VA, USA.

ASHRAE Handbook: Fundamentals, 2001, SI Edition, Georgia, USA.

ASHRAE Standard 34, 2010, "Designation and safety classification of refrigerants," *American Society of Heating, Refrigerating, and Air-conditioning Engineers Inc.*, Atlanta, GA, USA.

Baker, M., Touloukian, Y. S., and Hawkins, G. A., 1953, "Heat transfer film coefficients for refrigerants boiling inside tubes," *Ref. Eng.*, p. 986-991.

Bennett, D. L. and Chen, J.C., 1980, "Forced convective boiling in vertical tubes for saturated pure components and binary mixtures," *Journal of A.I.Ch.E.*, Vol. 26, p. 454-461.

Burkhardt, J., and Hahne, 1979, "Influence of oil on the nucleate boiling of R-11," *XVth International Congress of Refrigeration*, Vol. 2, p. 537-543.

Calm, J. M., 1996, "The toxicity of refrigerants," *Proceedings of the International Refrigeration Conference*, Purdue University, West Lafayette, IN, USA.

Calm, J. M., 2000, "Toxicity data to determine refrigerant concentration limits," *Report DE/CE 23810-110*, *Air Conditioning and Refrigeration Technology Institute (ARTI)*, Arlington, VA, USA.

Calm, J. M. 2001, "ARTI refrigerant database," *Air Conditioning and Refrigeration Technology Institute*, Arlington, VA, USA.

Calm, J. M., 2003, "The four R's for responsible responses to refrigerant regulation," *Engineered Systems Magazine*, p. 66-72.

BIBLIOGRAPHY

- Calm, J. M. and Domanski, P. A., 2004, "R-22 replacement status," *EcoLibrium*, 3(10), p. 18-24.
- Calm, J. M., 2007, "The next generation of refrigerants," *International Congress of Refrigeration*, Paper ICR07-B2-534, Beijing, China.
- Calm, J. M., 2008, "The next generation of refrigerants – Historical review, considerations, and outlook," *Int. J. Refrigeration*, Vol. 31, p. 1123-1133.
- Carrier, W. H., and Waterfill, R. W., 1924, "Comparison of thermodynamic characteristics of various refrigerating fluids," *Refrigerating Engineering*.
- Cavallini, A., Del Col, D., Doretti, L., Longo, G. A., Rossetto, L., 1998, "A new model for refrigerant vaporization inside enhanced tubes," *Third International Conference on Multiphase Flow*, Lyon.
- Cavallini, A., Del Col, D., Doretti, L., Longo, G. A., and Rossetto, L., 1999, "Refrigerant vaporization inside enhanced tubes: A heat transfer model," *Heat and Technology*, Vol.17, Part2, p. 29-36.
- Cavallini, A., Del, C. D., Doretti, L., Longo, G.A. and Rossetto, L., 1999, "A new computational procedure for heat transfer and pressure drop during refrigerant condensation inside enhanced tubes," *Enhanced Heat Transfer*, Vol. 6, pp. 441-456.
- Cavallini, A., Del Col, D., Doretti, L., Longo, G. A., Rossetto, L., 1999, "Enhanced in tube heat transfer with refrigerants," *International Congress of Refrigeration*, IIR/IIF, Sydney.
- Chaddock, J. B., and Mathur, A. P., 1979, "Heat transfer to oil-refrigerant mixtures evaporating in tubes," *Second Multiphase Flow and Heat Transfer Symposium*, University of Miami, USA.
- Chamra, L. M., and Webb, R. L., 1995, Boiling and evaporation in micro-fin tubes at equal saturation temperatures," *J. of Enhanced Heat Transfer*, Vol. 2, p. 219-229.
- Chamra, L. M., Kung, C. C., Tan, M. O., and Tang, S. S., 2003, "Evaluation of existing evaporative heat-transfer models in horizontal micro-fin tubes," *ASHRAE Transactions*, Vol. 109, Part 1.
- Chen, J. C., 1966, "A correlation for boiling heat transfer to saturated fluids in vertical flow," *Ind. Eng. Chem. Proc. Design and Dev.*, Vol. 5, No. 3, p. 322-339.

BIBLIOGRAPHY

Collier, J. G., and Thome, J. R., 1994, "Convective boiling and condensation," 3rd edition, Oxford University Press Inc., New York, USA.

Coombs, D. W., 2004 and amendment 2006, "HFC-32 assessment of anesthetic potency in mice by inhalation," *Huntingdon Life Sciences Ltd.*, Huntingdon, Cambridgeshire, England.

Coombs, D. W., 2005, "HFC-22: An inhalation study to investigate the cardiac sensitization potential in the beagle dog," *Huntingdon Life Sciences Ltd.*, Huntingdon, Cambridgeshire, England.

Cooper, M. G., 1984, "Saturation nucleate pool boiling: A simple correlation," 1st U.K. *National Conference on Heat Transfer*, Vol. 2, p. 785-793.

Cremaschi, L., Hwang, Y., and Radermacher, R., 2005, "Experimental investigation of oil retention in air conditioning systems," *Int. J. Refrigeration.*, Vol. 28, pp. 1018-1028.

Davidson, W. F., 1943, "Studies of heat transmission through boiler tubing at pressures from 500 to 3300 pounds," *ASME Transactions*, Vol. 65, p. 553-579.

Dickson, A. J., and Gouse, S. W., 1967, "Heat transfer and fluid flow in a horizontal tube evaporator – Phase III," *ASHRAE Transactions*.

Ding, G., Hu, H., and Wang, K., 2008, "Heat transfer characteristics of R-410A-oil mixture flow boiling inside a 7 mm straight microfin tube," *Int. J. Refrigeration*, Vol. 31, pp. 1081-1093.

Dittus, F. W., and Boelter, L. M. K., 1930, *University of California (Berkeley) Publishers*, England, Vol. 2, p. 443.

Domanski, P. A., 1999, "Evolution of refrigerant application," *Proceedings of International Congress on Refrigeration*, Milan, Italy.

Downing, R. C., 1966, "History of the organic fluorine industry," *Kirk-Othmer Encyclopedia of Chemical Technology*, 2nd edition, Vol. 9, p. 704-707, John Wiley and Sons, New York, NY, USA.

Downing, R. C., 1984, "Development of chlorofluoro-carbon refrigerants," *ASHRAE Transactions*, Vol. 90, Part 2B, p. 481-491.

Eckels, S.J., and Pate, M.B., 1994, "In-tube evaporation and condensation of refrigerant-lubricant mixtures of R-134a and R-12," *ASHRAE Transactions*, Vol. 97, No. 2, p. 62-71.

BIBLIOGRAPHY

- Eckels, S. J., Doerr, T. M., and Pate, M. B., 1994, "In-tube heat transfer and pressure drop of R-134a and ester lubricant mixtures in a smooth tube and a micro-fin tube: part 1 - Evaporation," *ASHRAE Transactions*, Vol. 100, Part 2, p. 265-282.
- Eckels, S. J., Doerr, T. M., and Pate, M. B., 1998a, "Heat transfer coefficients and pressure drops for R-134a and an ester lubricant mixture in a smooth tube and a micro-fin tube," *ASHRAE Transactions*, Vol. 104, Part 1A, p. 366-375.
- Evans, O., 1805, "The Abortion of a Young Steam Engineer's Guide," Philadelphia, PA, USA.
- Foster, H. K., and Zuber, N., 1955, *Journal of A.I.Ch.E.*, Vol. 1, p. 531-535.
- Goto, M., Inoue, N., and Ishiwatari, N., 2001, "Condensation and evaporation heat transfer of R-410A inside internally grooved horizontal tubes," *Int. J. of Refrigeration*, Vol. 24, No. 7, p. 628-638.
- Greco, A., 2006, "Convective boiling of pure and mixed refrigerants: An experimental study of the major parameters affecting heat transfer," *Int. J. of Heat and Mass Transfer*, Vol. 51, p. 896-909.
- Green, G. H., and Furse, F. G., 1963, "Effect of oil on heat transfer from a horizontal tube to boiling R-11/oil mixtures," *ASHRAE Journal*, October, p. 63-68.
- Groll, E. A., and Shen, B., 2003, "Critical literature review of lubricant influence on refrigerant heat transfer and pressure drop," *Report prepared for Air conditioning and Refrigeration Technology Institute*.
- Gungor, K. E., and Winterton, W. H. S., 1986, "A general correlation for flow boiling in tubes and annuli," *Int. J. of Heat and Mass Transfer*, Vol. 29, No. 3, p. 351-358.
- Ha, S., and Bergles, A. E., 1993, "The influence of oil on local evaporation heat transfer inside a horizontal micro-fin tube," *ASHRAE Transactions*, Vol. 99, Part 1, pp. 1244-1256.
- Hambraeus, K., 1995, "Heat transfer of oil-contaminated R-134a in a horizontal evaporator," *Int. J. Refrigeration*, Vol. 18, No. 2, p. 87-99.
- Hamilton, L. J., Kedzierski, M. A., and Kaul, M. P., 2005, "Horizontal convective boiling of refrigerants and refrigerant mixtures within a micro-fin tube," *NISTIR 7243*, U.S. Department of Commerce, Washington, D.C.

BIBLIOGRAPHY

- Hasse, U., 1992, "Environment effects of refrigerants - Compression cycles for environmentally acceptable refrigeration, air-conditioning and heat pump systems," *International Institute of Refrigeration*, Paris, France, p. 10 –17.
- Hewitt, G. F., 1963, "Burnout and nucleation in climbing film flow," *AERE-R4374*.
- Hewitt, G. F., 1984, *Workshop on Two Phase Flow Processes*.
- Hrnjak, P. S., and Park, C. Y., 2007, "CO₂ and R-410A flow boiling heat transfer, pressure drop, and flow pattern at low temperatures in a horizontal smooth tube," *Int. J. Refrigeration*, Vol. 30, p. 166-178.
- Hughes, H. M., 1997, "Contemporary fluorocarbons," *Proceedings of ASHRAE/NIST Refrigerants Conference: Refrigerants for the 21st Century*, Gaithersburg, MD, USA.
- Incropera, F. P., and DeWitt, D. P., 1996, "Fundamentals of Heat and Mass Transfer," 4th edition, John Wiley & Sons.
- Jensen, M. K., and Jackman, D. L., 1984, "Prediction of nucleate pool boiling heat transfer coefficients of refrigerant-oil Mixtures," *Journal of Heat Transfer*, Vol. 106, p. 133-140.
- Jung, D. S., McLinden, M., Radermacher, R., and Didion, D., 1989, "A Study of Flow Boiling Heat Transfer with Refrigerant Mixtures," *Int. J. Heat and Mass Transfer*, Vol. 32., No. 9, p. 1751-1764.
- Kandlikar, S. G., 1990, "A general correlation for saturated two-phase flow boiling heat transfer inside horizontal and vertical tubes," *J. of Heat transfer*, Vol. 112, p. 219-228.
- Kandlikar, S. G., and Raykoff, T., 1997, "Predicting flow boiling heat transfer of refrigerants in micro-fin tubes," *J. Enhanced Heat Transfer*, Vol. 4, p. 257-268.
- Kandlikar, S. G., Lombardo, M., and Gupta, S. K., 1997, "Investigating the effect of heating method on pool boiling heat transfer," *Conference on Convective Flow and Pool Boiling II*, Paper II-3, Irsee, Germany.
- Kandlikar, S. G., 1998, "Boiling heat transfer with binary mixtures: Part II- Flow boiling in plain tubes," *J. of Heat Transfer*, Vol. 120, p. 388-394.
- Kattan, N., Favrat, D., and Thome, J. R., 1995, "R-502 and two near-azeotropic alternatives: Part 1 – In tube flow boiling tests," *ASHRAE Transactions*, Vol. 101, Pt. 1, p. 491 – 508.

BIBLIOGRAPHY

- Kattan, N., Thome, J. R., and Favrat, D., 1998a, "Flow boiling in horizontal tubes: Part 1 – Development of a diabatic two-phase flow pattern map," *ASME Transactions*, Vol. 120, p. 140-147.
- Kedzierski, M. A., 1993, "Simultaneous visual and calorimetric measurements of R-11, R-123, R-123/Alkylbenzene nucleate flow boiling," *Heat Transfer with Alternative Refrigerants*, ASME HTD-Vol. 243, p. 27-33.
- Kedzierski, M.A., and Kaul, M.P., 1993, "Horizontal nucleate flow boiling heat transfer coefficient measurements and visual observations for R-12, R-134a, and R-134a/polyol ester lubricant mixtures," *NISTIR 5144*, National Institute of Standards and Technology.
- Kedzierski, M. A., 1995, "Calorimetric and visual measurements of R-123 pool boiling on four enhanced surfaces," *NISTIR 5732*, U.S. Department of Commerce, Washington, D.C.
- Kedzierski, M. A., 1999, "Enhancement of R-123 pool boiling by the addition of n-hexane," *J. Enhanced Heat Transfer*, Vol. 6, No. 5, p. 343-355.
- Kedzierski, M. A., Choi, J. Y., and Domanski, P. A., 1999, "A generalized pressure drop correlation for evaporation and condensation of alternative refrigerants in smooth and micro-fin tubes," *NISTIR 6333*, U.S. Department of Commerce, Washington D.C.
- Kedzierski, M. A., 2000, "Refrigerant/lubricant mixture boiling heat transfer research at NIST," *All India Seminar on Future Trends in Mechanical Engineering*, Roorkee, India.
- Kedzierski, M. A., 2000a, "Enhancement of R-123 pool boiling by the addition of hydrocarbons," *Int. J. Refrigeration*, Vol. 23, p. 89-100.
- Kedzierski, M. A., 2003, "A semi-theoretical model for predicting refrigerant-lubricant mixture pool boiling heat transfer," *Int. J. Refrigeration*, Vol. 26, p. 337-348.
- Khanpara, J. C., Bergles, A. E., and Pate, M. B., 1987, "A comparison of in-tube evaporation of R-113 in electrically heated and fluid heated smooth and inner-fin tubes," *Advances in Enhanced Heat Transfer*, HTD-68, p. 35-45.
- Khanpara, J. C., Pate, M. B., and Bergles, A. E., 1987, "Local evaporation heat transfer in a smooth tube and a micro-fin tube using refrigerants 22 and 113," *Boiling and Condensation in Heat Transfer Equipment*, HTD, Vol. 85, p. 31 – 39.
- Khanpara, J. C., Bergles, A. E., and Pate, M. B., 1987a, "A comparison of in-tube evaporation of R-113 in electrically heated and fluid heated smooth and inner-fin tubes," *Advances in Enhanced Heat Transfer*, HTD-68, p. 35-45.

BIBLIOGRAPHY

- Kido, O., Taniguchi, M., Taira, T., and Uehara, H., 1995, "Evaporation heat transfer of HCFC22 inside an internally grooved horizontal tube," *ASME/JSME Thermal Engineering Conference*, Vol. 2, p. 323-330.
- Kim, M., and Shin, J., 2005, "Evaporating heat transfer of R-22 and R-410A in horizontal smooth and microfin tubes," *Int. J. Refrigeration*, Vol. 28, p. 940-948.
- Kim, S., Pehlivanoglu, N., and Hrnjak, P., 2010, "R-744 flow boiling heat transfer with and without oil at low temperatures in 11.2 mm horizontal smooth tube," *Proceedings of International Refrigeration and Air Conditioning Conference*, Purdue University, West Lafayette, IN, USA.
- Kuo, C. S., Wang, C. C., Cheng, W. Y., and Lu, D. C., 1995, "Evaporation of R-22 in a 7-mm micro-fin tube," *ASHRAE Transactions*, Vol. 101, Part 2, p. 1055-1061.
- Kutateladze, S. S., 1961, "Boiling heat transfer," *Int. J. of Heat and Mass Transfer*, Vol. 4, p. 31-45.
- Laesecke, A., 2002, Private communications by Kedzierski, NIST, Boulder, CO.
- Lemmon, E. W., Huber, M. L., and McLinden, M. O., 2006, "NIST reference fluid thermodynamic and transport properties," *REFPROP*, NIST standard reference database 23-Version 7.1.
- Lemmon, E. W., McLinden, M. O., and Huber, M. L., 2010, "NIST standard reference database 23, v. 9.0.," National Institute of Standards and Technology, Boulder, CO.
- Lim, T. W., and Kim, J. H., 2004, "An experimental investigation of heat transfer in forced convective boiling of R-134a, R-123, and R-134a/R-123 in a horizontal tube," *J. of Mechanical Science and Technology*, Vol. 18, No. 3, p. 513-525,
- Liu, Z., and Winterton, H. S., 1991, "A general correlation for saturated and subcooled flow boiling in tubes and annuli based on nucleate pool boiling," *Int. J. of Heat and Mass Transfer*, Vol. 34, p. 2759-2765.
- Lockhart, R. W., and Martinelli, R. C., 1947, "Proposed correlation of data for isothermal two-phase, two-component flow in pipes," *Chemical Engineering Progress*, Vol. 45, Part 1, p. 39-48.

BIBLIOGRAPHY

- Lottin, O., Guillemet, P., and Lebreton, J., M., 2003, "Effects of synthetic oil in a compression refrigeration system using R-410A – Part II: Quality of Heat Transfer and Pressure Losses within the Heat Exchangers," *Int. J. Refrigeration*, Vol. 26, p. 783-794.
- Manwell, S.P., and Bergles, A.E., 1990, "Gas-liquid flow patterns in refrigerant-oil mixtures," *ASHRAE Transactions*, Vol. 96, Part 2, p. 456-464.
- Mesler, R. B., 1977, "An alternate to the Dengler and Addoms convection concept of forced convection boiling heat transfer," *AIChE*, p. 448-453.
- Midgley Jr., T., and Henne, A. L., 1930, "Organic fluorides as refrigerants," *Industrial and Engineering Chemistry*, Vol. 22, p. 542-545.
- Midgley Jr., T., 1937, "From the periodic table to production," *Industrial and Engineering Chemistry* Vol. 29, Part 2, p. 239-244.
- Mishra, M. P., Varma, H. K., and Sharma, C. P., 1981, "Heat transfer coefficients in forced convection evaporation of refrigerant mixtures," *Letters in Heat and Mass Transfer*, Vol. 8, p. 127-136.
- Murata, K., and Hashizume, K., 1993, "Forced convective boiling of nonazeotropic refrigerant mixtures inside tubes," *Journal of Heat Transfer* Vol. 115, Part 3, p. 680-689.
- Nidegger, E., Thome, J. R., and Favrat, D. 1997, "Flow boiling and pressure drop measurements for R-134a/oil mixtures – part 1: Evaporation in a micro-fin tube," *HVAC&R Research*, Vol. 3, No. 1. p. 38 – 53.
- Nukiyama, S., 1934, "The maximum and minimum values of heat transmitted from metal to boiling water under atmospheric pressure," *Journal of Japan Soc. Mech. Eng.*, Vol. 37, p. 367.
- Oh, S. Y., and Bergles, A. E., 1998, "Experimental study of the effects of the spiral angle on evaporative heat transfer enhancement in micro-fin tubes," *ASHRAE Transactions*, Vol. 104, Part 2, p. 1137-1143.
- Ohadi, M. M., Darabi, J., Fanni, M. A., Dessiatoun, S. V., and Kedzierski, M. A., 1999, "Effect of heating boundary conditions on pool boiling experiments," *HVAC&R Research*, Vol. 5, No. 4, p. 283-296.
- Payne, W. V., and Domanski, P. A., 2002, "A Comparison of an R-22 and an R-410A air conditioner operating at high ambient temperatures," *Proceedings of the 9th International Conference*, R2-1, Purdue University, Indiana, USA.

BIBLIOGRAPHY

- Perkins, J., 1834, "Apparatus for producing ice and cooling fluids," *Patent 6662*, UK.
- Prasad, M., 2005, "Refrigeration and Air conditioning," *Revised 2nd Edition*, New Age International Ltd., Delhi, India.
- Radermacher, R., Ross, H., and Didion, D. A., 1983, "Experimental determination of forced convection evaporative heat transfer coefficients for non-azeotropic refrigerant mixtures," *ASME National Heat Transfer Conference*, ASME 83-WA/HT54.
- Ravigururajan, T. S., and Bergles, A. E., 1985, "General correlations for pressure drop and heat transfer for single-phase turbulent flow in internally ribbed tubes," *Augmentation of Heat Transfer in Energy Systems*, Vol. 52, p. 9-20.
- Reid, R. S., Pate, M. B., and Bergles, A. E., 1987, "Augmented in-tube evaporation of refrigerant 113," *Boiling and Condensation in Heat Transfer Equipment, HTD-85*, pp. 21-30.
- Rohsenow, W. M., Harnett, J. P., and Ganic, E. M., 1985, "Condensation," *Handbook of Heat Transfer*, 2nd edition, McGraw-Hill, New York.
- Rosen, M. J., 1978, *Surfactants and interfacial phenomenon*, John Wiley and Sons, New York, p. 57.
- Ross, H. D., 1986, "An investigation of horizontal flow boiling of pure and mixed refrigerants," *NBSIR-86-3450*, U.S. Department of Commerce, Washington, D.C., USA.
- Sami, S. M., Duong, T. N., and Snelson, W. K., 1993, "Study of flow boiling characteristics of R-134a in annulus of enhanced surface tubing," *Int. J. of Energy Research*, Vol. 17, Issue 8, p. 671-688.
- Sauer, H. J., Gibson, R. K., and Chongrungreong, S., "Influence of oil on nucleate boiling of refrigerants," *6th Int. Heat Transfer Conference*, Toronto, Vol. 1, p. 181-186.
- Sawant, N.N., Kedzierski, M.A., and Brown, J.S., 2007, "Effect of lubricant on R410A horizontal flow boiling," *NISTIR 7456*, U.S. Department of Commerce, Washington, D.C.
- Schlager, L. M., Pate, M. B., and Bergles, A. E., 1987, "A survey of refrigerant heat transfer and pressure drop emphasizing oil effects and in-tube augmentation," *ASHRAE Transactions*, Vol. 93, Part 1, p. 392-416.

BIBLIOGRAPHY

Schlager, L. M., Pate, M. B., and Bergles, A. E., 1988, "Evaporation and condensation of refrigerant-oil mixtures in a smooth tube and a micro-fin tube," *ASHRAE Transactions*, Vol. 94, Part 1, p. 149-166.

Schlager, L. M., Pate, M. B., and Bergles, A. E., 1989a., "Heat transfer and pressure drop during evaporation and condensation of R-22 in horizontal micro-fin tubes," *International J. Refrigeration*, Vol. 12, No. 1, p. 6-14.

Schlager, L. M., Pate, M. B., and Bergles, A. E., 1989b., "Evaporation and condensation heat transfer and pressure drop in horizontal, 12.7 mm micro-fin tubes with refrigerant 22," *Heat Transfer Fundamentals, Design, Applications, and Operating Problems* HTD-108, p. 205-213.

Schlager, L. M., Pate, M. B., and Bergles, A. E., 1989c., "Performance of micro-fin tubes with refrigerant-22 and oil mixtures," *ASHRAE Journal*, p. 17-28.

Schlager, L. M., Pate, M. B., and Bergles, A. E., 1989d., "A comparison of 150 and 300 SUS oil effects on refrigerant evaporation and condensation in a smooth tube and a micro-fin tube," *ASHRAE Transactions*, Vol. 95, Part 1, p. 387-397.

Schlager, L. M., Pate, M. B., and Bergles, A. E., 1990a., "Performance predictions of refrigerant-oil mixtures in smooth and internally finned tubes – Part I: Literature review," *ASHRAE Transactions*, Vol. 96.

Schlager, L. M., Pate, M. B., and Bergles, A. E., 1990b., "Performance predictions of refrigerant-oil mixtures in smooth and internally finned tubes – Part II: Design equations," *ASHRAE Transactions*, Vol. 96.

Schrock, V. E., and Grossman, L. M., 1959, "Forced convective boiling studies," *University of California, Institute of Engineering Research, Report No. 73308-UCX-2182*, Berkeley, California.

Seo, K., and Kim, Y., 2000, "Evaporation heat transfer and pressure drop of R-22 in 7 and 9.52 mm smooth and micro-fin tubes," *Int. J. of Heat and Mass Transfer*, Vol. 43, p. 2869-2882.

SES Technical Bulletin, 2004, "R-410A handling, properties, design, installation, and servicing," *Bulletin No. 17*, p. 1-7.

Shah, M. M., 1976, "A new correlation for heat transfer during boiling flow through pipes," *ASHRAE Transactions*, Vol. 88, Part 1, p. 185-196.

BIBLIOGRAPHY

- Shah, M. M., 1982, "Chart correlation for saturated boiling heat transfer: equations and further study," *ASHRAE Transactions*, Vol. 88, Part 1, p. 185-196.
- Singal, L. C., Sharma, C. P., and Varma, H. K., 1983, "Experimental heat transfer coefficient for binary refrigerant mixtures of R-13 and R-12," *ASHRAE Transactions*, p. 175-188.
- Singh, A., Ohadi, M. M., and Dessiatoun, S., 1996, "Flow boiling heat transfer coefficients of R-134a in a micro-fin tube," *Journal of Heat Transfer*, Vol. 118, p. 497 – 499.
- Song, S., and Bullard, C. W., 2002, "Effect of comfort constraints and compressor sizing on cycle efficiency of R-410A and R-744," Proceedings of 5th IIR-Gustav Lorentzen Conference on Natural Working Fluids, Guangzhou, China, p. 245 – 252.
- Staub, F. W., and Zuber, N., 1966, "Void fraction profiles, flow mechanisms and heat transfer coefficients for R-22 evaporating in a vertical tube," *ASHRAE Transactions*, p. 130.
- Stephan, K., 1963, "Influence of oil on heat transfer of boiling R-12 and R-22," *XIth International Congress of Refrigeration*, Vol. 1, p. 181-186.
- Stoecker, W. F. and Jones, J. W., 2001, "Refrigeration and Air-conditioning," 2nd edition, McGraw-Hill Inc.
- Taylor, B. N., and Kuyatt, C. E., 1994, "Guidelines for evaluating and expressing the uncertainty of NIST measurement results," *NIST Technical Note 1297*, U.S. Department of Commerce, Washington, D.C.
- Thome, J. R., 1995, "Comprehensive thermodynamic approach to modeling refrigerant-lubricating oil mixtures," *HVAC&R Research*, Vol. 1, No. 2, p. 110-126.
- Thome, J. R., 1996, "Boiling of new refrigerants: A State-of-the-art review," *Int. J. Refrigeration*, Vol. 19, p. 435-457.
- Thome, J. R., Nidegger, E., and Favrat, D. 1997, "Flow boiling and pressure drop measurements for R-134a/oil mixtures, Part 1: Evaporation in a micro-fin tube," *HVAC&R Research*, Vol.3, No. 1, p. 38–53.
- Thome, J. R., Zurcher, O., and Favrat, D. (1997), "Flow boiling and pressure drop measurements for R-134a/oil mixtures, Part 2: Evaporation in a plain tube," *HVAC&R Research*, Vol.3, No. 1, p. 54–64.

BIBLIOGRAPHY

Thome, J. R., Kattan, N., and Favrat, D., 1997, "Evaporation in micro-fin tubes: a generalized prediction model," *Proceedings of the Convective Flow and Pool Boiling Conference*, Kloster, Irsee.

Tichy, J. A., Duval, W. M. B., and Macken, N. A., 1986, "An Experimental investigation of heat transfer in forced-convection evaporation of oil-refrigerant mixtures," *ASHRAE Transactions*, Vol. 92, Part 2A, p. 450-460.

Tippets, F. E., 1962, *ASME Paper No. 62-WA-162*.

Treadwell, D. W., 1994, "Application of propane (R-290) to a single packaged unitary air-conditioning product," *ARI Flammability workshop*, Air-conditioning and Refrigeration Institute, Arlington, VA, USA.

Usmani, G. I., and Ravigururajan, T. S., 1999, "Two-phase flow heat transfer correlations for refrigerant-oil mixture flows inside augmented tubes," *Enhanced Heat Transfer*, Vol. 6, p. 405-418.

Yun, R., Kim, Y., Seo, K., and Kim, H., 2002, "A generalized correlation for evaporation heat transfer of refrigerants in micro-fin tubes," *Int. J. Heat and Mass Transfer*, Vol. 45, p. 2003-2010.

Webb, R. L., and Gupte, N. S., 1992, "A critical review of correlations for convective vaporization in tubes and tube banks," *Heat Transfer Engineering*, Vol. 13, No. 3, p. 58-81.

Webb, R. L., 1994, *Principles of Enhanced Heat Transfer*, *Wiley Interscience*.

Weber, F., 2000, "Simultaneous measurement of pressure, liquid and vapor density along the vapor-liquid equilibrium curve of binary mixtures of R-32 and R-125 of different composition," *Fluid Phase Equilibria*, Volume 174, Issues 1-2, p. 165-173.

Wei, W. J., Ding, G. L., Hu, H. T., Wang, K. J., 2007, "Influence of lubricant oil on heat transfer performance of refrigerant flow boiling inside small diameter tubes – Part II: Correlations," *Experiment Thermal Fluid and Science*, Vol. 32, part 1, p. 77-84.

Wilson, D. P., and Richard, R. G., 2002, "Determination of refrigerant lower flammability limits (LFLs) in compliance with proposed addendum to ANSI/ASHRAE Standard 34 – 1992 (1073-RP)," *ASHRAE Transactions*, Vol. 108, Part 2.

Wolverine Tube Inc., 2004, "Engineering Data Handbook III," Alabama, USA.

BIBLIOGRAPHY

Worsoe-Schmidt, P., 1960, "Some characteristics of flow pattern and heat transfer of Freon-12 evaporating in horizontal tubes," *The Journal of Refrigeration*, March-April, p. 40-43.

Zurcher, O., Thome, J. R., and Favrat, D. (1998), "In-tube flow boiling of R-407C and R-407C/oil mixtures, Part 1: Micro-fin tube," *HVAC&R Research*, Vol. 4, No. 4, p. 54-64.

Zurcher, O., Thome, J. R., and Favrat, D. (1998), "In-tube flow boiling of R-407C and R-407C/oil mixtures, Part 2: Plain tube results and predictions," *HVAC&R Research*, Vol. 4, No. 4, p. 54-64.